UNIVERSIDADE FEDERAL DO RIO GRANDE DO SUL
FACULDADE DE FARMÁCIA
PROGRAMA DE PÓS-GRADUAÇÃO EM CIÊNCIAS FARMACÊUTICAS

Modelagem Farmacocinética/Farmacodinâmica (PK/PD) da Quetiapina Nanoencapsulada em Modelo Animal de Esquizofrenia

FERNANDO OLINTO CARREÑO

Porto Alegre, 2019

UNIVERSIDADE FEDERAL DO RIO GRANDE DO SUL
FACULDADE DE FARMÁCIA
PROGRAMA DE PÓS-GRADUAÇÃO EM CIÊNCIAS FARMACÊUTICAS

Modelagem Farmacocinética/Farmacodinâmica (PK/PD) da Quetiapina Nanoencapsulada em Modelo Animal de Esquizofrenia

Tese apresentada por **Fernando Olinto Carreño** para obtenção do TÍTULO DE DOUTOR em Ciências Farmacêuticas

Orientador(a): Profa. Dra. Teresa Dalla Costa

Porto Alegre, 2019

Tese apresentada ao Programa de Pós-Graduação em Ciências Farmacêuticas, em nível de Doutorado Acadêmico da Faculdade de Farmácia da Universidade Federal do Rio Grande do Sul e aprovada com louvor em 16 de agosto de 2019, pela banca examinadora constituída por:

Profa. Dra. Andresa Heemann Betti
Universidade Feevale

Profa. Dra. Bibiana Verlindo de Araújo
Universidade Federal do Rio Grande do Sul

Prof. Dr. Hartmut Derendorf
University of Florida

Prof. Dr. Manuel Ibarra Viñales
Universidad de la República

CIP - Catalogação na Publicação

Carreño, Fernando
Modelagem Farmacocinética/Farmacodinâmica (PK/PD) da Quetiapina Nanoencapsulada em Modelo Animal de Esquizofrenia / Fernando Carreño. -- 2019.
240 f.
Orientadora: Teresa Dalla Costa.

Tese (Doutorado) -- Universidade Federal do Rio Grande do Sul, Faculdade de Farmácia, Programa de Pós-Graduação em Ciências Farmacêuticas, Porto Alegre, BR-RS, 2019.

1. nanocápsulas poliméricas de núcleo lipídico. 2. esquizofrenia. 3. poli(i:c). 4. modelo neurodesenvolvimental de esquizofrenia. 5. modelagem farmacocinética/farmacodinâmica. I. Dalla Costa, Teresa, orient. II. Título.

Elaborada pelo Sistema de Geração Automática de Ficha Catalográfica da UFRGS com os dados fornecidos pelo(a) autor(a).

Este trabalho foi desenvolvido no Laboratório de Farmacocinética e Modelagem PK/PD, Laboratório de Psicofarmacologia Experimental e Laboratório de Nanotecnologia Farmacêutica da Faculdade de Farmácia da Universidade Federal do Rio Grande do Sul e no Laboratório Nacional Agropecuário do Rio Grande do Sul (LANAGRO-RS) em Porto Alegre - RS e no *Pharmacometrics and Systems Pharmacology Group* da Universidade de Navarra em Pamplona – Espanha, com apoio financeiro do Programa de Pós Graduação em Ciências Farmacêuticas da UFRGS e do Conselho Nacional de Desenvolvimento Científico e Tecnológico - CNPq. O autor recebeu bolsa de estudos do CNPq e bolsa de doutorado sanduíche da Coordenação Nacional de Aperfeiçoamento de Pessoal de Nível Superior - CAPES.

AGRADECIMENTOS

À professora e orientadora Teresa Dalla Costa, por ter contribuído de forma ímpar com meu crescimento profissional, pelo exemplo profissional e comprometimento que tens com uma formação de excelência para teus alunos.

Às professoras Stela Rates, Ana Paula Herrmann, Sílvia Guterres e Karina Paese pelo apoio e orientação durante os experimentos realizados nos Laboratórios de Psicofarmacologia Experimental e Nanotecnologia Farmacêutica da UFRGS e também pelas importantes discussões científicas que fazem parte desta tese, foi um grande prazer trabalhar e aprender com vocês.

Al Prof. Iñaki Trocóniz me gustaría agradecerle el haberme brindado la oportunidad de realizar mi estancia en su grupo de investigación “Pharmacometrics and Systems Pharmacology” (P&SP) de la Universidad de Navarra. Gracias por tu dedicación, tus inestimables consejos y colaboración activa con esta tesis.

À veterinária Fabíola Schons Meyer e aos técnicos do biotério da bioquímica, em especial à Cláudia Kras, Cibele Kelm Marques e Luiza Falcão Funez. Sem o cuidado diário dedicado a cada um dos animais utilizados neste trabalho seria impossível chegar até aqui.

Ao Dr. Fabiano Barreto, pelo comprometimento e disponibilização do LC-MS/MS e do tempo, especialmente durante os finais de semana, para a concretização de experimentos que compõe esta tese.

À Victória Etges Helfer que topou embarcar nessa “aventura esquizofrênica” comigo e trabalhou ativa e incansavelmente ao meu lado em todas as etapas deste trabalho. A ti dedico uma medalha de ouro pela atuação como bolsista de iniciação científica nesta tese.

Às amizades que fiz nesse tempo de FACFAR: Izabel Almeida Alves, Bruna Torres, Graziela Lock, Keli Staudt, Ricardo Lorenzoni, Bruna Dias, Laura Olivo, Ana Lúcia Xavier. Por estarem sempre ao meu lado me dando força e animação para superar as dificuldades e alcançar meus objetivos.

Aos demais colegas do laboratório de farmacocinética e modelagem PK/PD com quem convivi durante essa trajetória e à professora Bibiana Verlindo de Araújo que além das discussões científicas nos seminários está sempre buscando proporcionar ao grupo diferentes experiências acadêmicas na área de farmacometria.

Me gustaría agradecer también a cada una de las personas que han sido parte del grupo P&SP mientras estuve allí: mi clon Diego, Nico, Vío, Belén, Itziar, Leire, Edu y Zinnia. Gracias por hacer mi estancia en el grupo muy alegre y de mucho aprendizaje (modelización, castellano, cultura y política española) y por brindarme vuestra compañía cuando echaba de menos a mi familia. Sois grandes personas y os deseo siempre lo mejor.

Aos colegas do grupo de Psicofarmacologia Experimental e Nanotecnologia Farmacêutica da UFRGS por sempre me receberem de braços abertos e com uma xícara de café.

Aos meus pais, Felipe e Maura Carreño, por terem incutido em mim os valores que me tornaram a pessoa que sou hoje. Por sempre permitirem que eu seguisse meu próprio caminho estando ao meu lado nas conquistas e derrotas.

À minha irmã Flávia Carreño, com quem tenho orgulho de compartilhar não apenas o gosto pela ciência mas também meu DNA. E ao Richard, que sempre vibra com as minhas conquistas e a quem eu tenho como um irmão.

E por fim, o agradecimento mais especial e carinhoso à Caroline, minha companheira de vida! O teu amor foi o pilar e a força motriz que me fizeram chegar até aqui. Eu amo você e amo a nossa família!

À minha família,

Caroline, Nix, Atena, Fly e quem ainda está por vir.

For such a model there is no need to ask the question "Is the model true?". If "truth" is to be the "whole truth" the answer must be "No". The only question of interest is "Is the model illuminating and useful?"

George. E.P. Box

RESUMO

A esquizofrenia (SCZ) é uma condição psiquiátrica debilitante que afeta aproximadamente 1% da população mundial. A alta variabilidade observada na resposta crônica ao tratamento da SCZ pode estar relacionada a disfunções da barreira hematoencefálica (BHE) que impactam no transporte de fármacos antipsicóticos (APD) para o sistema nervoso central (SNC). Com base na hipótese que a redução na penetração cerebral de fármacos para o SNC em pacientes com SCZ poderia estar associada à resistência à farmacoterapia foram desenvolvidas nanocápsulas poliméricas de núcleo lipídico (LNC) visando melhorar o *delivery* de APD para o cérebro. Buscando aumentar a compreensão do papel deste tipo de nanocarreador polimérico na disposição de fármacos para o SNC, nesta tese desenvolvemos um modelo farmacocinético/farmacodinâmico populacional (popPK/PD) capaz de descrever as alterações na farmacocinética plasmáticas e na distribuição cerebral da quetiapina (QTP) e nos níveis extracelulares corticais de dopamina após administração do fármaco em solução (FQ) ou nanoencapsulado (QLNC) a ratos machos e fêmeas hígidos e com SCZ experimental (SCZ-like). QLNC (1 mg/mL) foram obtidas por nanoprecipitação e apresentaram tamanho médio de 166 ± 39 nm, baixo índice de polidispersão (< 0,15) e alta eficiência de encapsulação (93 ± 1,38%). O modelo neurodesenvolvimental de SCZ induzido pela administração de ácido poliinosínico-policitidílico [poli(i:c)] a ratas prenhas foi utilizado para obter os animais com SCZ experimental. Ratas Wistar prenhas (GD15) receberam diferentes doses i.v *bolus* de poli(i:c). Déficits comportamentais na prole adulta (PND75) foram avaliados pelos testes de labirinto em cruz elevado (EPM), inibição de sobressalto por pré-pulso (PPI) e hiperlocomoção induzida pelo MK-801 em comparação à prole de fêmeas prenhas (GD15) que receberam volume equivalente de solução salina estéril (animais hígidos). Ratos SCZ-like foram tratados com FQ e QLNC havendo restauração dos déficits apresentados no PPI apenas quando o fármaco nanoencapsulado foi utilizado. Para a investigação PK amostras de plasma e microdialisado cerebral (hipocampo ventral – HIP e córtex pré-frontal medial - mPFC) foram coletadas de machos e fêmeas hígidos e SCZ-like após administração intravenosa de FQ (5 e 10 mg / kg) ou QLNC (5 mg/kg). Observou-se uma redução significativa da exposição cerebral livre à QTP quando ratos SCZ-like foram administrados com FQ em comparação com animais hígidos. Utilizando modelagem farmacocinética populacional (popPK), um modelo semi-mecanístico capaz de descrever a farmacocinética plasmática e a distribuição cerebral da QTP administrada como FQ a animais hígidos e SCZ-like foi desenvolvido. O transporte bidirecional da QTP através da BHE foi parametrizado como CL_{in} e CL_{out}. Animais SCZ-like apresentaram uma redução significativa no transporte através da BHE (CL_{in}: 0,019 L/h/Kg e CL_{out}: 0,017L/h/Kg) em comparação com animais naïve (CL_{in}: 0,045 L/h/Kg e CL_{out}: 0,023 L/h/kg). Além disso,

demonstrou-se que quanto pior o desempenho do animal no PPI, mais comprometido está o transporte de influxo de QTP através da BHE, indicando que a penetração de APD como a QTP está diminuida na SCZ e pode contribuir para a resistência observada ao tratamento farmacológico da doença. Aumento da exposição cerebral à QTP foi observado em animais SCZ-like quando QLNC foi administrada. O modelo popPK foi então expandido para descrever as diferentes características da QLCN: liberação da QTP *in vivo* do nanocarreador no plasma ($Krel_{FAST}$: 0,261 h^{-1} e $Krel_{SLOW}$: 0,00047 h^{-1}) e mecanismo de distribuição da QTP para os tecidos e cérebro governado pelo nanocarreador ($CL_{in,nano}$: 0,067 L/h/kg). Para investigação da PD um método bioanalítico versátil por CLAE-MS/MS foi desenvolvido e validado para determinação simultânea de monoaminas (MNT): dopamina (DA), ácido 3-4-diidroxifenilacético (DOPAC), ácido homovanílico (HVA), serotonina (5-HT) e ácido 5-hidroxi-indol-acético (5-HIAA) em amostras de microdialisado cerebral. O método foi aplicado para monitorar as alterações de concentração de MNT em amostras de dialisado obtidas do mPFC de prole de animais hígidos e SCZ-like antes e após a administração de QTP 5 mg/kg i.v. *bolus* (FQ e QLNC). Alterações na linha de base da DA após administração do fármaco não foram significativas em animais SCZ-like administrados com FQ. Quando ratos SCZ-like receberam QLNC, observou-se um aumento dos níveis de DA semelhantes aos observados em animais hígidos. Modelo de resposta indireta semi-mecanístico popPK/PD desenvolvido permitiu entender como FQ e QLNC afetam as concentrações extracelulares de DA. Um aumento de cerca de três vezes de no valor de EC_{50} (1,75 ng/mL para 4,97 ng/mL) para a QTP foi observado em ratos SCZ-like em comparação com animais hígidos. QLNC não alterou os parâmetros PD, pois não foram observadas alterações no EC_{50} após administração dessa formulação. No entanto, como a LNC modula a exposição cerebral à QTP foi observado um aumento dos níveis de DA no mPFC mostrando a importância do componente farmacocinético na variabilidade do tratamento farmacológico da SCZ. A abordagem presente nesta tese é útil para entender possibilidades e limitações dessas nanoformulações no *delivery* cerebral de fármacos, permitindo utilizar dessa estratégia para melhorar o tratamento farmacológico da SCZ.

Palavras-chave: nanocápsulas poliméricas de núcleo lipídico, esquizofrenia, poli(i:c), modelo neurodesenvolvimental de esquizofrenia, delivery cerebral, modelo popPK, modelo popPK/PD

ABSTRACT

Pharmacokinetic/Pharmacodynamic (PK/PD) Model of Quetiapine Lipid Core Nanocapsules in a Neurodevelopmental Animal Model of Schizophrenia

Schizophrenia (SCZ) is a debilitating psychiatric condition with a lifetime prevalence of 1% worldwide. The incidence of this psychic disorder is slightly higher in men than in women, and women have less severe symptoms and better prognosis. The high variability observed in chronic SCZ response to treatment may be partially related to blood-brain barrier (BBB) dysfunction and consequent alterations on antipsychotic drug transport to central nervous system (CNS). We hypothesized that limited drug delivery to CNS in SCZ patients could be associated with pharmacotherapy resistance and developed lipid core nanocapsules (LNC) aiming to improve drug targeting to the brain. Viewing to increasing the understanding of the role of this type of drug delivery systems in brain drug disposition, in the current study we developed a population pharmacokinetic/pharmacodynamic (popPK/PD) model capable of describing changes in QTP plasma and brain pharmacokinetics and dopamine levels in brain after drug administration in solution (FQ) or encapsulated (QLNC) to naïve and schizophrenia-like (SCZ-like) male and female rats. QLNC (1 mg/mL) were obtained by nanoprecipitation and presented average size of 166 ± 39 nm, low polydispersity index (< 0.15) and high encapsulation efficiency (93 ± 1.38%). Neurodevelopmental model of SCZ induced by the administration of viral mimic polyinosinic–polycytidilic acid [poly(i:c)] to pregnant rats, which has face, construct and predictive validity, was used to produce the SCZ-like animals. Pregnant Wistar dams (GD15) received different i.v. *bolus* doses of poly(i:c). SCZ-like deficits in male and female adult offspring (PND75) were accessed by elevated plus-maze (EPM), pre-pulse inhibition of the startle response (PPI) and MK-801-induced hyperlocomotion in comparison to offspring of pregnant dams (GD15) that received the same i.v. *bolus* volume of saline (naïve animals). SCZ-like animals were treated with FQ and QLNC showing restoration of the PPI deficits only when drug encapsulated was used. For PK investigation, plasma and brain microdialysis samples (ventral hippocampus – HIP and medium prefrontal cortex -mPFC) were collected from male and female, naïve and SCZ-like animals following intravenous dosing with FQ (5 and 10 mg/kg) or QLNC (5 mg/kg). A significant reduction of the extent of QTP unbound brain distribution was observed in SCZ-like animals dosed with FQ formulation when compared to naïve offspring. Using population model based approach (popPK) a semi-mechanistic two-compartment model was identifiable both in blood and in the brain after administration of FQ formulation to naïve and SCZ-like rats. Bi-directional transport of QTP across the BBB was parametrized as CL_{in} and CL_{out}. SCZ-like animals presented a significant reduction in the rate of BBB transport (CL_{in}: 0.019

L/h/Kg; and CL_{out}: 0.017 L/h/Kg) in comparison to naïve animals (CL_{in}: 0.045 L/h/Kg and CL_{out}: 0.023 L/h/Kg). Using the PPI test it was possible to demonstrate that the greater reduction in PPI, the more compromised is the influx transport across BBB, indicating that the cerebral penetration of antipsychotics such as QTP is decreased in SCZ and may contribute to the resistance observed with pharmacological treatment. An increased brain exposition was observed in SCZ-like animals when QLNC was administered. The popPK model was expanded to describe different features of the QLNC formulation. The final model describes QTP *in vivo* release from QLNC in plasma ($Krel_{FAST}$: 0.261 h-1 and $Krel_{SLOW}$: 0.00047 h-1) and support a mechanism of the LNC governing QTP distributing into brain and tissues ($Qnano_{TISSUE/BRAIN}$ 0.067 L/h/Kg). For the PD investigation, a versatile method was developed and validated for simultaneous determination of the monoamine neurotransmitters (MNT) dopamine (DA), 3-4-dyhydroxyphenilacetic acid (DOPAC), homovanilic acid (HVA), serotonin (5-HT) and 5-hydroxyindolacetic acid (5-HIAA) in rat brain microdialysate samples using high-performance liquid chromatography tandem mass spectrometry (LC-MS/MS). The method was applied for monitoring the concentration changes of MNT in microdialysate samples from mPFC of male and female naïve and SCZ-like animals before and after QTP 5 mg/kg i.v. *bolus* dosing as FQ and QLNC. Only DA showed differences form baseline after QTP dosing. Changes in DA baseline were not observed in SCZ-like animals after FQ dosing, however when the animals received QLNC formulation an increase in DA levels similar to that observes in naive animals was observed. A semi-mechanistic popPK/PD indirect response model was developed allowing understanding how FQ and QLNC formulation affects DA concentrations in naïve and SCZ-like rats. SCZ status increased QTP EC_{50} values about three times in comparison to naïve animals (from 1.75 ng/mL to 4.97 ng/mL). Nanoencapsulation did not alter PD parameters, since no alterations were observed in EC_{50} after QLNC dosing. However, because LNC modulate QTP brain delivery and increase in DA levels in mPFC was observed, showing the importance of the pharmacokinetic component to overcome the variability observed in SCZ pharmacological treatment. The present model-based approach is useful to better understand the possibilities and limitations of these nanoformulation in drug delivery to the brain opening the possibility to use this approach to improve SCZ-treatment limited response rates.

Keywords: Lipid core nanocapsules; schizophrenia; poly(i:c) model of schizophrenia; quetiapine; microdialysis, brain delivery, popPK model, popPK/PD model.

LISTA DE TABELAS

CAPÍTULO 1

Material suplementar

Table S1. Summary of the statistical tests and outcomes used for the cytokine maternal plasma levels evaluation. ……..…..…….....93

Table S2. Summary of the statistical tests and outcomes for the behavioral analyses conducted in saline and poly(i:c) offspring. ……..94

Table S3. Summary of the statistical tests and outcomes for the evaluation of quetiapine lipid core nanocapsules effect on PPI restoration in poly(i:c) animals. ……..…95

CAPÍTULO 2

Table 1. Mass spectrometry and retention times for each analyte. ……...……111

Table 2. Calibration curve regression parameters. ……...115

Table 3. Stability of MNTs in artificial cerebrospinal fluid. ……..…….117

Table 4. Effects of 5 mg/kg QTP systemic injection in MNT exposure in naïve and poly(i:c) offspring. ……..……...120

Material suplementar

Table S1. Intra and inter-assay precision and accuracy of the method for determining DA in quality control samples. ……125

Table S2. Intra and inter-assay precision and accuracy of the method for determining DOPAC in quality control samples. ……..…….……126

Table S3. Intra and inter-assay precision and accuracy of the method for determining HVA in quality control samples.……127

Table S4. Intra and inter-assay precision and accuracy of the method for determining 5-HT in quality control samples. ……...128

Table S5. Intra and inter-assay precision and accuracy of the method for determining 5-HIIA in quality control samples. ……..….129

CAPÍTULO 3

Table 1. Pharmacokinetic parameters estimate of the final QTP model.……...154

Material suplementar

Table S1. Pharmacokinetic parameters estimate for the external validation FQ model using probenecid dataset……..……..……...171

CAPÍTULO 4

Table 1. Population pharmacokinetic parameters used in the PK/PD modeling..…….....187

Table 2. Table 2. Parameter estimates of the final PK/PD model……..…...192

LISTA DE FIGURAS

CAPÍTULO 1

Figure 1. Cytokine plasma levels after single poly(i:c) injection to pregnant damns (GD15). ……..……..……...78

Figure 2. Effect of different poly(i:c) prenatal treatment doses on elevated plus maze……..……...80

Figure 3. Effects of different doses of poly(i:c) on sensorimotor gating assessed by the paradigm of prepulse inhibition (PPI) of the acoustic startle response……..……..……81

Figure 4. Locomotor responses of adult offspring exposed prenatally to saline or different doses of poly(i:c). ……82

Figure 5. Effects of FQ and QLNC treatment on prepulse inhibition of the acoustic startle response in poly(i:c) neurodevelopmental model of SC. ……83

Material suplementar

Figure S1. Sex difference in acoustic startle response after a 120-dB pulse. …….....91

Figure S2. Difference in acoustic startle response in a 120-dB pulse trial after administrations of different formulations. ……..……..……92

CAPÍTULO 2

Figure 1. Chemical structure of (A) dopamine - DA, (B) 3-4-dyhydroxyphenilacetic acid - DOPAC, (C) homovanilic acid - HVA, (D) serotonin – 5-HT and (E) 5-hydroxyindolacetic acid - 5-HIIA…..……...…...105

Figure 2. Effect of QTP (5 mg/kg i.v. *bolus*) on extracellular levels of DA (A), DOPAC (B), HVA (C), 5-HT (D) and 5-HIIA (E) at the mPFC of naïve (solid symbols) and poly(i:c) exposed (empty symbols) offspring…….…..118

CAPÍTULO 3

Figure 1. Deficit in sensorimotor gating assessed by the paradigm of prepulse inhibition (PPI) of the acoustic startle response…….....145

Figure 2. Schematic representation of the final QTP structural model for FQ and QLNC formulation…….....147

Figure 3. Correlation between model predicted individual CL_{in} and CL_{out} and prepulse inhibition response of the naïve and poly(i:c) animals……..…….....152

Figure 4. Visual predictive checks (VPCs) of the final population PK model for FQ and QLNC formulations stratified by total plasma, unbound plasma and the unbound brain stratified by naïve or SCZ-like rats. ……..…….....155

Figure 5. Simulated time course of FQ and QLNC in plasma and brain of naïve and SCZ-like rats……..……..…….....156

Figure 6. Simulated QTP total plasma and unbound brain concentrations following QLNC with different $Krel_{SLOW}$ rates administration to SCZ-like rats…….…….....157

Material suplementar

Figure S1. Individual and population fitted total plasma concentration *versus* time profiles using the final popPK model for FQ and QLNC formulations…..167

Figure S2. Individual and population fitted unbound plasma concentration *versus* time profiles using the final popPK model for FQ and QLNC formulations……..…..168

Figure S3. Individual and population fitted unbound brain concentration *versus* time profiles using the final popPK model for FQ and QLNC formulations…..169

Figure S4. Goodness of fit plots for FQ formulation model ……...170

Figure S5. Goodness of fit plots for QLNC formulation model ……..……...170

Figure S6. Individual and population fitted total plasma and unbound brain concentration *versus* time profiles following QTP 10 mg/kg i.v. dosing 30 min after 30 mg/kg probenecid (PROB) i.v. dosing using the final popPK model for FQ as an external validation……..……..172

Figure S7. Goodness of fit plots for the external validation using the probenecid dataset…….173

CAPÍTULO 4

Figure 1. Schematic representation of the full structural PK/PD model used to describe mPFC dopamine response after administration of FQ or QLNC formulation…….……..…..189

Figure 2. Simulated unbound brain concentration versus time profile of quetiapine after a single intravenous bolus dose of 5 mg/kg of FQ or QLNC formulations to naïve and SPR rats…….……..……..…..190

Figure 3. Observed and model-fitted dopamine concentrations in mPFC of naïve and SPR after administration of a single 5 mg/kg dose of FQ formulation intravenously……..……..……..…….191

Figure 4. Observed and model-fitted dopamine concentrations in mPFC of naïve and SPR after administration of a single 5 mg/kg dose of QLNC formulation intravenously…..……..……..……...……..193

Figure 5. Visual predictive checks (VPCs) of the final PK/PD model for naïve and SPR after administrations of FQ and QLNC formulations…..…….194

LISTA DE ABREVIATURAS

5-HIIA - 5-hydroxyindolacetic acid

5-HT - serotonin

ACF - artificial cerebrospinal fluid

APD - antipsychotic drugs

ASR - acoustic startle response

BHE - barreira hematoencefálica

BLK - blank lipid-core nanocapsules

CSF - cerebrospinal fluid

DA - dopamine

DOPAC - 3-4-dyhydroxyphenilacetic acid

EPM - elevate plus maze

FQ - quetiapine control formulation

fT - fator de penetração tecidual

GD - dia gestacional

HVA - ácido homovanílico

IL-10 - interleucina 10

IL-6 - interleucina 6

LCA - líquido cerebral artificial

LNC - lipid core nanocapsules

MIA - maternal immune activation

MNT - monoamine neurotransmitters

mPFC - medium prefrontal cortex

PND - postnatal-day

poly(i:c) - ácido poli-inosínico:policitidílico

popPK/PD - modelo populacional farmacocinético/farmacodinâmico

PPI - pre-pulse inhibition

PT - pre-natal treatment

QLNC - quetiapine lipid-core nanocapsules

QTP - quetiapina

SCZ - esquizofrenia

SPR – schizophrenia phenotyped rat

VEH - vehicle formulation

SUMÁRIO

INTRODUÇÃO 25

OBJETIVOS 33

2.1. Objetivo Geral 35

2.2. Objetivos Específicos 35

REVISÃO DE LITERATURA 37

3.1. Esquizofrenia: Aspectos Gerais 39

3.2. Diferenças Sexuais na Esquizofrenia 41

3.3. Status da Barreira Hematoencefálica em Transtornos Psicóticos 43

3.4. Modelos Animais de Esquizofrenia 46

3.5. Modelo Neurodesenvolvimental de Esquizofrenia por Ativação Imune Pré-Natal 49

3.6 Nanopartículas e *Delivery* de Antipsicóticos 53

3.7 Microdiálise como Ferramenta para Estudo da Distribuição Cerebral de Fármacos e Neurotransmissores 55

3.8 Modelagem Farmacocinética/Farmacodinâmica 57

CAPÍTULO 1 65

CAPÍTULO 2 97

CAPÍTULO 3 131

CAPÍTULO 4 175

DISCUSSÃO GERAL 201

CONCLUSÕES 217

REFERENCIAS GERAIS 221

ANEXOS 237

INTRODUÇÃO

A esquizofrenia (SCZ) é uma condição psiquiátrica crônica, heterogênea e debilitante desencadeada por fatores genéticos, epigenéticos e ambientais que interferem coletivamente com a maturação e o desenvolvimento normal do cérebro (INSEL, 2010; RAPOPORT, GIEDD & GOGTAY, 2012; MILLAN et al., 2016).

A SCZ acomete cerca de 1% da população mundial sendo normalmente diagnosticada em adultos jovens. Possui uma importante carga socioeconômica devido aos custos diretos e indiretos que decorrem da cessação de uma vida produtiva e independente e relacionado à assistência ao paciente durante a utilização de serviços hospitalares (INSEL, 2010; MILLAN et al., 2016).

O tratamento farmacológico da SCZ baseia-se principalmente no controle dos sintomas positivos da doença com o uso de antipsicóticos típicos, atípicos ou suas associações. Embora a importância desses tratamentos deva ser reconhecida, ainda existe uma alta variabilidade na resposta terapêutica: 60% dos pacientes respondem parcialmente e 30% são considerados resistentes ao tratamento com antipsicóticos (SUZUKI et al., 2011).

Além da alta variabilidade terapêutica, estudos publicados recentemente têm evidenciado diferenças importantes na fisiopatologia da esquizofrenia e na resposta ao tratamento farmacológico entre homens e mulheres (BALE & EPPERSON, 2015; HILL, 2016). No âmbito da pesquisa pré-clínica, porém, a utilização de fêmeas ainda é incomum em estudos para desenvolvimento de novos fármacos ou terapias com antipsicóticos, limitando a compreensão das alterações farmacocinéticas e farmacodinâmicas relacionadas às diferenças sexuais.

A alta variabilidade na resposta terapêutica pode estar associada a alterações na barreira hematoencefálica (BHE) causadas pela SCZ, como o aumento da expressão de transportadores de efluxo, por exemplo, que podem limitar a distribuição dos antipsicóticos para seu sítio de ação no sistema nervoso central (SNC). Relatos na literatura indicam que há uma forte influência reguladora do estrógeno na expressão de transportadores na BHE de ratos Wistar, podendo haver uma alteração dos mesmos em estados patológicos como a esquizofrenia (MORRIS; LEE; PREDKO, 2003). Essa

influência poderia resultar em alterações na penetração cerebral de fármacos antipsicóticos em fêmeas em comparação com machos.

A utilização de diferentes tipos de nanocarreadores de fármacos como nanopartículas poliméricas, lipossomas e nanopartículas lipídicas sólidas é uma estratégia promissora que poderia contribuir para melhorar o *delivery* cerebral de antipsicóticos devido a capacidade desses sistemas de modular a farmacocinética e a distribuição tecidual de fármacos (ABBOTT et al., 2010; GABATHULER, 2010; LINDQVIST et al., 2013).

O grupo de Nanotecnologia Farmacêutica da Universidade Federal do Rio Grande do Sul (UFRGS) desenvolveu e tem estudado extensivamente uma formulação de nanocarreadores poliméricos composta por uma dispersão de triglicerídeos do ácido cáprico e caprílico e monoestearato de sorbitana envelopados por uma parede polimérica formada de poli(ε-caprolactona) e recoberta com polissorbato 80: as nanocápsulas poliméricas de núcleo lipídico (LNCs) (JÄGER et al., 2009; VENTURINI et al., 2011; JORNADA et al., 2012; FIEL et al., 2014).

Utilizando a quetiapina (QTP), antipsicótico atípico de 2ª geração como fármaco modelo, obtivemos nanocápsulas poliméricas de núcleo lipídico com o fármaco (QLNC) e avaliamos o *delivery* cerebral em ratos Wistar machos sadios. Os resultados demonstraram que as QLNC foram capazes de alterar a farmacocinética plasmática da QTP administrada por via intravenosa, promovendo uma redução significativa no *clearance* total do fármaco e consequentemente um aumento significativo da meia-vida e da área sob a curva plasmática (ASC), quando comparado com a mesma dose do fármaco administrada em solução (CARREÑO, 2016a).

Através da técnica de microdiálise cerebral, que permite determinar as concentrações farmacologicamente ativas na biofase, demonstramos que as QLNCs atravessam a membrana luminal da BHE carreando a QTP, não permitindo que o fármaco nanoencapsulado interaja com os transportadores de efluxo (CARREÑO et al., 2016b). Esse fato foi evidenciado pela diferença significativa no fator de penetração hipocampal quando o fármaco foi administrado em solução (fT = 1,55 ± 0,17) ou nanoencapsulado (fT = 0,88 ± 0,21) na ausência e na presença da probenecida (fTsolução = 0,94 ± 0,15 e fTQLNC = 0,92 ± 0,13), um inibidor do transportador de influxo.

Na investigação da penetração cerebral da QTP nos estudos conduzidos previamente (CARREÑO, 2016a; 2016b), no entanto, foram utilizados ratos machos sadios. Desse modo, as alterações causadas na BHE tanto pela SCZ quanto pelas diferenças de gênero e, consequentemente, na distribuição cerebral do fármaco não foram investigadas. Além disso, a exposição hipocampal à QTP livre nos animais sadios que receberam o fármaco nanoencapsulado (ASC_{0-6h} = 259 ± 62 ng*h/mL/kg) foi semelhante à determinada nos animais que receberam o fármaco em solução (ASC_{0-6s} = 224 ± 51 ng*h/mL/kg), apesar de termos determinado aumento das concentrações cerebrais totais (ASC_{0-8h} de 3,47 µg·h/g para 5,94 µg·h/g) com o uso da QLNC. Embora sem quantificação, observou-se que os animais que recebiam as QLNC apresentavam efeito sedativo mais pronunciado do que os animais que recebiam o fármaco em solução, indicando a necessidade de determinação das concentrações livres da QTP em outras regiões cerebrais. Essas questões em aberto justificam a continuidade dos estudos com as QLNC em modelo animal capaz de mimetizar as alterações neuronais e os padrões comportamentais observados em pacientes esquizofrênicos, bem como investigar se o sexo pode alterar o padrão de distribuição do fármaco, tanto livre quando nanoencapsulado, nesse modelo de SCZ.

O modelo neurodesenvolvimental de esquizofrenia por injeção intravenosa de ácido poli-inosínico:policitidílico [poli(i:c)] a ratas prenhas (ZUCKERMAN et al., 2003; ZUCKERMAN & WEINER, 2005; PATRICH et al., 2016) resulta em filhotes que na idade adulta apresentam um fenótipo neurobiológico e comportamental muito semelhante ao observado na SCZ humana (PATRICH et al., 2016; PIONTKEWITZ, ARAD & WEINER, 2011). Esse modelo pré-clinico é considerado preditivo e confiável, podendo ser utilizado na investigação da disposição cerebral e efeito antipsicótico de fármacos e na extrapolação da investigação de novas estratégias terapêuticas farmacológicas (MÖLLER, SWANEPOEL & HARVEY, 2015).

Uma melhor compreensão da relação concentração livre versus efeito farmacológico nos locais-alvo do SNC é fundamental para o entendimento e desenvolvimento de novas terapias farmacológicas que sejam efetivas para doenças como a SCZ já que, ainda hoje, há uma escassez de informações sobre essas relações (SRINIVAS; MAFFUID; KASHUBA, 2018).

A modelagem farmacocinética-farmacodinâmica (modelagem PK/PD) é uma ferramenta matemática e estatística que objetiva estabelecer relações entre a exposição (PK) e o efeito (PD) de um fármaco e que tem sido cada vez mais utilizada para caracterizar e prever o curso temporal das respostas farmacodinâmicas tanto em estudos pré-clínicos quanto em estudos clínicos (DANHOF et al., 2008, HURTADO et al., 2014; ZIMMERMANN et al., 2015)

Através do desenvolvimento de um modelo PK/PD populacional (modelo popPK/PD) é possível investigar as fontes de variabilidade dos parâmetros farmacocinético e do efeito farmacodinâmico intra e inter-indivíduos, tais como condições patológicas, massa corporal, sexo, idade, entre outros, que causam alterações na resposta terapêutica, permitindo uma melhor compreensão da relação entre esses fatores e a exposição/efeito do fármaco (ZHOU et al., 2015). Além disso, os modelos popPK/PD permitem descrever, simular e prever o efeito farmacológico em função do tempo resultante de um regime posológico adotado em indivíduos saudáveis ou em uma condição patológica como a SCZ, como no presente caso, levando em consideração a variabilidade entre os indivíduos da população estudada (BARBOUR, SCALIONE & DERENDORF, 2010).

Os modelos popPK/PD pré-clínicos descritos na literatura para antipsicóticos utilizam dados de PK (concentrações de fármaco no plasma e no tecido cerebral) *in vivo* em animais saudáveis e dados de PD (ocupação de receptores dopaminérgicos, D2, e serotoninérgicos, 5-HT2A) *in vitro* para estabelecer uma relação temporal do efeito de fármacos como a risperidona e a olanzapina e realizar simulações para prever o efeito em humanos (JOHNSON et al., 2011, 2014; KOZIELSKA et al., 2012).

O desenvolvimento de um modelo popPK/PD para a QTP capaz de descrever a modulação da disposição livre cerebral do fármaco e o efeito farmacológico resultante da nanoencapsulação observados em modelo animal de esquizofrenia, tanto para machos quanto para fêmeas, representa uma estratégia inédita na literatura e permitirá determinar de que maneira os nanocarreadores modulam os parâmetros PK/PD desse antipisótico, permitindo avaliar as vantagens do seu uso e gerando ferramenta importante para investigação de posologias eficazes para o fármaco.

OBJETIVOS

2.1. Objetivo Geral

Estabelecer um modelo popPK/PD capaz de descrever as alterações farmacocinéticas e farmacodinâmicas da quetiapina nanoencapsulada em um modelo neurodesenvolvimental de esquizofrenia em ratos Wistar machos e fêmeas.

2.2. Objetivos Específicos

1. Implementar o modelo neurodesenvolvimental de esquizofrenia em ratos Wistar machos e fêmeas através da ativação imune pré-natal induzida por poly(i:c) nas condições do laboratório;

2. Validar metodologia bioanalítica para a quantificação dos neurotransmissores: dopamina, serotonina e seus metabólitos (ácido 3,4-diidroxifenilacético - DOPAC, ácido homovanílico - HVA e ácido 5-hidroxi-indolacético - 5-HIAA) por técnicas de cromatografia líquida de alta eficiência acoplada à espectrometria de massas (LC-MS/MS);

3. Avaliar comparativamente a farmacocinética plasmática e a distribuição cerebral da QTP, através de microdiálise hipocampal e cortical, em ratos Wistar machos e fêmeas com esquizofrenia experimental após administração intravenosa do fármaco em solução e encapsulado na LNC;

4. Estabelecer modelo populacional (popPK) para descrever a farmacocinética plasmática e cerebral (córtex pré-frontal e hipocampo) da QTP em animais sadios e em animais do modelo neurodesenvolvimental de esquizofrenia após administração do fármaco em solução ou nanoencapsulado (QLNC);

5. Investigar, por microdiálise cerebral, as alterações nos níveis intersticiais corticais de dopamina, serotonina e seus metabólitos de ratos Wistar machos e fêmeas sadios e com esquizofrenia experimental após a administração intravenosa de QTP em solução e encapsulado na LNC;
6. Estabelecer um modelo popPK/PD capaz de descrever as alterações na farmacocinética plasmática, na distribuição cerebral e na resposta à quetiapina livre e nanoencapsulada administrada a ratos Wistar machos e fêmeas sadios e em animais do modelo neurodesenvolvimental de esquizofrenia.

Os objetivos específicos desta tese foram organizados na forma de quatro capítulos que correspondem a artigos científicos e incluem uma breve revisão de cada tema, materiais e métodos, resultados e discussão. Os artigos encontram-se na sequência do texto da seguinte maneira:

Capítulo 01: "Quetiapine lipid core nanocapsules restore prepulse inhibition deficits in a neurodevelopmental model of schizophrenia in male and female rats", que reúne resultados referentes ao objetivo específico 1.

Capítulo 02: "A versatile LC-MS/MS method for determination of neurotransmitters in microdialysis samples applied to investigate the effect of quetiapine in schizophrenic like animals" que reúne resultados referentes ao objetivos específicos 2.

Capítulo 03: "Semi-mechanistic pharmacokinetic modeling of lipid core nanocapsules: understanding quetiapine plasma and brain disposition in a neurodevelopmental animal model of schizophrenia", que reúne resultados referentes aos objetivos específicos 3 e 4.

Capítulo 04: "Pharmacokinetic/pharmacodynamic modeling of cortical dopamine levels after quetiapine lipid core nanocapsules administration to schizophrenia phenotyped rat", proposta preliminar de artigo que reúne resultados referentes aos objetivos específicos 5 e 6.

REVISÃO DE LITERATURA

3.1. Esquizofrenia: Aspectos Gerais

A SCZ é um transtorno mental crônico e multifatorial caracterizado por distorções do pensamento, das emoções, da percepção de si mesmo e também por afetos inapropriados ou embotados (CANDIAGO et al., 2013; INSEL, 2010; KAHN; SOMMER, 2015; MILLAN et al., 2016; SILVA et al., 2017). Na nota descritiva Nº 397 publicada em 2016 pela Organização Mundial da Saúde (OMS) estima-se que a SCZ afeta mais de 21 milhões de pessoas em todo mundo, comprometendo consideravelmente o desempenho educativo e laboral do paciente, que sofre também com a estigmatização da doença e a discriminação social (SILVA et al., 2017).

Os portadores de SCZ apresentam sinais e sintomas característicos que podem ser classificados em “positivos”, “negativos” e “cognitivos”. As crises psicóticas recorrentes são o principal sintoma positivo e causam perda do contato com a realidade, principalmente através da desorganização do pensamento (transtorno do pensamento formal), alucinações visuais, auditivas, gustativas e táteis, bem como delírios do tipo paranóide. O conjunto de sintomas negativos caracteriza uma síndrome amotivacional representada por expressão emocional diminuída, isolamento social, incapacidade de sentir prazer (anedonia), perda da capacidade de tomada de decisões e ausência de força de vontade (abulia). Os sintomas cognitivos afetam o raciocino e a aprendizagem, causando déficits de memória, função executiva e linguagem (SAHIN; DOOSTDAR; NEILL, 2016).

Até o momento não foi identificado nenhum marcador bioquímico ou teste laboratorial para diagnosticar a SCZ (LAI et al., 2016). O diagnóstico da esquizofrenia é baseado em critérios estabelecidos no Manual Diagnóstico e Estatístico de Transtornos Mentais (DSM-5) da Associação Americana de Psiquiatria e na Classificação Internacional de Doenças e Problemas Relacionados à Saúde (CID), publicado pela OMS. Esses critérios consideram a presença e a duração de sintomas positivos, negativos e cognitivos e também o impacto desses sintomas na vida social e ocupacional do paciente. São consideradas, ainda, as associações com outras condições psiquiátricas, transtornos de humor e até mesmo a utilização de drogas de abuso.

Devido a sua alta complexidade, a SCZ pode ser classificada em diferentes subtipos clínicos, sendo os principais: *paranóide*, com predomínio de delírios persecutórios e alucinações; *hebefrênico*, também chamado de desorganizado, em que predominam os distúrbios afetivos do tipo inapropriado ou pueril; *catatônico*, com sintomas de rigidez, esturpor ou agitação psicomotora; *indiferenciado*, predomínio de comportamento incoerente e desorganizado associado a delírios e alucinações; *residual*, com predominância de sintomas negativos.

O tratamento clínico da esquizofrenia é realizado através de duas frentes de ação: a psicoterapia e o tratamento farmacológico. O acompanhamento psicoterápico busca a reabilitação psicossocial do paciente, o resgate da autonomia, individualidade e da capacidade de socialização (KRAUSE et al., 2018).

O tratamento farmacológico é direcionado para o controle dos sintomas positivos da doença através do uso de medicamentos antipsicóticos típicos ($AP_{TÍPICOS}$), como haloperidol, flufenazina, clorpromazina e tioridazina; e antipsicóticos atípicos ($AP_{ATÍPICOS}$), como clozapina, risperidona, quetiapina, olanzapina e aripiprazol (ASSION et al., 2018). O tratamento crônico com esses medicamentos pode causar rigidez, distonia e discinesia ($AP_{TÍPICOS}$) ou aumentar o risco de desenvolvimento de doenças como obesidade, hiperlipidemia e diabetes tipo II ($AP_{ATÍPICOS}$) resultando muitas vezes em falta de adesão ao tratamento (LAPPIN et al., 2018; PEREIRA, BUDOVICH & CLAUDIO-SAEZ, 2018; URBAN; CUBAŁA, 2017). Além disso, o tratamento com antipsicóticos falha em aproximadamente um terço dos pacientes diagnosticados com SCZ, mesmo quando os medicamentos são utilizados de maneira correta e nas doses e frequências de administração adequadas (GILLESPIE et al., 2017; SUZUKI et al., 2011; VOLPE et al., 2017).

3.2. Diferenças Sexuais na Esquizofrenia

É sabido que homens e mulheres apresentam diferenças significativas no risco, desenvolvimento e evolução da esquizofrenia (ABEL, DRAKE & GOLDSTEIN, 2010; GOGOS et al., 2015; MARKHAM, 2012; OCHOA et al., 2012). A incidência do transtorno é ligeiramente maior em homens do que em mulheres (razão 1,4: 1), existindo diferença significativa na idade média de início do primeiro surto psicótico, que ocorre geralmente entre 18-24 e entre 22-28 anos em homens e mulheres, respectivamente (GOGOS et al., 2015). Geralmente, homens apresentam sintomas mais severos e um pior prognóstico da doença do que mulheres. Além disso, apenas em mulheres há uma segunda idade de pico de incidência que ocorre entre 45-49 anos e um maior risco de desenvolvimento de SCZ na faixa etária entre 50-70 anos (SUN et al., 2016). Além disso, após o primeiro surto psicótico as mulheres apresentam um melhor curso social da doença, ou seja, tendem a manter-se no emprego, apresentam menor número de hospitalizações e menores chances de isolamento social quando comparadas com homens nas mesmas condições (OCHOA et al., 2012)

Essas diferenças entre os sexos levaram ao surgimento da hipótese estrogênica da SCZ, que atribui aos hormônios ovarianos, especialmente aos estrogênios, um papel protetor no desenvolvimento da doença em mulheres (MARKHAM, 2012). Durante a puberdade, a menarca marca o aumento da produção de estrogênios que podem contribuir para o atraso no surgimento dos primeiros sintomas da doença em mulheres em comparação com os homens (MCGREGOR; RIORDAN; THORNTON, 2017). Kiliçaslan e colaboradores (2014), em seu estudo com 289 pacientes diagnosticadas com SCZ, encontraram uma associação inversamente proporcional entre a idade do primeiro surto psicótico e a idade da menarca. Além disso, o segundo pico de incidência de SCZ ocorre apenas em mulheres e no período da menopausa, onde há uma rápida redução dos níveis de estrógeno e progesterona (GOGOS et al., 2015; SUN et al., 2016). Mulheres diagnosticadas com SCZ no período pré-menopausa apresentam um melhor prognóstico da doença e respondem melhor ao tratamento com antipsicóticos, necessitando de doses menores dos

fármacos, quando comparadas com mulheres mais velhas ou homens portadores de SCZ (ABEL, DRAKE & GOLDSTEIN, 2010).

Em estudo realizado por Huber e colaboradores (2004) os hormônios sexuais estradiol, progesterona, prolactina e hormônio luteinizante foram dosados em amostras de sangue coletadas de um grupo de 50 mulheres internadas por surto psicótico, sendo 23 delas diagnosticadas com SCZ, ficou evidente que as taxas de recaída e o número de hospitalizações foram maiores durante períodos de flutuação de estrogênio, por exemplo, durante o início da fase folicular do ciclo menstrual, após o parto ou no período pós-menopausa (RUBIN et al., 2010).

Embora seja evidente a relação entre os níveis de estrogênios e a ação protetora contra o desenvolvimento de SCZ em mulheres, outro fator importante que explica a idade precoce e a maior incidência de SCZ em homens é a exposição à testosterona, que pode ser considerada um fator de risco para a doença (MARKHAM, 2012). A testosterona e a desidroepiandrosterona (DHEA) possuem papel no neurodesenvolvimento, pois influenciam a conectividade sináptica e a diferenciação neuronal (MELCANGI, PANZICA & GARCIA-SEGURA, 2011). Em seu estudo de meta-análise, Misiak e colaboradores (2018) encontraram níveis elevados de DHEA em todos os grupos de pacientes esquizofrênicos analisados. Considerando apenas os pacientes em primeiro surto psicótico, há uma elevação com os níveis de testosterona livre, mas não de testosterona total. Além disso, pacientes em recidiva aguda apresentam níveis significativamente mais altos de testosterona total que também estavam elevados em pacientes do sexo feminino com múltiplos episódios de crises psicóticas. Os autores concluíram que existem mudanças dinâmicas dos níveis de testosterona e DHEA em pacientes com esquizofrenia e que esses podem ser mecanismos ativados em resposta ao estresse associado à experiência de psicose aguda.

Apesar das diferenças sexuais relacionadas à SCZ serem passíveis de serem reproduzidas em modelos animais, ainda existem poucos estudos, principalmente relacionados a alterações na farmacocinética e farmacodinâmica de terapias farmacológicas para a SCZ, que incluem fêmeas em suas análises e, quando incluem, utilizam um número amostral reduzido o

que acaba não tendo relevância significativa na interpretação dos resultados, não permitindo que as diferenças sexuais sejam adequadamente exploradas.

Apesar de alguns autores justificarem a ausência de fêmeas nos estudos alegando que a expressão do fenótipo é mais forte nos machos, essa estratégia parece ser uma boa alternativa apenas do ponto de vista da redução de custos experimentais. O desenvolvimento de estudos comparativos em ambos os sexos permite decifrar as complexas alterações que ocorrem no neurodesenvolvimento de machos e fêmeas, permitindo um delineamento de novas estratégias terapêuticas direcionadas e, portanto mais eficientes.

3.3. Status da Barreira Hematoencefálica em Transtornos Psicóticos

Alterações patológicas na BHE estão bem descritas e são reconhecidas como um fator central para o desenvolvimento de uma série de distúrbios neurológicos, por exemplo, a esclerose múltipla (BELL et al., 2018), o acidente vascular cerebral (ZHANG et al., 2018) e a epilepsia (VAN VLIET, ARONICA & GORTER, 2015).

Entretanto, a relação entre a BHE e os transtornos psicóticos como a SCZ recebeu menos atenção e somente com o avanço das técnicas para detecção de biomarcadores em amostras biológicas, dos exames de imagem (RM, PET Scan) e das bases imunológicas da SCZ, que ocorreu nas últimas duas décadas, é que houve um aumento dos esforços para entender o papel desta barreira biológica no transtorno (POLLAK et al., 2018). De maneira geral, mudanças patológicas na BHE podem incluir: aumento da permeabilidade vascular com extravasamento de conteúdo do interstício cerebral para a circulação sistêmica ou de proteínas plasmáticas para o interstício; expressão alterada de canais iônicos e transportadores de efluxo ou influxo nas células endoteliais e gliais; alterações em claudinas e integrinas que formam as zônulas de oclusão; e aumento da transmigração de leucócitos (POLLAK et al., 2018; TENREIRO et al., 2016). Essas alterações causam perturbações da homeostase cerebral e podem afetar diretamente a sinalização neuronal. Porém, não existe até o momento nenhum estudo conclusivo que evidencie se as alterações de BHE são causa ou ocorrem em consequência à disfunção dos neurônios descrita para a SCZ (POLLAK et al., 2018).

As evidências de comprometimento da BHE em transtornos psicóticos têm sido comprovadas através do estudo de biomarcadores no líquor (LCR), na circulação sistêmica (biomarcadores séricos), através da análise *post mortem* de cérebros de pacientes esquizofrênicos e também, por estudos de neuroimagem *in vivo*.

A técnica considerada padrão ouro para avaliar a permeabilidade das barreiras cerebrais em seres humanos é o coeficiente de albumina (AlbQ), que consiste na razão entre a concentração de albumina (Alb) presente no LCR e a concentração sérica desta proteína. Em indivíduos saudáveis a concentração de Alb no LCR é aproximadamente 200 vezes menor do que no sangue.

Estudo realizado por Endres e colaboradores (2015) analisou 180 amostras de LCR obtidas de pacientes psicóticos e encontrou uma elevação no número de leucócitos, um aumento da concentração de proteínas totais e um AlbQ elevado para os pacientes com diagnóstico de esquizofrenia. Valores semelhantes foram obtidos em um estudo anterior realizado por Bechter e colaboradores (2010) com amostras de LCR coletadas de 63 pacientes, sendo 24 pacientes com transtornos afetivos e 39 pacientes com esquizofrenia. Dentre os pacientes esquizofrênicos, 23% apresentaram AlbQ aumentado o que poderia ser indicativo de aumento de permeabilidade através da BHE. No entanto, um aumento no AlbQ também pode estar relacionado com uma diminuição na taxa de renovação do LCR, aumento da resistência do fluxo subaracnoideo ou bloqueio das vilosidades do tecido aracnóideo que podem causar um redução do *clearance* de proteínas do LCR para o sangue venoso (BECHTER et al., 2010)

Apesar de estudos *post mortem* com cérebros de pacientes esquizofrênicos possuírem uma série de limitações devido ao reduzido número de amostras, falta de casos controle adequados e normalmente envolverem amostras de pacientes que estavam em tratamento com antipsicóticos (POLLAK et al., 2018), através deles é possível evidenciar alterações de microvasculatura que podem estar relacionados de forma direta com um padrão anormal de estruturação da BHE em pacientes SCZ. Harris e colaboradores (2008) obtiveram amostras de córtex pré-frontal (PFC) provenientes do cérebro de 12 pacientes esquizofrênicos e 12 casos-controle e isolaram a microvasculatura cerebral através de microdissecação a laser.

Através da análise de RNA os autores concluíram que houve um *downregulation* em genes envolvidos com transporte de íons, adesão e proliferação em células endoteliais da microvasculatura cerebral de pacientes esquizofrênicos quando comparados com os controles. Outros estudos também demonstraram redução no número de oligodendrócitos e redução no número de astrócitos adjacentes aos capilares que formam a BHE em diferentes regiões cerebrais, como o córtex pré-frontal e o hipocampo, a partir de autópsias realizadas em cérebros de pacientes esquizofrênicos comparados com seus respectivos controles (VOSTRIKOV; ORLOVSKAYA; URANOVA, 2008; WEBSTER et al., 2001).

Considerando que grande porcentagem dos antipsicóticos atualmente prescritos para o tratamento de SCZ, tais como quetiapina, aripiprazol, olanzapina e paliperidona, é substrato para transportadores de influxo e efluxo na BHE (CARREÑO et al., 2016b; MOONS et al., 2011; WOLKING et al., 2015), alterações na expressão ou atividade desses transportadores poderia explicar, pelo menos de forma parcial, a resistência ao tratamento com antipsicóticos.

Bernstein e colaboradores (2016), em um estudo *post mortem* com tecido cerebral de 13 pacientes esquizofrênicos e nove casos controles avaliaram, através de imunohistoquímica quantitativa, a densidade numérica da expressão de glicoproteína-P (P-gp) em capilares da BHE obtidos de diferentes regiões cerebrais e não obtiveram nenhuma diferença significativa entre os dois grupos. Em contrapartida, De Klerk e colaboradores (2010), em estudo clínico com 10 pacientes portadores de SCZ utilizando a técnica de tomografia por emissão de prótons (PET Scan) e [^{11}C]verapamil como substrato, foram capazes de quantificar a função da glicoproteína-P (P-gp) *in vivo*, demonstrando que a captação do verapamil foi reduzida no córtex, nos gânglios basais e na amígdala dos pacientes esquizofrênicos. Essa redução teve correlação com o aumento da atividade da P-gp nessas regiões cerebrais e, segundo os autores, pode ser um fator que contribui para a resistência aos antipsicóticos. Considerando as limitações na comparação entre os estudos de Bernstein e De Klerk é possível hipotetizar que, em pacientes portadores de SCZ, há uma alteração na atividade da P-gp, mas não em sua expressão.

Até o momento, no entanto, não há um completo entendimento das alterações da BHE na SCZ. Porém, já é possível perceber oportunidades para o desenvolvimento de estudos que contribuirão para a elucidação do papel da BHE na SCZ e o desenvolvimento de novas estratégias terapêuticas para o tratamento dessa doença.

3.4. Modelos Animais de Esquizofrenia

A tentativa de modelar condições psiquiátricas em animais é muitas vezes vista com certo ceticismo pela comunidade científica (BOKSA, 2007; LOW & HARDY, 2007). A esquizofrenia, por ser considerada uma condição exclusivamente humana, é um caso particularmente ilustrativo dessa descrença, já que até o momento não pôde ser totalmente recriada em animais (CORRADI, 2011; REISINGER et al., 2015).

Entretanto, do ponto de vista da pesquisa pré-clínica, a modelagem animal oferece uma plataforma essencial para o entendimento da neurobiologia da SCZ atuando como uma ferramenta de monitoramento rápido de numerosos elementos relacionados com o surgimento e progressão da doença (WILSON; TERRY, 2010). Além disso, com uso de modelos confiáveis e preditivos torna-se possível avaliar a resposta a agentes terapêuticos e projetar novas terapias farmacológicas para o tratamento da doença (JONES, WATSON & FONE, 2011). É fundamental, portanto, que os modelos animais de SCZ apresentem a tríade de requisitos de validade: de face, de constructo e preditiva para que possuam um alto valor translacional (MEYER, 2014; NESTLER; HYMAN, 2010).

A validade de face representa o grau de homologia de sintomas entre o modelo animal e a condição humana que se pretende simular. Para a esquizofrenia, este é um grande desafio há ser enfrentado tendo em vista a natureza dos sintomas da doença, como alucinações e delírios, que até o momento não são possíveis de serem determinados em animais (LIPSKA & WEINBERGER, 2000; MARCOTTE, PEARSON & SRIVASTAVA, 2001; WILSON & TERRY, 2010). Pode-se, porém, estabelecer um paralelo entre sintomas e comportamentos que sabidamente possuem um impacto importante na doença em humanos e que são modelados com sucesso em animais.

Alterações do filtro sensório motor, comportamento social prejudicado, déficits na inibição latente e disfunções cognitivas são características comportamentais capazes de serem modeladas em animais e que correspondem à sintomatologia da SCZ em humanos (BUHUSI et al., 2017; DODELL-FEDER, TULLY & HOOKER, 2015; GEYER, 2006). Modelos que utilizam hiperlocomoção induzida por afetaminas têm sido comumente descritos na literatura e mimetizam o tônus hiperdopaminérgico (BRISCH et al., 2014) e o comportamento estereotipado frequentemente descrito em pacientes esquizofrênicos (CALZAVARA et al., 2011; MAVRIKAKI; NOMIKOS; PANAGIS, 2010). Esses modelos são especialmente úteis na pesquisa pré-clínica para triagem de novos compostos com atividade antipsicótica (HERRMANN et al., 2014; HERRMANN et al., 2017). Além disso, a elevação da atividade locomotora devido à utilização de antagonistas dos receptores de glutamato (ROENKER et al., 2011; ZAVITSANOU et al., 2014) está baseada em alterações do receptor de N-metil-D-aspartato (NMDA) observadas em análises *post mortem* de cérebros de pacientes com SCZ (RUBIO, DRUMMOND & MEADOR-WOODRUFF, 2012).

A replicação da neurobiologia subjacente aos sintomas da patologia humana no modelo animal é denominada validade de constructo (BELZUNG; LEMOINE, 2011; WILSON; TERRY, 2010). Novamente, para a SCZ esta é uma tarefa desafiadora, uma vez que, por sua característica multifatorial e complexa, os substratos neurobiológicos relacionados aos sinais e sintomas da doença ainda não estão claramente elucidados (KAHN & SOMMER, 2015). Entretanto, através de estudos *post mortem* ou de ressonância magnética *in vivo* é possível identificar anomalias estruturais e moleculares presentes em cérebros de pacientes com SCZ (JUNG et al., 2010; KAHN & SOMMER, 2015) e, ao modelar tais alterações em animais, torna-se possível estabelecer a validade de constructo necessária (LIPSKA & WEINBERGER, 2000; MARCOTTE, PEARSON & SRIVASTAVA, 2001; NESTLER & HYMAN, 2010). Na literatura estão descritos modelos onde foi possível mimetizar a desorganização neuronal do córtex pré-frontal (volume reduzido, distribuição laminar de neurônios alterada, elevada densidade neuronal) (BOLKAN, CARVALHO POYRAZ & KELLENDONK, 2016; BUCKLEY, 2005; SIMPSON & KELLENDONK, 2017), as alterações em neurônios GABAérgicos, a redução de

axônios e as alterações na expressão gênica de subunidades de receptores NMDA (BOGART & O'DONNELL, 2018; PRYTKOVA & BRENNAND, 2017), bem como o aumento dos ventrículos e a diminuição da massa cinzenta (LAZAR, NEUFELD & CAIN, 2011; WILSON & TERRY, 2010) presentes em pacientes portadores de SCZ.

A validade preditiva pode ser definida como o grau com que o modelo é capaz de demonstrar em animais a resposta farmacológica esperada em humanos e permitir prever a eficácia de um novo agente terapêutico (BELZUNG; LEMOINE, 2011; JONES; WATSON; FONE, 2011). A busca de compostos com potencial ação antipsicótica ou de novas estratégias de tratamento para a SCZ está baseada, principalmente, na capacidade que as substâncias possuem em modular os sintomas positivos da doença. Em animais isso pode ser demonstrado através do *screening* de compostos ou formulações em testes como inibição de sobressalto por pré-pulso, modelos de memória de trabalho e modelos envolvendo desafios com anfetamina (ANTONIO et al., 2016; DIMER et al., 2014; DIMER et al., 2015; FONSECA et al., 2015; HERRMANN et al., 2014, 2017; NEVES et al., 2017).

Um estudo realizado por Flores e colaboradores (2016) identificou aproximadamente 20 diferentes tipos de modelos animais de esquizofrenia, todos com suas vantagens e limitações. Esses modelos podem ser divididos, de acordo com a classificação proposta por Jones e colaboradores (2011), em quatro categorias gerais de indução: i) modelos do neurodesenvolvimento, como modelo de isolamento social, modelos de exposição pré-natal a toxinas ou compostos químicos (LODGE, 2013; REISINGER et al., 2015; SWANEPOEL; MÖLLER; HARVEY, 2017); ii) modelos farmacológicos, como modelo de sensibilização à anfetamina ou à fenciclidina (SAHIN; DOOSTDAR; NEILL, 2016); iii) modelos de lesão, como lesão neonatal do hipocampo ventral ou do córtex pré-frontal (BRADY, 2016; FLORES; MORALES-MEDINA; DIAZ, 2016); e iv) modelos de manipulação genética, como utilização de animais *knockout* para genes específicos que produziriam nos animais alterações cerebrais ou comportamentos tipo esquizofrênico (COBA et al., 2018; LEE et al., 2018; NAKAO et al., 2018; OKAZAKI et al., 2018).

A utilização dos modelos que envolvem manipulações farmacológicas em animais adultos ou ainda lesão de regiões cerebrais apresenta

desvantagens do ponto de vista etiológico e limitações devido à falta de alterações em sistemas neurais que irão refletir de forma mais precisa a fisiopatologia da SCZ (FLORES, MORALES-MEDINA & DIAZ, 2016; JONES, WATSON & FONE, 2011; WILSON & TERRY, 2010). Além disso, modelos que utilizam a manipulação de fatores de susceptibilidade genética, apesar de serem considerados uma ferramenta importante para estudos biológicos, não permitem a modificação de mais de um gene por geração, distanciando-se da etiológica genética da SCZ em humanos (HENRIKSEN; NORDGAARD; JANSSON, 2017)

No escopo desta revisão de literatura será discutido apenas o modelo neurodesenvolvimental por ativação imune pré-natal, com enfoque para a administração de poli(i:c) a ratas prenhas, que foi o modelo escolhido para o desenvolvimento do trabalho.

3.5. Modelo Neurodesenvolvimental de Esquizofrenia por Ativação Imune Pré-Natal

A utilização de modelos neurodesenvolvimentais de SCZ apresenta forte validade etiológica e podem produzir anormalidades em múltiplos circuitos neuronais, aproximando-os da fisiopatologia da doença (MEYER et al., 2005; WILSON; TERRY, 2010; HADAR et al., 2015a; HADAR et al., 2015b).

Modelos neurodesenvolvimentais de SCZ por ativação imune pré-natal em roedores desenvolveram-se baseados em estudos epidemiológicos realizados em humanos que correlacionam o risco aumentado de desenvolvimento da doença com indivíduos nascidos de mães que tiveram infecções durante o período gestacional. Esses modelos possuem validade de face, construto e preditiva bem estabelecidas na literatura (BROWN & DERKITS, 2010; BROWN, 2012; KHANDAKER et al., 2013; NIELSEN, BENROS & MORTENSEN, 2014; NIELSEN, LAURSEN & AGERBO, 2016; WEBER-STADLBAUER, 2017).

No contexto de estudos que mimetizaram em roedores os mecanismos fisiopatológicos da SCZ através da ativação imune pré-natal, uma série de exemplos bem sucedidos podem ser citados, como a exposição de ratas ou camundongas prenhas ao vírus *influenza* humano (FATEMI et al., 2002;

FATEMI et al., 2017; GARBETT et al., 2012; LANDREAU et al., 2012; MEYER, 2014; XIA et al., 2014), à endotoxina bacteriana lipopolissacarideo (LPS) (BATINIĆ et al., 2016; DE SOUZA et al., 2015; RÉUS et al., 2017; SANTOS-TOSCANO et al., 2016), e ao poli(i:c), um RNA dupla fita sintético (ARSENAULT et al., 2014; MEYER, 2014; PATRICH et al., 2016; REISINGER et al., 2015; ROSE et al., 2017).

Em mamíferos o poli(i:c) atua como um potente agente imunoestimulante, pois mimetiza uma infecção por retrovírus de fita dupla através da ativação de receptores do tipo Toll-3 (MATSUMOTO & SEYA, 2008; ZAVITSANOU et al., 2014; REISINGER et al., 2015). A ativação destes receptores induz cascatas de sinalização celular relacionadas com processos infecciosos que geram um desbalanço entre citocinas pró-inflamatórias (ex. interleucinas IL-1β, IL-6, fator de necrose tumoral: TNF-α, e interferons do tipo I: INF-α e INF-β) e anti-inflamatórias (ex. interleucina IL-10 e fator de crescimento TGF-β) na circulação sistêmica materna, na placenta e no líquido amniótico (MEYER, FELDON & YEE, 2009; ALTAMURA et al., 2013; FINEBERG & ELLMAN, 2013) e induzem respostas inflamatórias no cérebro do feto em desenvolvimento, como ativação microglial, alterações na maturação de oligodendrócitos e aumento da geração de espécies reativas de oxigênio (DEBNATH, VENKATASUBRAMANIAN & BERK, 2015), levando a distúrbios do neurodesenvolvimento que podem estar associados à doenças neuropsiquiátricas como SCZ e autismo (MEYER et al., 2005; RAPOPORT, GIEDD & GOGTAY, 2012; MEYER, 2014; HADAR et al., 2015a; KHANDAKER et al., 2015; PATRICH et al., 2016; MILLAR, BILKEY & WARD, 2017;DONEGAN, BOLEY & LODGE, 2018).

É importante ressaltar que, apesar do neurodesenvolvimento fetal ser comprometido de forma semelhante em ratos e camundongos, o nível de comprometimento é significativamente dependente do período gestacional escolhido, da dose de poli(i:c) utilizada e da via e frequência de administração utilizadas (LI et al., 2009; MEYER & FELDON, 2012).

Estudos revisados neste trabalho e que utilizaram a ativação imune pré-natal descrevem o período compreendido entre o 9º e o 17º dia gestacional como sendo a janela de tempo mais significativa para a obtenção de animais adultos com endofenótipo patológico que se assemelha à SCZ (MEYER et al.,

2005; PIONTKEWITZ, ARAD & WEINER, 2011; MEYER & FELDON, 2012; MEYER, 2014; HADAR et al., 2015a,b.; MATTEI, SCHWEIBOLD & WOLF, 2015). As doses de poli(i:c) relatadas na literatura variam entre 0,5 e 20 mg/kg (MEYER; FELDON, 2012; COBA et al., 2018), com administrações pela via intravenosa e intraperitoneal em dose única ou múltiplas doses (ARSENAULT et al., 2014; REISINGER et al., 2015). Porém, a avaliação pormenorizada dos resultados obtidos entre as diferentes combinações desses fatores encontra-se além do escopo desta revisão de literatura. Ninhadas adultas de roedores (ratos ou camundongos) que passaram por ativação imune pré-natal serão referidas nesta revisão como animais poli(i:c).

Alterações neuroquímicas e histopatológicas estão descritas para animais poli(i:c) em regiões cerebrais que se assemelham àquelas encontradas na SCZ em humanos (MATTEI, SCHWEIBOLD & WOLF, 2015).

Zuckerman e colaboradores (2003) demonstraram que ratos poli(i:c) (GD15, 4 mg/kg, i.v) na idade adulta (90 dias) apresentaram alterações histopatológica no hipocampo e giro denteado em comparação com animais controle de mesma idade, além de hiperatividade dopaminérgica medida em fatias estriatais do cérebro desses animais. Ozawa e colaboradores (2006), utilizando administrações repetidas de poli(i:c) (GD12-GD17, 5 mg/kg, i.p.) em camundongas prenhas obtiveram ninhadas que apresentaram aumento do *turnover* dopaminérgico e redução de receptores do tipo D_2 no estriado, déficits significativos no teste de inibição de sobressalto por pré-pulso e reconhecimento de objetos e atividade locomotora aumentada no desafio com metanfetamina. Alterações dos níveis basais de neurotransmissores em regiões cerebrais relevantes para a SCZ, medidos em amostras de homogeneizado de tecido, foram demonstradas por Winter e colaboradores (2009) após desafio imune com poli(i:c) (GD9, 5 mg/kg, i.v.). Camundongos poli(i:c) adultos (12 semanas) apresentaram aumento de dopamina e seus principais metabólitos (DOPAC e HVA) no globo pálido e no córtex pré-frontal e redução dos níveis de serotonina no hipocampo, núcleo accumbens e globo pálido sem que houvesse alterações significativas nos níveis de GABA.

No entanto, Bitanihirwe e colaboradores (2010) administraram poli(i:c) a camundongas prenhas (GD17, 5 mg/kg, i.v.) e obtiveram redução nos níveis de dopamina e glutamato no hipocampo e córtex pré-frontal, de GABA no

hipocampo e de glicina no córtex pré-frontal nas ninhadas em idade adulta (80 dias). Essas ninhadas apresentaram também déficits significativos em experimentos de interação social e inibição latente, comportamento estereotipado e aumento da atividade locomotora induzida por apomorfina, além de anedonia, medida através do teste de preferência à sacarose.

Hadar e colaboradores (2015), com o objetivo de avaliar as alterações comportamentais e neurobiológicas ao longo do desenvolvimento do animal , utilizaram ratas Wistar prenhas (GD15) para o desafio imune com poli(i:c) (4 mg/kg, i.v.) e, a partir dessas fêmeas, obtiveram ninhadas poli(i:c) adolescentes (35 e 60 dias) e adultas (100 dias). Os autores demonstraram que o déficit pré-atencional, medido através da inibição de sobressalto por pré-pulso, surge apenas quando o animal atinge a idade adulta. Outro resultado bastante relevante, demonstrado pelos mesmos autores, está relacionado com as alterações de dopamina e serotonina no córtex pré-frontal medial, núcleo accumbens, globo pálido, putâmen caudado e hipocampo. Foi evidenciada uma atividade neuroquímica alterada no córtex pré-frontal medial e hipocampo dos ratos poli(i:c) já no período de adolescência, que persistiu na vida adulta, demonstrando um comprometimento precoce dessas estruturas cerebrais, enquanto que as alterações causadas pelo poli(i:c) no núcleo accumbens e globo pálido lateral aparecem apenas na idade adulta comprovando, portanto, a natureza desenvolvimental do modelo.

Crum e colaboradores (2017), através de imagens obtidas por ressonância magnética, demonstraram a evolução de anormalidades estruturais no cérebro de ratos poli(i:c) (GD15, 4 mg/kg, i.v.), evidenciando a redução de volume em regiões corticais, no hipocampo, amígdala, estriado, núcleo accumbens e ventrículos laterais em comparação com animais controle. Os resultados obtidos apresentam validade de construto robusta para achados clínicos de imagem descritos para indivíduos com alto risco clínico para desenvolvimento de transtornos psiquiátricos como a SCZ (SATTERTHWAITE et al., 2016).

3.6 Nanopartículas e *Delivery* de Antipsicóticos

Apesar do tratamento com antipsicóticos atualmente disponíveis na clínica contribuírem para o controle dos sintomas positivos da esquizofrenia, a falha terapêutica continua sendo um problema bastante importante culminando na falta de controle dos sintomas da SCZ e impactando diretamente na vida útil e no convívio social dos pacientes.

Essa falta de resposta ao tratamento pode estar associada a não adesão, a tomadas irregulares da medicação, ao uso de doses excessivas ou insuficientes, ou ainda, devido a interrupções frequentes, abuso de drogas ou aos diversos efeitos adversos, extrapiramidais e metabólicos, que ocorrem durante a utilização dos antipsicóticos (BARRETO et al., 2009). Ainda, mecanismos fisiológicos ou patológicos associados à doença como polimorfismo genético, alterações morfológicas cerebrais relacionadas à SCZ, indução de enzimas do metabolismo hepático devido ao uso crônico da medicação e interação do fármaco com proteínas de efluxo como P-gp presente na BHE, contribuem para o desenvolvimento da resistência aos fármacos antipsicóticos, podendo resultar em ineficácia terapêutica (LÖSCHER & POTSCHKA, 2005).

Nesse contexto, esforços têm sido conduzidos no desenvolvimento de estratégias para aumentar a biodisponibilidade, melhorar o efeito terapêutico e ainda reduzir os efeitos colaterais decorrentes da utilização dessa classe de fármacos. O estudo da utilização de sistemas nanoestruturados (nanopartículas poliméricas, lipossomas e nanopartículas lipídicas sólidas) expandiu-se nos últimos anos, por ser uma estratégia bastante promissora para o *delivery* de antipsicóticos através da BHE. O tamanho nanométrico dessas partículas favorece o aumento da penetração cerebral de compostos farmacologicamente ativos melhorando, na maioria dos casos, sua eficácia terapêutica (FOND, MACGREGOR & MIOT, 2013; POLLAK et al., 2018).

Yasir e Sara (2014) desenvolveram nanopartículas lipídicas sólidas contendo haloperidol (SLNP-Hal), um antipsicótico típico bastante utilizando na clínica e que apresenta pronunciado efeito extrapiramidal. Os autores, após administrarem a formulação por via intranasal a ratos Wistar machos, observaram aumento da exposição cerebral ($ASC_{cérebro}$) em homogeneizado de

tecido de aproximadamente 4 vezes quando comparado com o fármaco administrado em solução pela mesma via. Além disso, houve redução da exposição sistêmica ao fármaco. Essa estratégia permitiria a redução da dose do antipsicótico com redução de seus efeitos extrapiramidais.

Vieira e colaboradores (2016) desenvolveram nanocápsulas de clozapina com diferentes tipos de revestimentos (tween-80, quitosana e polietilenoglicol). Essas formulações foram testadas em ratos Wistar machos e os resultados demonstram que houve uma alteração do *clearance* total e do volume de distribuição do fármaco. Além disso, os animais apresentaram uma redução do comportamento estereotipado induzido por afentamina (AMP).

Utilizando ratos Wistar machos adultos, Dimer e colaboradores (2014, 2015) avaliaram os efeitos adversos, o perfil farmacocinético e a atividade antipsicótica das nanocápsulas de núcleo lipídico de olanzapina (OLA-LNC), demonstrando que os animais tratados com OLA-LNC apresentaram ganho de peso e níveis de colesterol total significativamente menores, aumentaram a exposição plasmática ao fármaco e diminuíram o comportamento estereotipado induzido por AMP.

Patel e colaboradores (2011) propuseram uma formulação de nanopartículas lipídicas sólidas contendo risperidona (SLN-Ris) para ser utilizada por via intranasal com o objetivo de melhorar a biodisponibilidade oral do fármaco, devido ao seu elevado metabolismo de primeira passagem, evitar que a Ris sofresse ação da P-gp presente na BHE e aumentar a biodistribuição cerebral (*targeting* para o cérebro). Os autores observaram aumento da exposição cerebral quando as SLN-Ris foram administrada por via intranasal a ratos Wistar machos em comparação com o fármaco administrado em solução.

Nosso grupo de pesquisa produziu (CARREÑO et al., 2015), através do método de deposição interfacial do polímero pré-formado, nanocápsulas de poli(ε-caprolactona) com núcleo lipídico composto por triglicerídeos de cadeia média (cáprico e caprílico) e monoestearato de sorbitano contendo quetiapina na concentração de 1 mg/mL (QLNC). Através da aplicação de um algoritmo proposto por Oliveira e colaboradores (2012) demonstramos que o fármaco se encontra majoritariamente disperso no núcleo e na parede polimérica da nanopartícula. O alto teor obtido para a formulação (~98%) além da alta eficiência de encapsulação obtida (~95%) corroboram os dados obtidos a partir

da aplicação do algoritmo (CARREÑO et al., 2016b). Além disso, em um estudo realizado com homogeneizado de tecido cerebral e hepático observamos um aumento da exposição à QTP em ambos os tecidos após administração de QLNC na dose de 5 mg/kg pela via intravenosa, em comparação com o fármaco administrado em solução (CARREÑO et al., 2016a).

O conjunto desses resultados demonstra que a utilização de nanopartículas apresenta grande potencial como nova estratégia terapêutica para o tratamento de SCZ, pois permite modular a farmacocinética e a farmacodinâmica de fármacos antipsicóticos.

3.7 Microdiálise como Ferramenta para Estudo da Distribuição Cerebral de Fármacos e Neurotransmissores

A microdiálise cerebral consiste na implantação de uma pequena sonda na região cerebral de interesse. A parte da sonda que fica em contato direto com o interstício cerebral contém uma membrana semipermeável, de *cutoff* definido, que é constantemente perfundida, a um fluxo baixo e constante (0.5 – 10 µL/min) com líquido cerebral artificial (LCA) (DARVESH et al., 2011; ZESTOS; KENNEDY, 2017). No local de implantação da sonda, cria-se um gradiente de concentração que permite a difusão e coleta no microdialisado de moléculas de baixo peso molecular tanto endógenas, como os neurotransmissores e seus metabólitos, como exógenas, como a fração livre - farmacologicamente ativa - de fármacos que atravessaram a BHE e atingiram o parênquima cerebral. Através da microdiálise cerebral é possível avaliar as alterações nos sistemas de neurotransmissores (dopaminérgico, serotoninérgico, glutamatérgico) resultantes da administração de fármacos, bem como o próprio fármaco no mesmo local.

Shilliam e colaboradores (2005) utilizaram a microdiálise cerebral em ratos para avaliar o efeito do tratamento oral agudo (10 mg/kg) e crônico (21 dias) com o antipsicótico clozapina no sistema dopaminérgico do núcleo accumbens. Os autores concluíram que o fármaco promove alterações tempo-dependente do sistema dopaminérgico na região investigada e que esta

poderia ser uma das explicações para a demora no surgimento da atividade antipsicótica exercida pelo fármaco.

Yamamura colaboradores (2009), buscando elucidar o mecanismo de ação da QTP, avaliaram por microdiálise os níveis extracelulares de norepinefrina, dopamina, serotonina, GABA e glutamato no córtex pré-frontal de ratos. Os resultados obtidos demonstram que, após administração de QTP nas doses de 10 mg/kg e 30 mg/kg pela via intraperitoneal, há uma elevação significativa dos níveis extracelulares de norepinefrina, dopamina e glutamato, sem que haja alterações nos níveis de serotonina e GABA na região cerebral investigada.

A microdiálise também tem sido utilizada para avaliação do *delivery* cerebral de fármacos inclusos em nanopartículas. Trabalho desenvolvido pelo nosso grupo de pesquisa (FREDDO, 2009) utilizou a técnica de MD cerebral para avaliar de forma comparativa a distribuição do ácido valpróico no córtex frontal de ratos Wistar quando o fármaco foi administrado em solução ou em uma formulação de nanocápsulas revestidas com quitosana. As nanocápsulas revestidas com quitosana promoveram um aumento de cinco vezes no fator de penetração cerebral do ácido valpróico em comparação com a penetração observada quando o fármaco foi administrado em solução.

Lindqvist e colaboradores (2013) desenvolveram uma formulação de lipossomas peguilados conjugados com glutationa contendo DAMGO e avaliaram em ratos a distribuição cerebral desse peptídeo quando administrado encapsulado ou em solução. Os autores observaram um aumento significativo da exposição cerebral ao composto bem como um prolongamento do efeito antinociceptivo quando o peptídeo foi administrado na nanoformulação.

A microdiálise cerebral também pode ser utilizada para investigar o efeito da modulação de proteínas transportadoras de influxo e efluxo e expressas na BHE. Postchka e colaboradores (2002), utilizando microdiálise cerebral em ratos e verapamil, inibidor não seletivo da P-gp, demonstraram que a distribuição de fenobarbital, lamotrigina e felbamato para o parênquima cerebral sobre efeito significativo do efluxo pela P-gp.

Recentemente relatamos, utilizando a microdiálise cerebral em ratos Wistar machos que tiveram os transportadores de influxo sensíveis a probenecida inibidos, que as QLNCs atravessam a membrana luminal da BHE

carreando a QTP, não permitindo que o fármaco nanoencapsulado interaja com os transportadores de influxo presentes na barreira (CARREÑO et al., 2016b).

Apesar do exposto, nenhum trabalho publicado até o momento utilizou a microdiálise para avaliar as alterações promovidas por nanopartículas contendo fármacos antipsicóticos nos níveis intersticiais de neurotransmissores, nem o comportamento farmacocinético de distribuição cerebral de antipsicóticos em modelos animais de SCZ.

3.8 Modelagem Farmacocinética/Farmacodinâmica

A farmacometria é uma área da ciência aplicada que, no desenvolvimento de fármacos, busca quantificar o efeito farmacológico através da utilização de modelagem matemática e simulações (MM&S) de perfis de concentração de fármaco *versus* tempo (PK), efeito farmacológico (PD), da (pato)fisiologia dos sistemas biológicos e de como estes interatuam. Esta abordagem constitui uma importante ferramenta para integrar conhecimentos e permitir a tomada de decisões racionais durante o desenvolvimento pré-clínico, translacional e clínico de fármacos (MOULD; UPTON, 2012; RIGGS; CREMERS, 2019).

Modelos farmacocinéticos populacionais (popPK) são utilizados para descrever estudos farmacocinéticos nos quais dados individuais de uma população são avaliados utilizando modelos não lineares de efeito misto Essa abordagem tem como objetivo principal encontrar parâmetros farmacocinéticos e suas fontes de variabilidade em uma determinada população (MOULD; UPTON, 2013) e com isso elucidar o impacto de diversos fatores individuais que usualmente afetam a farmacocinética.

Modelos não lineares referem-se ao fato de que a variável dependente (ex.: concentração plasmática de fármaco) está relacionada de maneira não linear com os parâmetros do modelo e com as variáveis independentes. Os efeitos mistos referem-se à parametrização do modelo e podem ser divididos em: (i) efeitos fixos - parâmetros que não variam entre os indivíduos da população e, (ii) efeitos aleatórios - parâmetros que variam entre os indivíduos de dada população (MOULD; UPTON, 2012).

Durante o desenvolvimento de um modelo farmacocinético populacional devem ser considerados cincos aspectos principais: (i) conjunto de dados; (ii) modelo estrutural, que descreve o perfil de concentração *versus* tempo típico para uma população; (iii) modelo estatístico, que está relacionado com a variabilidade no perfil de concentração típico dentro da população (ex.: variabilidade interindividual, variabilidade inter-ocasião); (iv) modelo de covariáveis, que explica a variabilidade através de características dos indivíduos (ex.: peso, altura, parâmetros fisiológicos, etc); (v) software utilizado na modelagem, que são capazes de integrar os dados e os modelos de forma conjunta e, através de distintos métodos de estimação de parâmetros para a parte estrutural, estatística e de covariáveis, descrever os dados (MOULD; UPTON, 2013; RIGGS; CREMERS, 2019).

Além disso, a integração de modelos farmacocinéticos populacionais (popPK) com dados de farmacodinâmica (PD) através da construção de modelos popPK/PD permite prever a variação do efeito farmacológico em relação a variação da concentração do fármaco no organismo em função do tempo. Desta forma, é possível relacionar exposição ao fármaco e resposta, obtendo um entendimento ainda mais robusto e preciso da ação farmacológica de um composto no organismo (UPTON; MOULD, 2014).

Modelos popPK/PD podem ser divididos em modelos empíricos (*"top-down"*) ou modelos mecanísticos (YU; WILSON, 2010). Os modelos empíricos descrevem, por exemplo, a variação de *endpoints* clínicos (ex.: variação de biomarcadores) em função do tempo, baseados no ajuste de uma função matemática aos dados observados, normalmente sem considerar o mecanismo de ação do fármaco. Apesar de serem modelos simples e descritivos, possuem menor poder de previsão do que os modelos mecanísticos (AIT-OUDHIA; MAGER; STRAUBINGER, 2014).

Por outro lado, os modelos mecanísticos descrevem os efeitos clínicos de um fármaco em função do tempo baseados em parâmetros obtidos *in vitro* e também em observações fisiológicas dos indivíduos. Esse tipo de modelo faz uma distinção clara de parâmetros específicos do fármaco (ex.: sítio de ação, afinidade com a proteína alvo, logP, solubilidade) e parâmetros específicos do sistema biológico com o qual o fármaco atua (ex.: densidade de receptores, progressão da doença, feedback homeostático, fluxo sanguíneo) (YU;

WILSON, 2010). Dessa forma, são modelos mais complexos e com uma capacidade de previsão mais robusta, já que é possível relacionar alterações que uma condição fisiopatológica pode causar em parâmetros específicos do sistema com alterações no efeito farmacológico (UPTON; MOULD, 2014).

Modelos PK/PD têm sido utilizados para compreender os processos de distribuição de fármacos no SNC, buscando principalmente caracterizar mecanismos de transporte de fármacos através da BHE. Como exemplo pode-se citar o estudo de Boström e colaboradores (2008) que utilizaram um modelo PK/PD para investigar como as diferenças no transporte através da BHE de oxicodona e morfina influenciam na potência desses dois fármacos em ratos Sprague-Dawley machos. Após os animais atingirem concentrações de *steady state* para morfina ou oxicodona foi utilizada a técnica de microdiálise para determinar as concentrações livres no plasma e no estriado (dados PK) e o efeito antinociceptivo de cada fármaco utilizando o teste de retirada da cauda (*tail-flick test*) da água quente (dados PD). Os dados PK foram utilizados para construção de um modelo farmacocinético populacional que descreve a taxa de transporte de morfina e oxicodona através da BHE (CL_{in} e CL_{out}) e a extensão (Kp,uu) de distribuição de ambos os fármacos no cérebro. O modelo PK foi então combinado aos dados de PD, descritos por um modelo de efeito linear (efeito = inclinação da linha de base x $C_{fármaco}$) para obtenção de um modelo PK/PD onde foi possível avaliar as diferenças nos parâmetros farmacodinâmicos da morfina e da oxicodona. A diferença de seis vezes na razão entre a concentração livre cerebral e a concentração livre no plasma (Kp,uu) prevista pelo modelo para oxicodona e morfina implica que, para a mesma concentração livre no plasma, as concentrações livres cerebrais da oxicodona serão seis vezes maiores que as de morfina, causando o maior efeito observado.

Além da descrição da relação entre os dados de PK e PD, existe um grande potencial de aplicação de modelos PK/PD para investigar mecanismos e simular cenários distintos com o uso de formulações farmacêuticas, especialmente nanotecnológicas. Através da modelagem PK/PD é possível entender o transporte, a captação, o *delivery* a partir da nanopartícula e a disposição de fármacos no plasma e em diferentes tecidos, assim como entender a contribuição dos nanocarreadores na modulação da resposta

terapêutica. Os modelos matemáticos desenvolvidos para formulações nanotecnológicas podem funcionar como uma ferramenta *in silico* para otimização desses nanocarreadores, já que permitem descrever *in vivo* parâmetros formulação dependente (ex.: a taxa de liberação do fármaco do nanocarreador) e compreender como esses parâmetros impactam na modulação da farmacocinética e da farmacodinâmica do fármaco nanoformulado.

Exemplos de modelos farmacocinéticos que descrevem a distribuição e a liberação de nanocarreadores estão descritos na literatura (LINDQVIST et al., 2013; LINDQVIST; FRIDÉN; HAMMARLUND-UDENAES, 2016; YUAN et al., 2019). Lindqvist e colaboradores (2013), por exemplo, desenvolveram uma formulação de lipossomas PEGilados decorados com glutationa (GSH) contendo o peptídeo opioide DAMGO e avaliaram a farmacocinética e a distribuição cerebral através de microdiálise cerebral e plasmática do peptídeo administrado em solução (free-DAMGO) e encapsulado na formulação lipossomal (GSH/PEG-DAMGO). A partir dos perfis de concentração livre-tempo plasmática e cerebrais obtidos foi construído um modelo popPK onde demonstrou-se que o efluxo através da BHE (CL_{out}) para free-DAMGO é 10 vezes maior que o influxo (CL_{in}) causando assim, uma baixa penetração desse peptídeo no cérebro. Além disso, através de simulações baseadas nos dados experimentais obtidos a partir dos dados de GSH/PEG-DAMGO foi possível explorar o mecanismo que explica a maior exposição cerebral quando o composto é administrado na formulação lipossomal. Simulações de diferentes taxas de liberação de DAMGO do lipossoma permitiram demonstrar que a extensão de distribuição cerebral do comporto pode ser regulada e que o mecanismo mais provável de distribuição de GSH/PEG-DAMGO para o cérebro é a fusão do lipossoma com a membrana luminal endotelial. Esse trabalho demonstra que a combinação de dados experimentais, modelagem matemática e simulações é útil para explorar e prever possibilidades e limitações no uso de sistemas nanoestruturados para *delivery* cerebral de fármacos. A limitação desse trabalho, no entanto, é que as formulações foram avaliadas em animais hígidos, sem doenças que poderiam afetar a BHE e alterar a disposição e a capacidade de distribuição dos nanocarreadores.

A modelagem farmacocinética de base fisiológica (PBPK) também tem sido uma ferramenta bastante útil para caracterizar e prever a disposição sistêmica, a exposição tecidual, a eficácia e a toxicidade de formulações contendo nanopartículas. De maneira geral, modelos PBPK assumem que o organismo é constituído de compartimentos que representam fisiologicamente órgãos, tecidos e outros espaços fisiológicos (JONES; ROWLAND-YEO, 2013). Entretanto, as aplicações, vantagens e desvantagens da utilização de modelos PBPK para nanoformulações não fazem parte do escopo desta tese.

Observa-se na literatura um aumento da utilização de estratégias de MM&S para avaliar a eficiência de fármacos em estudos pré-clínicos e clínicos de desordens do SNC tais como depressão, Alzheimer e esquizofrenia (SRINIVAS; MAFFUID; KASHUBA, 2018).

Olsen e colaboradores (2008), em um estudo pré-clínico, obtiveram concentrações plasmáticas totais no *steady state* para o antipsicótico típico haloperidol e para quatro antipsicóticos atípicos: sertindol, clozapina, risperidona e olanzapina (dados de PK), avaliaram a capacidade desses fármacos de suprimir a esquiva condicionada em um teste comportamental e determinaram *in vivo* a ocupação de receptores de dopamina (D_2) no estriado (dados PD) de ratos Wistar machos. O conjunto de dados PK e PD obtidos foi utilizado para a construção de um modelo PK/PD clássico (abordagem não populacional) capaz de relacionar a magnitude de ocupação de receptores D_2 necessária para suprimir a esquiva condicionada nos ratos com a concentração plasmática necessária para obter 50% da resposta relativa ao fármaco (EC_{50}). Esses resultados foram comparados com valores reportados para ocupação de receptores D_2 e EC_{50} de pacientes esquizofrênicos responsivos ao tratamento com antipsicóticos. Os autores obtiveram boa correlação entre os níveis plasmáticos eficazes na supressão da resposta de esquiva condicionada em ratos e aqueles terapeuticamente eficazes em pacientes para o haloperidol, clozapina e risperidona, ma o modelo PK/PD previu valores 3 e 4 vezes mais altos para o sertindol e a olanzapina, respectivamente. Assim, o modelo proposto pode atuar como um guia para a determinação de concentrações plasmáticas efetivas de potenciais antipsicóticos no cenário clínico, o que poderia acelerar o processo geral de desenvolvimento de fármacos.

Johnson e colaboradores (2011) desenvolveram um modelo PK/PD populacional hibrido semi-mecanístico e baseado na fisiologia capaz de prever o curso temporal da ocupação de receptores de dopamina (D_2) no estriado de ratos Wistar machos após administração intravenosa, intraperitoneal ou subcutânea de olanzapina em dose única variando entre 0.01 e 40 mg/kg. Para construção do modelo foram utilizadas concentrações cerebrais totais obtidas por homogeneizado de tecido, concentrações plasmáticas totais além da taxa de ocupação de receptores D_2 obtida *in vivo*. A validade do modelo proposto foi confirmada pela boa concordância entre as constantes e parâmetros estimados pelo modelo e os valores da taxa de dissociação *in vitro* obtidos da literatura. Segundo os autores, a vantagem do modelo desenvolvido é que, uma vez que o mesmo inclui a cinética de ligação aos receptores e a farmacocinética plasmática e cerebral da olanzapina como base para previsão da ocupação de receptores *in vivo,* esta estratégia pode ser utilizada para escalonamento de informações obtidas *in vitro* e no cenário pré-clínico para os cenários clínicos.

Baseados nesse modelo desenvolvido por Johnson e colaboradores, Kozielska e colaboradores (2012) foram capazes de descrever o perfil de concentração plasmático, a exposição cerebral total e a ocupação de receptores dopaminérgicos D_2 e serotoninérgicos 5-HT2A dos antipsicóticos atípicos risperidona e paliperidona em ratos. Os autores apontam que foi necessário realizar ajustes no modelo estrutural como a inserção de um parâmetro que considera a formação do metabólito ativo da paliperidona e a adição de um efluxo deste metabólito através da BHE. Simulações realizadas com o modelo proposto demonstraram que o padrão de distribuição cérebro:plasma é um forte influenciador da afinidade do fármaco pelos receptores investigados e, por isso, os autores tiveram que adicionar a afinidade aos receptores 5-HT2A no modelo desenvolvido. Desta forma obtiveram um modelo que também apresenta capacidade translacional de cenários pré-clínicos para clínicos.

Em um estudo clínico com pacientes esquizofrênicos que receberam tratamento com antipsicóticos típicos e atípicos, Pilla Reddy e colaboradores (2013) caracterizaram a evolução dos escores de três subescalas (positiva, negativa e geral) da escala de síndrome positiva e negativa (PANSS), utilizada para avaliar o grau de esquizofrenia em pacientes. Utilizando um modelo

PK/PD os autores foram capazes de diferenciar o efeito dos antipsicóticos nos diferentes domínios de sintomas da esquizofrenia, revelando, por exemplo, que a olanzapina apresenta um efeito superior no tratamento de sintomas negativos em comparação com outros antipsicóticos não-clozapínicos.

Diante do exposto, esta tese objetivou investigar as alterações de disposição cerebral e de efeito da QTP carreada por nanocápsulas poliméricas de núcleo lipídico (QLNC) em um modelo animal de esquizofrenia através do desenvolvimento de um modelo PK/PD, buscando ampliar o entendimento do papel desse tipo de nanocarreador no *delivery* cerebral e no efeito anitpsicótico.

CAPÍTULO 1

QUETIAPINE LIPID CORE NANOCAPSULES RESTORE PREPULSE INHIBITION DEFICITS IN A NEURODEVELOPMENTAL MODEL OF SCHIZOPHRENIA IN MALE AND FEMALE RATS

Carreño F[1*], Helfer VE[1], Staudt KJ[1], Paese K[1], Meyer FS[2], Herrmann AP[3], Guterres SS[1], Rates SMK[1], Dalla Costa T[1]

[1]Programa de Pós-Graduação em Ciências Farmacêuticas, Faculdade de Farmácia, Universidade Federal do Rio Grande do Sul;
[2]Centro de Reprodução e Experimentação de Animais de Laboratório, Instituto de Ciências Básicas da Saúde, Universidade Federal do Rio Grande do Sul;
[3]Programa de Pós-Graduação em Farmacologia e Terapêutica, Instituto de Ciências Básicas da Saúde, Universidade Federal do Rio Grande do Sul.

ABSTRACT

Lipid core nanocapsules (LNC) has been extensively studied as a new treatment strategy to improve therapeutic effects of antipsychotic drugs. We investigated the efficacy of quetiapine LNCs (QLNCs) on the poly(i:c) model of schizophrenia in both male and female rats using the pre-pulse inhibition of startle response (PPI) test paradigm after evaluating the outcomes of three different poly(i:c) doses administered to pregnant damns at GD15 on neurodevelopmental outcomes of maternal immune activation (MIA) in adult male and female offspring. QTP solution was not capable of producing a reversal in the sensorimotor gating-disruptive effect caused by the prenatal poly(i:c) exposure. The same dose of QTP given as QLNCs significantly improved PPI-impairment. This is the first study reporting the restoration of the PPI deficits in a neurodevelopmental model of SCZ using LNCs. This is a promising delivery system strategy to improve antipsychotic effects contributing to the development of better SCZ pharmacological treatments.

Keywords: lipid core nanocapsules; schizophrenia; poly(i:c) model of schizophrenia; pre-pulse inhibition; quetiapine.

1. INTRODUCTION

Schizophrenia (SCZ) and its spectrum disorders are debilitating psychiatric conditions with lifetime prevalence around 1% worldwide (Millan et al., 2016). Around 60% of patients are non-responsive to pharmacological treatment or experience relapses throughout the course of the illness (Möller et al., 2015). Typical and atypical antipsychotic drugs (APD) side effects are responsible for patient's nonadherence to treatment emphasizing the urgent need for new treatment strategies (Lally et al., 2016; Yang and Tsai, 2017).

Lipid core nanocapsules (LNC) has been extensively studied as a novel treatment strategy to improve bioavailability, therapeutic effects and to reduce adverse effects of APD (Dimer et al., 2015, 2014; Fonseca et al., 2015)

Quetiapine lipid-core nanocapsules (QLNC) intravenously administered to male naïve Wistar rats increased quetiapine (QTP) plasma exposure by reducing total clearance and also increased the drug's brain and liver exposure in comparison to the drug administered in solution (Carreño et al., 2015, 2016). These results, however, might have limit translation to patients due to the lack of neural alterations related to SCZ pathophysiology (Flores et al., 2016).

Based on the neurodevelopmental hypothesis of schizophrenia, one rodent model that shows construct, face and predictive validity is based on prenatal treatment with polyinosinic-polycytidylic acid - poly(i:c), a synthetic analog of double-stranded RNA (dsRNA) (Hadar et al., 2015a; Patrich et al., 2016). Poly(i:c) is a potent mammalian immunogen that triggers the production and release of many pro-inflammatory cytokines such as IL-1β, IL-6 and type I interferon (Meyer & Feldon, 2012). The poly(i:c) model successfully accounts for several aspects of SCZ epidemiology and pathophysiology, including sex differences (Hill, 2016; Kokras and Dalla, 2014; Meyer & Feldon, 2012).

One of the most consistently observed behavioral findings reported in after prenatal treatment with poly(i:c) at different gestational periods is the deficit in prepulse inhibition of startle response (PPI) (Yee et al., 2011). This paradigm is a multimodal and cross-species phenomenon that is thought to provide an operational measure of the sensorimotor gating deficits observed in schizophrenia and has preclinical relevance for the exploration of novel

therapeutic pharmacological strategies, such as the use of nanocarriers (Möller et al., 2015).

Given the above, here we sought to investigate the potential efficacy of QLNCs in male and female offspring exposed to maternal immune activation (MIA) using the PPI test paradigm.

2. MATERIALS AND METHODS

2.1 Drugs, chemicals and reagents

Quetiapine hemifumarate (purity ≥ 98.0%) was kindly donated by Prati-Donaduzzi Medicamentos Genéricos (Brazil). Polyinosic-polycytidylic acid sodium salt (#P1530), (+)-MK-801 hydrogen maleate (dizocilpine) and rat IL-6 and IL-10 ELISA kits (#RAB0311 and #RAB0246) were obtained from Sigma-Aldrich (Brazil). Polysorbate 80 (Tween® 80) was purchased from Delaware (Brazil). Sterile pyrogen-free 0.9% NaCl was obtained from HalexIstar (Brazil). Ultrapure water was obtained using a Millipore Milli-Q® system. All other chemical and reagents were of analytical grade and obtained from commercial sources.

2.2. Quetiapine Lipid Core Nanocapsules (QLNC) preparation

QTP lipid-core nanocapsules (QLNC – 1 mg/mL) were obtained by nanoprecipitation of the preformed polymer as previously published (CARREÑO et al., 2016). Blank lipid-core nanocapsules (BLK) batches were prepared in the same manner, without QTP. The QLNC and BLK formulations were physicochemically characterized and the results were similar to those previously published (Carreño et al., 2016, 2015).

A control formulation (FQ, 5 mg/mL) was prepared first dissolving quetiapine in acetic acid (99%), then saline 0.9% containing P-80 in the same concentration used in QLNC preparation was added and the pH was adjusted to 6.5 ± 0.5 using NaOH (8 M). The vehicle formulation (VEH) was made in the same manner without QTP.

2.2 Animals and breeding method

This study was previously approved by the Ethics Committee on the Use of Animals from the Federal University of Rio Grande do Sul (UFRGS/CEUA, protocol #31001). Male (300 – 350 g) and female (200 – 275 g, nulliparous) Wistar breeders were raised in conventional (open-top) caging system, under controlled environmental conditions (22 ± 2 °C, 65% humidity in a 12 h light/dark cycle) with free access to standard rodent chow and filtered water.

For the systemic poly(i:c) challenge, female rats were mated according to a timed-mating breeding scheme (Pritchett-Corning et al., 2009). The estrous cycle was monitored daily, and three females in proestrus or estrus were housed together with one male overnight (between 18 p.m. to 8 a.m.). In the next morning, vaginal smears were analyzed under a microscope. The observation of spermatozoa in the smear was confirmation of gestational day zero (GD0). Positive females were housed together (n = 3/cage) until the day of the systemic poly(i:c) challenge. All pregnant damns were weighed every morning (between 8 a.m. to 10 a.m.) from GD0 to GD18.

2.3. Systemic poly(i:c) challenge

Poly(i:c) 4 mg/mL stock solution was prepared in sterile pyrogen-free 0.9% NaCl according to manufacturer instructions. Final 2 mg/mL and 0.5 mg/mL sterile solutions were prepared in the same vehicle and stored at -20 ± 1 °C until use.

In the morning of GD15 (between 8 a.m. to 10 a.m.) pregnant damns were randomly allocated to different groups (n = 6–8 dams/group) and received either a single intravenous injection (2 mL/kg) of sterile saline (SAL group) or different doses of poly(i:c): 1 mg/kg (P1 group), 4 mg/kg (P4 group), 8 mg/kg (P8 group) via the lateral tail vein.

Blood samples (100 µL) were collected (n = 3 dams/group) in predetermined times (4, 8 and 24 h) after treatment to characterize cytokine (IL-6 and IL-10) plasma levels by ELISA using commercial kits. Females were housed individually until the birth of their offspring. No randomization procedure was adopted in order to place the cages in the rack.

Twenty-four hours after birth, the litters were weighed, pups were sex-typed based on anogenital distance and nests were culled to eight pups per litter (4 males and 4 females, whenever possible). At postnatal day 21 (PND21) pups were weaned and group-housed with littermates (n = 4/cage) based on their gender and treatment groups. Animals were not handled aside from weighing at predetermined days (PND21, PND40, PND70) and twice weekly cage changes.

2.4 Offspring behavioral phenotyping

The long-term behavioral alterations of the prenatal manipulation were assessed when the offspring reached the adult stage of development (PND70). A cohort of animals (from 6 – 8 litters/group) was used for the behavioral phenotyping and both males (n = 16/group) and females (n = 15 - 16/group) were included in each phenotypic characterization but tested in different days in a randomized within-group and across-group order.

All testing was conducted during the light phase of the light-dark cycle, and one hour prior to the beginning of the behavioral tests animals were transferred in their home cages to the behavioral facility and placed in a holding room to habituate to the surroundings with food and water *ad libitum.*

From the holding room, animals were placed individually into smaller transport cages and transported to the adjacent behavioral testing room, returning directly to their home cages at the end of each test session. The interval between each test was one week. All apparatuses used were cleaned with ethanol 30% before the first and between each animal tested.

2.4.1 Elevated plus maze test

In order to characterize a possible innate anxiety-like behavior in the poly(i:c) offspring, the elevated plus maze test (EPM) was selected. Test was based on the model described by Lister (1987) and performed according to Walf (2007). Experiments were video-recorded and analyzed with the ANY-maze tracking software (Stoelting Co., Wood Dale, IL, USA).

2.4.2 Prepulse inhibition of acoustic startle reflex (PPI)

Sensorimotor gating deficit was assessed using the paradigm of PPI of the acoustic startle response and was chosen based on previous literature findings demonstrating reduced PPI following prenatal poly(i:c)-induced MIA. An acoustic startle chamber (Insight®, Brazil) was used for the PPI test. Animals were allowed to acclimate to the box for 5 min under a 68 dB background noise level. Before initializing the experimental session, the startle response of each rat was normalized by a train section of 10 startle pulse alone trials (120 dB, 50 ms, 15 ± 8 s interval). The test was started with different trial types in random order over a 22 min period: pulse alone (120 dB, 50 ms), background noise (68 dB), prepulse (PP 71, 77 or 85 dB, 20 ms) + pulse, with an interpulse delay of 100 ms from onset to onset. A total of 10 presentations of each trial type was given with the interval between two trials varying randomly from 15 ± 8 s. PPI was indexed by percent inhibition of the startle response according to the formula: % PPI = 100 – [(response to prepulse + pulse trial/pulse alone trial) x 100].

2.4.3 Sensitivity to dizocilpine (MK-801)

The locomotor response to MK-801 challenge was accessed in open field arena (75 cm x 75 cm, 50 cm high opaque walls). Rats were placed in the center of the open field to measure basal locomotor activity for 30 min. Subsequently, they were briefly removed from the arena, administered intraperitoneally with 0.3 mg/kg of (+) MK-801 (Sigma Aldrich, Brazil) and immediately returned to the same apparatus for an additional 50 min interval. Experiments were video-recorded and analyzed with the ANY-maze tracking software (Stoelting Co., Wood Dale, IL, USA).

2.5. Effect of Quetiapine Lipid Core Nanocapsules on PPI

Based on the dose-response curve outcomes, a new cohort of 15 pregnant damns were injected with 4 mg/kg poly(i:c) following the protocol described in section 2.3.

After PND70 male (n = 56) and female (n = 52) offspring were submitted to PPI protocol (session 2.4.2) on two different days. The pre-test

section was performed one day before the test to access PPI deficits in the offspring (data not shown). On the test day, rats were randomly divided into 4 groups and were intravenously injected with: VEH (1 mL/kg), FQ FQ (5 mg/kg), BLK (1 mL/kg), and QLNC (5 mg/kg). Sixty minutes after administration rats were placed in the startle chamber and the PPI measurement was started. All animals were tested in a randomized within-group and across group order. Male and female rats were tested on different days.

2.6 Statistical Analysis

Statistical analysis was performed using the IBM®software SPSS® Statistics v. 23 and GraphPad Prism v.7.04, with statistical significance set to $p < 0.05$.

Repeated measures two-way ANOVA was used to identify the main effects of the poly(i:c) dose and time and their interactions in maternal plasma cytokine levels and maternal cumulative body weight gain. The effects of different doses of poly(i:c) in litter size prior to culling as well as sex ratio within litters were accessed using one-way ANOVA.

Data from all the offspring behavioral phenotyping tests were first analyzed by full-factorial parametric ANOVA using prenatal poly(i:c) exposure and sex as between-subject factors. However, whenever there were no significant sex-specific effects the data of the two sexes were combined for the final analysis and presentation of the results.

Effects of FQ and QLNC formulations on PPI were analyzed by repeated measures three-way ANOVA using formulation, prepulse intensity and sex as main factors. However, as no sex-specific effects were found data of the two sexes were combined for the final analysis and presentation of the results. All analyses that reached significance were followed by Bonferroni multiple comparison tests ($\alpha = 0.05$).

3. RESULTS

3.1. Maternal outcomes of poly(i:c) dose-response curve

3.1.1. Maternal cytokine plasma levels

After the injection of poly(i:c), a significant treatment x time interaction $F_{6,16} = 17.04$, $p < 0.0001$) was found in IL-6 maternal plasma levels: 4 hours after poly(i:c) challenge, the highest dose tested (P8) induced the largest significant increase in IL-6 maternal plasma levels ($p < 0.001$) but no differences were found between the lowest dose (P1) and saline injections ($p > 0.05$) (Figure 1A – Table S1).

The same significant interaction between treatment and time ($F_{6,16} = 10.27$, $p < 0.0001$) was found for the increase in IL-10 maternal plasma levels after poly(i:c) dosing, however the difference was significant eight hours following a single injection of poly(i:c) (Figure 1B).

An interaction between treatment and time ($F_{6,16} = 53.48$, $p<0.0001$) was also observed for the IL-6/IL-10 plasma ratio. Dams for P4 and P8 groups showed significantly higher ratios than those observed for saline group four hours after poly(i:c) dosing ($p < 0.01$), indicating that both doses induced an imbalance between pro-inflammatory and anti-inflammatory cytokines in the maternal blood circulation (Figure 1C).

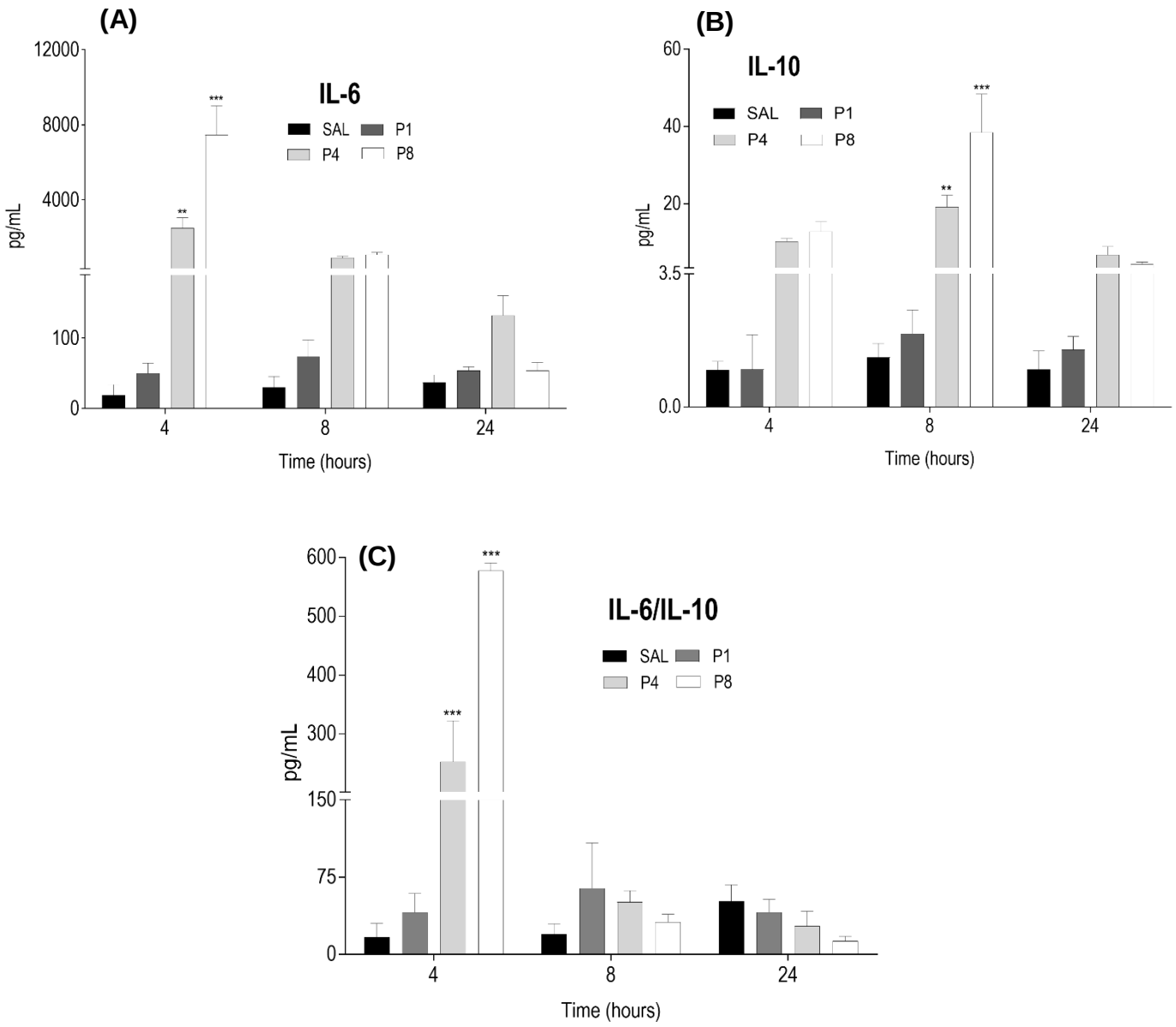


Figure 1. **Cytokine plasma levels after single poly(i:c) injection to pregnant damns (GD15).** (A) Maternal IL-6, (B) IL-10 plasma levels and (C) IL-6/IL-10 ratio at 4, 8 and 24 h after saline or poly (I:C) i.v single injection. SAL: Saline injected damns, P1: poly(i:c) 1 mg/kg injected damns, P4: poly(i:c) 4 mg/kg injected damns, P8: poly(i:c) 8 mg/kg injected damns, (n = 3/group; Mean ± S.E.M). **: $p < 0.01$ vs. saline; ***: $p < 0.0001$ vs. saline. RM Two-Way ANOVA, Bonferroni *post hoc*, $\alpha = 0.05$.

3.1.2. Non-significant outcomes

No significant alterations were found in cumulative maternal body weight gain (SAL: 123 ± 4 g; P1: 120 ± 5 g; P4: 118 ± 5 g; 121 ± 6 g), miscarriage rate (< 2%), litter size prior to culling (SAL: 10 ± 2; P1: 9 ± 2; P4: 10 ± 1; P8: 11 ± 2 pups per litter, $p > 0.05$) or sex ratio within litters (SAL: 1.0 ± 0.4 ; P1: 1.7 ± 1.4; P4: 1.1 ± 0.2; P8: 1.2 ± 0.4 male/female pups ratio per litter, $p > 0.05$).

3.2. Behavioral Outcomes of Poly(i:c) Offspring

3.2.1. Elevated plus maze

Effects of prenatal treatment with poly(i:c) on percentage of time spent and frequency of entries in the open arms are presented in Figure 2A. A significant main effect of prenatal treatment was found in the percentage of time spent in open arms ($F_{3,126} = 4.60$, $p = 0.004$). Animals from P8 offspring spent less time in the open arm compared to saline offspring ($p < 0.01$). Considering the frequency of open arms entries, no significant main effects or interactions were found.

The total distance traveled in EPM apparatus showed a significant interaction between prenatal treatment and sex ($F_{1,118} = 5.41$, $p = 0.002$). Males from poly(i:c) offspring presented a reduction in locomotor activity compared to saline male offspring and to females from the same poly(i:c) treatment group ($p < 0.01$). However, for females, only the highest tested dose caused a significant reduction in locomotor activity ($p < 0.01$) (Figure 2B).

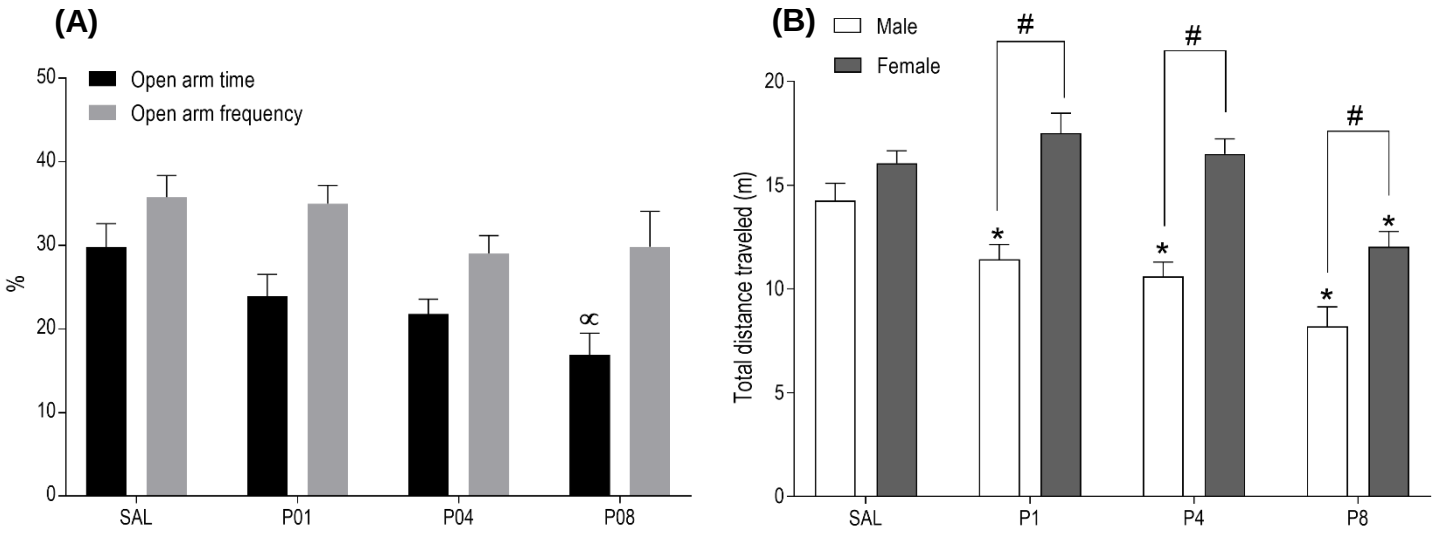


Figure 2. **Effect of different poly(i:c) prenatal treatment doses on elevated plus maze.** (A) Percentage of time spent and frequency of entries in open arm were reduced in the highest poly(i:c) dose tested. As long as no sex-specific effects were found, data from both sexes were combined for the final presentation. (B) All poly(i:c) males offspring traveled less in the EPM apparatus in comparison to SAL, however only the highest dose tested caused this behavior in females. SAL: saline offspring, P1: poly(i:c) 1 mg/kg offspring, P4: poly(i:c) 4 mg/kg offspring, P8: poly(i:c) 8 mg/kg offspring. **α**: $p < 0.05$ in comparison with the saline offspring; #: $p < 0.05$ when compared to females at same poly(i:c) treatment offspring. *****: $p < 0.05$ in comparison with SAL offspring. n = 15 – 16 animals/group; Mean ± S.E.M. Two-Way ANOVA, *post hoc* Bonferroni ($\alpha = 0.05$).

3.2.2. Prepulse inhibition of the startle response

Poly(i:c) prenatal exposure did not affect the startle reactivity to the 120-dB pulse-alone trial (Table S2). However, we observed a significant main effect of sex ($F_{1,118} = 31.72$, $p < 0.001$) reflecting a higher startle reactivity amplitude in male in comparison to female offspring (Figure S1).

The results obtained from the PPI were first analyzed by repeated measures three-way ANOVA with main factors of pre-natal (PT) treatment, sex and prepulse intensity (PP: 71, 77, 85 dB). Significant main effects of PT ($F_{3,118} = 52.14$, $p < 0.0001$) and PP ($F_{2,236} = 161.04$, $p < 0.0001$) were found. No main effect of sex ($p > 0.05$) or a significant two-way interaction between PT and sex ($p > 0.05$) were observed.

Data from both sexes were then combined and further analyzed by repeated measures two-way ANOVA, which revealed a significant interaction

between pre-natal treatment and prepulse intensity ($F_{6,244}$ = 11.15, p < 0.0001). *A* reduced prepulse inhibition of P4 and P8 when compared to saline and P1 (p < 0.05) was observed (Figure 3).

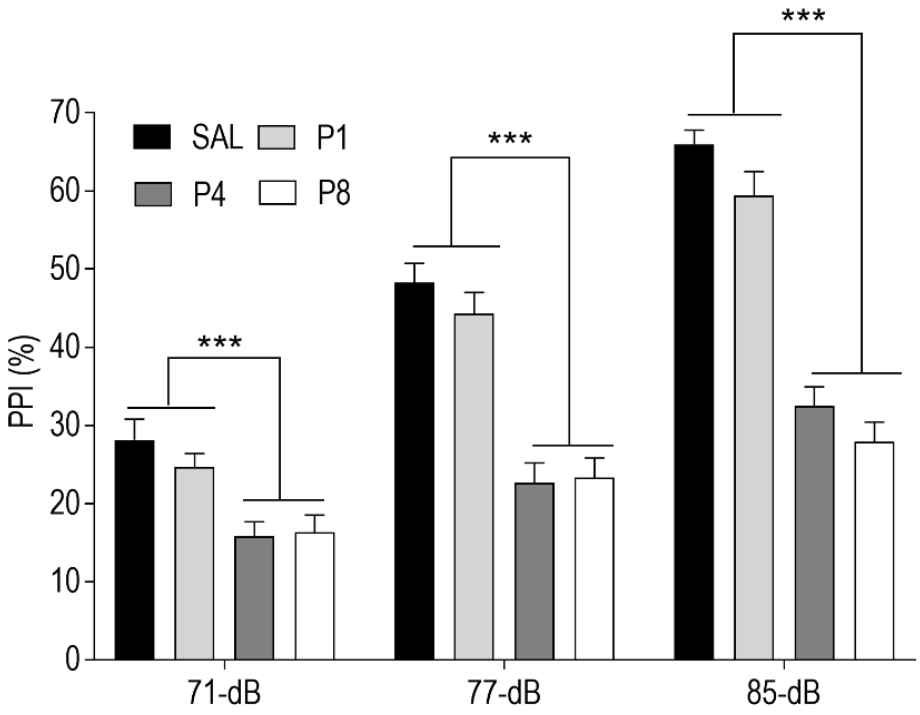


Figure 3. **Effects of different doses of poly(i:c) on sensorimotor gating assessed by the paradigm of prepulse inhibition (PPI) of the acoustic startle response** (A) Bar plot shows percentage pre-pulse inhibition (%PPI) across all prepulse stimuli used (71, 77 and 85 dB) in one pulse (120 dB) for different saline and poly(i:c) prenatal exposure. SAL: saline offspring, P1: poly(i:c) 1 mg/kg offspring, P4: poly(i:c) 4 mg/kg offspring, P8: poly(i:c) 8 mg/kg offspring. *: p < 0.05 difference between P4 and P8 compared to P1 and SAL offspring based on *post hoc* Bonferroni (α = 0.05). n = 15-16 animals/group, all values are mean ± S.E.M. As long as no sex-specific effects were found data from two sexes were combined for final presentation. Main effect of prepulse intensity is presented in table S2 (Supplementary Material).

3.2.3. Sensitivity to dizocilpine

Results obtained after MK-801 administration were analyzed by three-way repeated measures ANOVA with main factors of PT treatment, sex and 5-min bins. Significant main effects of PT ($F_{3,118}$ = 17.01, $p < 0.001$) and bin ($F_{9,1062}$ = 38.48, $p < 0.001$), and interactions between PT x bin ($F_{27,1062}$ = 5.52, $p < 0.0001$) and bin x sex ($F_{9,1062}$ = 3.34, $p < 0.0001$) were found.

However, there was no main effect of sex ($p > 0.05$) and data from both sexes were combined for further analysis. We also did not found a significant interaction between sex and PT ($p > 0.05$). Animals from P4 and P8 offspring showed increased locomotor activity in response to (+)-MK-801 while the lowest poly(i:c) dose tested (P1 group – 1 mg/kg) presented a locomotor response similar to that obtained in saline groups (Figure 4).

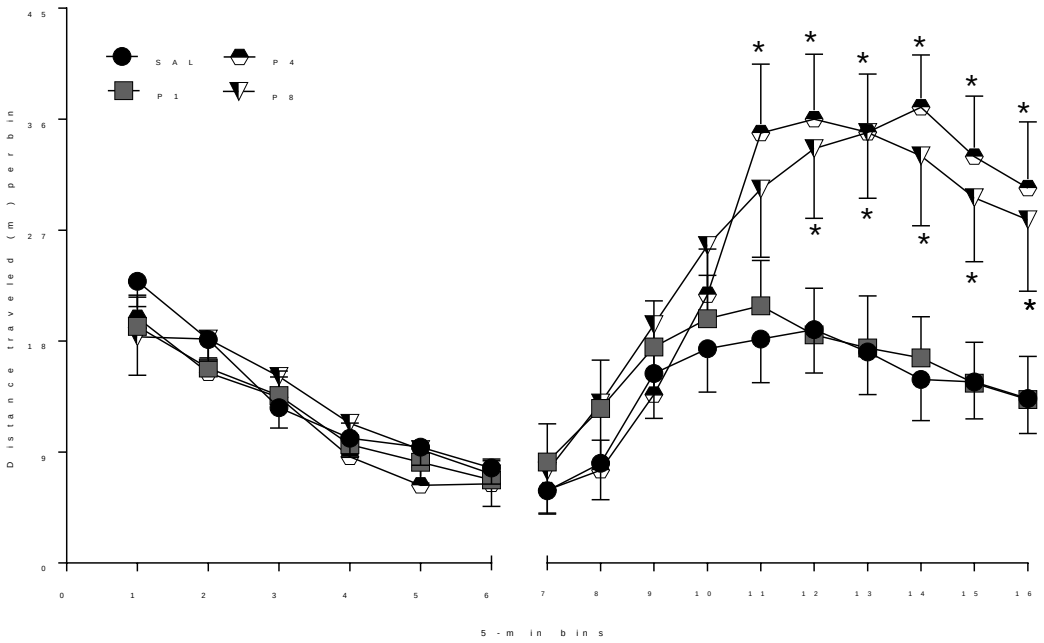


Figure 4. **Locomotor responses of adult offspring exposed prenatally to saline or different doses of poly(i:c).** Distance traveled per bin after (basal locomotor; bin 1-6) and before (bins 7-16) 0.3 mg/kg MK-801 i.p administration to male and to female rats (data from both sex combined for final analysis and presentation). Data show mean ± S.E.M, n = 30-32. RM-Two-Way ANOVA *post hoc* Bonferroni, (α = 0.05). SAL: saline offspring, P1: poly(i:c) 1 mg/kg offspring, P4: poly(i:c) 4 mg/kg offspring, P8: poly(i:c) 8 mg/kg offspring. * $p < 0.05$ compared to saline and P1 groups.

3.3. Effects of QLNC on PPI

Startle reactivity after 120 dB pulse alone trial was not altered by any formulations tested and males displayed higher startle reactivity amplitude in comparison to females (Figure S2, Table S3).

When PPI data were analyzed by factorial ANOVA, no main effect of sex or interactions between sex and the other factors analyzed were observed ($p > 0.05$, Table S3). Then, data from males and females were combined for further analysis and data presentation.

When combined data were analyzed by repeated measures two-way ANOVA a significant main effect of treatment ($F_{3,315} = 26.69$, $p < 0.0001$) and prepulse ($F_{2,315} = 34.73$, $p < 0.0001$) were found. However, there was no significant interaction between them ($p > 0.05$).

Groups injected with FQ formulation did not present improvement in PPI deficits compared to animals that received VEH or BLK formulations in all tested prepulse intensities ($p > 0.05$). However, a significant improvement in PPI deficit was observed for QLNC in comparison to BLK ($p < 0.001$), VEH ($p < 0.001$) and FQ ($p < 0.05$) formulations at 71, 77 and 85 dB (Figure 5).

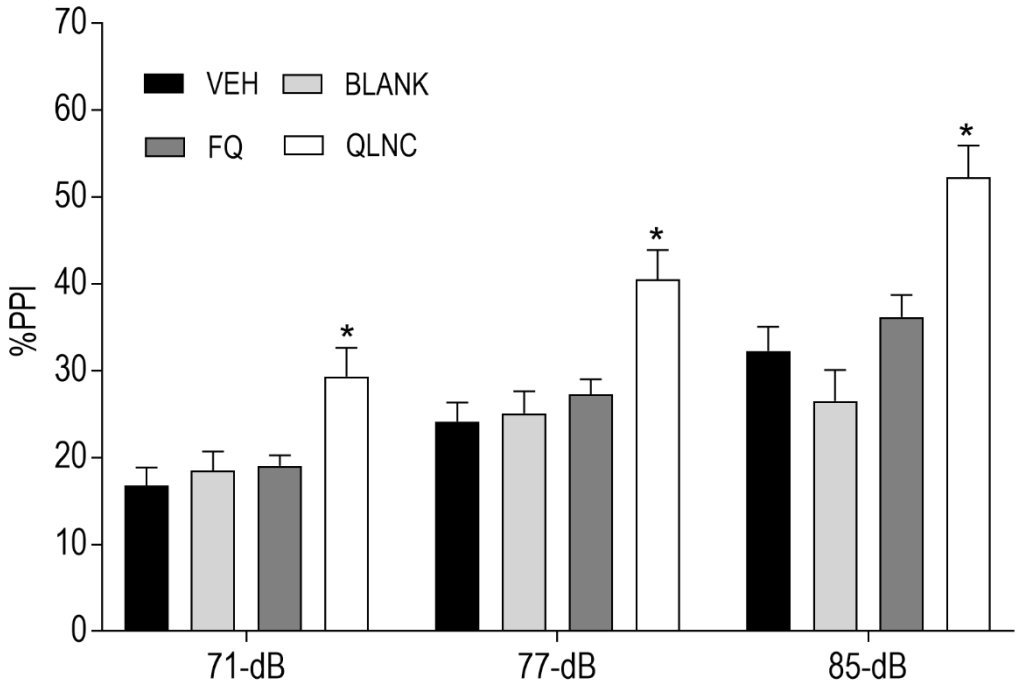


Figure 5. **Effects of FQ and QLNC treatment on prepulse inhibition of the acoustic startle response in poly(i:c) neurodevelopmental model of SCZ.** (A) Percent prepulse inhibition (%PPI) as a function of the 3 distinct prepulse levels (71, 77 and 85 dB) in one pulse (120 dB) for

males and females treated with vehicle (VEH – 1 mg/kg), blank lipid-core nanocapsules (BLK – 1 ml/kg), quetiapine solution (FQ – 5 mg/kg) and quetiapine lipid-core nanocapsules (QLNC – 5 mg/kg). n = 28-32 animals/group, all values are mean ± S.E.M. RM-Two-Way ANOVA *post hoc* Bonferroni, ($\alpha = 0.05$).*: $p<0.05$ compared to VEH, BLK and FQ formulations.

4. DISCUSSION

In the present study, we investigated the efficacy of QLNCs on the poly(i:c) model in both male and female rats using the PPI test. Considering that some studies indicates gender differences in PPI responses (Lehmann et al.,1999), we also evaluated the outcomes of three different poly(i:c) doses administered to pregnant damns at GD15 on neurodevelopmental outcomes of MIA in adult male and female offspring.

Poly(i:c) intravenous injection to pregnant Wistar rats acutely resulted in significant increase in maternal plasma levels of the pro-inflammatory cytokine IL-6 (4 h after dose) and anti-inflammatory cytokine IL-10 (8 h after dose) in a dose-dependent manner. Moreover, there was a significant imbalance between these two cytokines in maternal circulation four hours after dose. Exposure to imbalanced pro- and anti-inflammatory cytokines in prenatal life, resulting from administration of poly(i:c) to the pregnant damn, may cause abnormal development of the brain and a multitude of behavioral abnormalities observed in adult rodents (Fineberg & Ellman, 2013; Meyer et al., 2009).

Results of EPM indicate that male offspring from the higher poly(i:c) doses tested (4 mg/kg and 8 mg/kg) were, in general, more sensitive to poly(i:c) prenatal treatment than female offspring due to a significant reduction in time spent and entries to the open arms of the apparatus, similar to the findings by Yee and colleagues (2011) using pregnant Sprague Dawley rats and with poly(i:c) (4 mg/kg) at GD15. They observed that prenatal poly(i:c) exposure alone or in combination with juvenile stress increased anxiety-related behavior on the EPM. However, they did not report the time spent or the number of entries in closed arms neither the distance traveled in the EPM apparatus. Based on our findings we postulate that a more reasonable explanation for the alterations observed is the EPM is a reduction in locomotor activity rather than an increase in innate anxiety-related behavior caused by prenatal poly(i:c) exposure. This reduction in locomotor activity in the poly(i:c) animals might be

related to an increase in repetitive behavior such as self-grooming as observed for adult C57 mouse after prenatal exposure to poly(i:c) (20 mg/kg at GD12.5) (Schwartzer et al., 2013; Xuan and Hampson, 2014).

An increased hyperlocomotion induced by MK-801 was observed for poly(i:c) offspring. There is a broad spectrum of evidences in literature that rats prenatally exposed to poly(i:c) present hyperlocomotor activity in response to the N-methyl-D-aspartate receptor (NMDAR) antagonist MK-801 (Braun et al., 2012; Bronson et al., 2011; Vorhees et al., 2015; Zuckerman and Weiner, 2005). NMDAR hypofunction is one of the hypotheses involved in the pathophysiology of SCZ (Rahman et al., 2017). The present results corroborate these findings. Both male and female animals from P04 and P08 groups presented a more pronounced increase in locomotor activity after MK-801 dosing, although not in a dose response manner. Animals from the lowest poly(i:c) dose (1 mg/kg) did not differ from the controls, showing that this dose does not render the animals more sensitive to NMDAR blockade. Wolff and Bilkey (2008) suggested that low doses of poly(i:c) do not induce sufficient cytokine imbalance to alter fetal brain development. This hypothesis agrees with the present results, since maternal plasma levels of IL-6 and IL-10 for the 1 mg/kg dose were not altered.

In agreement with previously reports (Bikovsky et al., 2016; Hadar et al., 2015a, 2015b) in the current study adult poly(i:c) offspring exhibited significant preattentional sensorimotor gating deficits manifested as a reduction in PPI. The baseline acoustic startle response (ASR) for males was significantly higher than that observed for females even for those animals prenatally exposure to poly(i:c) (1, 4 and 8 mg/kg). Lehmann and colleagues (1999), working with Wistar rats, showed that ASR (120 dB pulse) is higher in males than in females in this rat strain. In this context, we assumed that in the present study all poly(i:c) doses tested did not modify the baseline ASR.

Although there are evidences in the literature that innate immune activation during critical periods of prenatal brain development have effects on the brain of adult rats in a sex-specific manner, the overall findings of our study did not corroborate this hypothesis. Factors such as type and dose of immunogen used, time of administration (early *vs.* late gestational period)

among others might interact with sex to play a significant role in the absence of differences observed in our study.

We further investigated the effects of nanoencapsulation of QTP on PPI response using a 4 mg/kg poly(i:c) dose. The analysis of mean PPI across all prepulse evaluated shows that QTP solution, administered intravenously at 5 mg/kg dose, was not capable of producing a reversal in the sensorimotor gating-disruptive effect caused by the prenatal poly(i:c) exposure. On the other hand, the same dose of QTP given as QLNCs resulted in significant improvement of PPI-impairment. One explanation for this finding might be related to the modulation of QTP drug delivery to the brain promoted by the nanocapsules. As reported previously by our research group, nanoencapsulation of QTP produces increased total brain exposure to the drug, determined in brain homogenates of male naïve Wistar rats (Carreño et al., 2016). These previous findings together with the present results leads to the assumption that the same increased exposure may be expected in the brain of female Wistar rats.

To the best of our knowledge, this is the first study reporting the restoration of the PPI deficits in a neurodevelopmental model of SCZ using drug encapsulated into LNC. This is a promising delivery system strategy to improve antipsychotic effects contributing to the development of SCZ new treatment strategies. Further studies are necessary to better understand free and nanoencapsulated QTP brain distribution in this neurodevelopmental SCZ model.

5. CONTRIBUTORS

TDC conceived the project and got the financial support. FC, APH, SMKR and TDC designed the experimental protocol. FC, VEH and KJS performed all the experiments. FSM provide the veterinary support during experimental protocol design and execution. KP and SSG supervised the lipid core nanocapsules preparation and characterization. FC, TDC, SMKR and APH performed the data analysis. FC, APH, SMKR and TDC wrote the manuscript. All authors approved the final manuscript.

6. ACKNOWLEDGMENTS

The authors acknowledge Dr. Liberato Brum Junior (Prati Donaduzzi, Toledo – PR, Brazil) for kindly providing quetiapine fumarate and technical support from the Animal's Facility staff (UFRGS/Biochemistry Department). This study was financed in part by CNPq/Brazil (Process 421767/2016-2) and by the Coordenação de Aperfeiçoamento de Pessoal de Nível Superior - Brazil (CAPES) - Finance Code 001. The authors also thank CNPq for the individual grant.

7. REFERENCES

Bikovsky, L., Hadar, R., Soto-Montenegro, M.L., Klein, J., Weiner, I., Desco, M., Pascau, J., Winter, C., Hamani, C., 2016. Deep brain stimulation improves behavior and modulates neural circuits in a rodent model of schizophrenia. Exp. Neurol. 283, 142–150.

Braun, A. a, Skelton, M.R., Vorhees, C. V, Williams, M.T., 2012. Comparison of the elevated plus and elevated zero mazes in treated and untreated male Sprague-Dawley rats. Pharmacol. Ther. 97, 406–415.

Bronson, S.L., Ahlbrand, R., Horn, P.S., Kern, J.R., Richtand, N.M., 2011. Individual differences in maternal response to immune challenge predict offspring behavior: contribution of environmental factors. Behav. Brain Res. 220, 55–64.

Carreño, F., Paese, K., Silva, C. M., Guterres, S.S., Dalla Costa, T., 2015. Characterizing the mechanism of quetiapine distribution in lipid-core nanocapsules pseudo-phases using a validated lc/uv method. Quim. Nova. 38, 1181–1186.

Carreño, F., Paese, K., Silva, C.M., Guterres, S.S., Dalla Costa, T., 2016. Pharmacokinetic Investigation of Quetiapine Transport across Blood–Brain Barrier Mediated by Lipid Core Nanocapsules Using Brain Microdialysis in Rats. Mol. Pharm. 13, 1289–1297.

Dimer, F.A., Pigatto, M.C., Boque, C.A., Pase, C.S., Roversi, K., Pohlmann, A.R., Burger, M.E., Rates, M.K., Dalla Costa, T., Guterres, S.S., 2015. Nanoencapsulation Improves Relative Bioavailability and Antipsychotic Effect of Olanzapine in Rats. J. Biomed. Nanotechnol. 11, 1482–93.

Dimer, F.A., Pigatto, M.C., Boque, C.A., Pase, C.S., Roversi, K., Pohlmann, A.R., Burger, M.E., Rates, S.M.K., Costa, T.D., Guterres, S.S., 2014. Nanoencapsulation improves relative bioavailability and antipsychotic effect of olanzapine in rats. J. Biomed. Nanotechnol. 11, 1482–1493.

Fineberg, A.M., Ellman, L.M., 2013. Inflammatory cytokines and neurological and neurocognitive alterations in the course of schizophrenia. Biol. Psychiatry 73, 951–66.

Flores, G., Morales-Medina, J.C., Diaz, A., 2016. Neuronal and brain morphological changes in animal models of schizophrenia. Behav. Brain Res. 301, 190–203.

Fonseca, F.N., Betti, A.H., Carvalho, F.C., Gremião, M.P.D., Dimer, F.A., Guterres, S.S., Tebaldi, M.L., Rates, S.M.K., Pohlmann, A.R., 2015. Mucoadhesive Amphiphilic Methacrylic Copolymer-Functionalized Poly(ε-caprolactone) Nanocapsules for Nose-to-Brain Delivery of Olanzapine. J. Biomed. Nanotechnol. 11, 1472–1481.

Hadar, R., Soto-Montenegro, M.L., Götz, T., Wieske, F., Sohr, R., Desco, M., Hamani, C., Weiner, I., Pascau, J., Winter, C., 2015a. Using a maternal immune stimulation model of schizophrenia to study behavioral and neurobiological alterations over the developmental course. Schizophr. Res. 166, 238–247.

Hadar, R., Soto-Montenegro, M.L., Götz, T., Wieske, F., Sohr, R., Desco, M., Hamani, C., Weiner, I., Pascau, J., Winter, C., 2015b. Using a maternal immune stimulation model of schizophrenia to study behavioral and neurobiological alterations over the developmental course. Schizophr. Res. 166, 238–47.

Hill, R.A., 2016. Sex differences in animal models of schizophrenia shed light on the underlying pathophysiology. Neurosci. Biobehav. Rev. 67, 41–56.

Kokras, N., Dalla, C., 2014. Sex differences in animal models of psychiatric disorders. Br. J. Pharmacol. 171, 4595–4619.

Lally, J., Gaughran, F., Timms, P., Curran, S.R., 2016. Treatment-resistant schizophrenia: current insights on the pharmacogenomics of antipsychotics. Pharmgenomics. Pers. Med. 9, 117–129.

Lehmann, J., Pryce, C.R., Feldon, J., 1999. Sex differences in the acoustic startle response and prepulse inhibition in Wistar rats. Behav. Brain Res. 104, 113–117.

Lister, R.G., 1987. The use of a plus-maze to measure anxiety in the mouse. Psychopharmacology. 92, 180-185.

Meyer, U., Feldon, J., 2012. To poly(I:C) or not to poly(I:C): Advancing preclinical schizophrenia research through the use of prenatal immune activation models. Neuropharmacology 62, 1308–1321.

Meyer, U., Feldon, J., Yee, B.K., 2009. A review of the fetal brain cytokine imbalance hypothesis of schizophrenia. Schizophr. Bull.

Millan, M.J., Andrieux, A., Bartzokis, G., Cadenhead, K., Dazzan, P., Fusar-Poli, P., Gallinat, J., Giedd, J., Grayson, D.R., Heinrichs, M., Kahn, R., Krebs, M.-O., Leboyer, M., Lewis, D., Marin, O., Marin, P., Meyer-Lindenberg, A., McGorry, P., McGuire, P., Owen, M.J., Patterson, P., Sawa, A., Spedding, M., Uhlhaas, P., Vaccarino, F., Wahlestedt, C., Weinberger, D., 2016. Altering the course of schizophrenia: progress and perspectives. Nat. Rev. Drug Discov. 15, 485 - 515.

Möller, M., Swanepoel, T., Harvey, B.H., 2015. Neurodevelopmental Animal

Models Reveal the Convergent Role of Neurotransmitter Systems, Inflammation, and Oxidative Stress as Biomarkers of Schizophrenia: Implications for Novel Drug Development. ACS Chem. Neurosci. 6, 987–1016.

Patrich, E., Piontkewitz, Y., Peretz, A., Weiner, I., Attali, B., 2016. Maternal immune activation produces neonatal excitability defects in offspring hippocampal neurons from pregnant rats treated with poly I:C. Sci. Rep. 6, 19106.

Pritchett-Corning, K.R., Chang, F.T., Festing, M.F.W., 2009. Breeding and housing laboratory rats and mice in the same room does not affect the growth or reproduction of either species. J. Am. Assoc. Lab. Anim. Sci. 48, 492– 498.

Rahman, T., Zavitsanou, K., Purves-Tyson, T., Harms, L.R., Meehan, C., Schall, U., Todd, J., Hodgson, D.M., Michie, P.T., Weickert, C.S., 2017. Effects of Immune Activation during Early or Late Gestation onN-Methyl-d-Aspartate Receptor Measures in Adult Rat Offspring. Front. psychiatry 8, 77.

Schwartzer, J.J., Careaga, M., Onore, C.E., Rushakoff, J.A., Berman, R.F., Ashwood, P., 2013. Maternal immune activation and strain specific interactions in the development of autism-like behaviors in mice. Transl. Psychiatry. 3, e240-9.

Vorhees, C. V., Graham, D.L., Braun, A.A., Schaefer, T.L., Skelton, M.R., Richtand, N.M., Williams, M.T., 2015. Prenatal immune challenge in rats: Effects of polyinosinic-polycytidylic acid on spatial learning, prepulse inhibition, conditioned fear, and responses to MK-801 and amphetamine. Neurotoxicol. Teratol. 47, 54–65.

Walf, A.A., Frye, C.A., 2007. The use of the elevated plus maze as an assay of anxiety-related behavior in rodents.Nature Protocol. 2, 322-328.

Wolff, A.R., Bilkey, D.K., 2008. Immune activation during mid-gestation disrupts sensorimotor gating in rat offspring. Behav. Brain Res. 190, 156–159.

Xuan, I.C.Y., Hampson, D.R., 2014. Gender-Dependent Effects of Maternal Immune Activation on the Behavior of Mouse Offspring. PLoS One 9, e104433.

Yang, A.C., Tsai, S.-J., 2017. New Targets for Schizophrenia Treatment beyond the Dopamine Hypothesis. Int. J. Mol. Sci. 18, 1689 -1703.

Yee, N., Ribic, A., de Roo, C.C., Fuchs, E., 2011. Differential effects of maternal immune activation and juvenile stress on anxiety-like behaviour and physiology in adult rats: No evidence for the “double-hit hypothesis.” Behav. Brain Res. 224, 180–188.

Zuckerman, L., Weiner, I., 2005. Maternal immune activation leads to behavioral and pharmacological changes in the adult offspring. J. Psychiatr. Res. 39, 311–23.

SUPPLEMENTARY MATERIAL

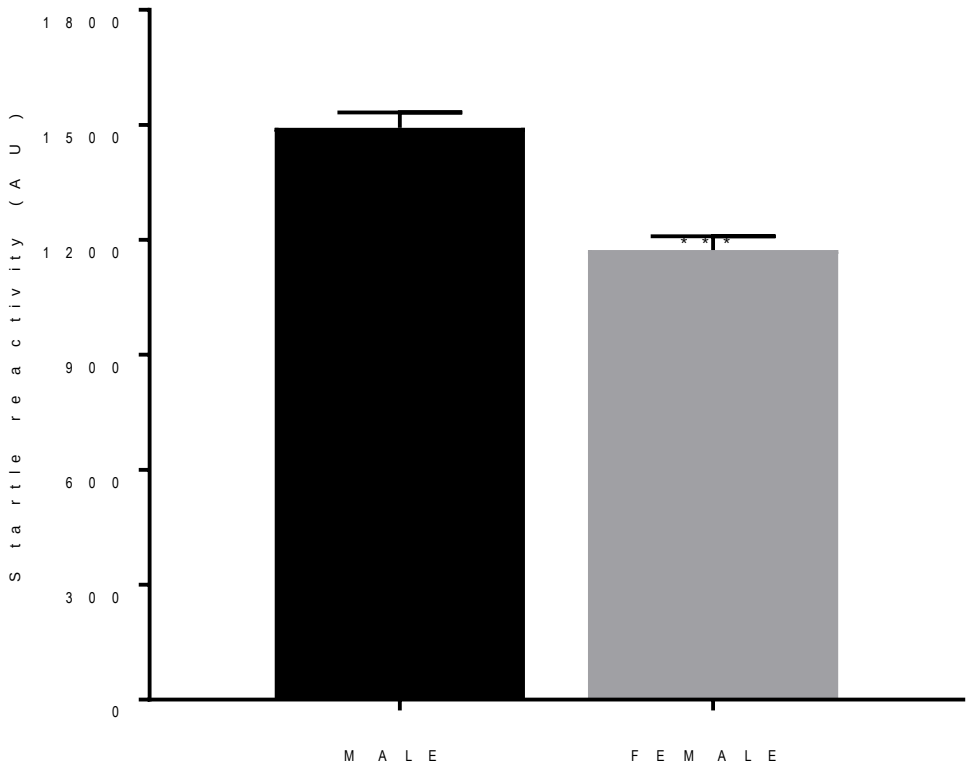


Figure S1. **Sex difference in acoustic startle response after a 120-dB pulse.** Bar plot shows startle reactivity expressed in arbitrary units (AU) for saline and poly(i:c) male and female offspring. ***: $p < 0.05$ difference between females compared to male offspring based on Bonferroni *post hoc* test ($\alpha = 0.05$). As long as no poly(i:c) prenatal exposure effects were founded data from all treatments were combined for final presentation. n = 60-64 animals/group, values are mean ± S.E.M from 10 distinct trials.

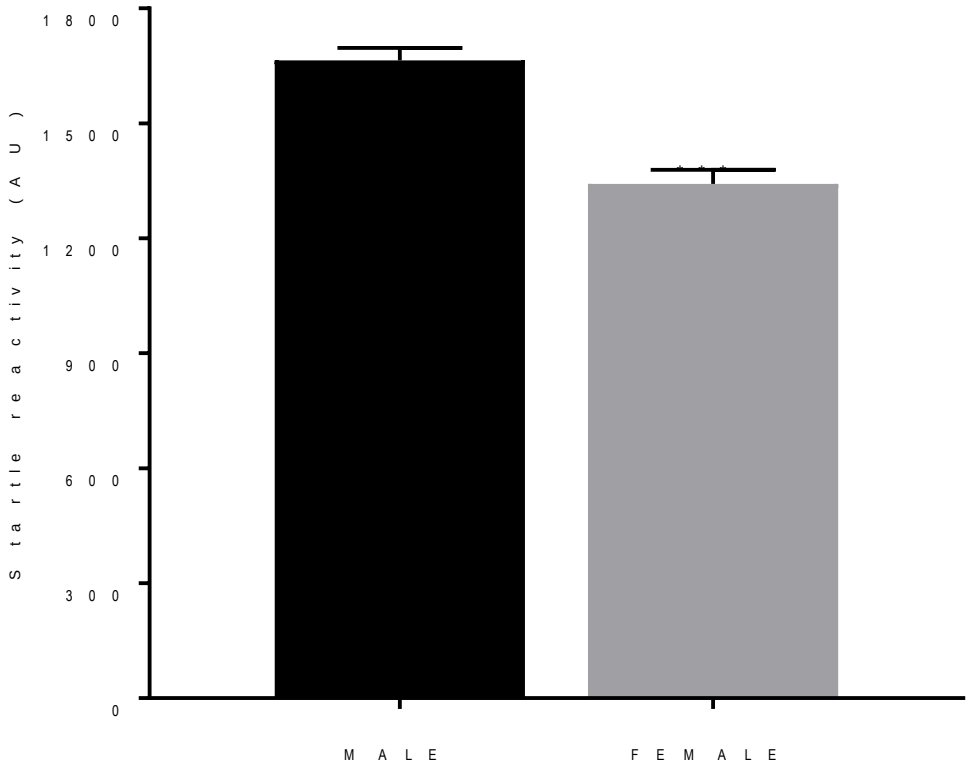


Figure S2. **Difference in acoustic startle response in a 120-dB pulse trial after administrations of different formulations.** Bar plot shows startle reactivity expressed in arbitrary units (AU) for poly(i:c) male and female offspring treated with vehicle (VEH – 1 mg/kg), blank lipid-core nanocapsules (BLK – 1 ml/kg), quetiapine solution (FQ – 5 mg/kg) and quetiapine lipid-core nanocapsules (QLNC – 5 mg/kg). ***: $p < 0.05$ difference between females compared to male offspring based on Bonferroni *post hoc* test ($\alpha = 0.05$). As long as no treatment effects were founded data from all formulations were combined for final presentation. n = 54-56 animals/group, values are mean ± S.E.M from 10 distinct trials.

Table S1. Summary of the statistical tests and outcomes used for the cytokine maternal plasma levels evaluation.

Measurment	Dependent Measures	ANOVA	Effects	DF	F-Value	P-Value
Cytokine maternal plasma levels	IL-6	4 x 2 (MIA x Time)	MIA	3	20.68	**0.004*** **
			Time	2	31.6	**<0.001*** **
			MIA x Time	6	17.04	**<0.001*** **
	IL-10	4 x 2 (MIA x Sex)	MIA	3	13.17	**0.001*** **
			Time	2	22.91	**<0.001*** **
			MIA x Time	6	10.27	**<0.001*** **
	IL-10/IL-6	4 x 2 (MIA x Sex)	MIA	3	16.25	**0.009*** **
			Time	2	99.51	**<0.001*** **
			MIA x Time	6	53.48	**<0.001*** **

IL: interleukin, MIA: Maternal immune activation, DF: degrees of freedom. Significant effects ($p < 0.05$).

Table S2. Summary of the statistical tests and outcomes for the behavioral analyses conducted in saline and poly(i:c) offspring.

Behavioral Test	Dependent Measures	ANOVA	Effects	DF	F-Value	P-Value
Elevated Plus Maze	Open arm entries (%)	4 x 2 (MIA x Sex)	MIA	3	1.52	0.213
			Sex	1	0.51	0.475
			MIA x Sex	3	2.13	0.061
	Time in open arm (%)	4 x 2 (MIA x Sex)	MIA	3	4.60	**0.004**
			Sex	1	0.52	0.470
			MIA x Sex	3	0.79	0.501
	Total distance traveled (m)	4 x 2 (MIA x Sex)	MIA	3	18.49	**< 0.001**
			Sex	1	45.60	**< 0.001**
			MIA x Sex	3	5.41	**0.002**
Prepulse inhibition	PPI (%)	4 x 2 x 3 (MIA x Sex x Prepulse)	MIA	3	52.14	**<0.001**
			Sex	1	1.72	0.191
			MIA x Sex	3	0.97	0.406
			Prepulse	2	161.04	**<0.001**
	Startle reactivity (AU)	4 x 2 (MIA x Sex)	MIA	3	1.73	0.164
			Sex	1	31.72	**< 0.001**
			MIA x Sex	3	0.970	0.410
Locomotor response to MK-801	Distance traveled after MK-801 injection	4 x 2 x 10 (MIA x Sex x Bin)	MIA	3	17.01	**<0.001**
			Sex	1	2.97	0.087
			MIA x Sex	3	0.879	0.454
			Bin	9	38.48	**<0.001**

MIA: maternal immune activation; PPI: prepulse inhibition; DF: degree of freedom. Significant effects ($p < 0.05$).

Table S3. Summary of the statistical tests and outcomes for the evaluation of quetiapine lipid core nanocapsules effect on PPI restoration in poly(i:c) animals.

Measurment	Dependent Measures	ANOVA	Effects	DF	F-Value	P-Value
Effects of QLNC on PPI	PPI (%)	2 x 3 x 2 (Formulation x Prepulse x sex)	Formulation	3	21.58	**<0.001*** **
			Sex	1	1.33	0.251
			Formulation x Sex	3	1.15	0.331
			Prepulse	2	65.03	**<0.001*** **
	Startle reactivity (AU)	2 x 2 (Formulation x Sex)	Formulation	3	2.12	0.102
			Sex	1	17.481	**<0.001*** **

PPI: prepulse inhibition; DF: degree of freedom. Significant effects ($p < 0.05$).

CAPÍTULO 2

A VERSATILE LC-MS/MS METHOD FOR DETERMINATION OF NEUROTRANSMITTERS IN MICRODIALYSIS SAMPLES APPLIED TO INVESTIGATE THE EFFECT OF QUETIAPINE IN SCHIZOPHRENIC-LIKE ANIMALS

Carreño F[1], Helfer VE[1], Staudt KJ[1], Olivo, LB[1], Barreto, F[2], Herrmann, AP[4], Rates SMK[3], Dalla Costa T[1]

[1]Pharmacokinetics and PK/PD Modeling Laboratory, Pharmaceutical Sciences Graduate Program, Faculty of Pharmacy, Federal University of Rio Grande do Sul;

[2]National Laboratory Network for Agriculture and Livestock - LANAGRO

[3]Experimental Psychopharmacology Laboratory, Pharmaceutical Sciences Graduate Program, Faculty of Pharmacy, Federal University of Rio Grande do Sul;

[4]Pharmacology and Therapeutics Graduate Program, Basic Health Science Institute, Federal University of Rio Grande do Sul.

HIGHLIGHTS

- An LC-MS/MS bioanalytical method was developed and validated for *in vivo* monitoring of monoamines (DA, DOPAC, HVA, 5-HT and 5-HIIA) in microdialysate samples. The method was selective, precise, accurate and sensitive.
- Method addressed the minimization of analytical time and sample volumes using positive and negative ionization in a single LC-MS/MS run analysis without any derivatization or cleanup steps, bringing advantages compared to other previously published methods.
- The method was successfully applied to determine interstitial monoamine concentrations following quetiapine intravenous administration to animals from a neurodevelopmental model of schizophrenia.
- Differently from naïve animals, no alterations were found in any monoamines extracellular levels after quetiapine dosing to schizophrenic-like animals in comparison to the baseline shading a light on the limited response rate to antipsychotic drugs observed in chronic schizophrenic patients.

ABSTRACT

A versatile method was developed and validated for simultaneous determination of the monoamine neurotransmitters (MNT) dopamine (DA), 3-4-dyhydroxyphenilacetic acid (DOPAC), homovanilic acid (HVA), serotonin (5-HT) and 5-hydroxyindolacetic acid (5-HIAA) in rat brain microdialysate samples using high-performance liquid chromatography tandem mass spectrometry (LC-MS/MS). The method allowed for small sample volume, using positive and negative ionization mode in a single run analysis without any derivatization or cleanup steps. Analytes were quantified at concentrations ranging from 100 ng/mL to 0.05, 10, 0.5, 0.1 or 1 ng/mL (lower limit of quantification, LLOQ) of DA, DOPAC, HVA, 5-HT and 5-HIIA, respectively, showing linearity ($r > 0.98$), accuracy, and precision (R.S.D ± 15%) according to validation limits accepted by international guidelines. The method was successfully applied for monitoring the concentration changes of MNT in microdialysate samples from medium prefrontal cortex of Wistar rats in a neurodevelopmental model of schizophrenia before and after quetiapine 5 mg/kg i.v. *bolus* dose administration. No alterations in MNTs were observed in schizophrenic-like animals in comparison to the baseline shading a light on the limited response rate to antipsychotic drugs observed in chronic schizophrenic patients.

Key-words: Monoamine neurotransmitters; LC-MS/MS; Method validation; Neurodevelopmental model of schizophrenia; Poly(i:c); Quetiapine.

1. INTRODUCTION

Monoamine neurotransmitters (MNT), such as dopamine (DA), serotonin (5-HT) and its main metabolites (Figure 1), are one of the major classes of neurotransmitters involved in Central Nervous System (CNS) chemical communication [1,2] and play their role in the pathophysiology of several neuropsychiatric disorders such as depression, Parkinson's disease, drug addiction and schizophrenia [3,4].

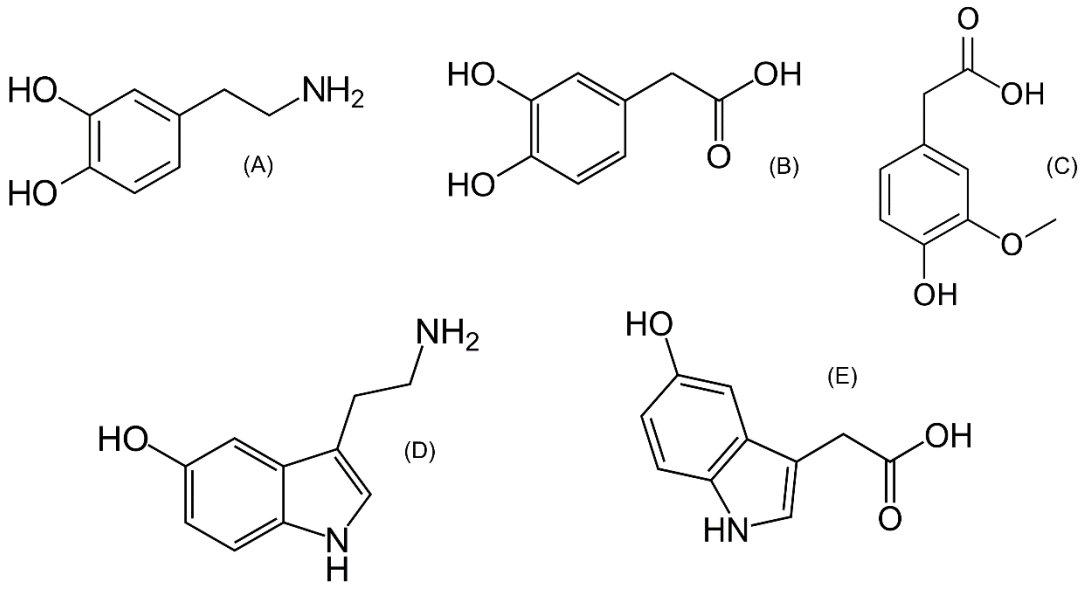


Figure 1. Chemical structure of (A) dopamine - DA, (B) 3-4-dyhydroxyphenilacetic acid - DOPAC, (C) homovanilic acid - HVA, (D) serotonin – 5-HT and (E) 5-hydroxyindolacetic acid - 5-HIIA.

Hypofunctionality of the medium prefrontal cortex (mPFC) has been proposed as an underlying dysfunction in schizophrenia, especially on negative and cognitive symptoms [5]. Hadar et al. [6], using post mortem HPLC analysis showed that in a neurodevelopmental animal model of schizophrenia rats presented distinct dopamine and serotonin changes in mPFC. The ability of the atypical antipsychotic drugs, such as quetiapine (QTP), to increase MNT levels in mPFC might play a role in their clinical effectiveness for treating schizophrenia [7,8].

Intracerebral *in vivo* microdialysis has been used to characterize the effects of psychotropic drugs, such as QTP, on biogenic amines extracellular levels on CNS in different brain regions of freely behaving rats [7-9]. However, the studies are generally conducted in naïve animals and the influence of SCZ alterations on MNT levels has not been addressed.

In microdialysis CNS experiments, perfusion fluid is continuously flushed through the probe inserted in the brain and diffused extracellular analytes are collected in the microdialysate for subsequent quantification. Microdialysis offers a very clean dialysate (protein free) sample, which requires no further cleanup procedure, making direct injection a feasible option [10–12].

The development of a bioanalytical methodology for the quantification of neurotransmitters in microdialysate samples represents an analytical challenge and is of continuing interest. The combination of very low basal levels of extracellular MNT together with slow perfusion rate (0.5 – 2 µL/min) and short sampling intervals (20-30 min) leads to a need for a highly sensitive assay method that allows for quantification of each neurotransmitter with minimal interference [13].

Several methods have been reported for the determination of MNT in microdialysis samples using gas chromatography (GC) and high-performance liquid chromatography (LC) techniques [14]. GC requires that the substance to be analyzed is volatile and normally volatilization of the analytes is achieved by chemical derivatization [15]. Although, GC coupled with mass spectrometry (MS) has been reported for quantification of neurotransmitter derivatives in plasma, cerebrospinal fluid (CSF) and extracted brain tissue, the sensitivity of GC assays is inadequate for the detection of extracellular levels of MNT in brain microdialysate [16]. Moreover, the GC assay includes time-consuming sample preparation and clean-up procedures and insufficient specificity.

By comparison, HPLC methods coupled to electrochemical detection (ECD), fluorescence (FLD) and ultraviolet (UV) have been routinely used for the quantification of MNT concentrations in MICRODIALYSIS samples and offer the benefits of simplicity and stability [14]. However, neurotransmitters such dopamine and serotonin are low molecular weight polar compounds and their retention times in standard reversed-phase HPLC systems is generally poor,

leading to the use of ion-paring and hydrophobic interaction mechanisms to separate these polar analytes [14].

ECD is known to present lack in reproducibility mainly because of hysteretic degradation of the electrode. Furthermore, Hows et al [17] demonstrated that dopamine levels measured by ECD could be overestimated due to artifacts. FLD and UV detectors show lack of sensitivity to cope with the small volumes of the microdialysis samples [14].

To overcome these problems, MS can be used as a selective tool because the detection of the analyte correlates both, the structural information and its molecular weight, increasing both the sensitivity and selectivity of the method [18]. Ji et al [19] have reported a LC-MS/MS method for simultaneous determination of MNT in mPFC microdialysis samples by diethylation labeling using cyanoborohydride reagent. Song et al [20] developed a robust LC-MS method for the determination of 17 neurotransmitters by derivatization with benzoyl chloride under mild conditions. Greco et al. [14] have reported a method for simultaneous determination of DA, norepinephrine (NE) and 5-HT in striatum rat brain using LC-MS/MS method that requires a derivatization process using (5-N-succinimidoxy-5-oxopentyl)triphenylphosphonium bromide (SPTPP) before the analysis. Although all cited methods showed good sensitivity and short runtimes, derivatization, especially its optimization, is a time-consuming and labour-intensive step.

Recently, Suomine et al. [4] have reported a ultra performance liquid chromatography tandem mass spectrometry (UPLC-MS/MS) method for the determination of MNT in human brain microdialysis samples. The analytical method requires minimal sample pretreatment and low injection volume (15 µL). However, its time consuming with long running time (25 min) and two separate runs for each sample because the analytical method require positive and negative ionization for all analytes investigated.

In the present work we demonstrate the development and validation of a method for simultaneous determination of DA, 3-4-dyhydroxyphenilacetic acid (DOPAC), homovalinic acid (HVA), 5-HT and 5-hydroxyindolacetic acid (5-HIAA) in low sample volume, using positive and negative ionization in a single LC-MS/MS run analysis without any derivatization or cleanup steps. The

method was applied in a microdialysis study aiming to investigate mPFC MNT alterations in a neurodevelopmental animal model of schizophrenia.

2. MATERIALS AND METHODS

2.1 Drugs, chemical and reagents

Analytical primary standards of DA, DOPAC, HVA, 5-HT and 5-HIAA were purchase from Sigma Aldrich (Brazil). QTP hemifumarate (>99.0%) was kindly donated by Pratti Donaduzzi Pharmaceutical Laboratory (Toledo, Brazil). Acetonitrile and methanol (LC-MS grade) were purchased from Merck (Kirkland, WA, USA) and formic acid from J.T.Backer (LC grade, Center Valley, PA, USA). Ultrapure water was obtained from a Milli-Q water purification system (Millipore, Bedford, MA, USA). All other chemicals and reagents were analytical grade.

Since catechol and indoles are subject to oxidative breakdown all samples require the addition of antioxidant. The antioxidant mixture used for standard stock solution (AM-SS) consisted of 0.1 M HCl, 5 mM $Na_2S_2O_5$, 300 µM of EDTA and the antioxidant mixture used for samples (AM-S) consisted of 0.27 mM Na_2EDTA, 3.3 mM L-cysteine, 0.5 mM ascorbic acid and 0.1 M acetic acid – pH 3.2. Microdialysis were performed using a modified artificial cerebrospinal fluid (ACF) consisted of NaCl 145 mM; KCl 2.7 mM; CaCl2 1.2 mM; MgCl2 1mM, ascorbic acid 10 nM - pH 6.2.

QTP solution (5 mg/mL) was prepared first dissolving the drug in acetic acid (99%), then 0.9% saline containing polysorbate 80 (78 mg/mL) was add and the pH was adjusted to 6.5 ± 0.5 using NaOH (8 M).

2.2 Preparation of standard solutions, calibration standards and quality controls

Series of stock solutions of DA, DOPAC, HVA, 5-HT and 5-HIAA were prepared by weighing the standards in different volumetric flasks and dissolving each with AM-SS solution described above to obtain a final concentration of 10 µg/mL. An aliquot of each stock was pipetted into a new volumetric flask to generate a mixed stock solution containing all five MNT and diluted to volume with the same solvent to a final concentration of 1 µg/mL.

Subsequent working solutions were prepared by diluting the mixed stock solution with ACF and calibrators were prepared at ten concentration for each of the neurotransmitters, excepted for DOPAC, as following: DA (0.05, 0.1, 0.25, 1.0, 2.5, 5, 15, 25, 50, 100 ng/mL), DOPAC (10, 15, 25, 50, 75, 100 ng/mL), HVA (0.5, 1.0, 2.5, 5, 10, 15, 25, 50, 75, 100 ng/mL), 5-HT (0.1, 0.25, 0.5, 1.0, 2.5, 5, 10, 25, 50, 100 ng/mL), 5-HIIA (1.0, 2.5, 5, 10, 15, 25, 50, 75, 100 ng/mL). Quality control (QC) were prepared at low (QCL - 0.15 ng/mL for DA; 20 ng/mL for DOPAC, 1.5 ng/mL for HVA, 0.3 ng/mL for 5-HT and 3 ng/mL for 5-HIIA), medium (QCM - 55 ng/mL for all compounds) and high (QCH - 80 ng/mL for all compounds) concentrations. To prevent MNT degradation working solutions were diluted 1:2 using the AM-S solution and directly injected into LC-MS/MS system. Furthermore, during preparation and storage samples were always protected from light.

2.3 Chromatographic and MS/MS conditions

Liquid chromatography – electrospray ionization – tandem mass spectrometry (LC-ESI-MS/MS) measurements were carried out on an Agilent 1200 LC series (Agilent Technologies®, USA) coupled to a triple-quadrupole mass spectrometer (PI 500 LC–MS/MS, Applied Biosystems, MDS Sciex, Toronto, Canada) equipped with an electrospray ionization source (ESI)

Chromatographic separation was achieved in a pentafluorophenyl column (Thermo Scientific Gold PFP Hypersil, 2,1 x 150 mm, 1.9 µm). The eluents used were A: 0.1% formic acid and B: acetonitrile + 0.1% formic acid. The gradient used in the analysis of microdialysis samples was: B 5% 0-3 min, 85% 3-5 min, 95% 6-8 min, 5% 8-8.5, 5% 8.5-10 min followed by an equilibration time of 4 min with a total run time of 15 min. The flow rate was 0.2 mL/min, and the column oven temperature was kept at 40 ºC

Microdialysate samples were diluted 1:2 using the AM-S solution and directly injected into the system without the need of internal standard or cleanup process. The samples were maintained at 10ºC in the autosampler before injection of 20 µL. To avoid contamination of the ion source by the modified ACF's solution the flow from the LC was direct to waste for the first minutes of the gradient.

For the mass spectrometric analysis, the ESI source operating in both positive and negative mode was set with the following parameters: ion spray (IS) voltage: 5500 V and -4500 V for the positive and negative modes, respectively; curtain gas: 30 psi; nebulizer gas (GS1): 55 psi; auxiliary gas (GS2): 55 psi; source temperature: 650 ºC. Nitrogen was used as the nebulizer and collision gas. Table 1 shows the instrument settings optimized for product ions of each compound, including the values for declustering potential (DP), entrance potential (EP), collision energy (CE) and collision cell exit potential (CXP). Acquisition was performed in multiple reaction monitoring (MRM) mode, and all data were processed using Analyst version 1.4.2 software (Applied Biosystems).

Table 1. Mass spectrometry and retention times for each analyte.

Compound	t_R (min)	MRM transition (m/z)	Dwell time (msec)	DP (V)	EP (V)	CE (V)	CXP (V)
Positive mode $[M-H]^+$							
DA	3.02	154.097 > 137	50	36	10	25	12
		154.097 > 91.1	50	36	10	29	14
		154.097 > 119	50	36	10	23	18
5-HT	3.19	176.929 > 160.1	50	56	10	13	10
		176.929 > 132	50	46	10	27	18
		176.929 > 115	50	46	10	37	18
5-HIIA	7.74	191.967 > 146	50	36	10	19	10
		191.967 > 119	50	41	10	39	18
Negative mode $[M-H]^-$							
DOPAC	4.50	166.881 > 123.1	50	-25	-10	-14	-13
		166.881 > 95	50	-15	-10	-16	-53
HVA	8.21	180.917 > 122	50	-10	-10	-20	-9
		180.917 > 137	50	-40	-10	-10	-7

DA: dopamine; DOPAC: 3-4-dyhydroxyphenilaetic acid; HVA: homovanilic acid; 5-HT: serotonin; 5-HIIA: 5-hydroxyindolacetic acid.
t_R: retention time; DP: declustering potential; EP: entrance potential; CE: collision energy; CXP: exit collision cell potential

2.4 Validation of the bioanalytical method

The bioanalytical method was validated in compliance with the USA Food and Drug Administration (FDA) guidelines [20-21] . The performance parameters evaluated were linearity, lower limit of quantification, precision (intra and inter-assay) and accuracy. Because MNTs are endogenous compounds present in brain selectivity was not determined since all brain samples will contain the analytes.

Linearity was evaluated through replicate analysis (n = 6) of standards curves to obtain a calibration equation. Linear regression (1/X weight scheme) of the concentration standard versus peak area was used to calculate corresponding MNT concentrations in microdialysate samples.

Intra and inter-day precisions and accuracy, evaluated on two consecutive days using six replicate of which QC (QCL, QCM, QCH) and lower limit of quantification (LLOQ) samples in ACF solution, were given as the relative standard deviation (R.S.D.%). Accuracy was calculated as relative error (R.E %). Precision and accuracy should be within ± 15% except for the LLOQ where it should not exceed ± 20% R.S.D.

Stability studies were performed in triplicate for the lowest and highest concentrations of QC samples after three freeze-thaw cycles (- 80 ºC ± 1 ºC/room temperature) and after a short-term stability at -20 ºC for 6 hours trying to simulate a real experimental day condition, since samples were collected and immediately transferred to a -20 ºC freezer before storing at – 80 ± 1 ºC. Samples were considered stable if the deviation from original concentration was within ± 15%.

2.5 Applicability of the bioanalytical method using microdialysis for MNT monitoring

To prove the applicability of the LC-MS/MS method, microdialysis experiments were performed in Wistar rats. Extracellular monoamine concentrations were monitored under basal conditions as well as in response to an intravenous injection of quetiapine.

2.5.1 Microdialysis system

The microdialysis system consisted of a CMA 120 system for freely moving animals (CMA®, Sweden). A PHD 2000 syringe pump (Harvard Apparatus, Holliston, USA) and gas-tight syringes (500 µL, Hamilton company, USA). A FEP MICRODIALYSIS tubing (1.2 µL/100 mm length – CMA, Sweden) were used to provide ACF solution through CMA 12 concentric microdialysis probe (3 mm, PAES membrane, 20 kDa cutoff – CMA®, Sweden). All syringes and microdialysis tubing used were wrapped in aluminum foil and samples were collected in amber microcentrifuge tubes placed in ice bath.

2.5.1 Animals and surgery procedure

In vivo experiments were carried out according to the Brazilian guidelines for animal experiments (Conselho Nacional de Controle de Experimentação Animal, CONCEA – Brazil) and were approved by the Federal University of Rio Grande do Sul Ethics Committee in Animal Use (CEUA/UFRGS #31001).

Male Wistar rats (250 – 300 g) were obtained from the Central Animal Facilities of the University's Biochemistry Department (Porto Alegre, Brazil). Animals were raised in conventional (open-top) caging system (3 rats/cage) in controlled conditions (22 ± 2ºC, 65% humidity, 12h light/dark cycle) and had *ad libitum* access to standard rodent chow (Nuvilab® – Nuvital/Brazil) and filtered water.

Neurodevelopmental animal model of schizophrenia was based on the model described by Hadar et al. [6]. Briefly, pregnant Wistar dams (gestational day 15) received poly (i:c) 4 mg/kg i.v. *bolus* dose via lateral tail vein. SCZ-like deficits in the adult offspring (PND75, P-offspring) were confirmed by elevated plus-maze, pre-pulse inhibition of the startle response and MK-801 induced hyperlocomotion in comparison to offspring (N-offspring) of pregnant dams (GD15) that received the same i.v. *bolus* volume of saline (data no shown).

For the microdialysis experiments, animals from P-offspring (n = 5 male rats) and N-offspring (n = 5 male rats) were anesthetized (ketamine/xilazine/acepromazine: 100 mg/kg -10 mg/kg - 2 mg/kg; i.p.),

received pre-emptive analgesia (ketoprofen, 5 mg/kg, subcutaneously) and local anesthesia (5 mg/kg lidocaine - 2 mg/kg bupivacaine; s.c.). Using a stereotaxic apparatus, a microdialysis guide cannulas were surgically implanted into the mPFC (A: +3.2 mm, L: +0.8 mm, V: -5.2 mm relative to bregma).

After surgery recovery for 48 h, the guide cannulas were replaced by the microdialysis probe which was continuously perfused with ACF solution at 1 µL/min. Following a 1-hour equilibration period, microdialysis samples were collected with a temporal resolution of 20 min (4 samples) in order to determine MNT basal concentration levels in rat's mPFC. Then, all animals were intravenously injected, via lateral caudal vein, with a single dose (5 mg/kg) of QTP solution (5 mg/mL) and microdialysis samples were collected every 20 min up to 280 min after drug administration (15 samples).

During all collection interval samples were kept on ice and one part of antioxidative mixture in four parts of microdialysate samples were added to prevent MNT degradation. Collected samples were storage at - 80 ± 2 ºC until analysis.

2.6 Statistical analysis

Using the software Phoenix® 64 v. 8.1 (Certara®, Princeton, NJ, USA) individual MNT brain concentration *vs.* time profiles obtained were used to determine the basal ($AUC_{0\text{-}80min}$) and after treatment ($AUC_{100\text{-}380min}$) area under the MNT brain concentration vs. time curve as well as the MNT brain maximum concentration observed (C_{max}) after QTP dosing.

Statistical analysis was performed using GraphPad Prism software version 7.04 with statistical significance set to $p < 0.05$. Baseline, treatment AUC and C_{max} were analyzed by Student's t-test and the effects of QTP on extracellular monoamine levels at each sampling time were compared using repeated-measures two-way ANOVA with Bonferroni multiple comparison ($\alpha = 0.05$).

3. RESULTS AND DISCUSSION

The aim of this study was to develop and validate a fast and simple method for determination of five MNTs in rodent brain ECF using microdialysis coupled with LC-MS/MS without the need of samples derivatization. Chromatographic separation was optimized to achieve good efficiency and short analysis time.

3.1 Validation of the bioanalytical method

3.1.1 Linearity and LLOQ

Linearity was defined using six calibrations curves prepared in ACF solution spiked with MNT mixture. These curves were prepared in ten distinct concentrations, excepted for DOPAC for which six concentrations were used.

Correlation coefficient (R) was calculated by linear regression applying weighting factor (1/x). All analytes showed satisfactory linearity with R values above 0.98. The LLOQ for each analyte was defined as the lowest concentration for which imprecision (R.S.D) was not higher than 20% (Table 2).

Table 2. Calibration curve regression parameters.

Compound	**Range (ng/mL)**	**Mean Regression Equation**	**Correlation coefficient (R)**
DA	0.05 – 100	Y = 39161.67 - 792.48	0.994 – 0.999
DOPAC	10 – 100	Y = 16086.83 - 19015.77	0.981 – 0.999
HVA	0.5 – 100	Y = 1079.50 - 70.85	0.990 – 0.996
5-HT	0.1 – 100	Y = 59057.67 - 2245.17	0.993 – 0.997
5-HIIA	1 – 100	Y = 85508.17 – 42429.83	0.981 – 0.998

DA: dopamine; DOPAC: 3-4-dyhydroxyphenilacetic acid; HVA: homovalinic acid; 5-HT: serotonin; 5-HIAA: 5-hydroxyindolacetic acid. n = 6 calibration curves/compound.

3.1.2 Precision and accuracy

Precision and accuracy of MNT determination were evaluated in spiked samples using 6 replicates on two different days. Inter and intra-day precision and accuracy for the MNT during validation experiments are shown in Tables S1 to S5 (Supplementary material). Intra-day and inter-day precisions (R.S.D) of the method were within 2.33 – 12.14 % and 4.56 – 10.52 %, respectively for all MNT analyzed.

The accuracy of the method for QCs ranged between 85.35 – 114.80 % and for LLOQ between 84.91 – 115.53 for all MNTs. All results regarding precision and accuracy were within acceptable criteria for bioanalytical methods [20-21].

3.1.3 Stability test

The results from the stability test are presented in Table 3. All analytes showed to be stable after three freeze-thaw cycles from -80 ºC to room temperature (R.S.D ranged from 4.04 – 14.70 % for all MNT) and for 6 h at -20 ºC (R.S.D range from 4.03 – 13.83 % for all MNT).

Table 3. Stability of MNTs in artificial cerebrospinal fluid.

Stability Conditions	Compound	Nominal Concentration (ng/mL)	Mean ± S. D[a]	R.S.D. (%)	C.V. Accuracy Range (%)
Three freeze-thaw cycles (-80 ºC/room temperature)	DA	0.15	0.14 ± 0.02	14.28	87.98 – 110.18
		80	76.45 ± 4.71	6.78	86.15 – 111.90
	DOPAC	20	23.54 ± 1.43	6.10	85.30 – 101.30
		80	82.45 ± 6.77	8.33	88.54 – 112.89
	HVA	1.5	1.65 ± 0.14	8.97	85.67 – 110.29
		80	77.45 ± 3.13	4.04	88.34 – 105.45
	5-HT	0.3	0.34 ± 0.05	14.70	89.45 – 112.45
		80	79.56 ± 4.34	5.45	86.45 – 99.54
	5-HIIA	3.0	3.23 ± 0.43	13.47	87.54 – 101.54
		80	82.30 ± 5.43	6.60	88.54 – 103.30
Storage -20 ± 1 ºC (6 h)	DA	0.15	0.13 ± 0.01	7.69	86.15 – 104.28
		80	82.34 ± 6.39	7.76	85.89 – 103.14
	DOPAC	20	22.14 ± 2.18	9.84	86.45 – 101.19
		80	77.56 ± 5.67	7.32	85.67 – 113.30
	HVA	1.5	1.51 ± 0.21	13.83	88.92 – 112.34
		80	82.34 ± 5.53	6.72	85.78 – 109.57
	5-HT	0.3	0.38 ± 0.05	13.15	88.67 – 113.29
		80	79.85 ± 7.21	9.10	85.89 – 107.81
	5-HIIA	3.0	3.12 ± 0.12	4.03	89.39 – 109.38
		80	83.33 ± 4.57	5.48	89.30 – 103.45

DA: dopamine; DOPAC: 3-4-dyhydroxyphenilacetic acid; HVA: homovalinic acid; 5-HT: serotonin; 5-HIAA: 5-hydroxyindolacetic acid.
[a]Mean of 3 replicates/QC sample/compound. S.D.: standard deviation; R.S.D.: relative standard deviation; C.V.: coefficient of variation.

3.2 Applicability of the bioanalytical method using microdialysis for MNT monitoring

The presented bioanalytical method was successfully applied to investigate MNT changes before and after QTP intravenous administration to naïve and poly(i:c) prenatally exposed male Wistar rats. Microdialysis sample

schedule and bioanalytical method sensitivity were adequate to allow adequate characterization of concentration versus time profile of all MNT investigated (Figure 2).

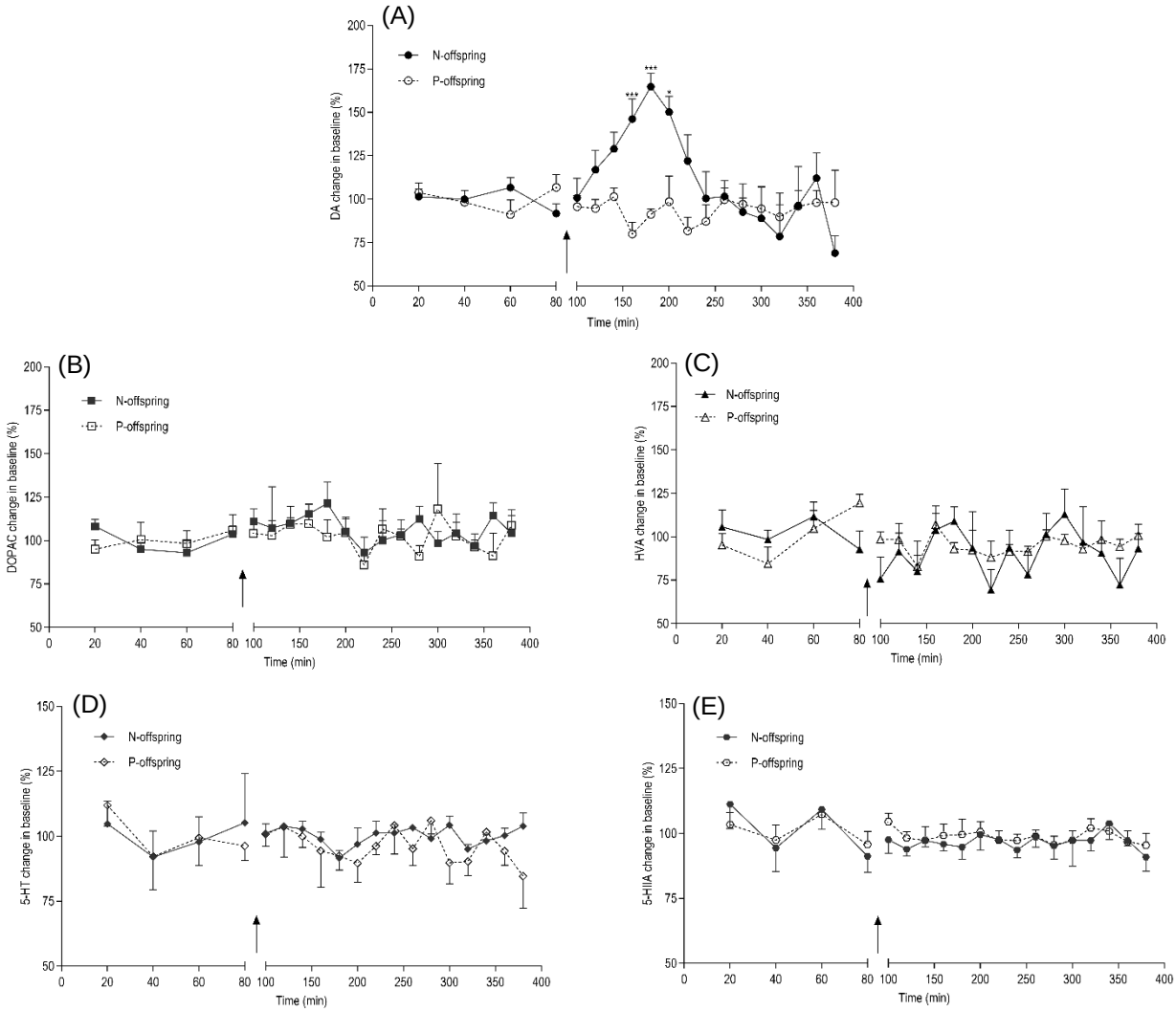


Figure 2. Effect of QTP (5 mg/kg i.v. *bolus*) on extracellular levels of DA (A), DOPAC (B), HVA (C), 5-HT (D) and 5-HIIA (E) at the mPFC of naïve (solid symbols) and poly(i:c) exposed (empty symbols) offspring. Arrows indicates systemic administration of QTP. Data represents mean ± S.E.M (n = 5/group). RM-Two-Way ANOVA *post hoc* Bonferroni, (α = 0.05). * $p < 0.05$, *** $p < 0.001$. QTP: quetiapine; DA: dopamine; DOPAC: 3-4-dyhydroxyphenilacetic acid; HVA: homovalinic acid; 5-HT: serotonin; 5-HIAA: 5-hydroxyindolacetic acid

In vivo brain microdialysis allowed to measure basal extracellular levels of MNT in the mPFC rats under freely behaving condition. Since the measured values were not corrected for *in vivo* probe recovery, it can be only used for the accurate quantification of changes relative to basal values.

In line with previous results [23,24] prenatal exposure to poly(i:c) did not promote changes in the mPFC basal dopamine and DOPAC levels in comparison to naïve animals (Table 4, $AUC_{0\text{-}80min}$). Although Hadar et al. [6] found lower levels of DOPAC measured in mPFC micropunches of poly(i:c) offspring, they reported no alterations in other neurotransmitters (HVA, 5-HT, 5-HIIA) in this brain region.

Following QTP dosing to naïve offspring, DA levels rapidly increased within 1.6 hours to a concentration ca. 65% greater than the basal, significantly increasing the AUC after treatment, which was not observed for P-offspring group (Table 4, C_{max} and $AUC_{100\text{-}380min}$). After reaching the peak level the concentration slowly decreases, reaching the starting point about 2.5 hours after the injection (Figure 2A). No significant alterations from baseline were found for DOPAC, HVA, 5-HT and 5-HIIA levels in N-offspring within the time frame of the experiment (Figure 2B-E). This finding agrees with a previous study showing that after 5 mg/kg QTP (i.p.) to naïve Sprague-Dawley rats DA extracellular levels increased up to 57% in the prefrontal cortex [7].

Table 4. Effects of 5 mg/kg QTP systemic injection in MNT exposure in naïve and poly(i:c) offspring.

Compound	C_{max} after QTP dosing (ng/mL)		$AUC_{0\text{-}80min}$ - Basal (ng*min/mL)		$AUC_{100\text{-}380min}$ - Treatment (ng*min/mL)	
	N-Offspring	P-Offspring	N-Offspring	P-Offspring	N-Offspring	P-Offspring
DA	0.66 ± 0.01	0.42 ± 0.02***	28 ± 1	27 ± 1	123 ± 6	86 ± 3***
DOPAC	20.96 ± 1.20	18.42 ± 0.60	1133 ± 50	1088 ± 88	4156 ± 135	3796 ± 115
HVA	51.07 ± 3.59	41.55 ± 2.82	2474 ± 162	2236 ± 149	8750 ± 288	8683 ± 655
5-HT	0.65 ± 0.05	0.53 ± 0.04	41 ± 2	35 ± 5	131 ± 28	134 ± 36
5-HIIA	60.74 ± 4.58	52.71 ± 2.93	4558 ± 135	3950 ± 290	13886 ± 350	12606 ± 480

DA: dopamine; DOPAC: 3-4-dyhydroxyphenilacetic acid; HVA: homovalinic acid; 5-HT: serotonin; 5-HIAA: 5-hydroxyindolacetic acid.
Data represented mean ± S.D. Student's t-test *** $p < 0.01$

No alterations were found in any MNT extracellular levels after QTP dosing to schizophrenic like animals in comparison to the baseline (Table 4, Figure 2 A-E). In other words, poly(i:c) exposed animals (P-offspring) did not respond to the antipsychotic drug. One hypothesis to explain the lack of response in P-offspring is the neurodegenerative hypothesis of schizophrenia, with long-term alterations in blood-brain-barrier permeability after inflammatory events in early life [25] that might affect QTP brain distribution. This finding can help to explain the limited response rate to antipsychotic drugs observed in chronic schizophrenic patients [26].

4. CONCLUSIONS

In the present work a LC-MS/MS method for determination of DA, DOPAC, HVA, 5-HT and 5-HIIA has been developed and validated and presented advantages such as short run time, small sample volume and the possibility of quantification analytes in positive and negative electrospray mode in the same run compared with previously published bioanalytical methods for quantification of neurotransmitters in MICRODIALYSIS samples.

The method was successfully applied for quantification of these MNTs in mPFC cortex microdialysate samples from naïve and poly(i:c) prenatal exposed rats. No alterations in basal extracellular levels were found between groups. However, differently from naïve rats, P-offspring did not respond to QTP systemic administration indicating altered drug brain distribution. To the best of our knowledge this is the first report of lack of QTP alteration on DA levels in this animal model of schizophrenia. Whether these results are due to altered QTP brain pharmacokinetics in this animal model of schizophrenia is under investigation.

5. ACKNOWLEDGEMENTS

The authors acknowledge Dr. Liberato Brum Junior (Prati Donaduzzi, Toledo – PR, Brazil) for kindly providing quetiapine fumarate, and all technical support received from the Animal's Facility staff (UFRGS/Biochemistry Department). This study was financed in part by CNPq/Brazil (Process 421767/2016-2) and by the Coordenação de Aperfeiçoamento de Pessoal de Nível Superior - Brazil (CAPES) - Finance Code 001. The authors also thank CNPq for the individual grants.

6. CONTRIBUTORS

TDC conceived the project and got the financial support. FC, SMKR and TDC designed the experimental protocol. APH provide support and orientation with the neurodevelopmental animal model. FC, VEH, KJS and LBO performed all the method validation and animal experiments. FB developed the analytical method and performed all sample analysis. FC performed the data analysis. FC and TDC wrote the manuscript. All authors approved the final manuscript.

7. REFERENCES

[1] B. Ferry, E.P. Gifu, I. Sandu, L. Denoroy, S. Parrot, Analysis of microdialysate monoamines, including noradrenaline, dopamine and serotonin, using capillary ultra-high performance liquid chromatography and electrochemical detection, J. Chromatogr. B Anal. Technol. Biomed. Life Sci. (2014). doi:10.1016/j.jchromb.2014.01.023.

[2] K. Bera, A.K. Das, A. Rakshit, B. Sarkar, A. Rawat, B.K. Maity, S. Maiti, Fluorogenic Detection of Monoamine Neurotransmitters in Live Cells, ACS Chem. Neurosci. (2018). doi:10.1021/acschemneuro.7b00391.

[3] F. Panin, A. Cathala, P.V. Piazza, U. Spampinato, Coupled intracerebral microdialysis and electrophysiology for the assessment of dopamine neuron function in vivo, J. Pharmacol. Toxicol. Methods. (2012). doi:10.1016/j.vascn.2012.01.003.

[4] T. Suominen, P. Uutela, R.A. Ketola, J. Bergquist, L. Hillered, M. Finel, H. Zhang, A. Laakso, R. Kostiainen, Determination of Serotonin and Dopamine Metabolites in Human Brain Microdialysis and Cerebrospinal Fluid Samples by UPLC-MS/MS: Discovery of Intact Glucuronide and Sulfate Conjugates, PLoS One. 8 (2013) 2–10. doi:10.1371/journal.pone.0068007.

[5] K. Nakao, V. Jeevakumar, S.Z. Jiang, Y. Fujita, N.B. Diaz, C.A. Pretell Annan, K.L. Eskow Jaunarajs, K. Hashimoto, J.E. Belforte, K. Nakazawa, Schizophrenia-Like Dopamine Release Abnormalities in a Mouse Model

of NMDA Receptor Hypofunction, Schizophr. Bull. (2018). doi:10.1093/schbul/sby003.
[6] R. Hadar, M.L. Soto-Montenegro, T. Götz, F. Wieske, R. Sohr, M. Desco, C. Hamani, I. Weiner, J. Pascau, C. Winter, Using a maternal immune stimulation model of schizophrenia to study behavioral and neurobiological alterations over the developmental course, Schizophr. Res. 166 (2015) 238–247. doi:10.1016/j.schres.2015.05.010.
[7] L. Pira, R. Mongeau, L. Pani, The atypical antipsychotic quetiapine increases both noradrenaline and dopamine release in the rat prefrontal cortex, Eur. J. Pharmacol. 504 (2004) 61–64. doi:10.1016/j.ejphar.2004.09.053.
[8] S. Yamamura, K. Ohoyama, T. Hamaguchi, K. Kashimoto, M. Nakagawa, S. Kanehara, D. Suzuki, T. Matsumoto, E. Motomura, T. Shiroyama, M. Okada, Effects of quetiapine on monoamine, GABA, and glutamate release in rat prefrontal cortex, Psychopharmacology (Berl). 206 (2009) 243–258. doi:10.1007/s00213-009-1601-9.
[9] A.G. Zestos, R.T. Kennedy, Microdialysis Coupled with LC-MS/MS for In Vivo Neurochemical Monitoring, AAPS J. 19 (2017) 1284–1293. doi:10.1208/s12248-017-0114-4.
[10] N.G. Girondi, F. Barreto, M.C. Pigatto, T. Dalla Costa, Sensitive analytical method to quantify clindamycin in plasma and microdialysate samples: Application in a preclinical pharmacokinetic study, J. Pharm. Biomed. Anal. 153 (2018) 57–62. doi:10.1016/j.jpba.2018.02.005.
[11] E.C. Palma, J.V. Laureano, B.V. de Araújo, N.G. Meinhardt, A.T. Stein, T. Dalla Costa, Fast and sensitive HPLC/UV method for cefazolin quantification in plasma and subcutaneous tissue microdialysate of humans and rodents applied to pharmacokinetic studies in obese individuals, Biomed. Chromatogr. 32 (2018). doi:10.1002/bmc.4254.
[12] R. Lorenzoni, F. Barreto, R.V. Contri, B.V. de Araújo, A.R. Pohlman, T.D. Costa, S.S. Guterres, Rapid and sensitive LC-MS/MS method for simultaneous quantification of capsaicin and dihydrocapsaicin in microdialysis samples following dermal application, J. Pharm. Biomed. Anal. 173 (2019) 126–133. doi:10.1016/j.jpba.2019.05.029.
[13] A. Gottås, Ripel, F. Boix, V. Vindenes, J. Mørland, E.L. Øiestad, Determination of dopamine concentrations in brain extracellular fluid using microdialysis with short sampling intervals, analyzed by ultra high performance liquid chromatography tandem mass spectrometry, J. Pharmacol. Toxicol. Methods. 74 (2015) 75–79. doi:10.1016/j.vascn.2015.06.002.
[14] S. Greco, W. Danysz, A. Zivkovic, R. Gross, H. Stark, Microdialysate analysis of monoamine neurotransmitters-A versatile and sensitive LC-MS/MS method, Anal. Chim. Acta. 771 (2013) 65–72. doi:10.1016/j.aca.2013.02.004.
[15] J.Y. Hong, N.H. Park, M.S. Oh, H.S. Lee, H. Pyo, J. Hong, Profiling analysis of biogenic amines and their acidic metabolites in mouse brain tissue using gas chromatography-tandem mass spectrometry, J. Chromatogr. B Anal. Technol. Biomed. Life Sci. (2013). doi:10.1016/j.jchromb.2013.09.026.
[16] H. Ko, R.A. Lahti, D.J. Duchamo, M.E. Royer, A GC-MS procedure for the measurement of dopamine in mouse striatal tissue, Anal. Lett. (1974).

[17] M.E.P. Hows, L. Lacroix, C. Heidbreder, A.J. Organ, A.J. Shah, High-performance liquid chromatography/tandem mass spectrometric assay for the simultaneous measurement of dopamine, norepinephrine, 5-hydroxytryptamine and cocaine in biological samples, J. Neurosci. Methods. (2004). doi:10.1016/j.jneumeth.2004.03.021.

[18] R. Nirogi, P. Komarneni, V. Kandikere, R. Boggavarapu, G. Bhyrapuneni, V. Benade, S. Gorentla, A sensitive and selective quantification of catecholamine neurotransmitters in rat microdialysates by pre-column dansyl chloride derivatization using liquid chromatography-tandem mass spectrometry., J. Chromatogr. B. Analyt. Technol. Biomed. Life Sci. (2013). doi:10.1016/j.jchromb.2012.09.034.

[19] C. Ji, W. Li, X.-D. Ren, A.F. El-Kattan, R. Kozak, S. Fountain, C. Lepsy, Diethylation labeling combined with UPLC/MS/MS for simultaneous determination of a panel of monoamine neurotransmitters in rat prefrontal cortex microdialysates., Anal. Chem. 80 (2008) 9195–203. doi:10.1021/ac801339z.

[20] P. Song, O.S. Mabrouk, N.D. Hershey, R.T. Kennedy, In vivo neurochemical monitoring using benzoyl chloride derivatization and liquid chromatography-mass spectrometry., Anal. Chem. 84 (2012) 412–9. doi:10.1021/ac202794q.

[21] Fda, Cder, Bioanalytical Method Validation Guidance for Industry Biopharmaceutics Bioanalytical Method Validation Guidance for Industry Biopharmaceutics Contains Nonbinding Recommendations, 2018. http://www.fda.gov/Drugs/GuidanceComplianceRegulatoryInformation/Guidances/default.htmand/orhttp://www.fda.gov/AnimalVeterinary/GuidanceComplianceEnforcement/GuidanceforIndustry/default.htm.

[22] D. Zimmer, New US FDA draft guidance on bioanalytical method validation versus current FDA and EMA guidelines: Chromatographic methods and ISR, Bioanalysis. (2014). doi:10.4155/bio.13.298.

[23] L. Zuckerman, M. Rehavi, R. Nachman, I. Weiner, Immune Activation During Pregnancy in Rats Leads to a PostPubertal Emergence of Disrupted Latent Inhibition, Dopaminergic Hyperfunction and Altered Limbic Morphology in the Offspring: A Novel Neurodevelopmental Model of Schizophrenia, Neuropsychopharmacology. 28 (2003) 1778–1789. doi:10.1038/sj.npp.1300248.

[24] A. Luchicchi, S. Lecca, M. Melis, M. De Felice, F. Cadeddu, R. Frau, A.L. Muntoni, P. Fadda, P. Devoto, M. Pistis, Maternal immune activation disrupts dopamine system in the offspring, Int. J. Neuropsychopharmacol. (2016). doi:10.1093/ijnp/pyw007.

[25] H.B. Stolp, C.J. Ek, P.A. Johansson, K.M. Dziegielewska, N. Bethge, B.J. Wheaton, A.M. Potter, N.R. Saunders, Factors involved in inflammation-induced developmental white matter damage., Neurosci. Lett. 451 (2009) 232–6. doi:10.1016/j.neulet.2009.01.021.

[26] M.J. Millan, A. Andrieux, G. Bartzokis, K. Cadenhead, P. Dazzan, P. Fusar-Poli, J. Gallinat, J. Giedd, D.R. Grayson, M. Heinrichs, R. Kahn, M.-O. Krebs, M. Leboyer, D. Lewis, O. Marin, P. Marin, A. Meyer-Lindenberg, P. McGorry, P. McGuire, M.J. Owen, P. Patterson, A. Sawa, M. Spedding, P. Uhlhaas, F. Vaccarino, C. Wahlestedt, D. Weinberger, Altering the course of schizophrenia: progress and perspectives, Nat. Rev. Drug Discov. 15 (2016) 485. doi:10.1038/nrd.2016.28.

SUPPLEMENTARY MATERIAL

Table S1. Intra and inter-assay precision and accuracy of the method for determining DA in quality control samples.

Nominal Concentrations (ng/ mL)	Intra-day precision[a]				Inter-day precision[b]		C.V. Accuracy
	Day 1		Day 2				
	Mean ± S.D.	R.S.D. (%)	Mean ± S.D.	R.S.D. (%)	Mean ± S.D.	R.S.D (%)	Range (%)
0.05	0.060 ± 0.002	5.21	0.050 ± 0.006	12.05	0.054 ± 0.005	9.89	87.7 – 119.2
0.15	0.15 ± 0.01	4.84	0.14 ± 0.01	5.84	0.144 ± 0.008	5.85	89.19 – 105.2
55.0	55.69 ± 2.19	3.92	56.70 ± 3.51	6.18	56.19 ± 2.83	5.04	95.3 – 115.5
80.0	74.48 ± 4.18	6.46	76. 51 ± 1.93	2.53	75.40 ± 3.76	4.99	87.7 – 98.88

[a]Mean of replicates (n = 6/QC/compound); [b]Mean of two days (n = 12/QC/compound). S.D.: standard deviation, R.S.D: relative standard deviation, C.V.: coefficient of variation.

Table S2. Intra and inter-assay precision and accuracy of the method for determining DOPAC in quality control samples.

Nominal Concentrations (ng/ mL)	Intra-day precision[a]				Inter-day precision[b]		C.V. Accuracy
	Day 1		Day 2				
	Mean ± S.D.	R.S.D. (%)	Mean ± S.D.	R.S.D. (%)	Mean ± S.D.	R.S.D (%)	Range (%)
10.0	9.82 ± 1.10	11.24	9.92 ± 1.08	10.97	9.87 ± 0.99	10.11	86.29 – 114.51
20.0	20.81 ± 1.62	7.77	20.52 ± 2.14	10.40	20.66 ± 1.81	8.77	89.29 – 114.80
55.0	56.69 ± 1.89	3.33	55.10 ± 5.26	9.54	55.89 ± 3.87	6.90	88.02 – 109.22
80.0	80.95 ± 6.05	7.48	76.06 ± 6.51	8.57	78.50 ± 6.51	8.30	86.26 – 113.86

[a]Mean of replicates (n = 6/QC/compound); [b]Mean of two days (n = 12/QC/compound). S.D.: standard deviation, R.S.D: relative standard deviation, C.V.: coefficient of variation.

Table S3. Intra and inter-assay precision and accuracy of the method for determining HVA in quality control samples.

Nominal Concentrations (ng/mL)	Intra-day precision[a]				Inter-day precision[b]		C.V. Accuracy
	Day 1		Day 2				
	Mean ± S.D.	R.S.D. (%)	Mean ± S.D.	R.S.D. (%)	Mean ± S.D.	R.S.D (%)	Range (%)
0.5	0.53 ± 0.04	8.61	0.50 ± 0.06	12.14	0.51 ± 0.05	10.52	89.46 – 115.53
1.5	1.40 ± 0.08	5.75	1.48 ± 0.11	7.57	1.42 ± 0.09	6.31	86.92 – 108.24
55.0	51.40 ± 5.02	9.76	57.29 ± 2.58	4.50	54.34 ± 4.89	9.00	85.35 – 108.62
80.0	82.62 ± 3.00	3.63	91.48 ± 3.32	3.64	87.04 ± 5.52	6.34	98.77 – 113.63

[a]Mean of replicates (n = 6/QC/compound); [b]Mean of two days (n = 12/QC/compound). S.D.: standard deviation, R.S.D: relative standard deviation, C.V.: coefficient of variation.

Table S4. Intra and inter-assay precision and accuracy of the method for determining 5-HT in quality control samples.

Nominal Concentrations (ng/ mL)	Intra-day precision[a]				Inter-day precision[b]		C.V. Accuracy
	Day 1		Day 2				
	Mean ± S.D.	R.S.D. (%)	Mean ± S.D.	R.S.D. (%)	Mean ± S.D.	R.S.D (%)	Range (%)
0.1	0.090 ± 0.002	3.12	0.100 ± 0.009	8.67	0.096 ± 0.010	10.44	84.91 – 114.30
0.3	0.29 ± 0.02	6.17	0.32 ± 0.03	10.83	0.304 ± 0.027	8.98	88.14 – 113.30
55.0	54.75 ± 1.09	1.98	59.56 ± 3.47	5.83	57.15 ± 3.51	6.14	89.50 – 114.80
80.0	77.65 ± 4.49	5.79	82.08 ± 1.91	2.33	79.86 ± 4.02	5.04	88.35 – 114.22

[a]Mean of replicates (n = 6/QC/compound); [b]Mean of two days (n = 12/QC/compound). S.D.: standard deviation, R.S.D: relative standard deviation, C.V.: coefficient of variation.

Table S5. Intra and inter-assay precision and accuracy of the method for determining 5-HIIA in quality control samples.

Nominal Concentrations (ng/mL)	Intra-day precision[a]				Inter-day precision[b]		C.V. Accuracy
	Day 1		Day 2				
	Mean ± S.D.	R.S.D. (%)	Mean ± S.D.	R.S.D. (%)	Mean ± S.D.	R.S.D (%)	Range (%)
1.0	1.15 ± 0.03	3.30	1.10 ± 0.05	4.62	1.29 ± 0.05	4.56	105.80 – 119.10
3.0	2.75 ± 0.19	6.77	3.00 ± 0.19	6.28	2.88 ± 0.22	7.92	85.74 – 104.95
55.0	50.52 ± 3.21	6.35	56.66 ± 3.19	5.62	53.59 ± 4.42	8.26	87.51 – 111.51
80.0	85.32 ± 4.81	5.64	86.03 ± 5.45	6.45	85.67 ± 4.96	5.79	93.92 – 115.43

[a]Mean of replicates (n = 6/QC/compound); [b]Mean of two days (n = 12/QC/compound). S.D.: standard deviation, R.S.D: relative standard deviation, C.V.: coefficient of variation.

CAPÍTULO 3

SEMI-MECHANISTIC PHARMACOKINETIC MODELING OF LIPID CORE NANOCAPSULES: UNDERSTANDING QUETIAPINE PLASMA AND BRAIN DISPOSITION IN A NEURODEVELOPMENTAL ANIMAL MODEL OF SCHIZOPHRENIA

Carreño F[1], Helfer VE[1], Staudt KJ[1], Olivo, LB[1], Paese K[1], Meyer FS[2], Herrmann AP[3], Guterres SS[1], Rates SMK[1], Trocóniz, IF[4,5], Dalla Costa T[1]

[1]Programa de Pós-Graduação em Ciências Farmacêuticas, Faculdade de Farmácia, Universidade Federal do Rio Grande do Sul;

[3]Programa de Pós-Graduação em Farmacologia e Terapêutica, Instituto de Ciências Básicas da Saúde, Universidade Federal do Rio Grande do Sul;

[4]Pharmacometrics & Systems Pharmacology Research Unit, Department of Pharmaceutical Technology and Chemistry, School of Pharmacy and Nutrition, University of Navarra;

[5] IdiSNA, Navarra Institute for Health Research.

ABSTRACT

This study investigated plasma and brain disposition of quetiapine lipid core nanocapsules (QLNC) in naïve and schizophrenic (SCZ-like) rats and developed a semi-mechanistic model to describe changes in both compartments following administration of drug in solution (FQ) or nanoencapsulated. QLNC (1 mg/mL) presented 166 ± 39 nm, low polydispersity, and high encapsulation (93.0 ± 1.4%). Model building using experimental data from total and unbound plasma and unbound brain concentrations obtained by microdialysis after administration of single i.v. *bolus* dose of FQ or QLNC to naïve and SCZ-like rats. A two-compartment model was identifiable both in blood and in brain with a bi-directional drug transport across the blood-brain barrier (CL_{in} and CL_{out}). SCZ-like rats significant decrease in brain exposure with FQ (decrease in CL_{in}) was reverted by QLNC showing that nanocarriers govern quetiapine tissue distribution. Model simulations allowed exploring the potential of LCN for brain delivery.

Keywords: lipid core nanocapsules; schizophrenia; poly(i:c); microdialysis; population pharmacokinetics model; quetiapine.

1. INTRODUCTION

Schizophrenia (SCZ) is a chronic debilitating mental disorder most often presented in early adulthood with core symptoms of lose touch with reality, social withdraw and cognitive inflexibility (Moretti et al., 2018). Available psychotropic medicines face important challenges to produce efficacious treatments, since an important number of patients are non-responsive to pharmacological therapy. Most patients with SCZ will present multiple relapses during the course of the illness even when receiving medication in adequate dosage and treatment duration. Moreover, it is estimated that around 60% of SCZ patients respond partially to treatment and 30% of them are treatment resistant patients (Batail et al., 2014; Kennedy et al., 2014).

The development of new effective therapies for central nervous system (CNS) disorders is a huge challenge for the pharmaceutical industry (Lindqvist et al., 2016a, 2013). One important obstacle in this scenario is the blood-brain barrier (BBB) that significantly limits the ability of therapeutic agents to reach relevant concentrations at their targets in the CNS due to restrict paracellular and transcellular transport of endogenous and xenobiotic compounds to the brain (Carreño et al., 2016a; Lindqvist et al., 2013).

Nanoparticles are being developed as versatile platforms for modifying pharmacokinetic profile and pharmacological performance of loaded drugs (Yuan et al., 2019) and have been used as carriers for drug delivery to the brain (He et al., 2018; Lindqvist et al., 2016b; Carreño et al., 2016a, 2016b, 2015a; Dimer et al., 2014).

Nevertheless, little is known about the mechanisms by which nanocarriers improve *in vivo* drug's effect (Lindqvist et al., 2016a; Petros and DeSimone, 2010). An innovative way to improve the understanding of the key factors controlling plasma and brain drug disposition following loaded nanocarrier administration is the use of model based approaches (Lindqvist et al., 2016a). In the literature, there are some examples of population as well as physiologically based modeling of drugs incorporated into nanocarriers for CNS delivery (Lindqvist et al., 2016a; Moss and Siccardi, 2014).

The high variability in response associated to chronic SCZ response to treatment may be partially related to BBB dysfunction caused by the disease and

consequent alterations on antipsychotic drug transport to CNS. Assuming that limited drug delivery to CNS in schizophrenic patients could be associated with pharmacotherapy resistance we developed quetiapine (QTP) lipid core nanocapsules (LNC, QLNC) aiming to improve drug targeting to the brain.

In previous reports, we have shown that QLNC formulation systemically given to naïve rats significantly increased total QTP brain exposure, determined in tissue homogenate, in comparison to rats that received non-encapsulated drug (Carreño et al., 2016b). Furthermore, we demonstrated using microdialysis that the LNC promote QTP vectorization to the brain, increasing hippocampal free drug concentrations. We also showed that LNC are capable of carrying QTP across the BBB, avoiding influx transporters, instead of altering the barrier permeability (Carreño et al., 2016a). The former studies provided strong evidence that the developed QLNC modulate QTP pharmacokinetics and transport across the BBB, improving drug delivery to the brain. However, the studies were conducted in naïve animals and the influence of SCZ alterations on BBB was not addressed.

Although modeling and simulation has a great potential for elucidating the underlining mechanism of drug delivery from nanocarriers, there is a lack of quantitative evaluation of these systems performance in the course of diseases that can interfere with BBB drug's transport such as schizophrenia.

Neurodevelopmental model of SCZ induced by the administration of viral mimic polyinosinic–polycytidilic acid [poly(i:c)] to pregnant rats has substantial predictive validity already described in the literature, besides preclinical relevance for the exploration of novel therapeutic pharmacological strategies, such as the use of nanocarriers (Möller et al., 2015).

One of the most consistently observed behavioral findings reported in literature after prenatal treatment with poly(i:c) at different gestational periods is the deficit in prepulse inhibition of startle response (PPI) (Yee et al., 2011). Using this animal model we demonstrated that QTP solution was not capable of producing a reversal in the sensorimotor gating-disruptive effect caused by the prenatal poly(i:c) exposure. However, the same QTP dose given as nanoparticles significantly improved PPI impairment, indicating that this delivery system is a promising alternative to improve antipsychotic drug effects (Carreño et al., 2019).

In the current study we aim developing a semi-mechanistic pharmacokinetic model, using a populational (popPK) approach, capable of describing changes in

plasma and brain pharmacokinetics after administration of QTP in solution (FQ) or nanoencapsulated in lipid core nanocapsules (QLNC) to naïve and poly(i:c) prenatal exposed rats (SCZ-like), viewing to increase the understanding of the role of this drug delivery system when brain drug disposition is compromised.

2. MATERIALS AND METHODS

2.1. Chemicals and reagents

Quetiapine hemifumarate (purity) ≥ 98.0% was kindly donated by Pratti-Donaduzzi Medicamentos Genéricos (Brazil). Polyinosic-polycytidylic acid sodium salt (#P1530) was obtained from Sigma-Aldrich (Brazil). Polysorbate-80 (Tween® 80) was purchased from Delaware Química (Brazil). HPLC-grade methanol and acetonitrile were obtained from Merck (Brazil) and all other chemicals and reagents utilized were of analytical grade. Artificial cerebrospinal fluid (ACF) solution consisted of NaCl 145 mM; KCl 2.7 mM; $CaCl_2$ 1.2 mM; $MgCl_2$ 1mM, pH 6.2.

2.2. Quetiapine lipid core nanocapsules (QLNC) preparation

QTP lipid-core nanocapsules (QLNC – 1 mg/mL) were obtained by nanoprecipitation of the preformed polymer as previously published (Carreño et al., 2016b). All batches used in this study (n = 5) were physicochemically characterized and presented average size of 166 ± 39 nm, low polydispersity index (< 0.15), and high encapsulation efficiency (93.0 ± 1.4 %), similar to those LNC previously published (Carreño et al., 2016a, 2016b).

A control formulation (FQ, 5 mg/mL) was prepared first dissolving QTP in acetic acid (99%), then saline 0.9% containing P-80 (78 mg/mL) was added and the pH was adjusted to 6.5 ± 0.5 using NaOH (8 M).

2.3 Pharmacokinetic Study Design

2.3.1 Animals

This study was approved by the Ethics Committee in Animal Use from the Federal University of Rio Grande do Sul (UFRGS/CEUA #31001). Male (300 – 350 g) and female (200 – 270 g, nulliparous) Wistar breeders were obtained from the

Central Animal Facilities of University's Biochemistry Department (Porto Alegre, Brazil) and housed (3/cage) in a controlled environment (22 ± 2 °C, 65% humidity in a 12 h light/dark cycle) with free access to standard rodent chow and filtered water. The offspring were maintained in the same conditions.

2.3.2 Prenatal poly(i:c) challenge

Poly(i:c) 4 mg/mL stock solution was prepared in sterile pyrogen-free 0.9% NaCl according to manufacturer instructions and diluted to a final 2 mg/mL sterile solution in the same vehicle and stored at -20 ± 1 °C until use.

For the prenatal poly(i:c) challenge, female rats were mated according to a timed-mating breeding scheme (Pritchett-Corning et al., 2009). On the morning of gestational day 15 (GD15) pregnant damns (n = 6 dams) were given a single intravenous bolus injection of 4mg/kg of poly(i:c) via the lateral tail vein and females were housed individually until the birth of their offspring.

On post-natal day (PND) 1, pups were sexed, weighed and culled to eight pups per litter considering 4 females and 4 males (when possible). Weaning occurred at PND21 when pups where housed (4 animals/cage) according to sex and litter.

2.3.3 Pre-pulse inhibition of acoustic startle reflex

Sensory gating deficits as reflected in impaired PPI constitute one of the core features of schizophrenia. To confirm that the neurodevelopmental model of schizophrenia described in the literature was adequately induced in our laboratory, SCZ-like deficit in the adult offspring (PND75) was accessed by pre-pulse inhibition of the startle response (PPI) in comparison to a naïve rat's offspring.

Briefly, acclimatization (5 min, background noise, 68 dB) in the startle chamber (Insight®) was followed by 10 initial startle stimuli (120 dB). Test was started with different trial types in random order: pulse alone (120 dB), background noise (68 dB), pre-pulse (PP 71, 77 or 85 dB) + pulse. A total of 10 presentations of each trial type were given with an inter-stimulus interval randomized between 15 ± 8s. These results were used during model development.

2.3.4 Surgical procedure

Forty eight hours before plasma pharmacokinetic and brain microdialysis experiments adult male and female SCZ-like rats (post-natal day 75 – 85) were anesthetized (ketamine/xilazine/acepromazine: 100 mg/kg -10 mg/kg - 2 mg/kg; i.p.), received pre-emptive analgesia (ketoprofen, 5 mg/kg, s.c.) and local anesthesia (5 mg/kg lidocaine - 2 mg/kg bupivacaine, s.c.). This pharmacological combination, pre-emptive analgesia and addition of bupivacaine in local anesthesia for the management of postsurgical pain, resulted in reduction of weight loss and normal feeding behavior after surgery.

Using a stereotaxic apparatus (ASI instruments, USA) a CMA-12 guide cannula was placed into the ventral hippocampus (A: -5.20 mm; L:+4.80 mm; V:-4.50 mm relative to bregma; HIP groups) or medium prefrontal cortex (A: +3.2 mm, L: +0.8 mm, V: -5.2 mm relative to bregma; mPFC groups) (Paxinos and Watson, 2013). A Silastic® medical-grade tubing (Dow Corning, USA) was inserted in the right jugular vein and passed subcutaneously to the posterior surface of the neck, for total blood sampling. To avoid clotting, the jugular vein catheter was filled with heparin solution (100 IU/mL in phosphate buffer-saline pH: 7.4 ± 0.1). Animals recovered from the surgery in individual polypropylene boxes with food and water *ad libitum*.

2.3.5 *In vivo* microdialysis probe recovery

QTP *in vivo* relative recovery was determined by retrodialysis (RR_{RD}) in HIP and mPFC. After the surgery recovery period and 30 min before the start of the experiments, male and female (n = 4/brain region/sex) SCZ-like animals were placed in a CMA/120 system for freely moving animals and the guide cannula was carefully replaced with a CMA/12 microdialysis probe (3 mm, PAES membrane, 20 kDa cutoff – CMA®, Sweden). Probe was perfused with QTP 300 ng/mL solution in ACF at a flow rate of 2.0 µL/min for 1 h for equilibration. Microdialysate samples were collected each 30 min up to 120 min and injected directly into the LC system for quantification. *In vivo* RR_{RD} was calculated as described previously (Araujo et al., 2008).

Probe relative recovery *in vivo* did not differ between male and female rats and the mean value of 28.1 ± 5.3% and 31.1 ± 6.1% and for HIP and mPFC, respectively, was used to determine real QTP free brain concentrations.

2.3.6 Quetiapine plasma pharmacokinetic and unbound HIP and mPFC distribution

SCZ-like offspring were randomly divided in eight groups according to sex and treatment type: $FQ_{HIP,male}$ (n = 8); $QLNC_{HIP,male}$ (n = 7); $FQ_{HIP,female}$ (n = 7); $QLNC_{HIP,female}$ (n = 6), $FQ_{mPFC,male}$ (n = 6); $QLNC_{mPFC,male}$ (n = 6); $FQ_{mPFC,female}$ (n = 6); $QLNC_{mPFC,female}$ (n = 6). Naïve offspring were also divided in the following groups: $FQ_{naïve,male,mPFC}$ (n = 6), $QLNC_{naïve,male,mPFC}$ (n = 6) and $FQ_{naïve,female,HIP}$ (n = 6).

QTP total plasma pharmacokinetics and unbound brain concentrations, determined by microdialysis, were evaluated in awake animals after a single intravenous *bolus* dose via lateral tail vein of QTP solution (FQ groups - 10 mg/kg) or QLNC formulation (QLNC groups - 5 mg/kg).

In the day of the experiment, animals were placed individually in a CMA-120 system for freely moving animals and the guide cannula was replaced with a previous calibrated CMA/12 probe for microdialysis sampling. The microdialysis system was stabilized during 1 h with perfusion of ACF solution at a flow rate of 2.0 µL/min. After animals dosing, microdialysate samples were collected every 30 min up to 8 h. A previously validated HPLC-UV method was used to analyze microdialysate samples that were injected directly into the system without any processing (Carreño et al., 2016b).

Blood samples were collected through the jugular vein at scheduled time points (0.083; 0.25; 0.5; 1; 2; 4; 6; 8 h after dosing). Plasma obtained by centrifugation (1300 *g*, 10 min, at 4 ± 2° C) was stored at -80 °C ± 1° C until analysis. A previous validated HPLC-UV method was used for the quantification of QTP in plasma samples (Carreño et al., 2016a).

Results obtained for other male naïve groups that received FQ and QLNC, previously reported (Carreño et al., 2016b, 2016a), were also used during model building. Briefly, QTP total plasma pharmacokinetics and unbound HIP concentrations, determined by microdialysis, were evaluated in naïve awake animals after a single intravenous (i.v) *bolus* dose of 5 mg/kg (n = 7) and 10 mg/kg of FQ (n = 6) or 5 mg/kg QLNC (n = 7) via lateral tail vein. Plasma microdialysis

was performed in two groups (n = 6 animals/group). Each group received FQ (10 mg/kg) or QLNC (5 mg/kg) i.v. *bolus* administration via lateral tail vein.

2.4 Model-based data analysis

Data analysis was performed based on the population analysis approach using the software NONMEM (version 7.4, ICON Development Solutions, Ellicott City, MD, USA) and first-order conditional estimation method with interaction (FOCE-INTERACTION) was applied in all estimations.

A total of 1158 observations (356 total plasma samples, 42 unbound plasma samples and 760 brain microdialysate samples) from a total of 56 rats were used for the analysis of the FQ formulation and 886 observations (296 total plasma samples, 72 unbound plasma samples and 518 brain microdialysate samples) from a total of 40 rats were included in the analysis of QLNC formulation, including data from previous studies. Data below the quantification limit (BQL) were reported and kept in the data set since they represented less than 5% of the total data. Missing data were excluded from the analysis since they also represented less than 5% of the total data. All observations were natural logarithm transformed for the analysis.

Inter-individual variability (IIV) was modeled exponentially and expressed as coefficient of variation [CV (%)], and the non-diagonal elements of the omega (Ω) variance-covariance matrix were evaluated for significance. Intra-individual (residual) variability as described with an additive error model on the logarithm scale.

Model building was performed sequentially. First, a model to simultaneously described the total and unbound plasma concentrations in naïve and SCZ-like animals after the administration of the FQ formulation was developed, and thereafter, unbound HIP and mPFC data were added. The model for FQ formulation was expanded using the data from QLNC groups to describe different features of the QLNC formulation (plasma and tissue release from the nanocarrier, including an estimate for the fraction of the dose associated to the interface of the polymeric shell that is released as a burst after the administration of the nanocarrier). Microdialysate samples were described by the integral over each collection interval instead of a midpoint approach (Tunblad et al., 2004). All models were parametrized as a system of ordinary differential equations.

Model selection was based on the (i) changes in the minimum value of the objective (OFV) function approximately equal to -2*log(likelihood). The addition of a parameter in the models was considered statistically significant when the OFV dropped at least 3.84 ($p < 0.05$ for one degree of freedom), (ii) visual exploration of goodness of fit plots and (iii) precision of model parameters reflected as the relative standard error (RSE) computed as the ratio between the standard error and the parameter estimate.

The effects of the poly(i:c) exposure in all model parameters was investigated with stepwise covariate modeling (SCM), using a forward inclusion ($p < 0.05$) followed by backward elimination process ($p < 0.01$) (Wählby et al., 2002).

Evaluation of the selected PK model was performed through the simulation-based diagnostics prediction-corrected visual predictive checks (pcVPC) (Bergstrand et al., 2011). For each formulation and experimental group, one thousand simulated PK animal profiles were generated, then for each measurement time the 5^{th}, 50^{th}, and 95^{th} percentiles of were calculated and displayed graphically together with the experimental data. Parameter precision was evaluated from the analysis of five hundred simulated bootstrap datasets. The PsN (version 4.5.1) tool kit (Lindbom et al., 2005), the R (version 3.5.1) program, and the Xpose 4 (version 4.4.1) program (Jonsson and Karlsson, 1999) were used for automating and controlling the runs, data visualization, and graphical analysis (goodness-of-fit graphics, including pcVPCs and bootstrap analysis), respectively. The Pirana (version 2.9.8) program (Keizer et al., 2013) was used to keep track of run records and results.

2.5 Model validation and simulations

The selected model developed to describe total plasma and unbound brain concentrations after FQ administration was used to investigate the influence of probenecid on QTP transport across blood-brain barrier in naïve rats under the conditions described by Carreño et al (2016b) to externally validate the model performance under new experimental scenarios. The data set from QLNC animals administered with probenecid was too small to be used for model external validation.

The selected model was used to simulate plasma pharmacokinetics and brain disposition of FQ and QLNC to explore the differences observed in naïve and SCZ-like animals when received both formulations. Simulations were also performed viewing to demonstrate, in SCZ-like animals, the impact of alteration on the release rate of QTP from nanoparticles core (K_{SLOW}) by varying this parameter from $4.7x10^{-6}$ to $4.7x10^{-2}$ h^{-1}, keeping all the other parameters fixed.

3. RESULTS

3.1 Pre-pulse inhibition of acoustic startle reflex

The mean PPI (%) across all prepulse stimuli used for naïve and SCZ-like animals were analyzed by Student's t test ($\alpha = 0.05$) and were in agreement with our previous study (Carreño et al., 2019). Adult SCZ-like offspring exhibited significant preattentional sensorimotor gating deficits ($p < 0.01$) manifested as a reduction in PPI (Figure 1).

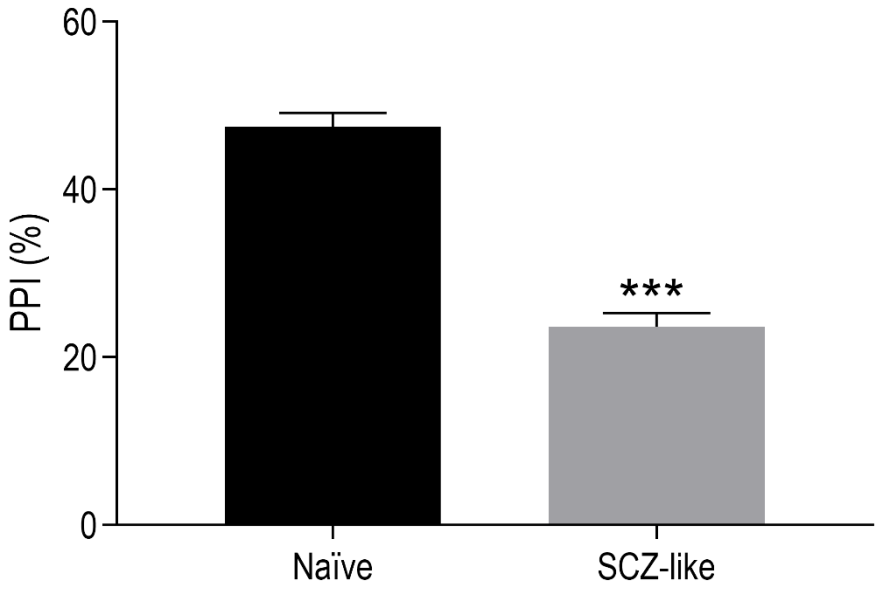


Figure 1. Deficit in sensorimotor gating assessed by the paradigm of prepulse inhibition (PPI) of the acoustic startle response. Bar plot depicts the mean %PPI across all prepulse stimuli used for males and females. *** $p < 0.01$ difference between SCZ-like animals compared to naïve. Student's t test ($\alpha = 0.05$), n = 18-22 animals/group, all values are mean ± S.E.M.

3.2. Population pharmacokinetic analysis

The schematic representation of the full PK model simultaneously describing the fate of total and unbound plasma concentrations and unbound concentrations in brain of QTP administered as single dose solution or encapsulated into lipid core nanocapsules to healthy or SCZ-like animals is shown in Figure 2.

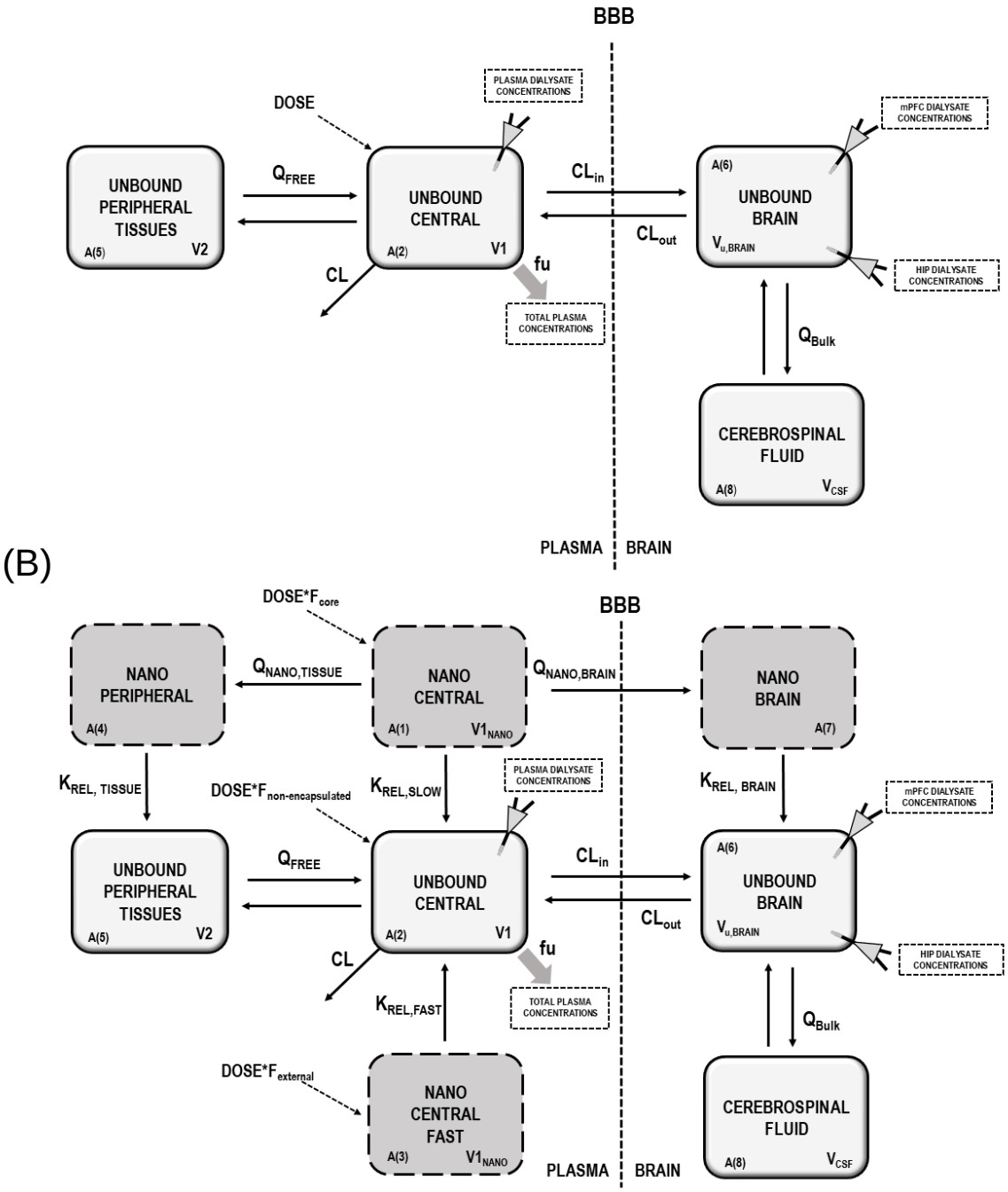


Figure 2**:** Schematic representation of the final QTP model for FQ (A) and QLNC (B) formulation. The compartment numbers used in EQs. 1 – 8 are given within parentheses. Abbreviations: BBB, blood-brain barrier; fu, unbound fraction; CL_{in}, influx clearance; CL_{out}, efflux clearance, CL, unbound QTP clearance; Q_{FREE}, unboud QTP intercompartmental clearance; Q_{bulk}, clearance from brain to cerebrospinal fluid; $Q_{NANO,BRAIN} = Q_{NANO,TISSUE}$, distribution rate constant of the nanoparticle to brain and tissue, respectively. V_1 and V_2 the central and the peripheral volume of distribution for the unbound QTP, respectively; $V_{u,BRAIN}$, unbound volume of distribution in the brain; V_{CSF}, volume of unbound cerebrospinal fluid; V_{1NANO}, volume of distribution for the nanoparticles in plasma; $K_{rel,slow}$, slow release constant of the drug from the nanocarrier in plasma; $K_{rel,fast}$, fast release constant of the drug in plasma; $K_{rel,tissue} = K_{rel,brain}$, release constant of drug from the nanocarrier in tissue/plasma.

3.2.1. Pharmacokinetic model after the administration of the FQ formulation

3.2.1.1. Plasma

With regard to the disposition of unbound QTP concentrations in plasma, a two compartments model described the data significantly better ($p < 0.01$) than the simpler one compartment model. On the other hand, increasing the number of distribution compartments did not improve the fit in a significant manner ($p > 0.05$). The distribution process between the peripheral and central compartments, and the elimination process are represented by Q_{Free} (distribution clearance) and CL (total plasma clearance), respectively. V_1, and V_2 correspond to the apparent volumes of distribution of the central and peripheral compartments, respectively. Total QTP plasma concentrations were described scaling the predicted unbound concentrations by $1/f_u$, where f_u, is the QTP unbound fraction in plasma.

3.2.1.2. Brain

Reversible transfer of unbound QTP between central compartment and brain through the BBB were described by the distribution clearances CL_{in} and CL_{out} parameterized in the model as $K_{in} \times V_1$ and $K_{out} \times V_{u,Brain}$, where K_{in} and K_{out} are the first order rate constant of influx and efflux, respectively. The value of $V_{u,Brain}$, the brain volume of distribution for unbound QTP, used in the current analysis was 3.4×10^{-4} L, calculated based on our previous work (Carreño et al., 2016b) according to the approach described by Tubland and coworkers (2004). During the model building process a model with same magnitude of CL_{in} and CL_{out} was fitted to the data resulting in a significantly worse fit ($p < 0.01$).

Disposition of unbound QTP concentrations in brain was significantly better described with a two compartments model in comparison to a model with just one compartment ($p < 0.01$). The cerebrospinal space was considered as the peripheral compartment within brain, with values of volume of distribution (V_{CSF}) of 2.5×10^{-4} L (calculated as described for $V_{u,Brain}$), and bulk flow (Q_{Bulk}) of 1.2×10^{-5} L/h (Ball et al., 2014).

3.2.2. Pharmacokinetic model after the administration of the LCN formulation

The current model considers that once QTP is released from the LNC formulations, the time course of unbound concentrations in plasma and brain, and total plasma concentrations are described by the model developed for the FQ formulation as explained above. Therefore, data following LNC dosing provide support to characterize the released kinetics in different tissues and distribution characteristics of the nanocarrier.

The final model considers that distribution of QTP within LNC is not homogenous. In fact fractions of the administered QTP dose which are assumed to be located in the core (F_{core}) or in the external layers ($F_{external}$) of the nanocarrier are released into the central unbound QTP compartment at first order rates described by the constants $K_{REL,\ SLOW}$, and $K_{REL,FAST}$, respectively. The remaining fraction of the dose ($F_{non\text{-}encapsulated}$), assumed to be non-encapsulated enters into the systemic circulation directly as free QTP in solution. Simpler models (i.e., homogeneous distribution of QTP within the formulation) were also tested resulting in worse fits.

QTP in the external layers ($F_{external}$) is rapidly released in the unbound QTP central compartment upon intravenous dosing. The model did not support a distribution of this fraction into the brain. However the core of the nanoparticles (F_{core}) containing QTP can be distributed irreversibly from the central compartment either to the brain or to the rest of the body releasing the drug from the LNC following first order processes governed by the $K_{REL,BRAIN}$ and $K_{REL,TISSUES}$ constants, respectively. Bidirectional transfer between compartments was also tested providing worse description of the data. The parameters $Q_{NANO,TISSUE}$ and $Q_{NANO,BRAIN}$ describe the unidirectional distribution clearances from the central compartment of the nanoparticles to the peripheral and brain compartments, respectively. Results showed than the estimates of $K_{REL,TISSUES}$, and $Q_{NANO,TISSUE}$ were not significant different from those corresponding to brain ($p > 0.05$), therefore both compartments shared the same parameters. $V_{1,NANO}$, represent the apparent volume of distribution of the nanoparticles in the central compartment.

The following set of ordinary differential equations define the model represented in Figure 2 and discussed above:

$$\frac{dA_1}{dt} = -\left(\frac{Q_{nano,tissue}}{V_{1,NANO}} + \frac{Q_{nano,brain}}{V_{1,NANO}} + K_{slow}\right) \cdot A_1 \quad (1)$$

$$\frac{dA_2}{dt} = -\left(\frac{CL}{V_1} + \frac{Q_{FREE}}{V_1} + \frac{CL_{in}}{V_1}\right) \cdot A_2 + \frac{CL_{out}}{V_{u,brain}} \cdot A_6 + K_{rel,slow} \cdot A_1 + K_{rel,fast} \cdot A_3 \quad (2)$$

$$\frac{dA_3}{dt} = -K_{rel,fast} \cdot A_3 \quad (3)$$

$$\frac{dA_4}{dt} = -K_{rel,tissue} \cdot A_4 + \frac{Q_{nano,tissue}}{V_{1,NANO}} \cdot A_1 \quad (4)$$

$$\frac{dA_5}{dt} = -\frac{Q_{FREE}}{V_2} \cdot A_5 + K_{rel,tissue} \cdot A_4 + \frac{Q_{FREE}}{V_1} \cdot A_2 \quad (5)$$

$$\frac{dA_6}{dt} = -\left(\frac{CL_{out}}{V_{u,brain}} + \frac{Q_{bulk}}{V_{u,brain}}\right) \cdot A_6 + \frac{CL_{in}}{V_1} \cdot A_2 + K_{rel,brain} \cdot A_7 + \frac{Q_{bulk}}{V_{CSF}} \cdot A_8 \quad (6)$$

$$\frac{dA_7}{dt} = -K_{rel,brain} \cdot A_7 + \frac{Q_{nano,brain}}{V_{1,NANO}} \cdot A_1 \quad (7)$$

$$\frac{dA_8}{dt} = -\frac{Q_{bulk}}{V_{CSF}} \cdot A_8 + \frac{Q_{bulk}}{V_{u,brain}} \cdot A_6 \quad (8)$$

where A_2, A_5, A_6 and A_8 represents the amounts of unbound drug in the central plasma compartment, peripheral plasma compartment, unbound brain plasma compartment and cerebrospinal fluid compartment, respectively; and the amount of QTP loaded into the nanocarrier in represented by A_1 and A_3 (central plasma compartment), A_4 (peripheral tissue compartment) and A_7 (brain tissue compartment).

The microdialysate plasma ($C_{dyalisate,plasma}$) and brain ($C_{dyalisate,brain}$) concentrations were expressed as the integral over each collection interval, represented by t1 and t2 divided by TIN, the sampling time interval for each microdialysate:

$$C_{dyalisate,plasma} = \left[\int_{t1}^{t2} \frac{A_1}{V_1}\, dt\right]/TIN$$

$$C_{dyalisate,brain} = \left[\int_{t1}^{t2} \frac{A_4}{V_{u,brain}}\, dt\right]/TIN$$

The total QTP plasma concentrations were expressed as $(A_1/V_1)/f_u$, and the QTP encapsulated concentrations as $(A_1+A_3)/V_{1,NANO}$.

3.3 Covariate analysis

The covariate analysis revealed that SCZ status (naïve or SCZ-like) showed an effect on CL_{in} and CL_{out} that were significantly reduced ($p < 0.01$) in SCZ-like animals with respect to the naïve condition, however neither weight nor gender influenced significantly any of the parameters of the model ($p > 0.05$).

Individuals CL_{in} and CL_{out} estimated by the model was plotted *versus* individual mean %PPI and a significant Pearson correlation coefficient was obtained, showing that the greater the preattentional sensorimotor gating deficits manifested as a reduction in PPI, the lower the CL_{in} and the higher the CL_{out} from the brain (Figure 3A and Figure 3B). Therefore, individual mean PPI was included in the final model as a semi-mechanistic way to better explain alterations in brain drug disposition in SCZ-like animals. The CL_{in} and CL_{out} of the SCZ-like animals was described as a function of the individual %PPI over %PPI mean. This inclusion lead to a drop in the objective function value (OFV) of 73.6 points and a better fit of the model to the data for the SCZ-like groups.

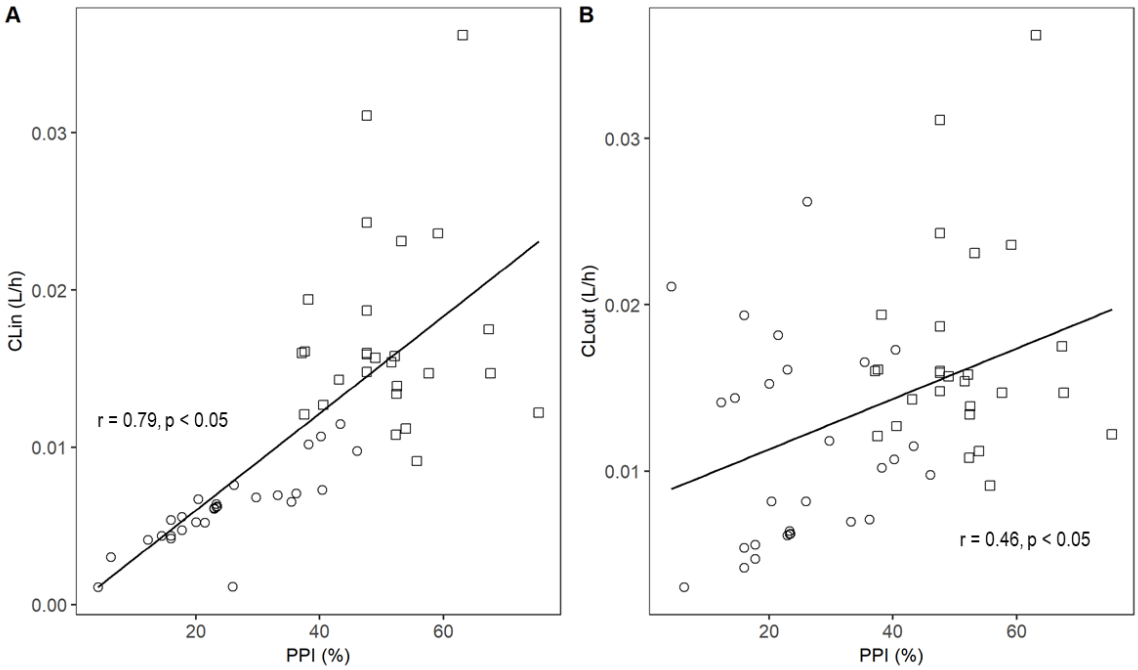


Figure 3. Correlation between model predicted individual CL_{in} (A) and CL_{out} (B) and prepulse inhibition response of the naïve (square) and poly(i:c) (dots) animals. Pearson correlation coefficient (α = 0.05) was obtained using the software GraphPad Prism (v. 7.0).

3.4 Model parameter estimates and model performance & evaluation

Model parameter estimates are listed in Table 1. The magnitude of the RSE indicates that all parameters were in general estimated with good precision. Data supported the estimation of IIV in the elimination clearance from the central compartment (CL) and in the parameters governing the bi-directional transport across BBB of unbound QTP. The magnitudes of IIV ranged from 17 to 67%. The estimate *in vivo* f_u was 0.24.

The fractions of the QTP dose that were non-encapsulated, fast and slow released from the nanocarriers were 7%, 8%, and 85%, respectively. *In vivo* first order release constants were 0.261 h^{-1} and 4.7 x 10^{-4} h^{-1} for the fast and slow release into the systemic circulation, and 0.0836 h^{-1} for the release taking place in the peripheral tissues and brain.

Individual predictions were able to describe observed total plasma, unbound plasma and unbound brain concentrations reasonably well (Figure S1-S3). Visual inspection of the basic goodness-of-fit plots did not reveal model misspecification (Figure S4 and S5). The visual predictive check (VPCs) confirmed that the model captures very well the overall tendency as well as the dispersion of the data for all the type of measurements and experimental scenarios (Figure 4).

Table 1. Pharmacokinetic parameters estimate of the final QTP model.

Parameters	Estimate (% RSE)	Median bootstrap (95th percentile)	% CV for IIV (% RSE)	% Shrinkage
CL (L/h/Kg)	1.86 (16)	1.79 (1.92)	22.9 (2)	6.10
V1 (L/Kg)	1.31 (08)	1.32 (1.34)	-	-
V2 (L/Kg)	1.73 (20)	1.76 (1.85)	-	-
Q (L/h/Kg)	1.08 (34)	1.06 (1.18)	-	-
fu (%)	24.2 (12)	23.9 (25.8)	-	-
$CL_{in,}$naïve (L/h/Kg)	0.045 (10)	0.043 (0.049)	16.7 (12)	17.3
$CL_{out,}$naïve (L/h/Kg)	0.023 (14)	0.021 (0.027)	26.4 (23)	21.3
CL_{in},SCZ (L/h/Kg)	0.019 (16)	0.016 (0.022)	55.6 (17)	15.8
$CL_{out,}$SCZ (L/h/Kg)	0.017 (7)	0.014 (0.018)	66.7 (21)	22.4
V_1nano (L/Kg)	0.77 (13)	0.74 (0.84)	-	-
$Krel_{FAST}$ (h^{-1})	0.261 (4)	0.231 (0.241)	-	-
$Krel_{SLOW}$(10^{-4} h^{-1})	4.7 (25)	4.2 (5.7)	-	-
$Krel_{TISSUE/BRAIN}$ (h^{-1})	0.0836 (35)	0.0791 (0.0861)	-	-
$Qnano_{TISSUE/BRAIN}$ (L/h/Kg)	0.067 (11)	0.061 (0.071)	-	-
F_{core} (%)	85 (11)	84 (86)	-	-
$F_{non\text{-}encapsulated}$ (%)	7 (36)	5 (8)	-	-
$F_{external}$ (%)	8	7 (9)	-	-

CL: clearance; *Q:* intercompartmental clearance; *V:* volume; RSE: relative standard error; IIV: interindividual variability; CV: coefficient of variation. Residual variability (%RSE) for FQ model was: 0.396 (7), 0.224 (8) and 0.124 (6) for total plasma, unbound plasma and unbound brain, respectively and IWRES shrinkage (%): 12.67. Residual variability (%RSE) for QLNC model was: 0.486 (6), 0.279 (28) and 0.232 (9) for total plasma, unbound plasma and unbound brain, respectively and IWRES shrinkage (%): 18.23. CL_{in} and CL_{out}: transport across BBB; SCZ*:* schizophrenia-like group; Krel: release constant, F: fraction of the dose.

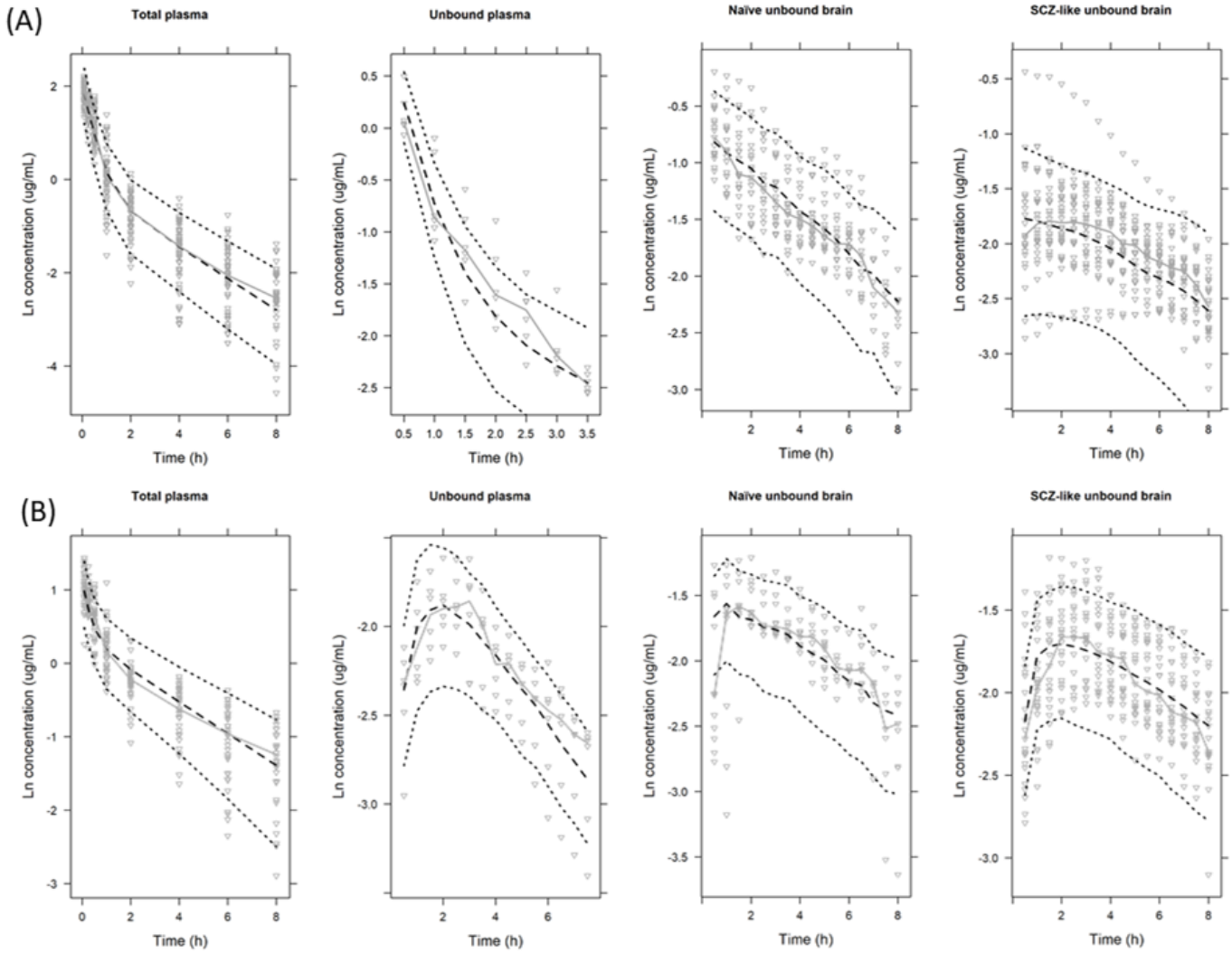


Figure 4. Visual predictive checks (VPCs) of the final population PK model for (A) FQ and (B) QLNC formulations stratified by total plasma, unbound plasma and the unbound brain stratified by naïve or SCZ-like rats. VPCs are based on 1000 simulations and show a comparison of the observations (triangles and thick lines for the median) with the 10^{th} and 90^{th} percentiles of the 1000 simulated profiles (dashed lines).

Using the parameters established by the final model, simulations of 100 concentration-time profiles of free QTP plasma and brain concentrations in naïve and SCZ-like animals were performed and the median of these profiles were plotted in Figure 5.

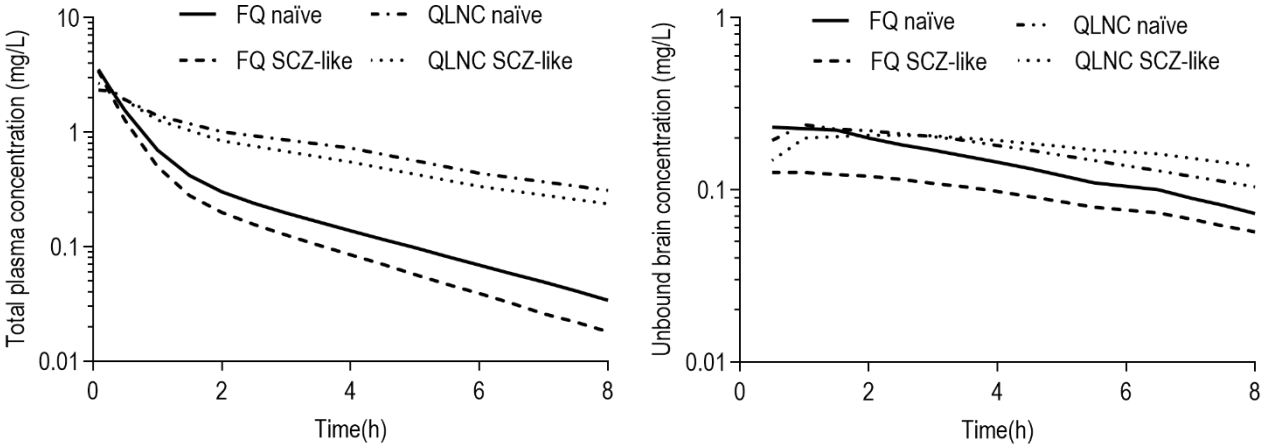


Figure 5. Simulated time course of FQ and QLNC in plasma and brain of naïve and SCZ-like rats. (A) QTP total plasma concentration-time profiles obtained after simulated i.v. bolus dosing of 5 mg/kg FQ or QLNC formulation; (B) QTP unbound brain concentration–time profiles obtained after simulated i.v. *bolus* dosing of 5 mg/kg FQ or QLNC formulation. Data show median of 100 simulated PK profiles.

Viewing to externally validate the final semi-mechanistic popPK model, a new set of QTP total plasma and unbound brain concentrations in naïve animals after FQ 5 mg/kg dose obtained 30 min after 30 mg/kg i.v. dosing of probenecid, an influx inhibitor, was used (CARREÑO et al, 2016b) (Figure S6 and S7). The model was able to characterize the influence of the influx inhibition on CL_{in} which was reduced from 0.045 L/h/kg (Table 1) to 0.028 L/h/kg (Table S1) indicating it's adequacy to describe the mechanism involved in QTP brain penetration.

The results of the alterations on total plasma and unbound brain concentrations when K_{slow} was varied are presented in Figure 7 for SCZ-like animals. One can observe that the higher the release rate from the nanoparticles core, the higher the total plasma and the lower the unbound brain concentrations.

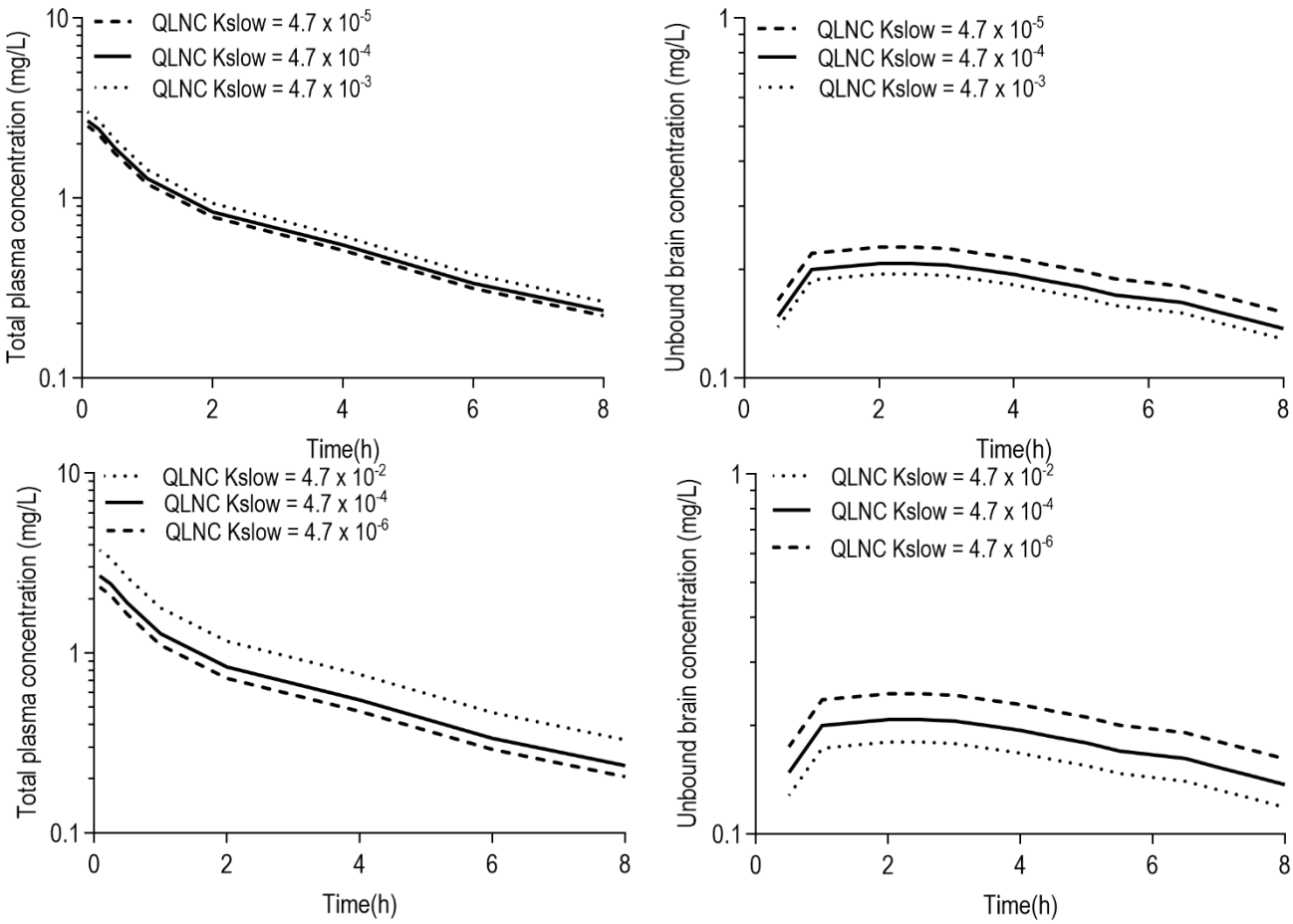


Figure 6. Simulated QTP total plasma (left panels) and unbound brain (right panels) concentrations following QLNC with different $Krel_{SLOW}$ rates administration to SCZ-like rats.

4. DISCUSSION

It has been reported that around 60% of schizophrenic patients are non-responsive to pharmacological treatment or experience relapses throughout the course of the illness (Möller et al., 2015). The incidence of the disorder is slightly higher in men than in women (ratio 1.4: 1) and, in general, men have more severe symptoms and a worse prognosis than women (OCHOA et al. al., 2012; SUN et al., 2016).

Pathological changes in BBB are well described and recognized as a central factor for the development of a number of neurological disorders. Although the high variability in chronic SCZ response to treatment may be partially related to BBB dysfunction, the relationship between BBB and psychotic disorders receives less

attention in the literature. Assuming that limited drug delivery to CNS in schizophrenic patients could be associated to pharmacotherapy resistance and that sex could affect drug's brain penetration is these patients, in the current study we used microdialysis to access free brain concentrations of QTP and population pharmacokinetic modeling to describe this drug penetration trough naïve and altered BBB (SCZ-like) of male and female Wistar rats following drug dosing as solution or nanoencapsulated into LNC.

No differences were found in any pharmacokinetic parameter for both formulations when data from male and female naïve or SCZ-like animals where compared within the same formulation group. This result indicates that sex does not influence QTP plasma pharmacokinetics and brain penetration even in the altered BBB condition investigated. For this reason, data from male and female animals were grouped for the following analysis.

Firstly we investigated the alterations in QTP plasma and brain disposition in SCZ-like in comparison to naïve animals following the administration of the drug in solution (FQ). Quetiapine plasma concentration *versus* time profiles were similar in SCZ-like and naïve rats suggesting that prenatal exposure to poly(i:c) does not affect QTP plasma disposition and elimination in adult offspring (Figure 6A and B). However, it is well known that only unbound concentrations at the target site are responsible for drug effect and relevant in predicting therapeutic efficacy.

A significant reduction of the extent of QTP unbound brain distribution was observed in SCZ-like animals dosed with FQ formulation when compared to naïve offspring (Figure 6C). Assuming CL_{in}/CL_{out} ratio as a measure of tissue penetration, the naïve animal's ratio of 1.96, indicative of QTP influx to the brain, is reduced to 1.11 in SCZ-like animals, a decrease of about 43%. Naïve rats present a normal brain development, however, the prenatal insult triggered by poly(i:c) impaired brain development of offspring leading to a long-term alterations in BBB permeability of the SCZ-like adult animals, mimicking what happens in humans, according to the neurodevelopmental hypothesis of SCZ. The semi-mechanistic model popPK final model allowed understanding the mechanisms underlying this reduced brain penetration, showing that SCZ-like animals present alterations in the influx transport across BBB represented by a reduction in the CL_{in} (from 0.045 L/h/kg to 0.019 L/h/kg)

when compared to the naïve animals (Table 1). Furthermore, using the PPI test, it was possible to demonstrated, for the first time, that the greater the preattentional sensorimotor gating deficit manifested as a reduction in PPI, the more compromised is the influx transport across BBB (Figure 3). Therefore, this result indicates that the cerebral penetration of antipsychotics such as QTP, which is an influx transport substrate, is decreased in SCZ and may contribute to the resistance observed with pharmacological treatment. If SCZ interferes with efflux transporters in the BBB remains to be investigated.

The model was externally validated using a set of data of naïve animals from previous study (CAREÑO et al., 2016b) that receive QTP in association with the influx transporter inhibitor probenecid. With this data set the parameter CLin was reduced (Table 1s) in the same magnitude observed when comparing naïve and SCZ-like animals (Table 1), indicating that any factor interfering with the influx transporter will have a significant impact on QTP brain exposure.

Our experimental setting allowed to investigate if the administration of QTP loaded into lipid core nanocarrier (QLNC) modified the drug delivery to the brain in naïve and SCZ-like animals. Normally the study of drug release kinetics from nanoparticles is carried out using *in vitro* data aiming to find a general model capable of describing a multi-mechanistic release. In the present study, using the model-based approach, we were able to describe the *in vivo* release kinetics of QTP from the QLNC in plasma and also support a mechanism of nanocarrier distribution and drug release into the brain and other tissues. In fact, we were able to demonstrate that QTP is released in plasma with two distinct first order rate constants: $Krel_{FAST}$: 0.261 h^{-1} and $Krel_{SLOW}$: 4.7 x 10^{-4} h^{-1}. The model predicts that approximately 8% of the drug is fastly released, and the remaining 85% is released more slowly (Table 1). These results are in accordance with the mechanism of QTP distribution in the LNC proposed previously, where we inferred that due to QTP logD in the formulation, it is distributed mainly in the inner pseudo-phase of the colloidal suspension (~95%) (Carreño et al., 2015).

The fast release of the QTP from LNC ($F_{external}$, $Krel_{FAST}$) could be characterized only in plasma, with a half-life on 2.7 h. In the brain we could characterize only the slow

release of the drug ($Krel_{TISSUE,BRAIN}$ = 0.0836 h^{-1}) which is different from the release in plasma because of the differences between tissue and blood environments.

We previously demonstrated that total concentrations measured in brain homogenates are increased in naïve animals administered with QLNC (Carreño et al., 2016a). However, unbound brain exposure to the drug was similar in naïve animals following FQ and QLNC i.v. dosing. We also showed, using the influx transporter inhibitor probenecid, that QLNC probably carries the drug into the brain, avoiding its interaction with BBB transporters (Carreño et al., 2016b). Using the model-based approach described in the present work it is now possible to understand these results. In naïve animals the rate of QTP distribution thought the BBB when the drug is given as FQ formulation is similar to that obtained when the drug is given as QLNC ($CL_{in,}$naïve: 0.045 L/h/kg and $Qnano_{TISSUE/BRAIN}$ 0.067 L/h/kg). When the BBB is unaltered, the rate of nanocarrier brain penetration ($Qnano_{TISSUE/BRAIN}$), which governs QTP distribution because 85 % of the drug is encapsulated, is similar to that observed for the unbound QTP brain penetration (CL_{in}).

When SCZ-like animals are administered with QLNC, part of the drug will be released in the blood, as already shown, but the higher amount of the drug will be carried across the BBB by the nanocarriers, avoiding the interaction with transporters at BBB. Once again, the nanocarrier governs QTP brain penetration with the same rate previously observed ($Qnano_{TISSUE/BRAIN}$ 0.067 L/h/kg). However, this rate is now higher than that observed for the unbound QTP brain penetration, which is reduced ($CL_{in,}$SCZ 0.019 L/h/kg) in SCZ-like animals, resulting in a increase in brain penetration. Comparing the increased brain exposition observed in SCZ-like animals when QLNC was administered, it is possible to note that the nanocarriers returned QTP concentrations levels similar to those observed in naïve animals (Figure 5).

The results demonstrate that LNC governs drug distribution to tissues and $Krel_{SLOW}$ in plasma determines the amount of drug remaining in the nanocarrier core, capable of penetrating the brain. The nanocarrier used in the present work is composed by a lipid-dispersed core (medium chain triglycerides and sorbitan monostearate) enveloped by a polymeric wall [poly(ε-caprolactone)] leading to a drug release kinetic

dependent on both the core viscosity (*in vivo* represented by F_{core} and $Krel_{SLOW}$) and the polymeric wall (*in vivo* represented by $F_{external}$ and K_{FAST}). Drug release rate from this nanoparticle decreases according to the increase in the polymer concentration (CRUZ et al, 2006) or depending on medium chain triglycerides and/or sorbitan monostearate concentrations. For example, an increase in sorbitan monoestearate concentration might cause a resistance to drug diffusion from the core of the LNC (Jäger et al, 2009), altering $Krel_{SLOW}$.

Simulations were performed varying the $Krel_{SLOW}$ 10 to 100-times up and down (Figure 6) viewing to understand the impact of this parameter on QTP brain distribution in SCZ-like animals. It is possible to observe that a 10-times increase in $Krel_{SLOW}$ will increase plasma total concentration and reduce unbound brain concentrations. Opposite effect would be produced by decreasing the $Krel_{SLOW}$ in the same magnitude. The alterations in brain unbound concentrations observed with this small alteration in $krel_{SLOW}$, however, may not have a significant clinical impact. The more the $Krel_{SLOW}$ is increased, the higher is the drug amount released in plasma and the less effective is the nanocarrier to overcome the BBB alterations produced in SCZ-like animals. It would take a 100-times increase on $Krel_{SLOW}$ to have a significant reduction on QTP unbound brain concentrations. In other words, only a 100-times increase on drug release from the LNC core could compromise the significant improvement of QTP brain penetration produced by the QLNC on SCZ-like animals.

The improvement in QTP delivery to the brain observed with LNC sheds light upon the pharmacokinetic component of the antipsychotic treatment resistant, opening the possibility to use this approach to improve SCZ treatment limited response rates.

The innovative strategy described in the present work, combining experimental microdialysis and mechanistic pharmacokinetic modeling applied to the investigation of nanocarrier tissue penetration investigated in diseased animals allowed to understand the drug delivery from the nanostructure *in vivo* and to construct a tool that can be used to simulate distinct outcomes for the development of nanocarriers with tailored delivery rates.

5. CONCLUSION

QTP brain exposure in reduced in SCZ-like rats in comparison to naïve animals, supporting the hypothesis that BBB dysfunction contributes to treatment failures. QTP encapsulation on LNC overcomes BBB disorder returning drug penetration to the levels observed in naïve animals.

A semi-mechanistic model of total and unbound plasma and unbound brain concentrations allowed the determination of the rate and extent of QTP brain distribution from FQ and QLNC formulations in naïve and SCZ-like exposed rats. The present model-based is useful for better understanding the potential of LCN for drug delivery to the brain, opening the opportunity of using this approach to design nanoformulations for improving SCZ-treatment limited response rates.

6. CONTRIBUTORS

TDC conceived the project, got the financial support and supervised the experiments. FC, APH, SMKR and TDC designed the experimental protocol. FC performed all animal experiments, sample quantification, data analysis and model building. VEH and KJS performed the animal experiments and samples quantification. FSM provide the veterinary support during experimental protocol design and execution. KP and SSG supervised the lipid core nanocapsules preparation and characterization. IFT supervised the data analysis and model building process. FC, IFT and TDC wrote the manuscript. All authors approved the final manuscript.

7. CONFLICT OF INTEREST

The authors declare no conflict of interest

8. ACKNOWLEDGMENTS

The authors acknowledge Dr. Liberato Brum Junior (Prati Donaduzzi, Toledo – PR, Brazil) for kindly providing quetiapine fumarate and technical support from the Animal's Facility staff (UFRGS/Biochemistry Department). This study was financed by

CNPq/Brazil (Process 421767/2016-2) and by the Coordenação de Aperfeiçoamento de Pessoal de Nível Superior – Brazil (CAPES) - Finance Code 001.

9. REFERENCES

Bergstrand, M., Hooker, A.C., Wallin, J.E., Karlsson, M.O., 2011. Prediction-corrected visual predictive checks for diagnosing nonlinear mixed-effects models. AAPS J. 13, 143–51. https://doi.org/10.1208/s12248-011-9255-z

Carreño, F., Paese, K., Silva, C. de M., Guterres, S.S., Costa, T.D., 2015a. Characterizing the mechanism of quetiapine distribution in lipid-core nanocapsules pseudo-phases using a validated LC/UV method. Quim. Nova 38, 1181–1186. https://doi.org/10.5935/0100-4042.20150137

Carreño, F., Paese, K., Silva, C. de M., Guterres, S.S., Costa, T.D., Carreño, F., Paese, K., Silva, C. de M., Guterres, S.S., Costa, T.D., 2015b. CHARACTERIZING THE MECHANISM OF QUETIAPINE DISTRIBUTION IN LIPID-CORE NANOCAPSULES PSEUDO-PHASES USING A VALIDATED LC/UV METHOD. Quim. Nova 38, 1181–1186. https://doi.org/10.5935/0100-4042.20150137

Carreño, F., Paese, K., Silva, C.M., Guterres, S.S., Dalla Costa, T., 2016a. Pharmacokinetic Investigation of Quetiapine Transport across Blood–Brain Barrier Mediated by Lipid Core Nanocapsules Using Brain Microdialysis in Rats. Mol. Pharm. 13, 1289–1297. https://doi.org/10.1021/acs.molpharmaceut.5b00875

Carreño, F., Paese, K., Silva, C.M., Guterres, S.S., Dalla Costa, T., 2016b. Pre-clinical investigation of the modulation of quetiapine plasma pharmacokinetics and tissues biodistribution by lipid-core nanocapsules. J. Pharm. Biomed. Anal. 119, 152–158. https://doi.org/10.1016/J.JPBA.2015.11.027

Dimer, F.A., Pigatto, M.C., Boque, C.A., Pase, C.S., Roversi, K., Pohlmann, A.R., Burger, M.E., Rates, S.M.K., Costa, T.D., Guterres, S.S., 2014. Nanoencapsulation improves relative bioavailability and antipsychotic effect of olanzapine in rats. J. Biomed. Nanotechnol. 11, 1482–1493. https://doi.org/10.1166/jbn.2015.2082

He, Q., Liu, J., Liang, J., Liu, X., Li, W., Liu, Z., Ding, Z., Tuo, D., 2018. Towards Improvements for Penetrating the Blood–Brain Barrier—Recent Progress from a

Material and Pharmaceutical Perspective. Cells. https://doi.org/10.3390/cells7040024

Jonsson, E.N., Karlsson, M.O., 1999. Xpose--an S-PLUS based population pharmacokinetic/pharmacodynamic model building aid for NONMEM. Comput. Methods Programs Biomed. 58, 51–64.

Keizer, R.J., Karlsson, M.O., Hooker, A., 2013. Modeling and simulation workbench for NONMEM: Tutorial on Pirana, PsN, and Xpose. CPT Pharmacometrics Syst. Pharmacol. https://doi.org/10.1038/psp.2013.24

Lindbom, L., Pihlgren, P., Jonsson, N., 2005. PsN-Toolkit - A collection of computer intensive statistical methods for non-linear mixed effect modeling using NONMEM. Comput. Methods Programs Biomed. https://doi.org/10.1016/j.cmpb.2005.04.005

Lindqvist, A., Fridén, M., Hammarlund-Udenaes, M., 2016a. Pharmacokinetic considerations of nanodelivery to the brain: Using modeling and simulations to predict the outcome of liposomal formulations. Eur. J. Pharm. Sci. 92, 173–182. https://doi.org/10.1016/j.ejps.2016.07.003

Lindqvist, A., Rip, J., Gaillard, P.J., Björkman, S., Hammarlund-Udenaes, M., 2013. Enhanced brain delivery of the opioid peptide DAMGO in glutathione pegylated liposomes: a microdialysis study. Mol. Pharm. 10, 1533–41. https://doi.org/10.1021/mp300272a

Lindqvist, A., Rip, J., Van Kregten, J., Gaillard, P.J., Hammarlund-Udenaes, M., 2016b. In vivo Functional Evaluation of Increased Brain Delivery of the Opioid Peptide DAMGO by Glutathione-PEGylated Liposomes. Pharm. Res. https://doi.org/10.1007/s11095-015-1774-3

Möller, M., Swanepoel, T., Harvey, B.H., 2015. Neurodevelopmental Animal Models Reveal the Convergent Role of Neurotransmitter Systems, Inflammation, and Oxidative Stress as Biomarkers of Schizophrenia: Implications for Novel Drug Development. ACS Chem. Neurosci. 6, 987–1016. https://doi.org/10.1021/cn5003368

Moss, D.M., Siccardi, M., 2014. Optimizing nanomedicine pharmacokinetics using physiologically based pharmacokinetics modelling. Br. J. Pharmacol. https://doi.org/10.1111/bph.12604

Paxinos, G., Watson, C., 2013. The Rat Brain in Stereotaxic Coordinates : Hard Cover Edition. Elsevier Science.

Petros, R.A., DeSimone, J.M., 2010. Strategies in the design of nanoparticles for therapeutic applications. Nat. Rev. Drug Discov. 9, 615–27. https://doi.org/10.1038/nrd2591

Pritchett-Corning, K.R., Chang, F.T., Festing, M.F.W., 2009. Breeding and housing laboratory rats and mice in the same room does not affect the growth or reproduction of either species. J. Am. Assoc. Lab. Anim. Sci. 48, 492–8.

Tunblad, K., Hammarlund-Udenaes, M., Jonsson, E.N., 2004. An integrated model for the analysis of pharmacokinetic data from microdialysis experiments. Pharm. Res. https://doi.org/10.1023/B:PHAM.0000041468.00587.c6

Wählby, U., Jonsson, E.N., Karlsson, M.O., 2002. Comparison of stepwise covariate model building strategies in population pharmacokinetic-pharmacodynamic analysis. AAPS PharmSci. https://doi.org/10.1208/ps040427

Yuan, D., He, H., Wu, Y., Fan, J., Cao, Y., 2019. Physiologically Based Pharmacokinetic Modeling of Nanoparticles. J. Pharm. Sci. 108, 58–72. https://doi.org/10.1016/j.xphs.2018.10.037

Supplementary Material

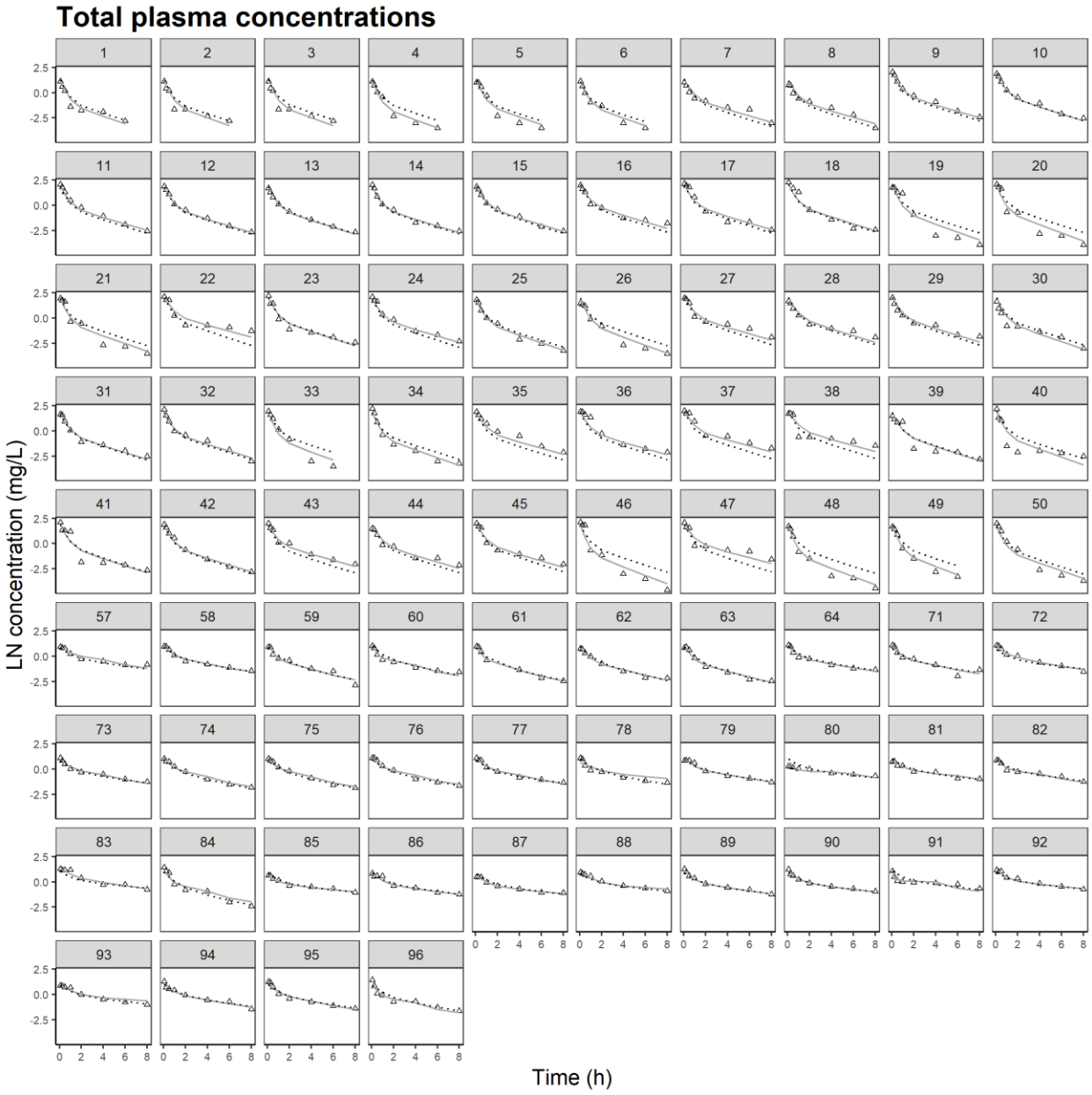


Figure S1. Individual and population fitted total plasma concentration *versus* time profiles using the final popPK model for FQ (1 -50) and QLNC (57-96). Triangles, observations; solid lines, individual model predictions (IPRED); dotted lines, population model predictions (PRED).

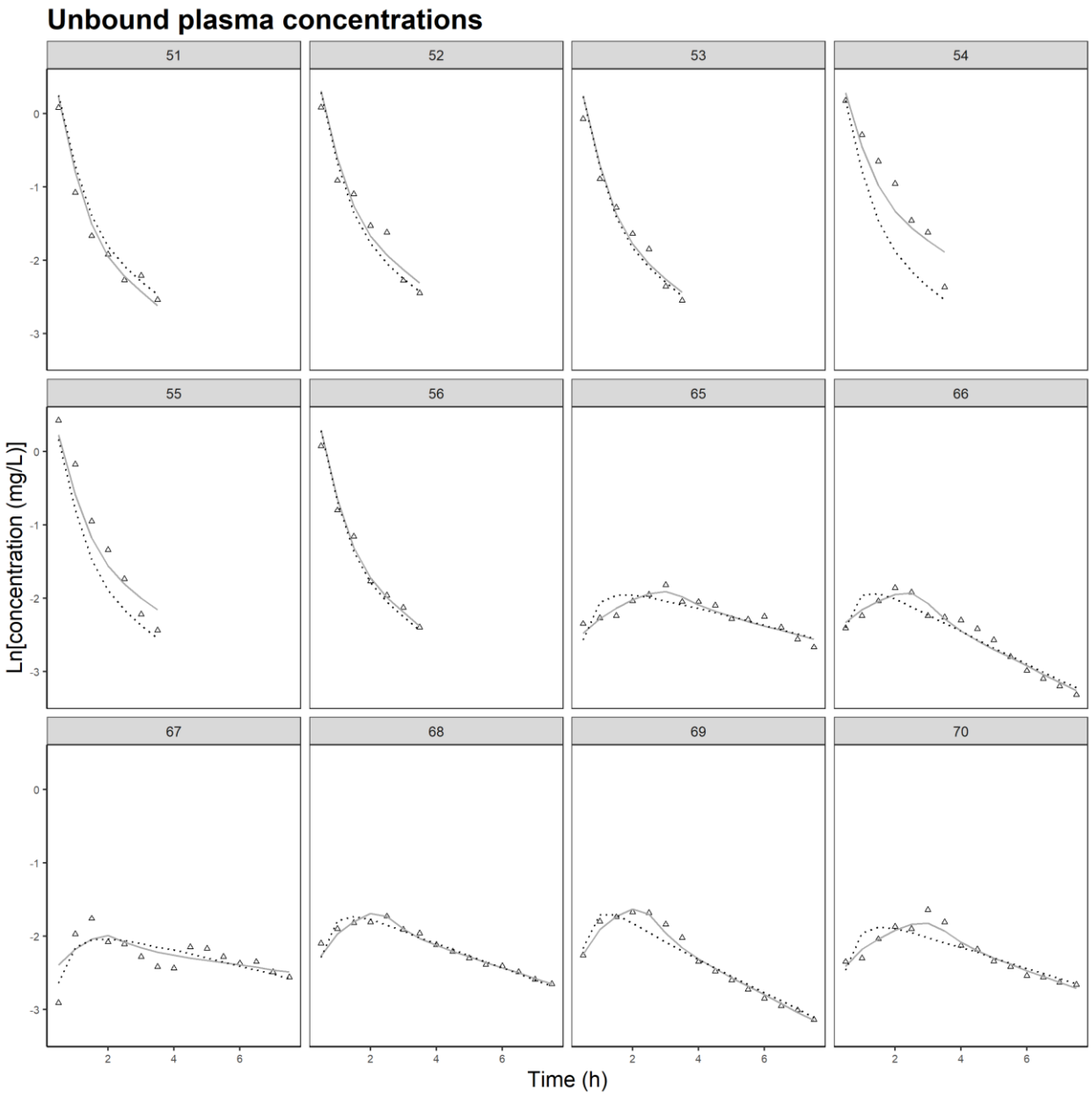


Figure S2. Individual and population fitted unbound plasma concentration *versus* time profiles using the final popPK model for FQ (51 - 56) and QLNC (65 - 70). Triangles, observations; solid lines, individual model predictions (IPRED); dotted lines, population model predictions (PRED).

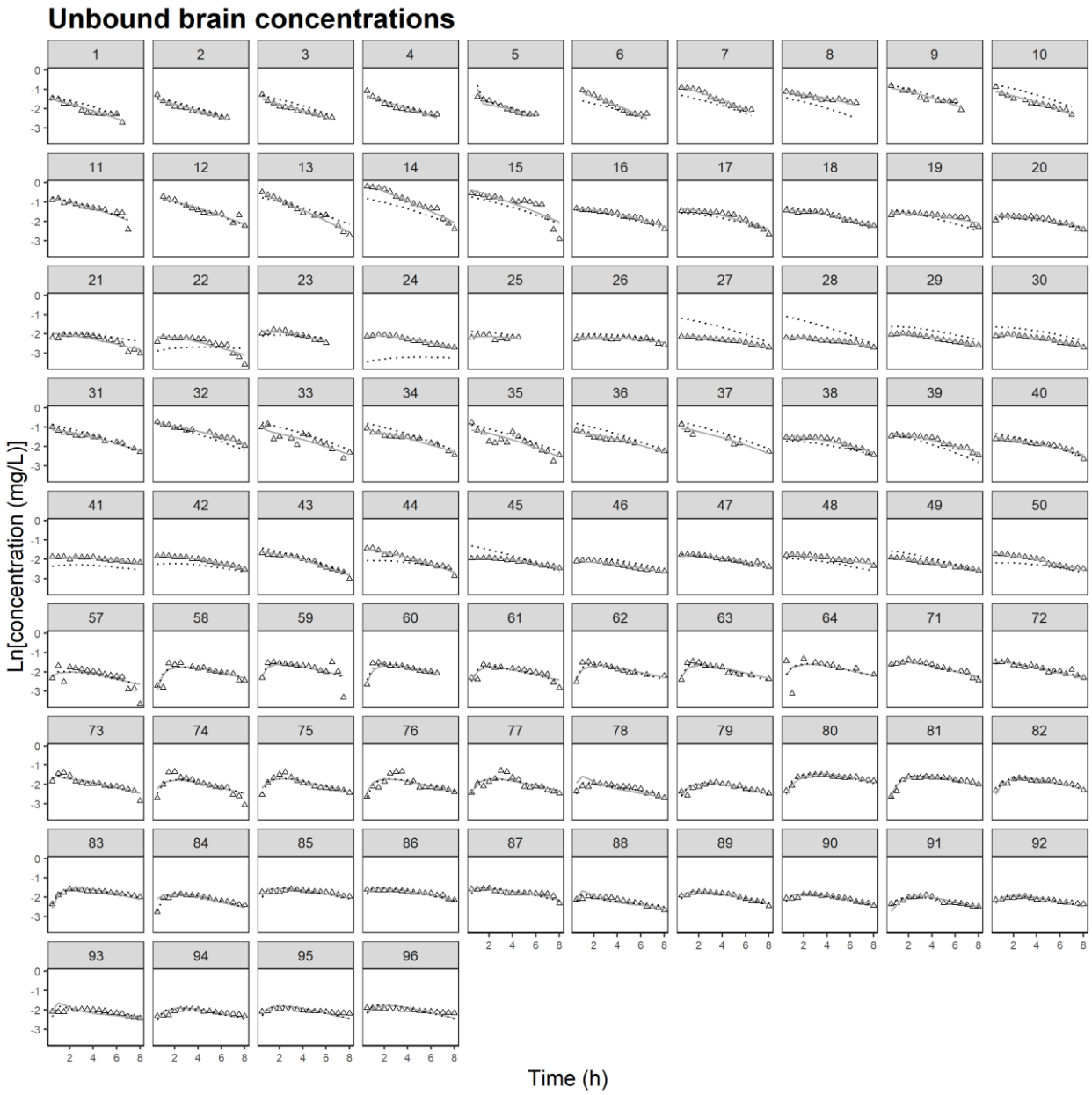


Figure S3. Individual and population fitted unbound brain concentration *versus* time profiles using the final popPK model for FQ (1 -50) and QLNC (57-96). Triangles, observations; solid lines, individual model predictions (IPRED); dotted lines, population model predictions (PRED).

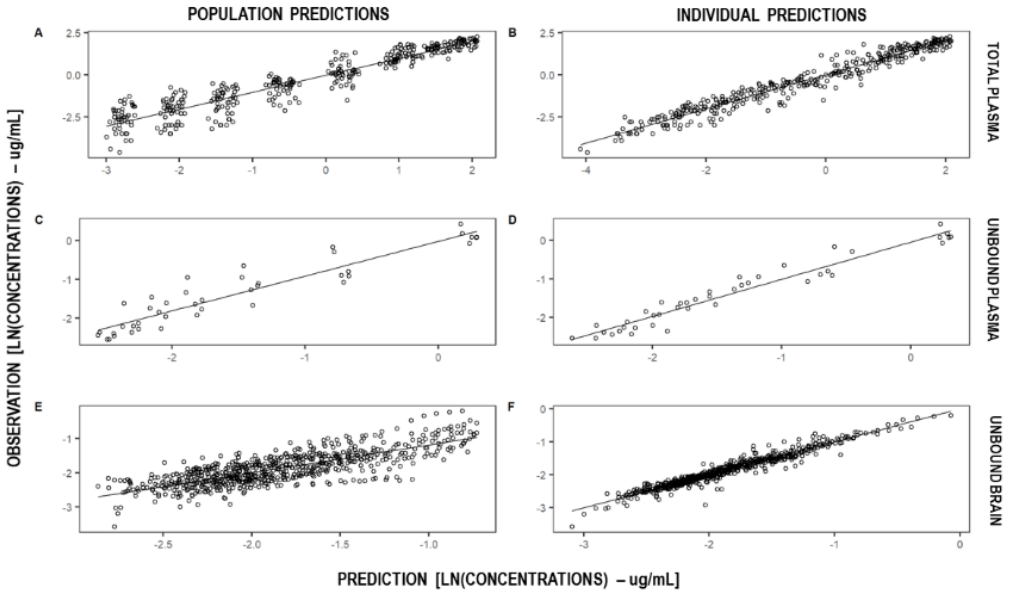


Figure S4. Goodness of fit plots for FQ formulation model. Observed data, population predictions (A, C and E) and individual predictions (B, D, F) of the total plasma, unbound plasma and unbound brain concentrations.

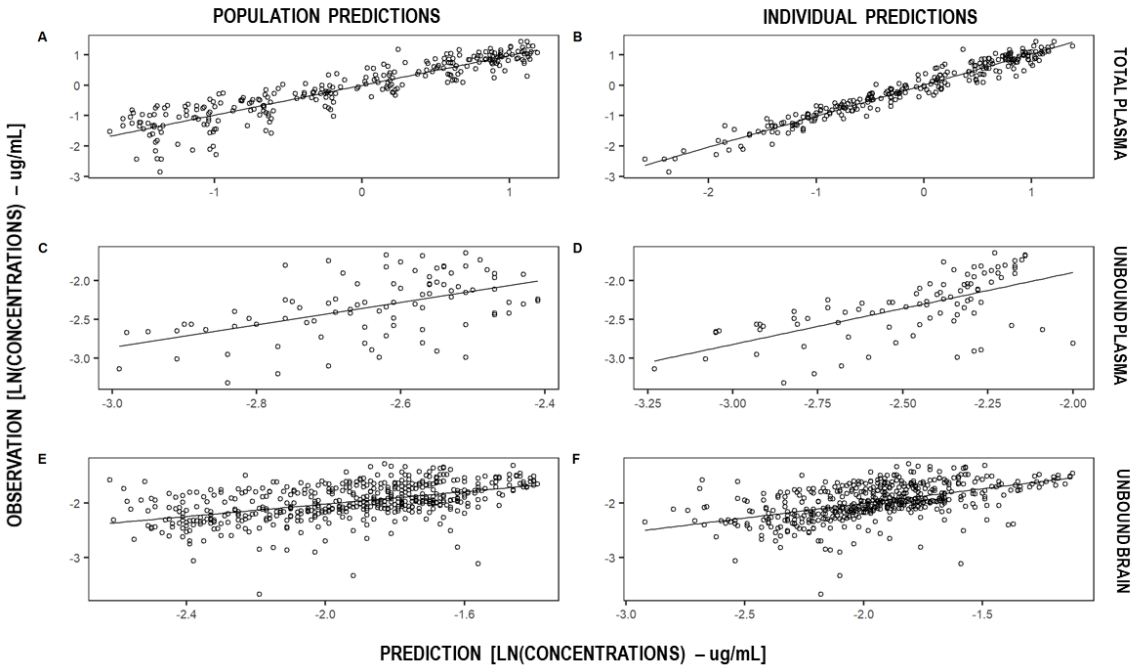


Figure S5. Goodness of fit plots for QLNC formulation model. Observed data, population predictions (A, C and E) and individual predictions (B, D, F) of the total plasma, unbound plasma and unbound brain concentrations.

Table 1S. Pharmacokinetic parameters estimate for the external validation FQ model using probenecid dataset.

Parameters	**Estimate (% RSE)**	**Median bootstrap (95th percentile)**	**% CV for IIV (% RSE)**	**% Shrinkage**
CL (L/h/Kg)	1.41 (5)	1.47 (1.52)	34.6 (15)	9.98
V1 (L/Kg)	1.22 (08)	1.27 (1.32)	-	-
V2 (L/Kg)	1.94 (19)	2.01 (2.10)	-	-
Q (L/h/Kg)	0.94 (24)	1.11 (1.12)	-	-
fu (%) FIX	24.2	-	-	-
$CL_{in,probenecid}$ (L/h/Kg)	0.028 (13)	0.030(0.037)	-	-
$CL_{out,probenecid}$ (L/h/Kg)	0.029 (11)	0.031(0.034)	-	-

CL: clearance; *Q:* intercompartmental clearance; *V:* volume; RSE: relative standard error; IIV: interindividual variability; CV: coefficient of variation. Residual variability (%RSE) for the model was: 0.496 (9), 0.054 (12) for total plasma and unbound brain, respectively and IWRES shrinkage (%): 14.28. $CL_{in,probenecid}$ and $CL_{out,probenecid}$: transport across BBB in the presence of the influx inhibitor probenecid

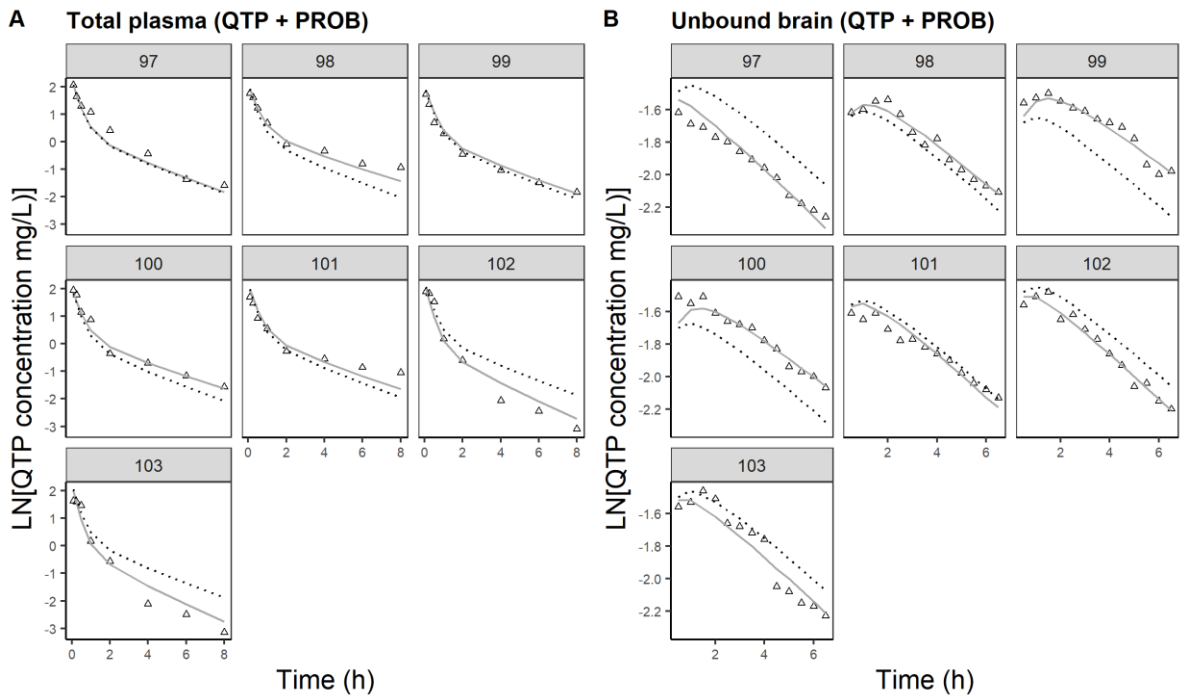


Figure S6. Individual and population fitted (A) total plasma and (B) unbound brain concentration *versus* time profiles following QTP 10 mg/kg i.v. dosing 30 min after 30 mg/kg probenecid (PROB) i.v. dosing using the final popPK model for FQ as an external validation. Triangles, observations; solid lines, individual model predictions (IPRED); dotted lines, population model predictions (PRED). All animals are naïve animals.

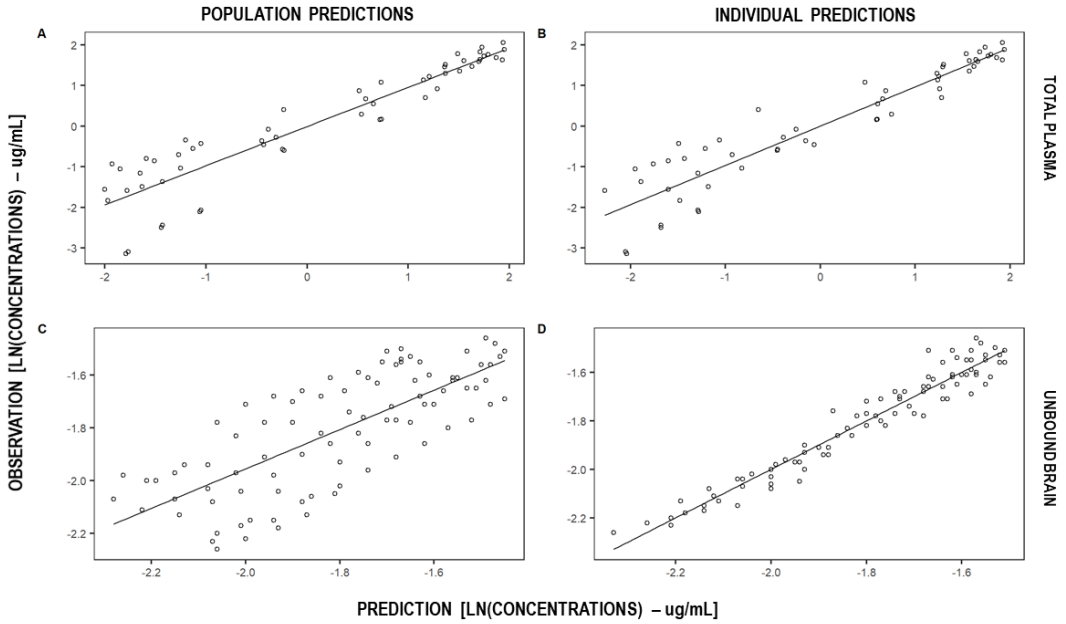


Figure S7. Goodness of fit plots for the external validation using the probenecid dataset. Observed data, population predictions (A, C) and individual predictions (B, D) of the total plasma and unbound brain concentrations

CAPÍTULO 4

PHARMACOKINETIC/PHARMACODYNAMIC MODELING OF CORTICAL DOPAMINE LEVELS AFTER QUETIAPINE LIPID CORE NANOCAPSULES ADMINISTRATION TO SCHIZOPHRENIA PHENOTYPED RAT

Carreño F[1], Helfer VE[1], Staudt KJ[1], Paese K[1], Meyer FS[2], Herrmann AP[3], Guterres SS[1], Rates SMK[1], Trocóniz, IF[4,5], Dalla Costa T[1]

[1]Programa de Pós-Graduação em Ciências Farmacêuticas, Faculdade de Farmácia, Universidade Federal do Rio Grande do Sul;

[2]Centro de Reprodução e Experimentação de Animais de Laboratório, Instituto de Ciências Básicas da Saúde, Universidade Federal do Rio Grande do Sul;

[3]Programa de Pós-Graduação em Farmacologia e Terapêutica, Instituto de Ciências Básicas da Saúde, Universidade Federal do Rio Grande do Sul;

[4]Pharmacometrics & Systems Pharmacology Research Unit, Department of Pharmaceutical Technology and Chemistry, School of Pharmacy and Nutrition, University of Navarra;

[5] IdiSNA, Navarra Institute for Health Research.

ABSTRACT

High variability in schizophrenia (SCZ) pharmacological treatment might be related to a pharmacodynamic component, due to alterations in antipsychotic drugs receptor binding or signal transduction and also be related to a pharmacokinetic component that affects biophase drug concentrations due to changes in penetration through the blood-brain-barrier (BBB) caused by the disease. Quetiapine lipid core nanocapsules have shown the capability of modulate drug delivery to the brain. In the present study, we described concentration-effect relationship after administrations of QTP as a solution or nanoencapsulated in SPR and naïve animals viewing to explore the PK and PD components of variability in SCZ response to treatment. A semi-mechanistic PK model was linked to an indirect response PD model to describe changes in dopamine extracellular concentrations in mPFC measured using intracerebral microdialysis. SCZ status increase EC_{50} values about 3 times reducing QTP pharmacological sensitivity in SPR in comparison to naïve after the administration of 5 mg/kg of FQ formulation. QLNC formulation was not capable of causes alterations in PD parameters. However, once the nanocarrier was able to modulate drug delivery to the brain there is an increase in DA levels in mPFC of SPR, highlighting the PK component of variability in SCZ pharmacological treatment. To the best of our knowledge, this is the first study that combine microdialysis and PK/PD modeling in a neurodevelopmental model of SCZ to investigate how a nanocarrier can modulate drug PK and PD contributing to development of new treatment strategies for SCZ.

1. INTRODUCTION

Schizophrenia (SCZ) is a disabling mental disorder that affects how a person think, feels and behaves. Besides the subjective experience of psychotic symptoms, SCZ patient's life expectancy is significantly shorter than the general population (SAHAETAL., 2007) and the mortality rate associated with this disorder outnumbers the one for cancer and other physical illnesses (MILLAN et al., 2016)

Antipsychotic drugs are the mainstay of SCZ and schizoaffective disorders pharmacological treatment and quetiapine (QTP), a second-generation antipsychotic drug, has an atypical profile against the positive, negative and cognitive symptoms of SCZ with a low propensity to induce extrapyramidal side effects (PIRA; MONGEAU; PANI, 2004; YAMAMURA et al., 2009).

Although its mechanism of action is not fully understood, QTP has the ability to increase catecholamine levels in prefrontal cortex with might play a role in its clinical effectiveness (ICHIKAWA et al., 2002; KRAUSE et al., 2018; PIRA; MONGEAU; PANI, 2004; YAMAMURA et al., 2009). A dysregulation in brain dopaminergic circuits with a reduced dopaminergic signaling in the mesocortical pathway has been proposed as an underlying dysfunction in SCZ, especially related to negative and cognitive symptoms (GRACE, 2016)

Unfortunately, current prescribed antipsychotic drug given to SCZ patients, including QTP, have limited response rate. About 60% of SCZ patients respond partially to treatment and 30% of them become treatment resistant patients (BATAIL et al., 2014)

This high therapeutic variability might be due to a pharmacodynamic component, due to alterations in antipsychotic drug receptor binding or signal transduction caused by SCZ and might be also related to a pharmacokinetic component that affects biophase antipsychotic concentrations due to changes in drug penetration through the blood-brain-barrier (BBB) and consequently delivery to the central nervous system (CNS) caused by the disease.

Assuming that limited drug delivery to CNS in schizophrenic patients could be associated with pharmacotherapy resistance we developed quetiapine lipid core nanocapsules (QLNC) aiming to improve drug targeting to the brain. In a previously

report (Capítulo 3) we combined brain microdialysis and population pharmacokinetic model-based approach to understand mechanistically the changes in plasma and brain pharmacokinetics after administration of QTP in solution (FQ) or nanoencapsulated (QLNC) to schizophrenia phenotyped rats (SPR). We demonstrate that QTP unbound brain exposure is reduced in SPR in comparison to naïve animals, supporting the hypothesis that BBB dysfunction contributes to treatment failures. Furthermore, QTP nanoencapsulation returned drug penetration to levels observed in naïve animals.

Pharmacokinetic/pharmacodynamic (PK/PD) modeling has been used to characterize the process between drug administration and its effect. Preclinical PK/PD models described in the literature for antipsychotic drugs use *in vivo* PK (plasma and tissue drug concentration) data and *in vitro* PD (dopaminergic and serotoninergic receptor occupancy) data to stablish a temporal relationship between drug concentration and effect. Antipsychotic drugs such as risperidone and olanzapine have been described by these models which were used to perform simulations and predictions of effect in humans (JOHNSON et al., 2011; KOZIELSKA et al., 2012)

In the present work we aimed to increase the understanding of the role of this drug delivery system by describing the development of a PK/PD model integrating the previously developed semi-mechanistic pharmacokinetic model to a different set of pharmacodynamic data - extracellular dopamine levels measured by microdialysis in naïve and SPR - viewing to explore the pharmacodynamic component of SCZ variability in response to treatment and the influence of QTP nanoencapsulation on this neurotransmitter levels.

2. MATERIALS AND METHODS

2.1. Quetiapine Lipid Core Nanocapsules (QLNC) preparation

QTP lipid-core nanocapsules (QLNC – 1 mg/mL) were obtained as described in previous report (CARREÑO et al., 2016a, CARREÑO et al., 2016b). Briefly, poly(ε-caprolactone) (PCL), medium chain triglycerides, sorbitan monoestearate and QTP were dissolved in acetone and ethanol. This organic phase was injected into an aqueous phase containing polysorbate 80 (P-80) in ultrapurified water under magnetic

stirring. Acetone was eliminated and the suspension concentrated under reduced pressure.

QTP control formulation (FQ, 5 mg/mL) was prepared first dissolving QTP in acetic acid (99%), then saline 0.9% containing P-80 in the same concentration used in QLNC preparation was added and the pH was adjusted to 6.5 ± 0.5 using NaOH (8 M).

2.2 Study Design

Experimental procedures described in the present study were approved by the Ethics Committee in Animal Use from the Federal University of Rio Grande do Sul (UFRGS/CEUA #31001) and were conducted in compliance with the principles of laboratory animal care from the National Council for Animal Experimentation (CONCEA/Brazil).

2.2.1 Animals

Pregnant Wistar rats and their offspring obtained from the Central Animal Facilities of University's Biochemistry Department (Porto Alegre, Brazil) were used throughout the study. All animals were housed (3/cage) in a controlled environment (22 ± 2 °C, 65% humidity in a 12 h light/dark cycle) with free access to standard rodent chow and filtered water. The offspring were maintained in the same conditions.

2.2.2 Neurodevelopmental animal model of schizophrenia

Neurodevelopmental animal model of schizophrenia was adapted previously in our laboratory (Capítulo 1) based on the model described by Hadar et al. (2015). Briefly, pregnant dams (gestational day 15) received single i.v. *bolus* dose of poly (i:c) 4 mg/kg (SPR offspring) or 2 mL/kg sterile saline (naïve offspring) via lateral tail vein. SPR deficits in the adult offspring (PND75) were confirmed by pre-pulse inhibition of the startle response (data no shown).

2.2.3 Pharmacokinetic study

The pharmacokinetics of FQ and QLNC formulations in naïve and SPR was previously investigated in plasma and brain, using microdialysis (CARREÑO et al., 2016a, 2016b), and a semi-mechanistic populational pharmacokinetic model capable of describe changes in both compartments was developed (Capítulo 3).

2.2.4 Pharmacodynamic study

The effect of FQ and QLNC on medial prefrontal cortex (mPFC) extracellular DA concentration was investigated using intracerebral microdialysis.

Naïve and SPR offspring were divided in eight groups according to disease status, sex and treatment type: $FQ_{naïve,male}$ (n = 7); $FQ_{naïve,female}$ (n = 6); $FQ_{SPR,male}$ (n = 6); $FQ_{SPR,female}$ (n = 6); $QLNC_{naïve,male}$ (n = 7); $QLNC_{naïve,female}$ (n = 6); $QLNC_{SPR,male}$ (n = 6); $QLNC_{SPR,female}$ (n = 6).

Each rat was anesthetized (ketamine/xilazine/acepromazine: 100 mg/kg -10 mg/kg - 2 mg/kg; i.p.), received pre-emptive analgesia (ketoprofen, 5 mg/kg, subcutaneously) and local anesthesia (5 mg/kg lidocaine - 2 mg/kg bupivacaine; s.c.). Using a stereotaxic frame, a microdialysis guide cannula was surgically implanted in the rat mPFC (A: +3.2 mm, L: +0.8 mm, V: -5.2 mm relative to bregma) according to the atlas of Paxinos and Watson (2013).

After a recovery period of 48 h, the guide cannula was carefully replaced with a CMA 12 concentric microdialysis probe (3 mm, PAES membrane, 20 kDa cutoff – CMA®, Sweden) and animals were placed in a CMA/120 system for freely moving animals 1 h prior to the start of the experiment for acclimatization.

Microdialysis probe was connected with flexible FEP tubing to a gas-tight syringe (500 µL, Hamilton company, USA) and a PHD 2000 syringe pump (Harvard Apparatus, Holliston, USA) was used to perfuse modified artificial cerebrospinal fluid (ACF) (NaCl 145 mM; KCl 2.7 mM; CaCl2 1.2 mM; MgCl2 1mM, ascorbic acid 10 nM - pH 6.2) solution at a rate of 1 µL/min. All syringes and microdialysis tubing used were wrapped in aluminum foil to prevent sample degradation.

Following a 1h equilibration period, 4 dialysate samples (temporal resolution of 20 min) wre collected in order to determine DA basal levels in mPFC. Immediately after baseline sample collection a single dose (5 mg/kg) of QTP as FQ (5 mg/mL) or QLNC (1 mg/mL) formulation was intravenously injected, via lateral caudal vein and 15 samples (20 min/sample) were collected up to 280 min.

Samples were collected in amber microcentrifuge tubes placed in ice bath and one part of antioxidative mixture (0.27 mM Na_2EDTA, 3.3 mM L-cysteine, 0.5 mM ascorbic acid and 0.1 M acetic acid – pH 3.2) in four parts of microdialysate samples were added to prevent DA degradation. Collected samples were storage at - 80 ± 2 ºC until analysis.

The quantification of DA in microdialysate samples was performed using a validated liquid chromatography – electrospray ionization – tandem mass spectrometry (LC-ESI-MS/MS) method (Capítulo 2). Briefly, mobile phase consisted of A: 0.1% formic acid and B: acetonitrile + 0.1% formic acid. The gradient used was B 5% 0-3 min, 85% 3-5 min, 95% 6-8 min, 5% 8-8.5, 5% 8.5-10 min followed by an equilibration time of 4 min with a total run time of 15 min. The flow rate was 0.2 mL/min, and the column oven temperature was kept at 40 ºC. Chromatographic separation was achieved in a pentafluorophenyl column (Thermo Scientific Gold PFP Hypersil, 2,1 x 150 mm, 1.9 µm). Microdialysate samples were directly injected into the system without the need of internal standard or cleanup process. For the mass spectrometric analysis, the ESI source operating in positive and acquisition was performed in multiple reaction monitoring (MRM) mode. Dopamine was monitored in three m/*z* transitions: 154.097 > 137, 154.097 > 91.1, and 154.097 > 119.

No attempt to correct for *in vitro* probe recovery was made in the present study given because *in vitro* recovery cannot be directly extrapolated to *in vivo* samples; given that, data was reported as directly measured in microdialysate samples.

2.3 Data analysis

Data analysis was performed by populational approach using the software NONMEM (version 7.4, ICON Development Solutions, Ellicott City, MD, USA) and first-order conditional estimation method with interaction (FOCE-INTERACTION) was applied in all estimations. The PsN (version 4.5.1) tool kit (LINDBOM; PIHLGREN; JONSSON, 2005), the R (version 3.5.1) program, and the Xpose 4 (version 4.4.1) program (JONSSON; KARLSSON, 1999) were used for automating and controlling the runs, data visualization, and graphical analysis (goodness-of-fit graphics, including pcVPCs and bootstrap analysis), respectively. The Pirana (version 2.9.8) program (KEIZER; KARLSSON; HOOKER, 2013) was used to keep track of run records and results.

A total of 468 observations from a total of 25 rats and 475 observations from a total of 25 rats of DA microdialysate samples were used for the analysis of the FQ and QLNC formulations, respectively. No data below the quantification limit (BQL) were reported and missing data were excluded from the analysis since they represented less than 5% of the total data. Inter-individual variability (IIV) was modeled exponentially and residual variability was described with a proportional model. Using the population pharmacokinetic parameters (PPP) method (Zhang et al., 2003) the semi-mechanistic PK model was linked to the response model first to describe concentration-effect relationship after the administration of FQ formulation and further after administering the QLNC formulation. Population PK parameters were fixed according to values presented in Table 1.

Table 1. Population pharmacokinetic parameters used in the PK/PD modeling.

Parameters	Population PK parameter value	% CV for IIV
CL (L/h/Kg)	1.86	22.9 (2)
V1 (L/Kg)	1.31	-
V2 (L/Kg)	1.73	-
Q (L/h/Kg)	1.08	-
fu (%)	24.2	-
$CL_{in,}$naïve (L/h/Kg)	0.045	16.7
$CL_{out,}$naïve (L/h/Kg)	0.023	26.4
CL_{in},SCZ (L/h/Kg)	0.019	55.6
$CL_{out,}$SCZ (L/h/Kg)	0.017	66.7
V_1nano (L/Kg)	0.77	-
$Krel_{FAST}$ (h^{-1})	0.261	-
$Krel_{SLOW}$(10^{-4} h^{-1})	4.7	-
$Krel_{TISSUE/BRAIN}$ (h^{-1})	0.0836	-
$Qnano_{TISSUE/BRAIN}$ (L/h/Kg)	0.067	-
F_{core} (%)	85	-
$F_{non\text{-}encapsulated}$ (%)	7	-
$F_{external}$ (%)	8	-

CL: clearance; *Q:* intercompartmental clearance; *V:* volume; RSE: relative standard error; IIV: interindividual variability; CV: coefficient of variation. CL_{in} and CL_{out}: transport across BBB; SCZ*:* schizophrenia-like group; V*:* volume; Krel: release constant, F: fraction of the dose.

After fixing the PK parameters, dopamine microdialysate samples were described by the integral over each collection interval (Tunblad, 2004), therefore, no assumptions regarding collection times were made.

Model selection was guided by: (i) changes in the minimum value of the objective (OFV) function approximately equal to -2*log(likelihood) (-2LL). For two nested models a decrease in 3.84 points in -2LL for an extra added parameter was considered significant at the 5% level, (ii) visual exploration of goodness of fit plots and (iii) precision of the model parameters (iii) precision of model parameters reflected as the relative standard error (RSE) computed as the ratio between the standard error and the

parameter estimate. Evaluation of the selected PK/PD model was performed through the simulation-based diagnostics prediction-corrected visual predictive checks (pcVPC) (BERGSTRAND et al., 2011).

3. RESULTS

3.1 PK/PD model building

The schematic representation of the full semi-mechanistic PK/PD model used to describe the mPFC dopamine response after administrations of QTP given as single dose as a solution or encapsulated into lipid core nanocapsules to naïve or SPR is shown in Figure 1.

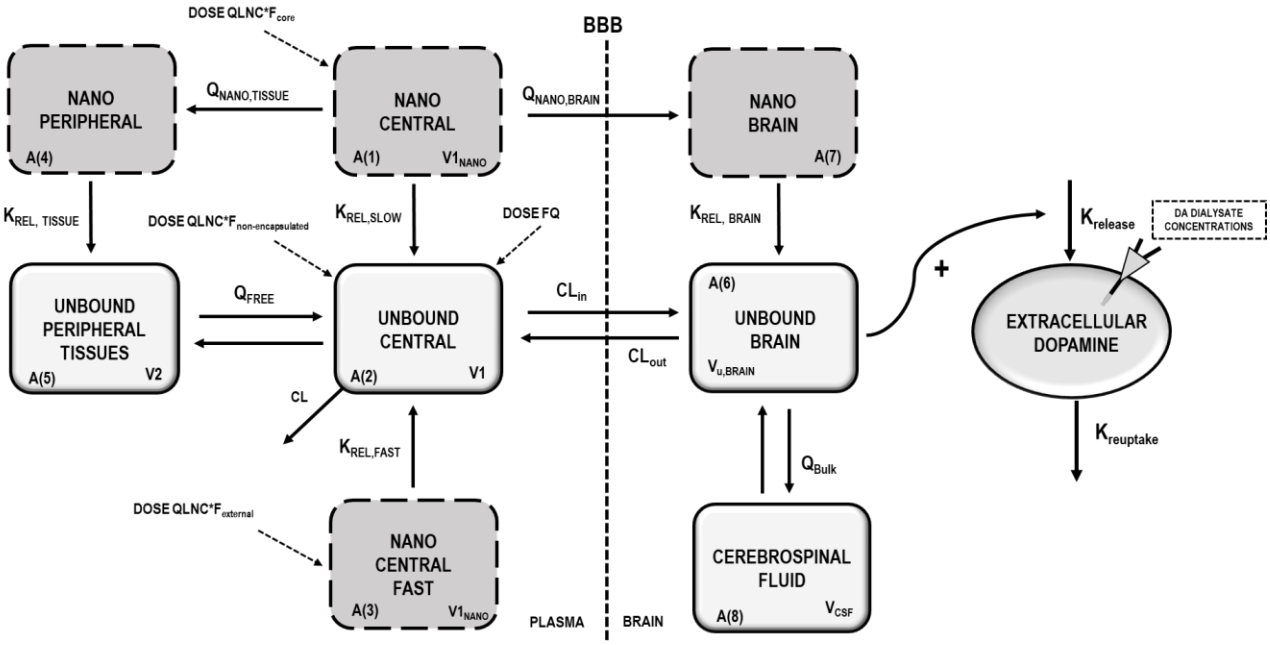


Figure 1. Schematic representation of the full PK/PD model used to describe mPFC dopamine response after administration of FQ or QLNC formulation. Abbreviations: BBB, blood-brain barrier; fu, unbound fraction; CL_{in}, influx clearance; CL_{out}, efflux clearance, CL, unbound QTP clearance; Q_{FREE}, unboud QTP intercompartmental clearance; Q_{bulk}, clearance from brain to cerebrospinal fluid; $Q_{NANO,BRAIN} = Q_{NANO,TISSUE}$, distribution rate constant of the nanoparticle to brain and tissue, respectively. V_1 and V_2 the central and the peripheral volume of distribution for the unbound QTP, respectively; $V_{u,BRAIN}$, unbound volume of distribution in the brain; V_{CSF}, volume of unbound cerebrospinal fluid; V_{1NANO}, volume of distribution for the nanoparticles in plasma; $K_{rel,slow}$, slow release constant of the drug from the nanocarrier in plasma; $K_{rel,fast}$, fast release constant of the drug in plasma; $K_{rel,tissue} = K_{rel,brain}$, release constant of drug from the nanocarrier in tissue/plasma, $K_{release}$, release rate constant of DA to intersticial space; $K_{reuptake}$, reuptake rate constant of DA from the extracellular space.

The typical simulated pharmacokinetic profile of unbound QTP concentrations after administration of a single intravenous 5 mg/kg dose of FQ or QLNC to naïve and SPR are represented in Figure 2.

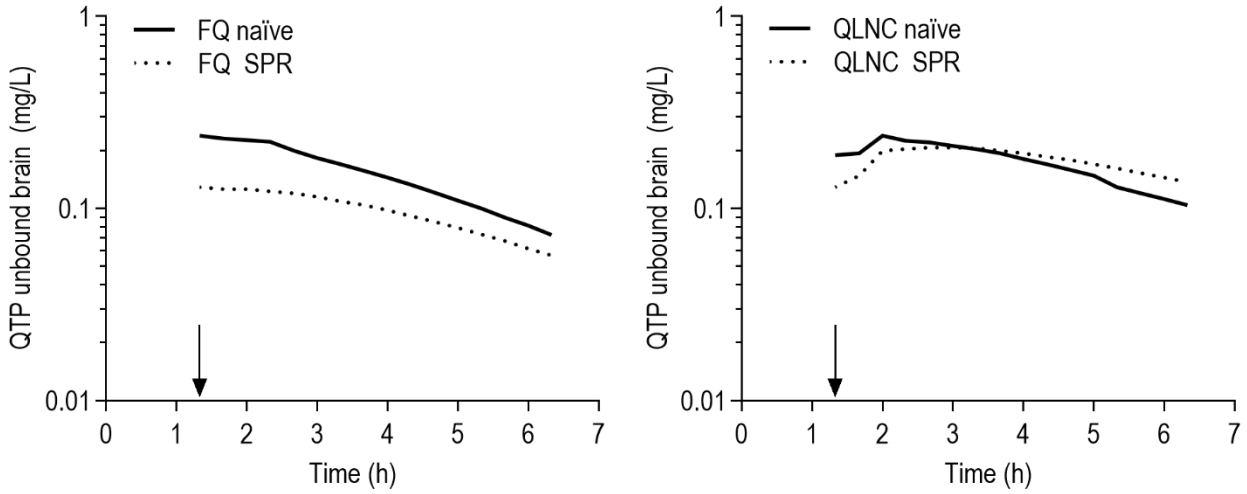


Figure 2. Simulated unbound brain concentration versus time profile of quetiapine after a single intravenous *bolus* dose of 5 mg/kg of FQ (left panel) or QLNC (right panel) formulations to naïve (solid line) and SPR (dotted line). Arrow represents the time when QTP formulations were given to the animals.

Based on measurement of extracellular mPFC dopamine levels using microdialysis an indirect response pharmacodynamic model (Equation 1) was used:

$$\frac{dDA}{dt} = K_{release} - K_{reuptake} \cdot DA \qquad (1)$$

where $K_{release}$ represents the zero-order rate for baseline DA input into the extracellular fluid (ECF), $K_{reuptake}$ represents the rate constant for the first order (DA concentration-dependent) rate of DA removal from ECF and DA is the dopamine levels in the extracellular fluid of the rat medial prefrontal cortex, which are expressed by the DA concentration in the microdialysate. Baseline DA levels (DA_0) and $K_{reuptake}$ were estimated from the modeling and $K_{release}$ was calculated as a secondary parameter from the baseline $K_{release} = DA_0 * K_{reuptake}$. QTP effect was implemented as stimulation of $K_{release}$ to describe the concentration-effect relationship (Equation 2).

$$\frac{dDA}{dt} = K_{release} \cdot \left[1 + \frac{E_{max} \cdot C_{unbound,brain}}{EC_{50} + C_{unbound,brain}}\right] - K_{reuptake} \cdot DA \qquad (2)$$

where $C_{unbound,brain}$ is the QTP unbound brain concentration, E_{max} is the theoretical maximum drug effect, and EC_{50} is the QTP unbound brain concentration associated with 50% of the maximum effect.

Other PD models were tested but neither linear, exponential or sigmoidal E_{max} model nor an inhibition of $K_{reuptake}$ (I_{max} model) described the data significantly better ($p > 0.05$).

3.2 PK/PD comparison of FQ and QLNC

Model building was performed sequentially. First, we used the QTP unbound brain concentrations simulated after the administration of FQ formulation to describe the alterations in prefrontal cortex DA levels in naïve and SPR when they were injected with this formulation. Pharmacodynamic model parameter estimates are listed in Table 2 and the magnitude of the RSE indicates that, in general, parameters were estimated with good precision. Data supported the estimation of IIV in the baseline DA concentration and EC_{50} parameters with magnitudes ranging from 21.4% to 44.9%.

Table 2. Parameter estimates of the final PK/PD model.

PD Parameters	Estimate (% RSE)	% CV for IIV (% RSE)	% Shrinkage
FQ formulation			
Baseline DA (ng/mL)	0.246 (8)	21.4 (18)	10.90
$K_{reuptake}$ (h^{-1})	1.1 (11)	-	-
Emáx	4.25 (16)	-	-
$EC_{50,\ naïve}$ (ng/mL)	1.75 (13)	44.9 (36)[a]	13.20
$EC_{50,\ SPR}$ (ng/mL)	4.97 (30)		
QLNC formulation			
Baseline DA (ng/mL)	0.293 (12)	23.4 (17)	18.56
$K_{reuptake}$ (h^{-1})	0.825 (16)	-	-
Emáx	4.25 FIX	-	-
$EC_{50,\ naïve}$ (ng/mL)	2.02 (16)	21.4 (23)[a]	21.98
$EC_{50,\ SPR}$ (mg/mL)	4.06 (21)		

[a]Individual variability was shared between both parameters. RSE (%): Relative standard error. CV: coefficient of variation. Residual variability (%RSE) for FQ model was: 0.278 (5). Residual variability (%RSE) for QLNC formulation was: 0.312 (9). Model parameters are defined in the text.

During covariate analysis gender did not influenced significantly any parameter of the model. However, EC_{50} was significantly higher ($p < 0.01$) in SPR group in comparison to naïve animals. The inclusion of the SCZ status (naïve or SPR) as a covariate lead to a drop in the objective function value (OFV) of 10.56 points and a better fit of the model to the data for the SPR group. The observed and model-fitted population and individual mPFC DA response-time profiles after FQ dosing are shown in Figure 3.

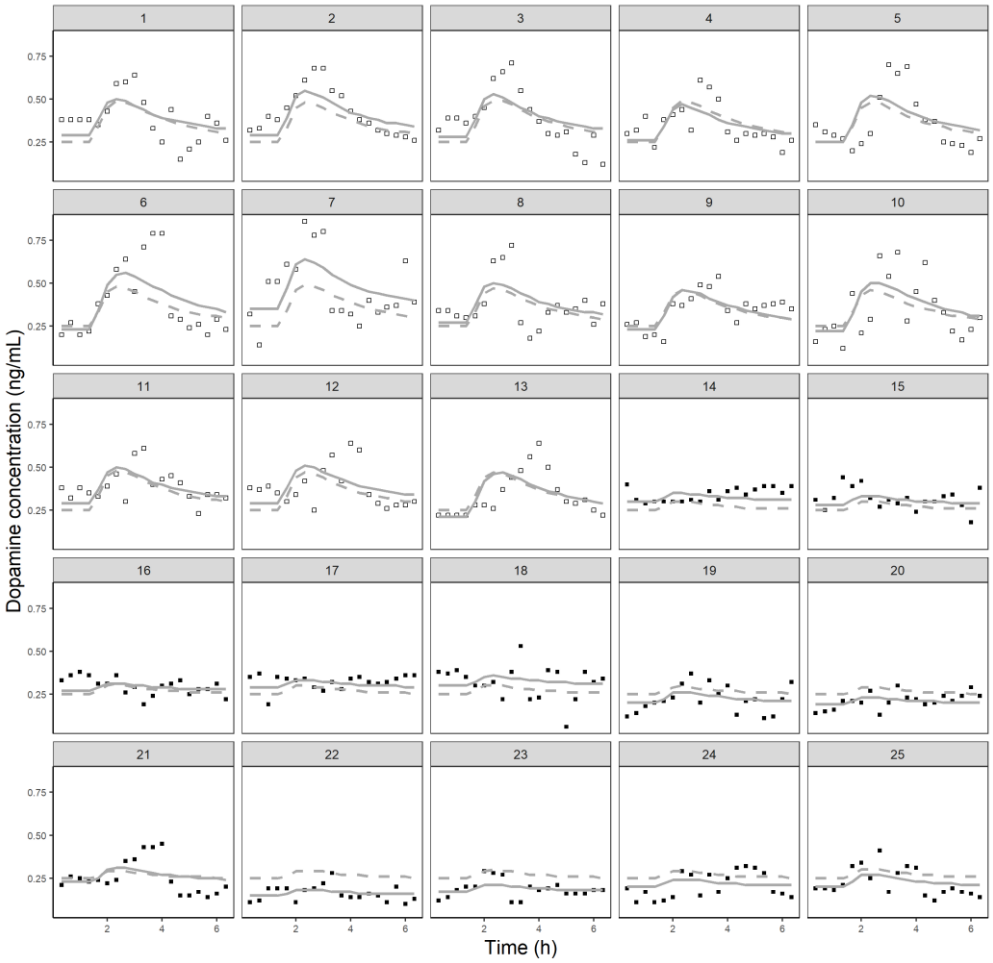


Figure 3. Observed and model-fitted dopamine concentrations in mPFC of naïve and SPR after administration of a single 5 mg/kg dose of FQ formulation intravenously. Open and filled squares represents observed dopamine concentrations in naïve rats and SPR, respectively. Dashed lines represent the model-fitted population dopamine concentrations (PRED) and the solid lines the individual dopamine concentrations (IPRED).

Assuming that SCZ did not causes alterations on E_{max}, since there is no IIV associated with this parameter, during model building this parameter was fixed. Unbound brain concentrations simulated after the intravenous administration of QLNC (5 mg/kg) was used to characterize the alterations in prefrontal cortex DA levels in naïve and SPR. PK/PD model parameter were estimated with good precision and IIV estimations of DA baseline concentration and EC_{50} were also supported by the data (Table 2). Although is possible to notice a significant increase in DA levels when SPR

were injected with QLNC formulation, there was no significant alteration on EC_{50} in comparison to SPR injected with the FQ formulation (Table 2). The observed and model-fitted population and individual mPFC DA response-time profiles after QLNC dosing are shown in Figure 3.

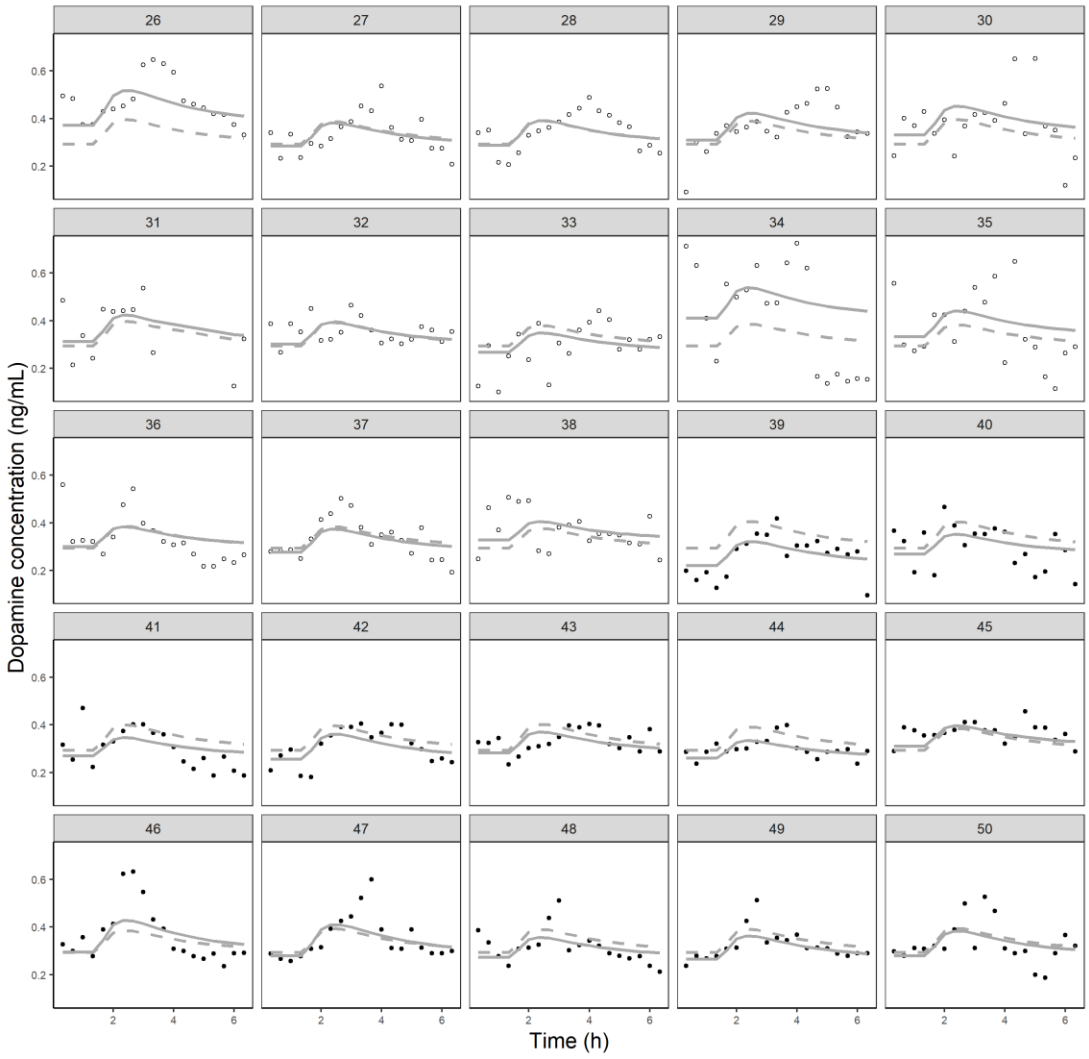


Figure 4. Observed and model-fitted dopamine concentrations in mPFC of naïve and SPR after administration of a single 5 mg/kg dose of QLNC formulation intravenously. Open and filled circles represent observed dopamine concentrations in naïve and SPR, respectively. Dashed lines represent the model-fitted population dopamine concentrations (PRED) and the solid lines the individual dopamine concentrations (IPRED).

Individual predictions were able to describe observed tendency reasonably well (Figure 3 and 4). The visual predictive check (VPCs) confirmed that the model captures very well the overall tendency as well as the dispersion of the data for all experimental scenarios (Figure 5).

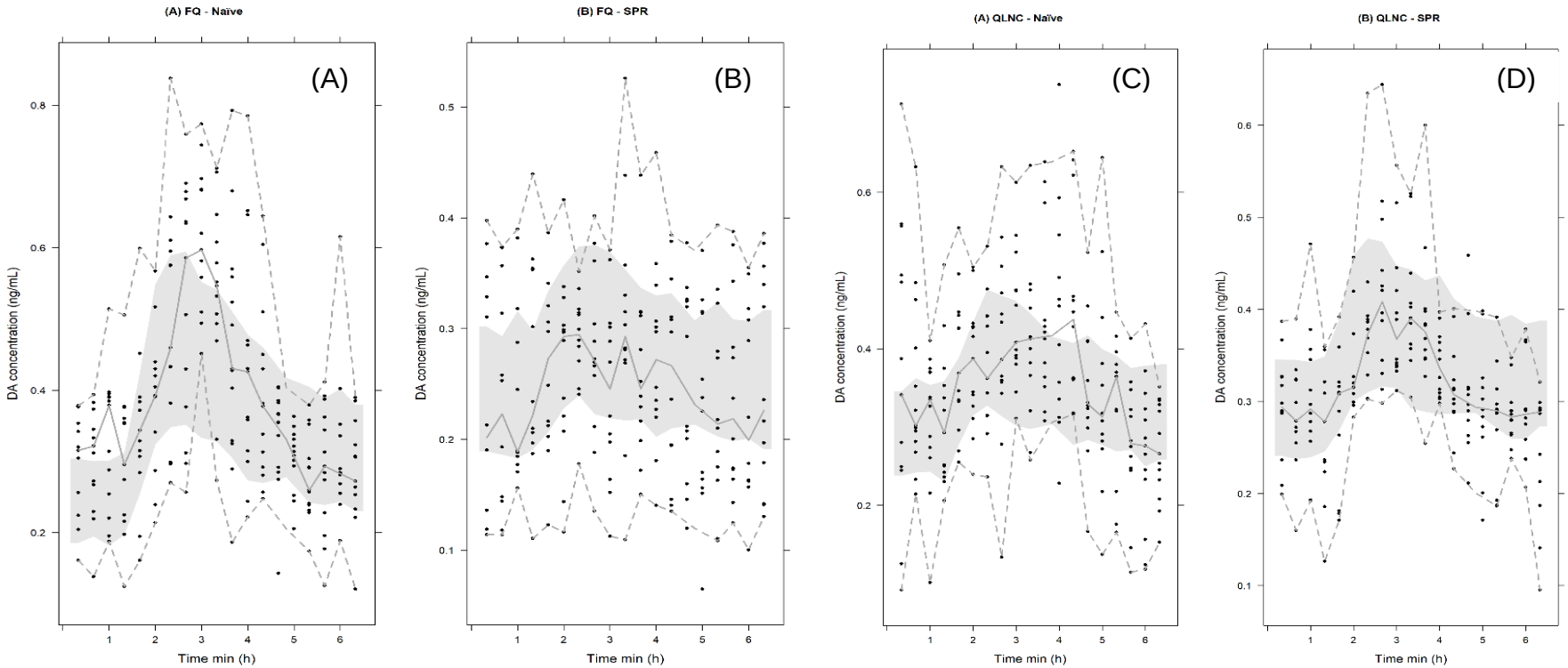


Figure 5. Visual predictive checks (VPCs) of the final PK/PD model for (A) FQ naïve, (B) FQ SPR, (C) QLNC naïve, and (D) QLNC SPR. VPCs are based on 1000 simulations and show a comparison of the observations (dots and thick lines for the median) with the 10th and 90th percentiles of the simulated profiles (dashed lines). Shaded area represents the 95% confidence interval of the 50th percentile of the simulated values.

4. DISCUSSION

In the present study we describe the *in vivo* concentration-effect relationship after administrations of QTP as a solution or nanoencapsulated to SPR and naïve animals viewing to explore the pharmacokinetic and pharmacodynamic components of variability in schizophrenic patient's response to pharmacological treatment.

A semi-mechanistic PK model developed previously, which takes into account the disease status on drug transport to the brain and the modulation of QTP delivery by LNC, was linked to an indirect response PD model to describe changes in dopamine extracellular concentrations in mPFC measured using intracerebral microdialysis.

Preclinical PK-PD models for antipsychotic drugs normally combines the drug transport across the BBB and the time course of D2 receptor occupancy which later can be utilized for translating PK-PD information from animals to human (KOZIELSKA et al., 2012). Although such models have greater value on antipsychotic drug development they do not consider alterations on drug´s pharmacokinetics and pharmacodynamics caused by SCZ status on active influx and efflux transporters as well as on the D2 receptors.

Using the PK/PD model developed here we were able to demonstrate, for the first time, that SCZ status increase EC_{50} values about 3 times reducing QTP pharmacological sensitivity in SPR in comparison to naïve after the administration of 5 mg/kg of FQ formulation (Table 2). Previously (Capítulo 1), we demonstrate that SPR did not respond to FQ formulation on pre-pulse inhibition test. Although the neurological pathway that governs PPI response and changes in DA levels in mPFC might not be correlated, one can infer that alterations on other neurotransmitter receptors due to SCZ can be expected, leading to the changes on drug potency similar to those observed for QTP EC_{50} in the present study. The increase in QTP EC_{50} combined with reduced unbound QTP brain concentrations following FQ dosing helps to understand the lack of response on PPI and highlight the importance of pharmacodynamic component of SCZ patient's high variability in response to treatment.

Nanoparticles did not causes alterations in PD parameters once the EC_{50} values for naïve and SPR groups when animals were injected with the QLNC

formulation are similar to those observed after FQ dosing (Table 2). However, because LCN were able to modulate QTP delivery to the brain an increase in DA levels in mPFC was observed. This result shows the importance of the pharmacokinetic component variability in SCZ pharmacological treatment and indicated that nanotechnology can be used to produce more effective antipsychotic treatments bypassing BBB alteration caused by the disease.

To the best of our knowledge, this is the first study that combines microdialysis and PK/PD modeling in a neurodevelopmental model of SCZ to investigate nanocarriers modulation of antipsychotic drug delivery, contributing to development of SCZ new treatment strategies.

Because we investigated a single QTP dose, the extrapolation possible with the PK/PD model developed here are limited. However, it is a starting point for a new approach for pre-clinical antipsychotic evaluation using mathematical modeling & simulation by correlating *in vivo* pharmacokinetic and pharmacodynamic data obtained from a predictive animal model of schizophrenia.

5. CONCLUSION

In conclusion, a semi-mechanist PK/PD model was developed for QTP using extracellular dopamine levels as pharmacodynamic response increasing the understanding of schizophrenia status and the role that LCN can have on the antipsychotic limited response to treatment.

6. ACKNOWLEDGMENTS

The authors acknowledge Dr. Liberato Brum Junior (Prati Donaduzzi, Toledo – PR, Brazil) for kindly providing quetiapine fumarate and technical support from the Animal's Facility staff (UFRGS/Biochemistry Department). This study was financed in part by CNPq/Brazil (Process 421767/2016-2) and by the Coordenação de Aperfeiçoamento de Pessoal de Nível Superior - Brazil (CAPES) - Finance Code 001. The authors also thank CNPq for the individual grant.

7. REFERENCES

BATAIL, J.-M. et al. Use of very-high-dose olanzapine in treatment-resistant schizophrenia. **Schizophrenia research**, [s. l.], v. 159, n. 2–3, p. 411–4, 2014. Disponível em: <http://www.ncbi.nlm.nih.gov/pubmed/25278103>. Acesso em: 5 abr. 2018.

BERGSTRAND, M. et al. Prediction-corrected visual predictive checks for diagnosing nonlinear mixed-effects models. **The AAPS journal**, [s. l.], v. 13, n. 2, p. 143–51, 2011. Disponível em: <http://www.ncbi.nlm.nih.gov/pubmed/21302010>. Acesso em: 25 jul. 2019.

GRACE, A. A. **Dysregulation of the dopamine system in the pathophysiology of schizophrenia and depression**, 2016.

HADAR, R. et al. Using a maternal immune stimulation model of schizophrenia to study behavioral and neurobiological alterations over the developmental course. **Schizophrenia Research**, [s. l.], v. 166, n. 1–3, p. 238–247, 2015. Disponível em: <http://dx.doi.org/10.1016/j.schres.2015.05.010>

ICHIKAWA, J. et al. Atypical antipsychotic drugs, quetiapine, iloperidone, and melperone, preferentially increase dopamine and acetylcholine release in rat medial prefrontal cortex: Role of 5-HT1A receptor agonism. **Brain Research**, [s. l.], v. 956, n. 2, p. 349–357, 2002.

JOHNSON, M. et al. Mechanism-based pharmacokinetic-pharmacodynamic modeling of the dopamine D2 receptor occupancy of olanzapine in rats. **Pharmaceutical research**, [s. l.], v. 28, n. 10, p. 2490–504, 2011. Disponível em: <http://www.ncbi.nlm.nih.gov/pubmed/21647790>. Acesso em: 23 jul. 2019.

JONSSON, E. N.; KARLSSON, M. O. Xpose--an S-PLUS based population pharmacokinetic/pharmacodynamic model building aid for NONMEM. **Computer methods and programs in biomedicine**, [s. l.], v. 58, n. 1, p. 51–64, 1999. Disponível em: <http://www.ncbi.nlm.nih.gov/pubmed/10195646>. Acesso em: 24 jul. 2019.

KEIZER, R. J.; KARLSSON, M. O.; HOOKER, A. Modeling and simulation workbench for NONMEM: Tutorial on Pirana, PsN, and Xpose. **CPT: Pharmacometrics and Systems Pharmacology**, [s. l.], 2013.

KOZIELSKA, M. et al. Pharmacokinetic-pharmacodynamic modeling of the D_2 and 5-HT (2A) receptor occupancy of risperidone and paliperidone in rats. **Pharmaceutical research**, [s. l.], v. 29, n. 7, p. 1932–48, 2012. Disponível em: <http://www.ncbi.nlm.nih.gov/pubmed/22437487>. Acesso em: 16 jul. 2019.

KRAUSE, M. et al. Antipsychotic drugs for patients with schizophrenia and predominant or prominent negative symptoms: a systematic review and meta-analysis. **European Archives of Psychiatry and Clinical Neuroscience**, [s. l.], v. 0, n. 0123456789, p. 0, 2018. Disponível em: <https://doi.org/10.1007/s00406-018-0869-3>

LINDBOM, L.; PIHLGREN, P.; JONSSON, N. PsN-Toolkit - A collection of computer intensive statistical methods for non-linear mixed effect modeling using NONMEM. **Computer Methods and Programs in Biomedicine**, [s. l.],

2005.

MILLAN, M. J. et al. Altering the course of schizophrenia: progress and perspectives. **Nature Reviews Drug Discovery**, [s. l.], v. 15, n. 7, p. 485, 2016.

PAXINOS, G.; WATSON, C. **The Rat Brain in Stereotaxic Coordinates : Hard Cover Edition.** [s.l.] : Elsevier Science, 2013.

PIRA, L.; MONGEAU, R.; PANI, L. The atypical antipsychotic quetiapine increases both noradrenaline and dopamine release in the rat prefrontal cortex. **European Journal of Pharmacology**, [s. l.], v. 504, n. 1–2, p. 61–64, 2004.

YAMAMURA, S. et al. Effects of quetiapine on monoamine, GABA, and glutamate release in rat prefrontal cortex. **Psychopharmacology**, [s. l.], 2009.

DISCUSSÃO GERAL

O presente trabalho visou contribuir para o entendimento das alterações farmacocinéticas e farmacodinâmicas relacionadas à nanoencapsulação de quetiapina em um nanocarreador polimérico de núcleo lipídico, permitindo elucidar como esse nanocarreador modula a disposição e o efeito farmacológico do fármaco quando há comprometimento da BHE devido à esquizofrenia experimental em ratos machos e fêmeas. Para atingir essa meta, utilizou-se uma estratégia experimental inovadora que combinou experimentos de microdiálise cerebral, para medida tanto do fármaco como de neurotransmissores, associados à modelagem matemática e simulação.

Doenças do SNC, tais como esquizofrenia, Parkinson, Alzheimer, depressão, ansiedade e epilepsia acometem milhões de pessoas em todo o mundo e são um grande problema de saúde pública. Apesar dos avanços das pesquisas científicas nas últimas décadas ter acelerado a compreensão dos mecanismos fisiopatológicos e bioquímicos dessas doenças, os progressos relacionados ao tratamento, especialmente novas farmacoterapias, foram mínimos.

Para que um fármaco seja capaz de exercer sua ação no SNC é necessário que o mesmo atravesse a BHE, que regula a penetração cerebral de substâncias nas células do epitélio vascular que compõe a barreira através de transporte paracelular (zônulas de oclusão e alta conduvitivade do endotélio) e transcelular (expressão de mecanismos de influxo e efluxo). Diferentes fatores podem alterar a passagem de fármacos na BHE, impedindo a manutenção de concentrações cerebrais suficientes para exercer efeito farmacológico desejado.

A utilização de nanocarreadores como nanopartículas lipídicas sólidas, lipossomas e nanopartículas poliméricas tem demonstrado ser uma estratégia promissora para melhorar o *delivery* cerebral de fármacos (CARREÑO et al., 2015, 2016a, 2016b; LINDQVIST et al., 2013; VIEIRA et al., 2016). Trabalhos conduzidos anteriormente pelo nosso grupo de pesquisa em Farmacocinética e Modelagem PK/PD tem buscado compreender as alterações farmacocinéticas relacionadas à nanoencapsulação de fármacos e a interação desses nanocarreadores com as barreiras fisiológicas do SNC.

Carreño e colaboradores (2016a) demonstraram que nanocápsulas poliméricas de núcleo lipídico contendo quetiapina (QLNC) foram capazes de

aumentar a exposição tecidual total ao fármaco, medida em homogeneizado cerebral e hepático de ratos Wistar machos hígidos[1], porém não foram capazes de alterar as concentrações livres (não ligadas a proteínas) cerebrais em comparação com a QTP administrada em solução (FQ). Após administração de probenecida, inibidor de transporte de influxo, a penetração cerebral da QTP administrada como solução, determinada a partir do fator de penetração, foi reduzida 1,55 ± 0,17 para 0,94 ± 0,15. Esse resultado comprova que a QTP é substrato para transportadores de influxo presentes na BHE, uma vez que a penetração cerebral do fármaco é maior que a unidade em condição fisiológica, sendo reduzida para valor próximo a um quando o transportador de influxo é inibido. No entanto, a penetração cerebral do fármaco nanoencapsualdo não foi alterada (0,88 ± 0,21 e 0,92 ± 0,13, respectivamente), evidenciando que a QTP nanoencapsulada é carreada para o parênquima cerebral pela LNC e não está disponível para interagir com transportadores presentes na BHE (CARREÑO et al., 2016b).

Sabe-se da literatura que aproximadamente 60% dos pacientes esquizofrênicos não respondem ao tratamento farmacológico ou apresentam recaídas ao longo do curso da doença (AMATO et al., 2017). Alterações patológicas na BHE são reconhecidas como um fator central para uma série de distúrbios neurológicos (STOLP et al., 2009; VARATHARAJ; GALEA, 2017). Embora haja uma alta variabilidade na resposta crônica ao tratamento da SCZ, a relação entre esquizofrenia, alterações da BHE e falta de resposta farmacológica aos antipsicóticos é pouco explorada na literatura atualmente. Ainda menos investigada é a possível influência do componente farmacocinético na variabilidade da resposta farmacológica aos antipsicóticos nesses pacientes.

Sabe-se, ainda, que a incidência desse distúrbio psíquico é ligeiramente maior em homens do que em mulheres, sendo que as mulheres apresentam sintomas menos severos e melhor prognóstico (LI et al., 2016). Uma das hipóteses para explicar as diferenças entre os sexos observadas no curso e prognóstico da SCZ postula que há uma proteção estrogênica na BHE, uma vez que a expressão de transportadores de influxo e efluxo sofre

[1] No presente trabalho, o termo hígido usado em português corresponde ao termo *naïve* usado nos textos em inglês.

influência reguladora desse hormônio, podendo estar alterada nessas pacientes (MORRIS; LEE; PREDKO, 2003).

Diante desse cenário, os resultados promissores com as QLNC obtidos previamente originaram novos questionamentos: “Existem diferenças na exposição à QTP em diferentes regiões cerebrais, provocadas por diferenças de distribuição das nanocápsulas no parênquima cerebral?; “É possível descrever *in vivo* a liberação da QTP a partir das QLNC?”; “De que maneira as QLNC modulam a farmacocinética da QTP se a BHE está alterada, como na esquizofrenia?”; “Há diferenças na penetração cerebral das QLNC em machos e fêmeas hígidos e com alterações na BHE, como ocorre na esquizofrenia?; “É possível correlacionar as concentrações cerebrais livres da QTP administrada como FQ e como QLNC com as concentrações cerebrais de neurotransmissores utilizando ferramentas de farmacometria?”

Nesse contexto, a hipótese central explorada nesta tese foi que a resistência à farmacoterapia em pacientes esquizofrênicos poderia estar associada a alterações da BHE que limitam a penetração de antipsicóticos para o parênquima cerebral e que as QLNC seriam capazes de sobrepor essas limitações, controlando o *delivery* cerebral e melhorando a eficácia da QTP nesses pacientes.

Como nos estudos anteriores investigamos a penetração cerebral da QLNC somente em ratos Wistar machos hígidos, tornou-se fundamental avaliar as diferenças de disposição e resposta dos sistemas nanoencapsulados em um modelo animal preditivo e confiável, capaz de mimetizar as alterações cerebrais encontradas na esquizofrenia, como é o modelo de ativação da resposta imune materna por poli(i:c), utilizando para tanto machos e fêmeas.

O desenho experimental desta tese foi, portanto, dividido em quatro etapas: a) etapa de implementação do modelo neurodesenvolvimental de esquizofrenia; b) etapa PK, que teve como objetivo avaliar comparativamente os parâmetros farmacocinéticos plasmáticos e a distribuição da QTP administrada como FQ e como QLNC no hipocampo e córtex pré-frontal em modelo de esquizofrenia em ratos Wistar machos e fêmeas; c) etapa PD, cujo objetivo foi investigar as alterações nos parâmetros farmacodinâmicos promovido pela nanoencapsulação no mesmo modelo experimental. Nas

etapas PK e PD a microdiálise cerebral foi utilizada para coleta de amostras de líquido intersticial para quantificação da QTP e neurotransmissores, respectivamente. A escolha das regiões cerebrais para o estudo foi fundamentada nas hipóteses bioquímicas descritas na literatura para a gênese de sinais e sintomas característicos da esquizofrenia; e d) etapa de farmacometria, na qual, utilizando os dados coletados, foram desenvolvidos modelos semi-mecanísticos popPK e PK/PD, capazes de descrever as alterações na farmacocinética plasmática, na distribuição cerebral e na resposta à quetiapina nanoencapsulada em animais com esquizofrenia experimental.

O modelo de ativação imune pré-natal é induzido em ratas prenhas por injeção intravenosa de ácido poli-inosínico:policitidílico [poli(i:c)], um RNA dupla fita, mimetizando uma infecção viral por ativação de receptores *toll-like* 3 (PATRICH et al., 2016; ZUCKERMAN et al., 2003; ZUCKERMAN; WEINER, 2005). As citocinas pró-inflamatórias liberadas durante a resposta imune materna são capazes de alterar a neurogênese dos embriões que, na idade adulta, apresentarão alterações anatômicas (afinamento do córtex límbico e aumento da densidade de empacotamento neuronal), déficit comportamental (diminuição da inibição de pré-pulso, perturbação no aprendizado e aumento da resposta a anfetaminas) e alteração da neuroquímica cerebral (hipofunção dopaminérgica no córtex pré-frontal, por exemplo) resultando em um fenótipo neurobiológico e comportamental similar ao da esquizofrenia (PATRICH et al., 2016; PIONTKEWITZ; ARAD; WEINER, 2011).

Uma vez que os mecanismos pelos quais insultos virais durante a neuro-ontogênese podem causar uma patologia latente no SNC ainda não estão completamente elucidados, o sucesso do modelo proposto depende da capacidade da dose de poli(i:c) administrada produzir uma resposta imune materna adequada, consistente e com a liberação de citocinas pró-inflamatórias que irão interferir com o desenvolvimento normal do cérebro fetal (ZUCKERMAN et al., 2003; ZUCKERMAN; WEINER, 2005). Desse modo, foi necessário determinar a dose ótima de poli(i:c) capaz de gerar prole com sinais e sintomas de esquizofrenia na idade adulta nos animais provenientes do Biotério do Departamento de Bioquímica/UFRGS, através do

teste de diferentes doses do composto (P1 - 1 mg/kg; P4 - 4 mg/kg e P8 - 8 mg/kg).

Considerando que o poli(i:c) produz um desbalanço na resposta inflamatória mediado por aumento da expressão das interleucinas pró-inflamatórias e anti-inflamatórias, entre elas respectivamente IL-6 e IL-10, uma forma direta de demonstrar o sucesso na ativação imune é evidenciar o aumento dessas interleucinas na circulação sistêmica das ratas prenhas.

A administração intravenosa de poli(i:c) em ratas Wistar prenhas resultou em um aumento significativo dos níveis plasmáticos da citocinas pró-inflamatória IL-6 (4 horas pós-dose) e da citocina anti-inflamatória IL-10 (8 horas pós-dose) em comparação com as fêmeas prenhas que receberam volume equivalente de solução salina estéril, de forma dose dependente. Além disso, houve também um desequilíbrio significativo na razão entre IL-6/IL-10 na circulação sistêmica das ratas (Capítulo 1). Essas citocinas causam alterações na barreira hematoplacentária e impactam diretamente no desenvolvimento cerebral da prole.

As alterações comportamentais após a exposição pré-natal a diferentes doses de poli(i:c) foram avaliadas quando a prole atingiu a idade adulta (PND70) através dos testes de labirinto em cruz elevado (LCE), inibição de sobressalto por pré-pulso (PPI) e hiperlocomoção induzida por MK-801.

Houve uma redução significativa na distância total percorrida, no tempo gasto e no número de entradas nos braços abertos do labirinto em cruz elevado, especialmente em machos descendentes de mães que foram injetadas com as doses de poli(i:c) de 4 e 8 mg/kg, não havendo diferenças entre essas duas doses. Com base nesses achados, postulamos que a exposição pré-natal ao poli(i:c) não foi capaz de provocar nos animais alterações relacionadas à ansiedade nata. A redução na distância total percorrida no aparato pode estar relacionada ao aumento de comportamento tipo repetitivo (*self-grooming*) durante uma situação estressante, apesar desta medida não ter sido avaliada no presente trabalho. Trabalhos publicados na literatura utilizando cepas de camundongos C57 reportaram que após exposição pré-natal ao poli(i:c), camundongos adultos apresentaram aumento de *self-grooming* quando comparados com proles expostas a salina (SCHWARTZER et al., 2013; XUAN; HAMPSON, 2014).

Os resultados obtidos no teste de hiperlocomoção induzida por MK-801 corroboram estudos prévios descritos na literatura de que a ativação da resposta imune materna (MIA) causa na prole atividade hiperlocomotora em resposta ao antagonista do receptor NMDA, MK-801 e a hipofunção deste receptor é uma das hipóteses envolvidas na fisiopatologia da SCZ.

Tanto animais machos quanto fêmeas dos grupos P4 e P8 apresentaram um aumento pronunciado da atividade locomotora após administração de MK-801, embora esse aumento não tenha sido dose-dependente. Além disso, os animais provenientes da menor dose de poli(i:c) investigada (P1- 1 mg/kg) não diferiram dos controles que receberam salina.

Wolff e Bilkey (2008) sugerem, em seu estudo que doses de poli(i:c), que não são capazes de gerar um desbalanço significativo de citocinas na circulação sistêmica das mães não são capazes de causar alterações no desenvolvimento cerebral dos fetos. Nossos resultados concordam com essa hipótese já que os níveis plasmáticos de IL-6 e IL-10 para a dose de 1 mg/kg não foram diferentes daqueles obtidos para as fêmeas prenhas do grupo controle.

Por fim, um dos achados comportamentais mais consiste observados e descritos na literatura após a MIA com poli(i:c) em diferentes períodos gestacionais é o déficit na inibição de sobressalto induzida por pré-pulso. Este paradigma é um fenômeno multimodal e interespecífico que fornece uma medida operacional dos déficits sensoriais e cognitivos observados na SCZ. Corroborando relatos anteriores (BIKOVSKY et al., 2016; HADAR et al., 2015a, 2015b), no presente estudo, a prole de animais P4 e P8 exibiram uma redução do PPI em comparação com animais do grupo salina e P1.

Embora existam evidências na literatura de que a MIA durante períodos críticos do desenvolvimento pré-natal do cérebro cause efeitos em ratos adultos de maneira sexo-específica (REISINGER et al., 2015), o conjunto de achados deste trabalho não corrobora essa hipótese. Fatores como a dose de poli(i:c) utilizada e o tempo de gestação no qual foi feita a administração, entre outros, podem interagir com o sexo e desempenhar um papel significativo na ausência de diferenças observadas no presente estudo.

Com a relevância pré-clínica que o teste de PPI apresenta para a exploração de estratégias terapêuticas farmacológicas para a SCZ,

investigamos os efeitos da nanoencapsulação da QTP na resposta ao PPI em comparação com a QTP administrada em solução utilizando a prole proveniente de ratas prenhas administradas com poli(i:c). A QTP na dose de 5 mg/kg administrada por via intravenosa à prole P4 não foi capaz de produzir uma reversão no déficit de PPI causado pela MIA. Por outro lado, a mesma dose de QLNC resultou em uma melhora significativa do comprometimento dos animais no PPI. A hipótese para explicar esse resultado é de que a QLNC modula a exposição cerebral à QTP. Em estudo prévio, animais que receberam quetiapina nanoencapsulada apresentaram um aumento de cerca de duas vezes na exposição cerebral ao fármaco medida em homogeneizado de tecido (Carreño et al., 2016a). Até o presente momento, este é o primeiro trabalho que relata a restauração dos déficits de PPI em um modelo neurodesenvolvimental de SCZ utilizando antipsicótico nanoencapsulado e demonstram o potencial de aplicação das nanopartículas no tratamento farmacológico da SCZ.

A etapa seguinte da tese foi a avaliação comparativa da farmacocinética plasmática e da distribuição cerebral da QTP, através de microdiálise em duas distintas regiões cerebrais (hipocampo e córtex) de ratos Wistar machos e fêmeas com SCZ experimental após administração intravenosa do fármaco em solução ou nanoencapsulado (Capítulo 3).

O conjunto de dados de concentração plasmática total, concentração hipocampal e cortical livre versus tempo, juntamente com os resultados obtidos em trabalhos anteriores desenvolvidos por Carreño e colaboradores (2015, 2016a, 2016b) foram utilizados para o desenvolvimento de um modelo farmacocinético semi-mecanístico utilizando uma abordagem populacional capaz de descrever as alterações na farmacocinética plasmática e cerebral após a administração de QTP em solução (FQ) ou nanoencapsulada (QLNC) em animais de ambos os sexos hígidos e provenientes do modelo neurodesenvolvimental de SCZ [de agora em diante denominados poli(i:c)] buscando aumentar a compreensão do papel desse nanocarreador na disposição cerebral quando a BHE está comprometida pela doença.

Assim como observado nos resultados dos experimentos comportamentais, a utilização do sexo como covariável no modelo popPK desenvolvido não alterou os parâmetros farmacocinéticos estimados quando animais machos e fêmeas hígidos ou poli(i:c) administrados com a mesma

formulação (FQ ou QLNC) foram comparados dentro do mesmo grupo. Esse resultado indica que o sexo não influencia a farmacocinética plasmática e a penetração cerebral da QTP, mesmo na condição de BHE alterada.

Utilizando o modelo popPK desenvolvido para FQ foi possível simular a exposição plasmática e cerebral livre em animais hígidos e poli(i:c). Não houve alteração significativa nos perfis de concentração plasmática *versus* tempo quando animais hígidos e poli(i:c) foram comparados, demonstrando que a exposição pré-natal a MIA não afeta a disposição e a eliminação plasmática da QTP. No entanto, as concentrações livres cerebrais são as responsáveis pelo efeito terapêutico sendo mais relevantes que as concentrações plasmáticas. Uma redução significativa da exposição cerebral à QTP foi observada nos animais poli(i:c) em relação aos animais hígidos quando o fármaco foi administrado como FQ. Isso pode ser explicado pelo insulto pré-natal desencadeado pela MIA que prejudicou o desenvolvimento cerebral da prole, resultado em alterações de longo prazo na BHE dos animais adultos. Assumindo que as alterações da BHE observadas no modelo poli(i:c) mimetizam o que acontecem em humanos com SCZ, concentrações cerebrais menores de QTP seriam esperadas em pacientes esquizofrênicos que recebem o fármaco não-encapsulado.

Através do modelo semi-mecanístico desenvolvido foi possível entender o mecanismo pelo qual essa alteração na BHE ocorre. Os animais com SCZ experimental apresentam redução no transporte por influxo através da BHE, o que pode ser observado pela redução do parâmetro CL_{in} de 0,045 L/h/kg para 0,019 L/h/kg (Tabela 1, Capítulo 3) quando comparado aos animais hígidos. Em estudo prévio com probenecida havíamos evidenciado que a QTP é substrato para transportadores de influxo na BHE, havendo uma redução do fator de penetração cerebral de 39,4% quando o inibidor de influxo é utilizado em associação com o fármaco (CARREÑO et al., 2016b). Utilizando o modelo popPK desenvolvido nesta tese foi possível confirmar esse achado, observando-se uma redução de CL_{in} de 38% nos animais poli(i:c), indicando que a SCZ experimental inibe os transportadores de influxo de modo semelhante ao observado com o inibidor, levando à redução da exposição cerebral à QTP.

Este resultado inédito pode auxiliar no entendimento da resistência ao tratamento farmacológico da SCZ, já que a disposição cerebral de antipsicóticos como a QTP, que penetra no cérebro por difusão e influxo, poderá estar diminuída em pacientes esquizofrênicos. Além disso, esse resultado também corrobora e explica a falta de resposta dos animais poli(i:c) que receberam FQ no teste do PPI. Utilizando o modelo popPK foi possível prever o valor de CL_{in} individual para cada um dos animais que receberam FQ e correlacioná-los com os resultados do teste de PPI. Os resultados demonstram de maneira inédita que quanto maior o déficit pré-atencional no PPI, maior é o comprometimento do transporte da QTP através da BHE (Figura 3, Capítulo 3). Os resultados, no entanto, não permitem concluir se as alterações causadas no influxo através da BHE no modelo de SCZ são devidas à redução da expressão ou da atividade dos transportadores de influxo presentes na BHE. Para responder a esse questionamento, bem como para demonstrar se há também alteração no transporte por efluxo na BHE devido a SCZ, mais estudos são necessários.

O modelo popPK desenvolvido foi expandido para investigar a modulação da farmacocinética da QTP quando administrada como QLNC tanto em animais hígidos quanto em animais com SCZ experimental.

Normalmente, os estudos de cinética de liberação de fármacos a partir de nanocarreadores são realizados *in vitro* em ensaios de liberação utilizando saco de diálise. A interpretação quantitativa desses ensaios é facilitada pela utilização de modelos matemáticos de ordem zero, primeira ordem ou modelo de Higuchi, que traduzem matematicamente a curva de liberação em parâmetros relacionados com o nanocarreador em estudo, visando estabelecer uma correlação desses com os resultados farmacocinéticos obtidos *in vivo*.

No presente estudo, utilizando a modelagem popPK, fomos capazes de descrever a cinética de liberação da QTP a partir das QLNCs no plasma *in vivo* e propor um mecanismo de distribuição do nanocarreador para cérebro e outros tecidos, bem como de liberação da QTP nanocarreada nos mesmos.

É importante ressaltar que, durante o desenvolvimento da formulação de nanopartículas, a QTP foi escolhida como fármaco modelo levando em consideração as características físico-químicas da molécula, especialmente seu logD (2,6), que aumenta a eficiência de encapsulação neste tipo de

nanocarreador e a distribuição do fármaco majoritariamente no núcleo da partícula. A partir da aplicação do algoritmo desenvolvido por Oliveira e colaboradores (2012), foi possível propor a distribuição da QTP na estrutura das LNCs (CARREÑO et al., 2015), demonstrando que grande parte do fármaco encontra-se disperso no núcleo e na parede polimérica do nanocarreador (~95%) e o restante encontra-se em solução.

Através do modelo popPK desenvolvido foi possível demonstrar que as LNCs liberam a QTP no plasma com duas constantes distintas de primeira ordem: $Krel_{FAST}$ e $Krel_{SLOW}$ (Tabela 1, Capítulo 3). A partir do modelo demonstramos que 8% da dose de QTP administrada sofrerá uma liberação rápida no plasma, pois se encontra nas camadas poliméricas da nanoestrutura ($F_{external}$) e 85% da dose será liberada de maneira mais lenta, pois está dispersa no núcleo lipídico da nanoestrutura (F_{core}). Foi possível caracterizar que o F_{core} terá a capacidade de se distribuir para o cérebro e demais tecidos, liberando o fármaco nesses locais com velocidade distinta daquela determinada em plasma. O restante da dose administrada (~7%) está em solução no momento da administração da formulação, pois não foi nanoencapsulada ($F_{non\text{-}encapsualted}$). O conjunto desses resultados corrobora os dados obtidos no estudo prévio de Carreño e colaboradores (2015) e valida o mecanismo proposto de distribuição da QTP no nanocarreador.

Havíamos demonstrado anteriormente que as concentrações totais de QTP, determinadas em homogeneizado de tecido cerebral, estavam aumentadas em animais hígidos administrados com QLNC. No entanto, a exposição cerebral à QTP medida através de microdiálise no líquido extracelular de ratos Wistar machos hígidos era semelhante, independente da formulação administrada (FQ ou QLNC). Através do modelo popPK proposto foi possível explicar esse resultado. A taxa de distribuição da QTP administrada como FQ é similar àquela obtida quando o fármaco é administrado como QLNC (CL_{in},naïve = 0,045 L/h/kg *versus* $Qnano_{TISSUE/BRAIN}$ = 0,067 L/h/kg) para os animais hígidos. Entretanto, quando animais com SCZ experimental são administrados com QLNC o transporte do fármaco através da BHE será governado pelo nanocarreador ($Qnano_{TISSUE/BRAIN}$ = 0,067 L/h/kg), sendo maior do que o transporte do fármaco livre (não ligado às proteínas plasmáticas - 0,019 L/kg/h, Tabela 1, Capítulo 3), já que aproximadamente 85% da dose do

fármaco está nanoencapsulada no núcleo da partícula. Comparando o aumento da exposição cerebral observada em animais com SCZ experimental quando QLNC foi administrado, é possível notar que os nanocarreadores retornaram as concentrações de QTP aos níveis observados em animais hígidos (Figura 6, Capítulo 3).

Os resultados demonstram que a LNC governa a distribuição do fármaco para os tecidos e $Krel_{SLOW}$ no plasma determina a quantidade de fármaco remanescente no núcleo do nanocarreador, capaz de penetrar no cérebro. As QLNC são compostas por um núcleo lipídio disperso contendo triglicerídeos de cadeia média e monoestearato de sorbitano, envolto por uma parede polimérica [poli (ε-caprolactona)]. Esse sistema gera uma cinética de liberação do fármaco dependente da viscosidade do núcleo (representada no modelo como F_{core} e $Krel_{SLOW}$) e a da parede polimérica (representada in vivo por $F_{external}$ e $Krel_{FAST}$). A taxa de liberação de fármaco dessa nanopartícula ($Krel_{SLOW}$) diminui de acordo com o aumento na concentração do polímero ou na dependência concentrações de triglicerídeos de cadeia média e/ou de monoestearato de sorbitano. Nesse contexto, as similações realizadas variando em 10 e 100 vezes o valor de $Krel_{SLOW}$ permitiram entender o impacto desse parâmetro na pemetração crebral da QTP do animais poli(i:c) (Figura 6, Capítulo 3). Foi possível observar que um aumento de 10 vezes no $Krel_{SLOW}$ aumenta a concentração total no plasma e reduz as concentrações cerebrais livres, no entanto, essas alterações são pquenas e podem não ter um impacto clínico significativo.

As simulações também mostraram que, quanto maior o $Krel_{SLOW}$, maior a quantidade de fármaco liberada no plasma e menos eficaz é o nanocarreador para superar as alterações na BHE produzidas nos animais poli(i:c). Apenas um aumento de 100 vezes na liberação do fármaco a partir do núcleo da LNC poderia comprometer a melhora significativa na penetração cerebral da QTP pela QLNC em animais poli(i:c), o que na prática seria impossível de ser obtido, mesmo alterando as proporções dos componentes da formulação.

A quantificação da QTP em amostras de plasma, microdialisado cerebral e também do fármaco associado às nanocápsulas foi realizada através de metodologias previamente validadas e publicadas. Entretanto, para a etapa PD do trabalho era necessário desenvolver e validar

metodologia bioanalítica para a determinação das monoaminas dopamina, serotonina e seus metabólitos em amostras de microdialisado cerebral através de LC-MS/MS.

O método bioanalítico desenvolvido foi validado de acordo com as diretrizes do *Food and Drug Administration (*FDA, 2011) demonstrando-se seletivo, preciso, exato sensível e permitiu o monitoramento *in vivo* das monoaminas (DA, DOPAC, HVA, 5-HT e 5-HIIA) em amostras de microdialisado de córtex pré-frontal de ratos hígidos e com SCZ experimental. Entre as vantagens do método bioanalítico proposto em relação a outros métodos descritos na literatura destacam-se a minimização do tempo analítico (15 min) e do volume de amostra injetado (20 µL), além da quantificação de analitos em modo de eletrospray positivo e negativo na mesma corrida cromatográfica, sem a necessidade de etapas de derivatização ou extração das amostras (Capítulo 2). O método desenvolvido foi empregado com sucesso para avaliar os níveis basais de monoaminas em animais hígidos e do modelo neurodesenvolvimental de esquizofrenia e também as alterações após a administração das formulações avaliadas nesta tese (FQ e QLNC).

Os animais hígidos administrados com as formulação FQ e QLNC, ambos na dose de 5 mg/kg, apresentaram aumento significativo e semelhante dos níveis extracelulares de DA em relação à linha de base, diferentemente dos animais poli(i:c), que apresentaram alterações significativas equivalentes nos níveis desse neurotransmissor apenas após a administração de QLNC. Não foram observas diferenças significativas em relação à linha de base de nenhum dos outros compostos (DOPAC, HVA, 5-HT e 5-HIIA) em nenhum dos grupos investigados.

A integração do modelo popPK desenvolvido (Capítulo 2) com os dados de níveis extracelulares de DA permite explorar os componentes farmacocinético e farmacodinâmico da variabilidade de resposta ao tratamento farmacológico da SCZ, descrevendo a relação concentração-efeito *in vivo* das formulações investigadas.

O modelo popPK/PD desenvolvido permitiu demonstrar, pela primeira vez, que a SCZ experimental reduz a sensibilidade farmacológica à QTP, já

que o valor de EC_{50} estimado pelo modelo foi cerca de 3 vezes maior para os animais poli(i:c) em relação aos animais hígidos administrados com FQ.

Anteriormente (Capítulo 1) havíamos demonstrado que animais poli(i:c) não respondem à formulação FQ no teste comportamental do PPI. Embora a via neurológica que rege a resposta do PPI e as alterações nos níveis extracelulares de DA no mPFC possam não ser correlacionadas, o conjunto de resultados obtidos permite hipotetizar que alterações em outros receptores de neurotransmissores devido a SCZ podem levar a mudanças na potência de fármacos semelhantes àquelas observadas para o EC_{50} da QTP. A reduzida penetração cerebral da QTP somada ao aumento no valor do EC_{50} ajuda a entender a falta de resposta no PPI e destaca a importância do componente farmacodinâmico na alta variabilidade na resposta ao tratamento farmacológico na SCZ.

A utilização do fármaco nanoencapsulado (QLNC) não causou alterações nos parâmetros farmacodinâmicos da QTP. No entanto, como o nanocarreador modula o *delivery* cerebral da QTP foi observado um aumento nos níveis basais de DA no mPFC dos animais poli(i:c). Este resultado evidencia a importância do componente farmacocinético no tratamento farmacológico da SCZ e indica que a nanotecnologia pode ser usada na busca de tratamentos mais efetivos para a doença.

É importante ressaltar que a extrapolação possível com esse modelo PK/PD é limitada, já que, investigamos uma única dose do fármaco. No entanto, é um ponto de partida para uma nova abordagem de avaliação pré-clínica de antipsicóticos usando modelagem matemática & simulação para correlacionar dados obtidos *in vivo* em modelo animal preditivo de SCZ.

Assim, a presente tese apresenta uma abordagem conceitualmente inovadora na investigação do potencial terapêutico de nanopartículas para *delivery* cerebral: estudo farmacocinético pré-clínico em modelo experimental de doença, com investigação farmacocinética e farmacodinâmica utilizando técnica refinada para medir as concentrações livres do fármaco no local de ação e ferramentas de modelagem matemática & simulação para entender os mecanismos envolvidos na liberação *in vivo* do fármaco a partir do sistema nanoestruturado, sua distribuição tecidual e seu efeito.

As diferenças observadas na disposição farmacocinética cerebral e plasmática do fármaco em solução e nos nanocarreadores em animais hígidos e com esquizofrenia experimental, bem como as alterações nos níveis de DA após uso dessas formulações na situação hígido ou doente, permitiram demonstrar a importância da investigação pré-clínica na condição de doença em que o fármaco será utilizado, indicando que a avaliação de nanocarreadores em animais hígidos pode mascarar o potencial real dessas nanoestruturas para o *delivery* de fármacos.

A investigação das concentrações livres (farmacologicamente ativas) através de microdiálise plasmática e cerebral no local de ação dos antipsicóticos, e não somente as concentrações plasmáticas totais ou as concentrações teciduais totais obtidas em homogeneizado de tecidos, geralmente descritas nos estudos de penetração tecidual de nanopartículas, permitiram entender a função do nanocarreador na penetração do fármaco através da BHE, demonstrando seu papel determinante no transporte do fármaco no organismo.

Apesar das medidas farmacocinéticas de exposição ao fármaco, como área sob a curva de concentração *vs* tempo (ASC) e concentração plasmática máxima (C_{max}), geralmente relatadas nos estudo farmacocinéticos com nanopartículas serem relevantes para a aplicação biológica dessas formulações, o refinamento da análise dos dados farmacocinéticos utilizando ferramentas de MM&S utilizando neste trabalho permitiu o entendimento dos mecanismos envolvidos no *delivery* cerebral do fármaco em condição de doença, contribuindo para a construção de modelo popPK semi-mecanístico que pode ser utilizado no desenvolvimento de nanocarreadores customizados.

Por fim, diferentemente dos trabalhos tradicionais com nanopartículas, onde são avaliadas de modo independente as alterações farmacocinéticas e/ou farmacodinâmicas produzidas pelos nanocarreadores, no presente trabalho, através do uso de modelagem PK/PD, foi possível explorar o potencial terapêutico das nanopartículas, possibilitando a compreensão global do papel dessas LNCs no *delivery* cerebral da quetiapina.

CONCLUSÕES

O conjunto de resultados desse trabalhão permite concluir que o modelo neurodesenvolvimental de esquizofrenia em ratos Wistar machos e fêmeas, através da ativação da resposta imune materna induzida por poli(i:c), foi capaz de causar alterações comportamentais na prole e alterar o padrão de penetração cerebral da QTP, dando suporte a hipótese de que há um componente farmacocinético na variabilidade da resposta terapêutica observada no tratamento farmacológico da esquizofrenia.

A administração da QTP em uma nanopartícula polimérica de núcleo lipídico demonstrou ser capaz de governar a distribuição cerebral do fármaco, superando as alterações causadas pela SCZ experimental e retornando a exposição cerebral da QTP para os níveis observados em animais hígidos.

O desenvolvimento de um modelo farmacocinético semi-mecanístico através de uma abordagem populacional, que descreveu a farmacocinética plasmática e cerebral da QTP em animais hígidos e com SCZ experimental, representou uma estratégia inédita e permitiu entender o mecanismo pelo qual o nanocarreador modula o *delivery* cerebral do fármaco e evidenciar as vantagens de sua aplicação no tratamento da SCZ.

Utilizando a técnica de microdiálise cerebral foi possível medir os níveis intersticiais corticais de dopamina, serotonina e seus metabólitos e demonstrar que, na dose investigada (5 mg/kg), a FQ foi capaz de promover uma alteração nos níveis extracelulares de dopamina em animais hígidos, mas não foi capaz de alterar os níveis intersticiais de dopamina animais com SCZ experimental. Entretanto, quando os animais com SCZ experimental foram administrados com QLNC os níveis intersticiais de dopamina foram semelhantes aos encontrados em animais hígidos.

Através do modelo semi-mecanístico popPK/PD desenvolvido foi possível demonstrar a importância do componente farmacodinâmico na alta variabilidade de resposta farmacológica da SCZ e que as nanopartículas, apesar de não serem capazes de alterar os parâmetros PD da quetiapina, causam um aumento nos níveis basais de dopamina no mPFC dos animais poli(i:c) porque melhoram o *delivery* cerebral do fármaco.

Assim, o conjunto de dados desta tese é inovador e pode contribuir não apenas para uma melhor compreensão do componente farmacocinético

associado à variabilidade na resposta terapêutica da SCZ como também propõe uma estratégia de base nanotecnológica para resolvê-lo.

REFERÊNCIAS GERAIS

ABEL, K. M.; DRAKE, R.; GOLDSTEIN, J. M. Sex differences in schizophrenia. **International Review of Psychiatry**, v. 22, n. 5, p. 417–428, 2010.

ABBOTT, N. J.; PATABENDIGE, A. A. K.; DOLMAN, D. E. M.; YUSOF, S. R.; BEGLEY, D. J. Structure and function of the blood–brain barrier. **Neurobiology of Disease, Special Issue: Blood Brain Barrier**. v. 37, n. 1, p. 13–25, 2010.

AIT-OUDHIA, S.; MAGER, D.E.; STRAUBINGER, R. M. Application of pharmacokinetic and pharmacodynamic analysis to the development of liposomal formulations for oncology. **Pharmaceutics**, v. 6, n. 1, p. 137–74, 2014.

ALTAMURA, A. C. et al. Neurodevelopment and inflammatory patterns in schizophrenia in relation to pathophysiology. **Progress in Neuro-Psychopharmacology and Biological Psychiatry**, v. 42, p. 63–70, 2013.

AMERICAN PSYCHIATRIC ASSOCIATION (2014). Manual Diagnóstico e Estatístico de Transtornos Mentais – 5.ed.: DSM-5 (Artmed Editora)

ANTONIO, C. B. et al. LASSBio-579, a prototype antipsychotic drug, and clozapine are effective in novel object recognition task, a recognition memory model. **Behavioural Pharmacology**, v. 27, n. 4, p. 339–349, 2016.

ARSENAULT, D. et al. The different effects of LPS and poly I:C prenatal immune challenges on the behavior, development and inflammatory responses in pregnant mice and their offspring. **Brain, Behavior, and Immunity**, , v. 38, p. 77–90, 2014.

ALLARDYCE, J. et al. Association Between Schizophrenia-Related Polygenic Liability and the Occurrence and Level of Mood-Incongruent Psychotic Symptoms in Bipolar Disorder. **JAMA Psychiatry**, 75, p. 28-35, 2018.

BATINIĆ, B. et al. Lipopolysaccharide exposure during late embryogenesis results in diminished locomotor activity and amphetamine response in females and spatial cognition impairment in males in adult, but not adolescent rat offspring. **Behavioural Brain Research**, v. 299, p. 72–80, 2016.

BALE, T.L., EPPERSON, C.N. Sex differences and stress across the lifespan. **Nature Neuroscience**, v. 18, p. 1413-1420, 2015.

BARBOUR, A. SCAGLIONE, F., DERENDORF, H. Class-dependent relevance of tissue distribution in the interpretation of anti-infective pharmacokinetic/pharmacodynamic indices. **International Journal of Antimicrobial Agents**, v. 35, p. 431-438, 2010.

BARRETTO, E.M.; KAYO, M.; AVRICHIR, B.S.; SA, A.R.; CAMARGO, M.D.; NAPOLITANO, I.C.; NERY, F.G.; PINTO, J.A. JR.; BANNWART, S.; SCEMES S.; DI SARNO, E.; ELKIS H. A preliminary controlled trial of cognitive behavioral therapy in clozapine-resistant schizophrenia. **The Journal of Nervous and Mental Disease**, v. 197, n. 11, p. 865 -868, 2009.

BECHTER, K. et al. Cerebrospinal fluid analysis in affective and schizophrenic spectrum disorders: identification of subgroups with immune responses and blood-CSF barrier dysfunction. **Journal of psychiatric research**, v. 44, n. 5, p. 321–30, 2010.

BELL, J. S. et al. The cortical blood–brain barrier in multiple sclerosis: a gateway to progression? **Journal of Neurology**, 2018.

BELZUNG, C.; LEMOINE, M. Criteria of validity for animal models of psychiatric disorders: focus on anxiety disorders and depression. **Biology of Mood & Anxiety Disorders**, v. 1, p. 9, 2011.

BERNSTEIN, H.-G. et al. Morphometric analysis of the cerebral expression of ATP-binding cassette transporter protein ABCB1 in chronic schizophrenia: Circumscribed deficits in the habenula. **Schizophrenia research**, v. 177, n. 1–3, p. 52–58, 2016.

BITANIHIRWE, B. K. et al. Late Prenatal Immune Activation in Mice Leads to Behavioral and Neurochemical Abnormalities Relevant to the Negative Symptoms of Schizophrenia. **Neuropsychopharmacology**, v. 35, n. 12, p. 2462–2478, 2010.

BOGART, L. J.; O'DONNELL, P. Multiple long-range inputs evoke NMDA currents in prefrontal cortex fast-spiking interneurons. **Neuropsychopharmacology**, p. 1, 2018.

BOLKAN, S. S.; CARVALHO POYRAZ, F.; KELLENDONK, C. Using human brain imaging studies as a guide toward animal models of schizophrenia. **Neuroscience**, v. 321, p. 77–98, 2016.

BOSTRÖM, E.; HAMMARLUND-UDENAES, M.; SIMONSSON, U. S. H. Blood-brain barrier transport helps to explain discrepancies in in vivo potency between oxycodone and morphine. **Anesthesiology**, v. 108, p. 495-505, 2008.

BRADY, A. M. The Neonatal Ventral Hippocampal Lesion (NVHL) Rodent Model of Schizophrenia. In: **Current Protocols in Neuroscience**. Hoboken, NJ, USA: John Wiley & Sons, Inc., 2016. v. 77p. 9.55.1-9.55.17.

BRISCH, R. et al. The role of dopamine in schizophrenia from a neurobiological and evolutionary perspective: old fashioned, but still in vogue. **Frontiers in psychiatry**, v. 5, p. 47, 2014.

BROWN, A. S. Epidemiologic studies of exposure to prenatal infection and risk of schizophrenia and autism. **Developmental Neurobiology**, v. 72, n. 10, p. 1272–1276, 2012.

BROWN, A. S.; DERKITS, E. J. Prenatal Infection and Schizophrenia: A Review of Epidemiologic and Translational Studies. **American Journal of Psychiatry**, v. 167, n. 3, p. 261–280, 2010.

BUCKLEY, P. F. Neuroimaging of schizophrenia: structural abnormalities and pathophysiological implications. **Neuropsychiatric disease and treatment**, v. 1, n. 3, p. 193–204, 2005.

BUHUSI, M. et al. Chronic mild stress impairs latent inhibition and induces region-specific neural activation in CHL1-deficient mice, a mouse model of schizophrenia. **Behavioural Brain Research**, v. 333, p. 1–8, 2017.

CALZAVARA, M. B. et al. Effects of antipsychotics and amphetamine on social behaviors in spontaneously hypertensive rats. **Behavioural Brain Research**, v. 225, n. 1, p. 15–22, 2011.

CARREÑO, F.; PAESE, K.; SILVA, C. M.; GUTERRES, S.S.; DALLA COSTA, T.; Characterizing the mechanism of quetiapine distribution in lipid-core nanocapsules pseudo-phases using a validated LC/UV method. **Quimica Nova**, v. 38, p., 1181–1186, 2015.

CARREÑO, F. et al. Pre-clinical investigation of the modulation of quetiapine plasma pharmacokinetics and tissues biodistribution by lipid-core nanocapsules. **Journal of Pharmaceutical and Biomedical Analysis**, v. 119, p. 152–158, 2016. a.

CARREÑO, F. et al. Pharmacokinetic Investigation of Quetiapine Transport across Blood–Brain Barrier Mediated by Lipid Core Nanocapsules Using Brain Microdialysis in Rats. **Molecular Pharmaceutics**, v. 13, n. 4, p. 1289–1297, 2016. b.

COBA, M. P. et al. Dlgap1 knockout mice exhibit alterations of the postsynaptic density and selective reductions in sociability. **Scientific Reports**, v. 8, n. 1, p. 2281, 2018.

CORRADI, R. B. Schizophrenia as a Human Process. **The Journal of the American Academy of Psychoanalysis and Dynamic Psychiatry**, v. 39, n. 4, p. 717–736, 2011.

CRUM, W. R. et al. Evolution of structural abnormalities in the rat brain following in utero exposure to maternal immune activation: A longitudinal in vivo MRI study. **Brain, Behavior, and Immunity**, v. 63, p. 50–59, 2017.

DANHOF, M.; DE LANGE, E. C. M.; PASQUA, O. E. DELLA; PLOEGER, B. A.; VOSKUYL, R. A. Mechanism-based pharmacokinetic-pharmacodynamic (PK-PD) modeling in translational drug research. **Trends in Pharmacological Sciences**, v.29, n. 4, p.186–191, 2008.

DARVESH, A.S.; CARROLL, R.T.; GELDENHUYS, W.J.; GUDELSKY, G.A.; KLEIN, J.; MESHUL, C.K.; VAN DER SCHYF, C.J. In vivo brain microdialysis: advances in neuropsychopharmacology and drug discovery. **Expert Opinion on Drug Discovery**, v.6, p. 109-127, 2011.

DE KLERK, O. L. et al. Regional increase in P-glycoprotein function in the blood-brain barrier of patients with chronic schizophrenia: a PET study with [(11)C]verapamil as a probe for P-glycoprotein function. **Psychiatry research**, v. 183, n. 2, p. 151–6, 2010.

DE SOUZA, D. F. et al. Changes in Astroglial Markers in a Maternal Immune Activation Model of Schizophrenia in Wistar Rats are Dependent on Sex. **Frontiers in Cellular Neuroscience**, v. 9, p. 489, 2015.

DEBNATH, M.; VENKATASUBRAMANIAN, G.; BERK, M. Fetal programming of schizophrenia: Select mechanisms. **Neuroscience & Biobehavioral Reviews**, v. 49, p. 90–104, 2015.

DIMER, F. A. et al. Nanoencapsulation improves relative bioavailability and antipsychotic effect of olanzapine in rats. **Journal of Biomedical Nanotechnology**, v. 11, n. 8, p. 1482–1493, 2014.

DIMER, F. A. et al. Nanoencapsulation Improves Relative Bioavailability and Antipsychotic Effect of Olanzapine in Rats. **Journal of biomedical nanotechnology**, v. 11, n. 8, p. 1482–93, 2015.

DODELL-FEDER, D.; TULLY, L. M.; HOOKER, C. I. Social impairment in schizophrenia: new approaches for treating a persistent problem. **Current opinion in psychiatry**, v. 28, n. 3, p. 236–42, 2015.

DONEGAN, J. J.; BOLEY, A. M.; LODGE, D. J. Embryonic stem cell transplants

as a therapeutic strategy in a rodent model of autism. **Neuropsychopharmacology**, 2018.

ENDRES, D. et al. Immunological findings in psychotic syndromes: a tertiary care hospital's CSF sample of 180 patients. **Frontiers in Human Neuroscience**, v. 9, p. 476, 2015.

FATEMI, S.H.; EARLE, J.; KANODIA, R.; KIST, D.; EMAMIAN, E.S.; PATTERSON, P.H.; SHI, L.; SIDWELL, R. Prenatal viral infection leads to pyramidal cell atrophy and macrocephaly in adulthood: implications for genesis of autism and schizophrenia. **Cellular and Molecular Neurobiology**, v. 22 n.1, p. 25-33, 2002.

FATEMI, S. H. et al. The effects of prenatal H1N1 infection at E16 on FMRP, glutamate, GABA, and reelin signaling systems in developing murine cerebellum. **Journal of Neuroscience Research**, v. 95, n. 5, p. 1110–1122, 2017.

FIEL, L.A.; CONTRI, R.V.; BICA, J.F.; FIGUEIRÓ, F.; BATTASTINI, A.M.O.; GUTERRES, S.S.; POHLMANN, A.R. Labeling the oily core of nanocapsules and lipid- core nanocapsules with a triglyceride conjugated to a fluorescent dye as a strategy to particle tracking in biological studies. **Nanoscale Research Letters**, v. 9, n. 1, p. 233, 2014.

FINEBERG, A. M.; ELLMAN, L. M. Inflammatory cytokines and neurological and neurocognitive alterations in the course of schizophrenia. **Biological psychiatry**, v. 73, n. 10, p. 951–66, 2013.

FLORES, G.; MORALES-MEDINA, J. C.; DIAZ, A. Neuronal and brain morphological changes in animal models of schizophrenia. **Behavioural Brain Research**, v. 301, p. 190–203, 2016.

FREDDO, R.J. **Estudos para Obtenção e Caracterização de Sistemas Nanoparticulados Contendo Ácido Valpróico e Avaliação da Penetração Deste Através da Barreira Hematoencefálica**. 2009. 140f. Tese (Doutorado em Ciências Farmacêuticas) – Faculdade de Farmácia, Universidade Federal do Rio Grande do Sul, Porto Alegre, 2009. Disponível em: . Acesso em dezembro 2014.

FOND, G.; MACGREGOR, A.; MIOT, S. Nanopsychiatry-The potential role of nanotechnologies in the future of psychiatry: A systematic review. **European Neuropsychopharmacology**, v. 23, n. 9, p. 1067–1071, 2013.

FONSECA, F. N. et al. Mucoadhesive Amphiphilic Methacrylic Copolymer-Functionalized Poly(ε-caprolactone) Nanocapsules for Nose-to-Brain Delivery of Olanzapine. **Journal of Biomedical Nanotechnology**, v. 11, n. 8, p. 1472–1481, 2015.

GABATHULER, R. Approaches to transport therapeutic drugs across the blood-brain Barrier to treat brain diseases. **Neurobiology of Disease**, v. 37, n. 1, p. 48–57, 2010.

GARBETT, K. A. et al. Effects of maternal immune activation on gene expression patterns in the fetal brain. **Translational Psychiatry**, v. 2, n. 4, p. e98–e98, 2012.

GEYER, M. A. The family of sensorimotor gating disorders: comorbidities or diagnostic overlaps? **Neurotoxicity research**, v. 10, n. 3–4, p. 211–20, 2006.

GILLESPIE, A. L. et al. Is treatment-resistant schizophrenia categorically distinct from treatment-responsive schizophrenia? a systematic review. **BMC Psychiatry**, v. 17, n. 1, p. 12, 2017.

GOGOS, A. et al. **A Role for Estrogen in Schizophrenia: Clinical and Preclinical Findings**, 2015.

HADAR, R. et al. Using a maternal immune stimulation model of schizophrenia to study behavioral and neurobiological alterations over the developmental course. **Schizophrenia Research**, v. 166, n. 1–3, p. 238–247, 2015. a.

HADAR, R. et al. Using a maternal immune stimulation model of schizophrenia to study behavioral and neurobiological alterations over the developmental course. **Schizophrenia research**, v. 166, n. 1–3, p. 238–47, 2015. b.

HARRIS, L. W. et al. The Cerebral Microvasculature in Schizophrenia: A Laser Capture Microdissection Study. **PLoS ONE**, v. 3, n. 12, p. e3964, 2008.

HENRIKSEN, M.G., NORDGAARD, J., JANSSON, L.B. Genetics of Schizophrenia: Overview of Methods, Findings and Limitations. **Frontiers in human neuroscience**, v. 22, n. 11, p. 311:322, 2017

HERRMANN, A. P. et al. N-acetylcysteine prevents increased amphetamine sensitivity in social isolation-reared mice. **Schizophrenia Research**, v. 155, n. 1–3, p. 109–111, 2014.

HERRMANN, A. P. et al. Effects of N-acetylcysteine on amphetamine-induced sensitization in mice. **Revista Brasileira de Psiquiatria**, n. 0, p. 0–0, 2017.

HILL, R. A. Sex differences in animal models of schizophrenia shed light on the underlying pathophysiology. **Neuroscience and Biobehavioral Reviews**, v. 67, p. 41–56, 2016.

HUBER, T. J. et al. Psychotic disorders and gonadal function: evidence supporting the oestrogen hypothesis. **Acta Psychiatrica Scandinavica**, v. 109, n. 4, p. 269–274, 2004.

HURTADO, F. K. et al. Population pharmacokinetic modeling of the unbound levofloxacin concentrations in rat plasma and prostate tissue measured by microdialysis. **Antimicrobial Agents and Chemotherapy**, v. 58, n. 2, p. 678–686, 2014.

JÄGER, E.; VENTURINI, C. G.; POLETTO, F. S.; COLOMÉ, L. M.; POHLMANN, J. P. U.; BERNARDI, A.; BATTASTINI, A. M. O.; GUTERRES, S. S.; POHLMANN, A. R. Sustained release from lipid-core nanocapsules by varying the core viscosity and the particle surface area. **Journal of Biomedical Nanotechnology**, v. 5, n. 1, p. 130–140, 2009.

JOHNSON, M.; KOZIELSKA, M.; PILLA REDDY, V.; VERMEULEN, A.; BARTON, H. A.; GRIMWOOD, S.; DE GREEF, R.; GROOTHUIS, G. M. M.; DANHOF, M.; PROOST, J. H. Dopamine D2 receptor occupancy as a predictor of catalepsy in rats: a pharmacokinetic-pharmacodynamic modeling approach. **Pharmaceutical Research**, v.31, n. 10, p. 2605–2617, 2014.

JOHNSON, M.; KOZIELSKA, M.; REDDY, V. P.; VERMEULEN, A.; LI, C.; GRIMWOOD, S.; GREEF, R. de; GROOTHUIS, G. M. M.; DANHOF, M.; PROOST, J. H. Mechanism-based pharmacokinetic–pharmacodynamic modeling of the dopamine D2 receptor occupancy of olanzapine in rats. **Pharmaceutical Research**, v. 28, n. 10, p. 2490–2504, 2011.

JONES, H. M.; ROWLAND-YEO, K. Basic concepts in physiologically based pharmacokinetic modeling in drug discovery and development. **CPT: Pharmacometrics and Systems Pharmacology**, v. 14, p. 10-12, 2013.

JORNADA, D. S.; FIEL, L. A.; BUENO, K.; GERENT, J. F.; PETZHOLD, C. L.; BECK, R. C. R.; GUTERRES, S. S.; POHLMANN, A. R. Lipid-core nanocapsules: mechanism of self-assembly, control of size and loading capacity. **Soft Matter**, v. 8, n. 24, p. 6646–6655, 2012.

INSEL, T. R. Rethinking schizophrenia. **Nature**, v. 468, n. 7321, p. 187, 2010.

JONES, C. A.; WATSON, D. J. G.; FONE, K. C. F. Animal models of schizophrenia. **British journal of pharmacology**, v. 164, n. 4, p. 1162–94, 2011.

JUNG, W. H. et al. Structural Brain Alterations in Individuals at Ultra-high Risk for Psychosis: A Review of Magnetic Resonance Imaging Studies and Future Directions. **Journal of Korean Medical Science**, v. 25, n. 12, p. 1700, 2010.

KAHN, R. S.; SOMMER, I. E. The neurobiology and treatment of first-episode schizophrenia. **Molecular Psychiatry**, v. 20, n. 1, p. 84–97, 2015.

KOZIELSKA, M.; JOHNSON, M.; PILLA REDDY, V.; VERMEULEN, A.; LI, C.; GRIMWOOD, S.; DE GREEF, R.; GROOTHUIS, G. M. M.; DANHOF, M.; PROOST, J. H. Pharmacokinetic-pharmacodynamic modeling of the D2 and 5-HT2A receptor occupancy of risperidone and paliperidone in rats. **Pharmaceutical Research**, v. 29, n. 7, p. 1932–1948, 2012.

KHANDAKER, G. M. et al. Prenatal maternal infection, neurodevelopment and adult schizophrenia: a systematic review of population-based studies. **Psychological Medicine**, v. 43, n. 2, p. 239–257, 2013.

KHANDAKER, G. M. et al. Inflammation and immunity in schizophrenia: implications for pathophysiology and treatment. **The Lancet Psychiatry**, v. 2, n. 3, p. 258–270, 2015.

KILIÇASLAN, E. E. et al. Şizofreni Başlangıç Yaşı ile Menarş Yaşı Arasındaki İlişki. **Nöro Psikiyatri Arşivi**, v. 51, n. 3, p. 211–215, 2014.

KRAUSE, M. et al. Antipsychotic drugs for patients with schizophrenia and predominant or prominent negative symptoms: a systematic review and meta-analysis. **European Archives of Psychiatry and Clinical Neuroscience**, v. 0, n. 123456789, p. 0, 2018.

LAI, C.Y., SCARR, E., UDAWELA, M., EVERALL, I., CHEN, W.J., DEAN, B. Biomarkers in schizophrenia: A focus on blood based diagnostics and theranostics. **World Journal of Psychiatry**, v. 22, p. 102-117, 2016.

LANDREAU, F. et al. Effects of Two Commonly Found Strains of Influenza A Virus on Developing Dopaminergic Neurons, in Relation to the Pathophysiology

of Schizophrenia. **PLoS ONE**, v. 7, n. 12, p. e51068, 2012.

LAPPIN, J.M., WIJAYA, M., WATKINS, A., MORELL, R., TEASDALE, S., LEDERMAN, O., ROSENBAUM, S., DICK, S., WARD, P., CURTIS, J. Cardio-metabolic risk and its management in a cohort of clozapine-treated outpatients. **Schizophrenia Research**, v. 199, p. 367-373, 2018.

LAZAR, N. L.; NEUFELD, R. W. J.; CAIN, D. P. Contribution of nonprimate animal models in understanding the etiology of schizophrenia. **Journal of psychiatry & neuroscience : JPN**, v. 36, n. 4, p. E5-29, 2011.

LEE, J. H. et al. Impaired social behaviors and minimized oxytocin signaling of the adult mice deficient in the N -methyl- d -aspartate receptor GluN3A subunit. **Experimental Neurology**, v. 305, p. 1–12, 2018.

LI, Q. et al. Prenatal Immune Challenge Is an Environmental Risk Factor for Brain and Behavior Change Relevant to Schizophrenia: Evidence from MRI in a Mouse Model. **PLoS ONE**, v. 4, n. 7, p. e6354, 2009.

LINDQVIST, A.; RIP, J.; GAILLARD, P. J.; BJÖRKMAN, S.; HAMMARLUND-UDENAES, M. Enhanced brain delivery of the opioid peptide damgo in glutathione pegylated liposomes: a microdialysis study. **Molecular pharmaceutics**, v. 10, n. 5, p. 1533–1541, 2013.

LINDQVIST, A.; FRIDÉN, M.; HAMMARLUND-UDENAES, M. Pharmacokinetic considerations of nanodelivery to the brain: Using modeling and simulations to predict the outcome of liposomal formulations. **European Journal of Pharmaceutical Sciences**, v. 20, p. 173-182, 2016.

LIPSKA, B. K.; WEINBERGER, D. R. To model a psychiatric disorder in animals: Schizophrenia as a reality test. **Neuropsychopharmacology**, v. 23, n. 3, p. 223–239, 2000.

LODGE, D. J. The MAM rodent model of schizophrenia. **Current protocols in neuroscience**, v. Chapter 9, p. Unit9.43, 2013.

LÖSCHER, W.; POTSCHKA, H. Drug resistance in brain diseases and the role of drug efflux transporters. **Nature Reviews, Neuroscience**, v. 6, n.8, p. 591-602, 2005.

LOW, N. C.; HARDY, J. What Is a Schizophrenic Mouse? **Neuron**, v. 54, n. 3, p. 348–349, 2007.

MARCOTTE, E. R.; PEARSON, D. M.; SRIVASTAVA, L. K. Animal models of schizophrenia: a critical review. **Journal of psychiatry & neuroscience : JPN**, v. 26, n. 5, p. 395–410, 2001.

MARKHAM, J. A. Sex steroids and schizophrenia. **Reviews in Endocrine and Metabolic Disorders**, v. 13, n. 3, p. 187–207, 2012.

MATTEI, D.; SCHWEIBOLD ,R.; WOLF, S.A. Brain in flames - animal models of psychosis: utility and limitations. **Neuropsychiatric disease and treatment**, v. 11, p. 1313-1319, 2015.

MATSUMOTO, M.; SEYA, T. TLR3: Interferon induction by double-stranded RNA including poly(I:C). **Advanced Drug Delivery Reviews**, v. 60, n. 7, p.

805–812, 2008.

MAVRIKAKI, M.; NOMIKOS, G. G.; PANAGIS, G. Efficacy of the atypical antipsychotic aripiprazole in d-amphetamine-based preclinical models of mania. **The International Journal of Neuropsychopharmacology**, v. 13, n. 4, p. 541, 2010.

RIGGS, M.M.; CREMERS, S. Pharmacometrics and systems pharmacology for metabolic bone diseases. British Journal of Clinical Pharmacology, v. 85, p. 1049 – 1051, 2019.

MCGREGOR, C.; RIORDAN, A.; THORNTON, J. Estrogens and the cognitive symptoms of schizophrenia: Possible neuroprotective mechanisms. **Frontiers in Neuroendocrinology**, v. 47, p. 19–33, 2017.

MELCANGI, R. C.; PANZICA, G.; GARCIA-SEGURA, L. M. Neuroactive steroids: focus on human brain. **Neuroscience**, v. 191, p. 1–5, 2011.

MEYER, U. et al. Towards an immuno-precipitated neurodevelopmental animal model of schizophrenia. **Neuroscience & Biobehavioral Reviews**, v. 29, n. 6, p. 913–947, 2005.

MEYER, U.; FELDON, J. To poly(I:C) or not to poly(I:C): Advancing preclinical schizophrenia research through the use of prenatal immune activation models. **Neuropharmacology**, v. 62, n. 3, p. 1308–1321, 2012.

MEYER, U.; FELDON, J.; YEE, B. K. A Review of the Fetal Brain Cytokine Imbalance Hypothesis of Schizophrenia. **Schizophrenia Bulletin**, v. 35, n. 5, p. 959–972, 2009.

MILLAN, M. J. et al. Altering the course of schizophrenia: progress and perspectives. **Nature Reviews Drug Discovery**, v. 15, n. 7, p. 485, 2016.

MILLAR, J.; BILKEY, D. K.; WARD, R. D. Maternal immune activation alters sensitivity to action-outcome contingency in adult rat offspring. **Brain, Behavior, and Immunity**, v. 63, p. 81–87, 2017.

MISIAK, B. et al. Testosterone, DHEA and DHEA-S in patients with schizophrenia: A systematic review and meta-analysis. **Psychoneuroendocrinology**, v. 89, p. 92–102, 2018.

MÖLLER, M.; SWANEPOEL, T.; HARVEY, B. H. Neurodevelopmental Animal Models Reveal the Convergent Role of Neurotransmitter Systems, Inflammation, and Oxidative Stress as Biomarkers of Schizophrenia: Implications for Novel Drug Development. **ACS Chemical Neuroscience**, v. 6, n. 7, p. 987–1016, 2015.

MOONS, T. et al. Relationship between P-glycoprotein and second-generation antipsychotics. **Pharmacogenomics**, v. 12, n. 8, p. 1193–1211, 2011.

MORRIS, M.E., LEE, H.J., PREDKO, L.M. Gender differences in the membrane transport of endogenous and exogenous compounds. **Pharmacological Reviews**, v.55, n.22, p. 229-240, 2003.

MOULD, D.R.; UPTON, R.N. Basic concepts in population modeling, simulation, and model-based drug development. **CPT: Pharmacometrics & Systems Pharmacology**, v. 1, n. 9, p. 1-16, 2012.

MOULD, D.R.; UPTON, R.N. Basic Concepts in Population Modeling, Simulation, and Model-Based Drug Development—Part 2: Introduction to Pharmacokinetic Modeling Methods**. CPT: Pharmacometrics & Systems Pharmacology**, v. 2, p. 1-16, 2013.

MOULD, D.R.; UPTON, R.N. Basic Concepts in Population Modeling, Simulation, and Model-Based Drug Development—Part 3: Introduction to Pharmacodynamic Modeling Methods**. CPT: Pharmacometrics & Systems Pharmacology**, v. 3, p. 1-18, 2014.

NAKAO, K. et al. Schizophrenia-Like Dopamine Release Abnormalities in a Mouse Model of NMDA Receptor Hypofunction. **Schizophrenia Bulletin**, 2018.

NESTLER, E. J.; HYMAN, S. E. Animal models of neuropsychiatric disorders. **Nature neuroscience**, v. 13, n. 10, p. 1161–9, 2010.

NEVES, G. et al. Is Forced Swimming Immobility a Good Endpoint for Modeling Negative Symptoms of Schizophrenia? - Study of Sub-Anesthetic Ketamine Repeated Administration Effects. **Anais da Academia Brasileira de Ciências**, v. 89, n. 3, p. 1655–1669, 2017.

NIELSEN, P. R.; BENROS, M. E.; MORTENSEN, P. B. Hospital Contacts With Infection and Risk of Schizophrenia: A Population-Based Cohort Study With Linkage of Danish National Registers. **Schizophrenia Bulletin**, v. 40, n. 6, p. 1526–1532, 2014.

NIELSEN, P. R.; LAURSEN, T. M.; AGERBO, E. Comorbidity of schizophrenia and infection: a population-based cohort study. **Social Psychiatry and Psychiatric Epidemiology**, v. 51, n. 12, p. 1581–1589, 2016.

OCHOA, S. et al. Gender Differences in Schizophrenia and First-Episode Psychosis: A Comprehensive Literature Review. **Schizophrenia Research and Treatment**, v. 2012, p. 1–9, 2012.

OLIVEIRA, C.P.; VENTURINI, C.G.; DONIDA, B.; POLETTO, F.S.; GUTERRES, S.S.; POHLMAN, A.R. An algorithm to determine the mechanism of drug distribution in lipid-core nanocapsule formulation. **Soft Matter**, v.9, p. 1141-1150, 2012.

OKAZAKI, H. et al. Calcineurin knockout mice show a selective loss of small spines. **Neuroscience Letters**, v. 671, p. 99–102, 2018.

OZAWA, K. et al. Immune Activation During Pregnancy in Mice Leads to Dopaminergic Hyperfunction and Cognitive Impairment in the Offspring: A Neurodevelopmental Animal Model of Schizophrenia. **Biological Psychiatry**, v. 59, n. 6, p. 546–554, 2006.

PATEL, S.; CHAVHAN, S.; SONI, H.; BABBAR, A.K.; MATHUR, R.; MISHRA, A.K.; SAWANT, K. Brain targeting of risperidone-loaded solid lipid nanoparticles by intranasal route. **Journal of Drug Targeting**, v.19, n. 6, p. 468-474, 2011.

PATRICH, E. et al. Maternal immune activation produces neonatal excitability defects in offspring hippocampal neurons from pregnant rats treated with poly I:C. **Scientific Reports**, v. 6, p. 19106, 2016.

PEREIRA, L.; BUDOVICH, A.; CLAUDIO-SAEZ, M. Monitoring of Metabolic Adverse Effects Associated With Atypical Antipsychotics Use in an Outpatient

Psychiatric Clinic. **Journal of Pharmacy Practice**, p. 89719001775271, 2018.

PILLA REDDY, V. et al. Pharmacokinetic-pharmacodynamic modelling of antipsychotic drugs in patients with schizophrenia: part II: the use of subscales of the PANSS score. **Schizophrenia research**, v. 146, p. 144-152, 2013.

PIONTKEWITZ, Y.; ARAD, M.; WEINER, I. Risperidone administered during asymptomatic period of adolescence prevents the emergence of brain structural pathology and behavioral abnormalities in an animal model of schizophrenia. **Schizophrenia Bulletin**, v. 37, n. 6, p. 1257–1269, 2011.

POLLAK, T. A. et al. The blood-brain barrier in psychosis. **The lancet. Psychiatry**, v. 5, n. 1, p. 79–92, 2018.

POTSCHKA, H.; FEDROWITZ, M.; LÖSCHER, W. P-Glycoprotein-mediated efflux of phenobarbital, lamotrigine, and felbamate at the blood-brain barrier: evidence from microdialysis experiments in rats. **Neuroscience Letter**, v. 26, p. 173-176, 2002.

PRYTKOVA, I.; BRENNAND, K. J. Prospects for Modeling Abnormal Neuronal Function in Schizophrenia Using Human Induced Pluripotent Stem Cells. **Frontiers in cellular neuroscience**, v. 11, p. 360, 2017.

RAPOPORT, J.; GIEDD, J.; GOGTAY, N. Neurodevelopmental model of schizophrenia: update 2012. **Molecular psychiatry**, v. 17, n. 12, p. 1228–1238, 2012.

REISINGER, S. et al. **The Poly(I:C)-induced maternal immune activation model in preclinical neuropsychiatric drug discovery**, 2015. a.

REISINGER, S. et al. The Poly(I:C)-induced maternal immune activation model in preclinical neuropsychiatric drug discovery. **Pharmacology & Therapeutics**, v. 149, p. 213–226, 2015. b.

RÉUS, G. Z. et al. Ketamine potentiates oxidative stress and influences behavior and inflammation in response to lipolysaccharide (LPS) exposure in early life. **Neuroscience**, v. 353, p. 17–25, 2017.

ROENKER, N. L. et al. Effect of paliperidone and risperidone on extracellular glutamate in the prefrontal cortex of rats exposed to prenatal immune activation or MK-801. **Neuroscience letters**, v. 500, n. 3, p. 167–71, 2011.

ROSE, D. R. et al. Long-term altered immune responses following fetal priming in a non-human primate model of maternal immune activation. **Brain, Behavior, and Immunity**, v. 63, p. 60–70, 2017.

RUBIN, L. H. et al. Peripheral oxytocin is associated with reduced symptom severity in schizophrenia. **Schizophrenia Research**, v. 124, n. 1–3, p. 13–21, 2010.

RUBIO, M. D.; DRUMMOND, J. B.; MEADOR-WOODRUFF, J. H. Glutamate receptor abnormalities in schizophrenia: implications for innovative treatments. **Biomolecules & therapeutics**, v. 20, n. 1, p. 1–18, 2012.

SAHIN, C.; DOOSTDAR, N.; NEILL, J. C. Towards the development of improved tests for negative symptoms of schizophrenia in a validated animal model. **Behavioural Brain Research**, v. 312, p. 93–101, 2016.

SANTOS-TOSCANO, R. et al. Unaltered cocaine self-administration in the

prenatal LPS rat model of schizophrenia. **Progress in Neuro-Psychopharmacology and Biological Psychiatry**, v. 69, p. 38–48, 2016.

SATTERTHWAITE, T. D. et al. Structural Brain Abnormalities in Youth With Psychosis Spectrum Symptoms. **JAMA Psychiatry**, v. 73, n. 5, p. 515, 2016.

SHILLIAM, C.S.; DAWSON, L.A. The effect of clozapine on extracellular dopamine levels in the shell subregion of the rat nucleus accumbens is reversed following chronic administration: comparison with a selective 5-HT(2C) receptor antagonist. **Neuropsychopharmacology**, v. 30, p. 372-380, 2005.

SILVA, R., ALBUQUERQUE, S., MUNIZ, A.V., FILHO, P., RIBEIRO, S., PINHEIRO, P. R., ALBUQUERQUE, V. Reducing the Schizophrenia Stigma: A New Approach Based on Augmented Reality. **Computational intelligence and neuroscience**, v. 2017, p. 1-12, 2017.

SIMPSON, E. H.; KELLENDONK, C. Insights About Striatal Circuit Function and Schizophrenia From a Mouse Model of Dopamine D2Receptor Upregulation. **Biological psychiatry**, v. 81, n. 1, p. 21–30, 2017.

SRINIVAS, N., MAFFUID, K., KASHUBA A.D.M. Clinical Pharmacokinetics and Pharmacodynamics of Drugs in the Central Nervous System. **Clinical Pharmacokinetics**, v. 54, p. 1059-1074, 2018.

SUN, J. et al. Progesterone: The neglected hormone in schizophrenia? A focus on progesterone-dopamine interactions. **Psychoneuroendocrinology**, v. 74, p. 126–140, 2016. a.

SUZUKI, T. REMINGTON, G., MULSANT, BH., RAJJI, T.K., UCHIDA, H., GRAFF-GUERRERO, A., MAMO, D.C. Treatment resistant schizophrenia and response to antipsychotics: a review. **Schizophrenia Research**, v. 133, p. 54-62, 2011.

SWANEPOEL, T.; MÖLLER, M.; HARVEY, B. H. N-acetyl cysteine reverses bio-behavioural changes induced by prenatal inflammation, adolescent methamphetamine exposure and combined challenges. **Psychopharmacology**, p. 1–18, 2017.

TENREIRO, M. M. et al. Cellular response of the blood-brain barrier to injury: Potential biomarkers and therapeutic targets for brain regeneration. **Neurobiology of Disease**, v. 91, p. 262–273, 2016.

URBAN, A.; CUBAŁA, W. Therapeutic drug monitoring of atypical antipsychotics. **Psychiatria Polska**, v. 51, n. 6, p. 1059–1077, 2017.

VAN VLIET, E. A.; ARONICA, E.; GORTER, J. A. Blood–brain barrier dysfunction, seizures and epilepsy. **Seminars in Cell & Developmental Biology**, v. 38, p. 26–34, 2015.

VENTURINI, C.G., JÄGER, E., OLIVEIRA, C.P., BERNARDI, A., BATTASTINI, A.M.O., GUTERRES, S.S., POHLMANN, A.R. Formulation of lipid core nanocapsules. **Colloids and Surfaces A: Physicochemical and Engineering Aspects**, v. 375, p. 200-208, 2011.

VIEIRA, S. M. et al. A surface modification of clozapine-loaded nanocapsules improves their efficacy: A study of formulation development and biological assessment. **Colloids and Surfaces B: Biointerfaces**, v. 145, p. 748–756, 2016.

VOLPE, F. M. et al. Current inpatient prescription practices for the treatment of schizophrenia in public hospitals of Minas Gerais, Brazil. **Revista Brasileira de Psiquiatria**, v. 39, n. 2, p. 190–192, 2017.

VOSTRIKOV, V.; ORLOVSKAYA, D.; URANOVA, N. Deficit of pericapillary oligodendrocytes in the prefrontal cortex in schizophrenia. **The World Journal of Biological Psychiatry**, v. 9, n. 1, p. 34–42, 2008.

WEBER-STADLBAUER, U. Epigenetic and transgenerational mechanisms in infection-mediated neurodevelopmental disorders. **Translational Psychiatry**, v. 7, n. 5, p. e1113, 2017.

WEBSTER, M. J. et al. Immunohistochemical Localization of Phosphorylated Glial Fibrillary Acidic Protein in the Prefrontal Cortex and Hippocampus from Patients with Schizophrenia, Bipolar Disorder, and Depression. **Brain, Behavior, and Immunity**, v. 15, n. 4, p. 388–400, 2001.

WILSON, C.; TERRY, A. Neurodevelopmental Animal Models of Schizophrenia: Role in Novel Drug Discovery and Development. **Clinical Schizophrenia & Related Psychoses**, v. 4, n. 2, p. 124–137, 2010.

WINTER, C. et al. Prenatal immune activation leads to multiple changes in basal neurotransmitter levels in the adult brain: implications for brain disorders of neurodevelopmental origin such as schizophrenia. **The International Journal of Neuropsychopharmacology**, v. 12, n. 4, p. 513, 2009.

WOLKING, S. et al. Impact of Genetic Polymorphisms of ABCB1 (MDR1, P-Glycoprotein) on Drug Disposition and Potential Clinical Implications: Update of the Literature. **Clinical Pharmacokinetics**, v. 54, n. 7, p. 709–735, 2015.

XIA, Y. et al. Influenza vaccination during early pregnancy contributes to neurogenesis and behavioral function in offspring. **Brain, Behavior, and Immunity**, v. 42, p. 212–221, 2014.

YAMAMURA, S.; OHOYAMA, K.; HAMAGUCHI, T.; KASHIMOTO, K.; NAKAGAWA, M.; KANEHARA, S.; SUZUKI, D.; MATSUMOTO, T.; MOTOMURA, E.; SHIROYAMA, T.; OKADA, M. Effects of quetiapine on monoamine, GABA, and glutamate release in rat prefrontal cortex. **Psychopharmacology**, v. 206, n. 2, p. 243 – 258, 2009.

YASIR, M.; SARA, U.V. Solid lipid nanoparticles for nose to brain delivery of haloperidol: in vitro drug release and pharmacokinetics evaluation. **Acta Pharmaceutica Sinica B**, v. 4, n. 6, p. 454-463, 2014.

YEE, N. et al. Differential effects of maternal immune activation and juvenile stress on anxiety-like behaviour and physiology in adult rats: No evidence for the “double-hit hypothesis”. **Behavioural Brain Research**, v. 224, n. 1, p. 180–188, 2011.

YU, X.Q.; WILSON, A.G.E. The role of pharmacokinetic and pharmacokinetic/pharmacodynamic modeling in drug discovery and development. **Future Medicinal Chemistry**, v. 2, p. 923-928, 2010.

ZAVITSANOU, K. et al. Effect of maternal immune activation on the kynurenine pathway in preadolescent rat offspring and on MK801-induced hyperlocomotion in adulthood: Amelioration by COX-2 inhibition. **Brain, Behavior, and**

Immunity, v. 41, p. 173–181, 2014.

ZESTOS, A.G.; KENNEDY, R.T. Microdialysis Coupled with LC-MS/MS for In Vivo Neurochemical Monitoring. **The AAPS Journal**, v. 19, p. 1284-1293, 2017.

ZHANG, S. et al. Autophagy- and MMP-2/9-mediated Reduction and Redistribution of ZO-1 Contribute to Hyperglycemia-increased Blood–Brain Barrier Permeability During Early Reperfusion in Stroke. **Neuroscience**, v. 377, p. 126–137, 2018.

ZIMMERMANN, E.S., LAUREANO, J.V., DOS SANTOS, C.N., SCHMIDT, S., LAGISHETTY, C.V., DE CASTRO, W.V., DALLA COSTA, T. Simultaneous Semi mechanistic Population Analyses of Levofloxacin in Plasma, Lung, and Prostate To Describe the Influence of Efflux Transporters on Drug Distribution following Intravenous and Intratracheal Administration. **Antimicrobial Agents and Chemotherapy**, v. 30, p. 946-954, 2015.

ZUCKERMAN, L. et al. Immune Activation During Pregnancy in Rats Leads to a PostPubertal Emergence of Disrupted Latent Inhibition, Dopaminergic Hyperfunction and Altered Limbic Morphology in the Offspring: A Novel Neurodevelopmental Model of Schizophrenia. **Neuropsychopharmacology**, v. 28, n. 10, p. 1778–1789, 2003.

ZUCKERMAN, L.; WEINER, I. Maternal immune activation leads to behavioral and pharmacological changes in the adult offspring. **Journal of psychiatric research**, v. 39, n. 3, p. 311–23, 2005.

ANEXO

Anexo I

Carta de aprovação do projeto no comitê de ética no uso de animais (CEUA/UFRGS)

U F R G S
UNIVERSIDADE FEDERAL
DO RIO GRANDE DO SUL

PRÓ-REITORIA DE PESQUISA
Comissão De Ética No Uso De Animais

CEUA UFRGS

CARTA DE APROVAÇÃO

Comissão De Ética No Uso De Animais analisou o projeto:

Número: 31001
Título: Modelagem Farmacocinética/Farmacodinâmica (PK/PD) da Quetiapina Nanoencapsulada em Modelo Animal de Esquizofrenia

Vigência: 11/04/2016 à 31/08/2019

Pesquisadores:

Equipe UFRGS:

TERESA CRISTINA TAVARES DALLA COSTA - coordenador desde 11/04/2016
SILVIA STANISCUASKI GUTERRES - pesquisador desde 11/04/2016
STELA MARIS KUZE RATES - pesquisador desde 11/04/2016
Fabiola Schons Meyer - pesquisador desde 11/04/2016
Fernando Olinto Carreño - Aluno de Doutorado desde 11/04/2016

Equipe Externa:

Ana Pula Hermann - pesquisador desde 11/04/2016

Comissão De Ética No Uso De Animais aprovou o mesmo em seus aspectos éticos e metodológicos, para a utilização de 119 ratos Wistar de 90 dias de idade, 20 machos e 99 fêmeas, 176 ratos Wistar machos provenientes do cruzamento dos referidos animais e o descarte de 176 fêmeas recém-nascidas destes mesmos cruzamentos, todos provenientes do CREAL-UFRGS, de acordo com os preceitos das Diretrizes e Normas Nacionais e Internacionais, especialmente a Lei 11.794 de 08 de novembro de 2008, o Decreto 6899 de 15 de julho de 2009, e as normas editadas pelo Conselho Nacional de Controle da Experimentação Animal (CONCEA), que disciplinam a produção, manutenção e/ou utilização de animais do filo Chordata, subfilo Vertebrata (exceto o homem) em atividade de ensino ou pesquisa.

Porto Alegre, Sexta-Feira, 6 de Maio de 2016

MARCELO MELLER ALIEVI
Coordenador da comissão de ética

Anexo II

Carta de aprovação de adendo no comitê de ética no uso de animais (CEUA/UFRGS) para utilização de fêmeas

CEUA
UFRGS

PRÓ-REITORIA DE PESQUISA

COMISSÃO DE ÉTICA NO USO DE ANIMAIS

CARTA DE APROVAÇÃO/ADENDO

Processo Nº: 31001

TÍTULO: MODELAGEM FARMACOCINÉTICA/FARMACODINÂMICA (PK/PD) DA QUETIAPINA NANOENCAPSULADA EM MODELO ANIMAL DE ESQUIZOFRENIA

Pesquisador Responsável: TERESA CRISTINA TAVARES DALLA COSTA

Comissão De Ética no Uso De Animais aprovou o adendo ao projeto intitulado **"Modelagem Farmacocinética/Farmacodinâmica (PK/PD) da Quetiapina Nanoencapsulada em Modelo Animal de Esquizofrenia"**, em reunião realizada em 29/08/2016 - Sala 323 do Anexo 1 da Reitoria - Campus Centro - Porto Alegre - RS, em seus aspectos éticos e metodológicos, para a utilização de 119 ratos Wistar de 90 dias de idade, 20 machos e 99 fêmeas, provenientes do CREAL-UFRGS; aprova-se também a utilização de 176 ratos Wistar machos e 176 (75 adendo 1 + 101 adendo 2) ratos Wistar fêmeas provenientes do cruzamento dos referidos animais. O projeto está de acordo com os preceitos das Diretrizes e Normas Nacionais e Internacionais, especialmente a Lei 11.794 de 08 de novembro de 2008, o Decreto 6899 de 15 de julho de 2009, e as normas editadas pelo Conselho Nacional de Controle da Experimentação Animal (CONCEA), que disciplinam a produção, manutenção e/ou utilização de animais do filo Chordata, subfilo Vertebrata (exceto o homem) em atividade de ensino ou pesquisa.

Porto Alegre, 09 de setembro de 2016

Marcelo Meller Alievi
Coordenador da CEUA/UFRGS